



This electronic version (PDF) was scanned by the International Telecommunication Union (ITU) Library & Archives Service from an original paper document in the ITU Library & Archives collections.

La présente version électronique (PDF) a été numérisée par le Service de la bibliothèque et des archives de l'Union internationale des télécommunications (UIT) à partir d'un document papier original des collections de ce service.

Esta versión electrónica (PDF) ha sido escaneada por el Servicio de Biblioteca y Archivos de la Unión Internacional de Telecomunicaciones (UIT) a partir de un documento impreso original de las colecciones del Servicio de Biblioteca y Archivos de la UIT.

(ITU) للاتصالات الدولي الاتحاد في والمحفوظات المكتبة قسم أجراه الضوئي بالمسح تصوير نتاج (PDF) الإلكترونية النسخة هذه والمحفوظات المكتبة قسم في المتوفرة الوثائق ضمن أصلية ورقية وثيقة من نقلًا.

此电子版（PDF版本）由国际电信联盟（ITU）图书馆和档案室利用存于该处的纸质文件扫描提供。

Настоящий электронный вариант (PDF) был подготовлен в библиотечно-архивной службе Международного союза электросвязи путем сканирования исходного документа в бумажной форме из библиотечно-архивной службы МСЭ.

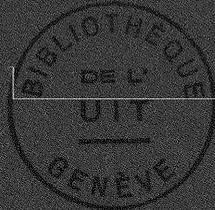


XVIIth PLENARY ASSEMBLY  
DÜSSELDORF, 1990



INTERNATIONAL TELECOMMUNICATION UNION

## HF TRANSMITTING ANTENNAS CHARACTERISTICS AND DIAGRAMMS



RECOMMENDATION 705 (SG 10)

**CCIR** INTERNATIONAL RADIO CONSULTATIVE COMMITTEE

Geneva, 1990

## CCIR

1. The International Radio Consultative Committee (CCIR) is the permanent organ of the International Telecommunication Union responsible under the International Telecommunication Convention "... to study technical and operating questions relating specifically to radiocommunications without limit of frequency range, and to issue recommendations on them..." (International Telecommunication Convention, Nairobi 1982, First Part, Chapter I, Art. 11, No. 83)\*

2. The objectives of the CCIR are in particular:

a) to provide the technical bases for use by administrative radio conferences and radiocommunication services for efficient utilization of the radio-frequency spectrum and the geostationary-satellite orbit, bearing in mind the needs of the various radio services;

b) to recommend performance standards for radio systems and technical arrangements which assure their effective and compatible interworking in international telecommunications;

c) to collect, exchange, analyze and disseminate technical information resulting from studies by the CCIR, and other information available, for the development, planning and operation of radio systems, including any necessary special measures required to facilitate the use of such information in developing countries.

\* See also the Constitution of the ITU, Nice, 1989, Chapter 1, Art. 11, No. 84.



XVIIth PLENARY ASSEMBLY  
DÜSSELDORF, 1990



INTERNATIONAL TELECOMMUNICATION UNION

## HF TRANSMITTING ANTENNAS CHARACTERISTICS AND DIAGRAMS



**RECOMMENDATION 705 (SG 10)**

**CCIR** INTERNATIONAL RADIO CONSULTATIVE COMMITTEE

Geneva, 1991

## RECOMMENDATION 705

## HF TRANSMITTING ANTENNAS CHARACTERISTICS AND DIAGRAMS\*

(Question 44/10, Study Programmes 44G/10 and 44H/10)

(1990)

The CCIR,

*considering*

- (a) that Resolution 76 decided to issue a separately published Recommendation containing a revised and complemented set of HF broadcasting antenna diagrams together with other relevant information;
- (b) that the diagrams published in this Recommendation should be easy to be understood and used by the planning and designing engineers, while retaining all the necessary useful information;
- (c) the experience gained with the previous editions of Antenna Diagrams;
- (d) the need to keep the cost of this publication as low as possible as expressed in Opinion 79;
- (e) that the characteristics of the HF antennas as contained in Annex I to this Recommendation have a wide application,

*unanimously recommends*

that the formulae as illustrated by sample diagrams and contained in Annex I to this Recommendation together with the corresponding computer programs should be used to evaluate the performance of HF transmitting antennas; particularly for planning purposes.

*Note* – Part 1 of Annex I gives comprehensive and detailed information on the theoretical characteristics of HF transmitting antennas.

Computer programs have been developed from the theory to calculate the radiation patterns and gain for the various included antenna types.

For any chosen antenna the available output data includes the directivity gain, the relative gain for a particular azimuth and elevation angle, tables of relative gain referred to the maximum and a number of different graphic outputs.

A few sample patterns are included to illustrate some of the possible outputs of the calculation procedure.

The real performance of antennas encountered in practice will deviate to a certain extent from its analytically calculated characteristics. To this purpose Part 2 gives advice about this deviation on the basis of the results of a comprehensive set of measurements carried out by various administrations with modern techniques.

---

\* The Director, CCIR, is requested to bring Chapter 2 of Part 2 of Annex I to the attention of the IEC.

## ANNEX I

## TABLE OF CONTENTS

	<i>Page</i>
<b>PART 1 – HF TRANSMITTING ANTENNA CHARACTERISTICS AND DIAGRAMS</b>	
1. Introduction.....	5
2. Geometrical representation of antenna radiation patterns.....	6
2.1 Graphical representation .....	6
3. Radiation patterns and gain calculation .....	7
3.1 General considerations.....	7
3.2 Radiation patterns.....	9
3.3 Directivity and gain .....	9
3.4 Effect of the ground.....	9
4. Arrays of horizontal dipoles .....	11
4.1 General considerations.....	11
4.2 Designation of arrays of horizontal dipoles .....	12
4.2.1 Arrays of horizontal dipoles arranged vertically (curtain antennas).....	12
4.2.2 Arrays of horizontal dipoles arranged horizontally (tropical antennas).....	13
4.2.3 Omnidirectional arrays of horizontal dipoles.....	13
4.2.3.1 Quadrant antennas .....	13
4.2.3.2 Crossed dipole antennas.....	14
4.3 Slewing.....	15
4.4 Arrays of horizontal dipoles arranged vertically.....	16
4.5 Arrays of horizontal dipoles arranged horizontally (tropical antennas).....	19
4.6 Omnidirectional arrays of horizontal dipoles.....	19
4.6.1 General considerations.....	19
4.6.2 Quadrant antennas .....	19
4.6.3 Crossed dipole antennas.....	21
4.7 Calculation of the patterns of horizontal dipole arrays .....	21
4.7.1 General considerations.....	21
4.7.1.1 Centre-fed half-wave dipole arrays .....	25
4.7.1.2 End-fed half-wave dipole arrays .....	25
4.7.2 Calculation of the array factor $S_z$ .....	25
4.7.2.1 Half-wave dipole arrays arranged vertically.....	26
4.7.2.2 Half-wave dipole arrays for tropical broadcasting.....	27

	<i>Page</i>
4.7.3 Calculation of the array factor $S_y$ .....	27
4.7.3.1 Centre-fed half-wave dipole arrays .....	28
4.7.3.2 End-fed half-wave dipole arrays .....	28
4.7.4 Calculation of the array factor $S_x$ .....	28
4.7.4.1 Aperiodic screen reflector antennas .....	29
4.7.4.2 Tuned reflector antennas .....	31
4.7.4.3 Centre-fed dipole arrays for tropical broadcasting .....	31
4.7.5 Calculation of the patterns for omnidirectional arrays of horizontal dipoles .....	32
4.7.5.1 Quadrant antennas .....	32
4.7.5.2 Crossed-dipole antennas .....	33
5. Log-periodic antennas .....	35
5.1 General considerations .....	35
5.2 Designation of log-periodic antennas .....	35
5.2.1 Horizontal log-periodic antennas .....	35
5.2.2 Vertical log-periodic antennas .....	36
5.3 Calculation of the patterns for horizontal log-periodic antennas .....	36
5.3.1 Basic theory .....	38
5.3.2 Calculation procedure .....	40
5.3.2.1 Approximate solution of the interior problem .....	41
5.4 Calculation of the patterns for vertical log-periodic antennas .....	47
5.4.1 Basic theory .....	49
5.4.2 Calculation procedure .....	49
6. Rhombic antennas .....	50
6.1 General considerations .....	50
6.2 Designation of rhombic antennas .....	50
6.3 Calculation of the patterns for rhombic antenna .....	51
7. Vertical monopoles .....	53
7.1 General considerations .....	53
7.2 Designation of vertical monopoles .....	53
7.3 Vertical monopole without an earth system .....	53
7.4 Vertical monopole with an earth system .....	55
7.4.1 Vertical monopole with an earth system consisting of a solid circular disk having infinite conductivity .....	55
7.4.2 Vertical monopole with an earth system consisting of a number of radial wires of given length and diameter .....	56
8. Pattern examples .....	59
References .....	59
Bibliography .....	60

## PART 2 – PRACTICAL ASPECTS OF HF TRANSMITTING ANTENNAS

1.	Introduction.....	61
2.	Measurements of antenna radiation patterns .....	61
	2.1 Method of measurement.....	61
	2.2 Considerations when using a helicopter for the measurements .....	61
	2.3 Measuring equipment.....	62
	2.4 Measurement procedures .....	62
	2.5 Processing the measured data.....	65
3.	Comparison of theoretical and measured radiation patterns .....	66
	3.1 Comparison of theoretical and measured front-to-back ratios.....	69
4.	Influence of surrounding environment on radiation patterns .....	70
	4.1 Ground topography .....	70
	4.2 Ground conductivity .....	72
	4.3 Other site structures .....	72
5.	Variations in practical antenna performance.....	74
	5.1 Azimuthal pattern .....	74
	5.2 Slewed pattern .....	76
6.	Suitability and application of antennas .....	77
	6.1 Horizontal dipole antennas.....	77
	6.2 Rotatable curtain antennas .....	77
	6.3 Rhombic antennas.....	78
	6.4 Fixed azimuth log-periodic antennas.....	78
	6.5 Rotatable log-periodic antennas .....	78
	Bibliography .....	78
	Annex I – Pattern examples.....	79

## PART 1

**HF transmitting antenna characteristics and diagrams****1. Introduction**

The aim of Part 1 of this Annex is to provide comprehensive and detailed information on the theoretical characteristics of HF transmitting antennas. The analytical approach followed is to calculate the pattern and directivity gain for any of the included antenna types. Although for the sake of simplicity the following basic assumptions have been used:

- antenna situated on flat homogeneous imperfect ground;
- antenna elements consisting of thin linear wires;
- sinusoidal current distribution in the radiating elements;

the algorithms, developed on the basis of current literature, were found to offer a good compromise between accuracy and ease of calculation.

The method of application of reflection coefficients with imperfect ground was verified as correct. The method of calculating the maximum gain of antennas has been adapted to correctly take into account the effect of different conductivities. The fundamental theoretical background has been studied and the appropriate formulae have been derived.

Computer programs have been developed to calculate the radiation patterns and gain for the following types of antennas, as used by administrations, for HF broadcasting and other services:

- arrays of half-wave horizontal dipoles;
- quadrant antennas and horizontal dipoles;
- log-periodic antennas;
- tropical antennas;
- rhombic antennas and
- vertical monopoles.

For the first time in a CCIR Recommendation, the computer programs are an integral part of the publication thus allowing the reader to perform his own calculation for any desired antenna type in varying conditions.

For a selected type of antenna the available output data include the directivity gain, the relative gain for a particular azimuth and elevation angle, tables of relative gain referred to the maximum and a number of different graphic outputs.

For this reason, only few example patterns are included to illustrate some of the possible outputs of the calculation procedure.

It is hoped that this Part will give the engineer a useful tool for the development, planning and operation of radio systems.

The real performance of antennas encountered in practice will deviate to a certain extent from their analytically calculated characteristics. Part 2 gives information about this deviation on the basis of the results of a comprehensive set of measurements carried out by various administrations using modern techniques.

## 2. Geometrical representation of antenna radiation patterns

An antenna can consist of a single element or an array of radiating elements. The spatial radiation distribution, or pattern, of an antenna can be represented by a three-dimensional locus of points, with each point having a value of cymomotive force\* (c.m.f.), based on a half-sphere above the ground centred at the antenna and of radius which is large compared to the physical and electrical dimensions of the antenna.

The c.m.f. at a point on the sphere is indicated in dB below the maximum c.m.f., which is labelled 0 dB.

The three-dimensional radiation pattern is based on the reference coordinate system of Fig. 1.

In a spherical polar coordinate system the following parameters are defined:

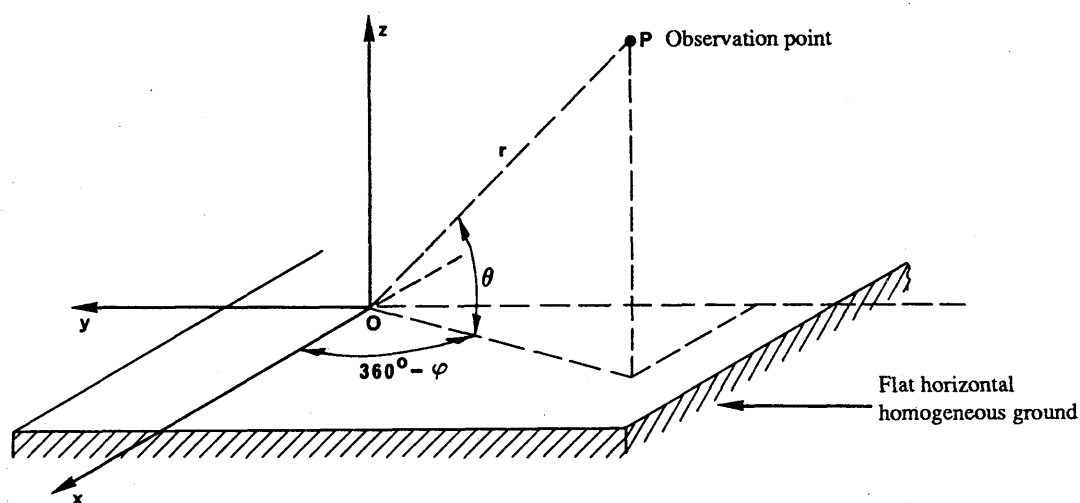
$\theta$ : elevation angle from the horizontal ( $0^\circ \leq \theta \leq 90^\circ$ )

$\varphi$ : azimuthal angle from the x-axis ( $0^\circ \leq \varphi \leq 360^\circ$ )

$r$ : distance between the origin and the distant observation point where the far field is calculated.

FIGURE 1

The reference coordinate system



### 2.1 Graphical representation

Several representations of a three-dimensional radiation pattern are possible. Very frequently a set of particular sections of the radiation pattern at specific elevation angles (azimuthal patterns) and at specific azimuthal angles (vertical patterns) is used to describe the full radiation pattern. The most important sections are the azimuthal patterns at the elevation angle at which the maximum c.m.f. occurs and the vertical pattern at the azimuthal angle at which the maximum c.m.f. occurs. These are referred to as the horizontal radiation pattern (HRP) and the vertical radiation pattern (VRP) respectively.

\* Definition of cymomotive force and specific cymomotive force (see Recommendation 561):

The cymomotive force at a given point in space is the product of the electric field strength at that point produced by the antenna and the distance from that point to the antenna. This distance must be large enough for the reactive components of the field to be negligible.

The c.m.f. in volts is numerically equal to the electric field strength in mV/m at a distance of 1 km.

The specific cymomotive force at a point in space is the c.m.f. at that point when the power radiated by the antenna is 1 kW.

A sinusoidal transformation, also called a "Sanson-Flamsteed" projection, is then used to represent the hemisphere and the contours in the plane of the paper.

The antenna is located in the centre of a sphere as in Fig. 2 in the reference coordinate system of Fig. 1.

In this projection, the point  $P(\theta, \varphi)$  on the sphere for the quadrant  $0^\circ \leq \varphi \leq 90^\circ$ ,  $0^\circ \leq \theta \leq 90^\circ$ , is transformed onto the point  $P'(\theta', \varphi')$  on a plane where  $\theta' = \theta$  and  $\varphi' = \varphi \cos\theta$ . A similar transformation is applied to the other quadrants.

In the Sanson-Flamsteed projection shown in Fig. 3 for the upper hemisphere, the equator is represented by a horizontal line and the central meridian at  $\varphi = 0^\circ$  becomes a line perpendicular to the equator forming the vertical axis.

The parallels of the hemisphere are straight lines equally spaced on the central meridian in proportion to the elevation angle. The meridians are portions of sine waves equally spaced in proportion to the azimuth angle  $\varphi$ , all passing through the pole of the hemisphere.

Two important properties of this projection are that equal areas within the hemisphere remain equal in the plane of the paper, and that azimuthal patterns for constant elevation angles, i.e. conic sections, are represented as straight lines parallel to the equator.

The horizontal reference plane through the  $270^\circ$  to  $90^\circ$  azimuth is in most cases a plane of symmetry of the antenna. To represent the whole hemisphere, two diagrams are needed: the forward radiation pattern and the backward radiation pattern. The first of these represents the radiation in the quarter sphere above ground between the azimuth angles  $270^\circ$ ,  $0^\circ$  and  $90^\circ$ , while the second contains the radiation in the other quarter sphere above the ground ( $90^\circ$ ,  $360^\circ$  and  $270^\circ$ ).

The contours of equal field strength are labelled with relative gain values referred to that in the direction of maximum radiation which is marked 0 dB.

The values adopted for the contours are the following (in dB attenuation relative to the maximum):

3, 6, 10, 15, 20, 25, 30.

Each diagram shows:

- the value of the elevation angle  $\theta$  (degrees), of the direction of maximum radiation;
- the value (dB) of the directivity gain relative to an isotropic antenna in free space\*,  $G_i$ .

### 3. Radiation patterns and gain calculation

#### 3.1 General considerations

The following assumptions have been used in the calculation of the radiation patterns and the gain of the types of antenna included in this Part:

- the antenna is situated on a flat, homogeneous ground (coinciding with the x-y plane). For the case of typical imperfect ground, a conductivity  $\sigma = 0.01$  S/m and dielectric constant (relative permittivity)  $\epsilon = 4.0$  (average ground), have been used as default values;
- antenna elements are thin linear wires;
- the currents in the radiating elements are sinusoidally distributed.

\* For definitions see RR 154 and CCIR Recommendation 573, Volume XIII.

FIGURE 2  
The spherical coordinate system

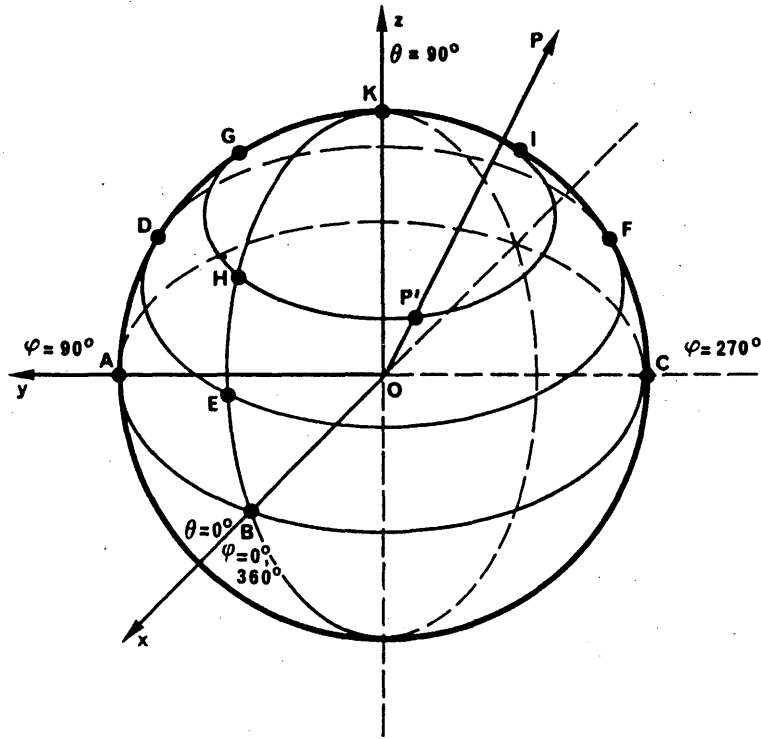
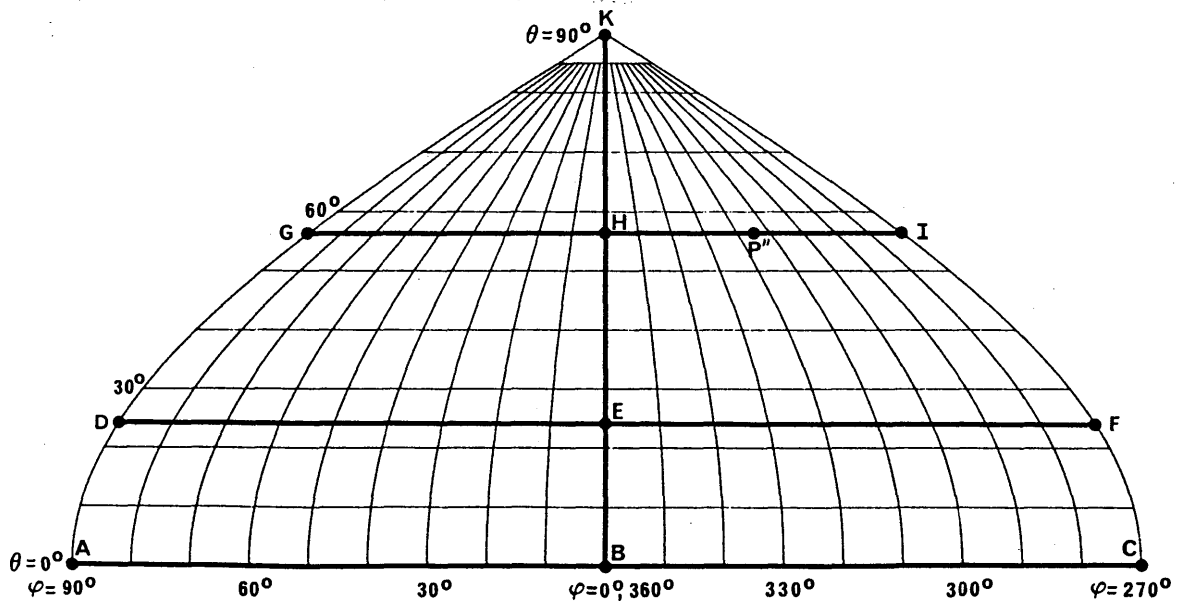


FIGURE 3  
The Sanson-Flamsteed projection



### 3.2 Radiation patterns

In the reference coordinate system of Fig. 1, the normalized radiation pattern function is given by the following expression:

$$F(\theta, \varphi) = K |E(\theta, \varphi)| = K |f(\theta, \varphi)| \cdot |S|$$

where:

- $K$ : normalizing factor to set  $|F(\theta, \varphi)|_{max} = 1$ , i.e. 0 dB;
- $E(\theta, \varphi)$ : total field contributed by the array;
- $f(\theta, \varphi)$ : element pattern function;
- $S$ : array factor depending on the space distribution of the elements.

Expressing the total field in terms of its components in a spherical coordinate system, gives:

$$|E(\theta, \varphi)| = \left[ |E_{\theta}(\theta, \varphi)|^2 + |E_{\varphi}(\theta, \varphi)|^2 \right]^{1/2}$$

### 3.3 Directivity and gain

The directivity,  $D$ , of an antenna is defined as the ratio of its maximum radiation intensity (or power flux-density) to the radiation intensity of an isotropic source radiating the same total power. It can be expressed by:

$$D = \frac{4\pi \cdot |E(\theta, \varphi)|_{max}^2}{W_0} = \frac{4\pi \cdot |E(\theta, \varphi)|_{max}^2}{\int_0^{2\pi} \int_{-\pi/2}^{\pi/2} |E(\theta, \varphi)|^2 \cos \theta \, d\theta \, d\varphi}$$

where:

- $W_0$ : radiation intensity of the isotropic source.

The above definition of directivity is a function only of the shape of the antenna radiation pattern.

The directivity gain relative to an isotropic antenna in free space is given by:

$$G_i = 10 \log_{10} D$$

The above definition assumes 100% efficiency of the antenna system. To take into account an antenna efficiency of less than 100%, it is necessary to define the antenna gain as the ratio of its maximum radiation intensity to the maximum radiation intensity of a reference antenna with the same input power.

### 3.4 Effect of the ground

Using the assumptions given in § 3.1, and also that the antenna is located in the coordinate system of Fig. 1, where the x-y plane represents a flat homogeneous ground, the far field produced at the observation point  $P(r, \theta, \varphi)$ , including the ground reflected part, can be derived as follows.

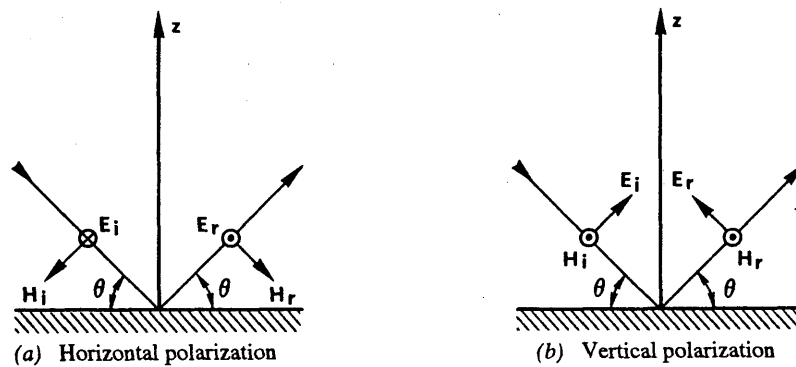
If the incident radiation on the ground is assumed to have a plane wavefront, the following two different cases can be considered:

- a) horizontal polarization,
- b) vertical polarization.

In the case of *horizontal polarization*, the incident (direct) electric vector is parallel to the reflecting x-y plane (and hence perpendicular to the plane of incidence, i.e. the plane containing the direction of propagation and the perpendicular to the reflecting surface, as shown in Fig. 4(a)).

In the case of *vertical polarization*, the incident electric vector is parallel to the plane of incidence while the associated incident magnetic vector is parallel to the reflecting surface, as shown in Fig. 4(b).

FIGURE 4  
Wave reflection on imperfect ground



The total far-field components above ground can then be expressed as follows:

- (a) Horizontal polarization

$$E_h = E_i(r_1) + E_r(r_2) = E_i(r_1) + R_h E_i(r_2)$$

where:

- $E_h$ : total horizontal component;
- $r_1$ : direct distance between the antenna and the observation point;
- $r_2$ : distance from the image of the antenna to the observation point;
- $E_i$ : direct electric field;
- $E_r$ : reflected electric field;
- $R_h$ : complex reflection coefficient for horizontally polarized waves defined as:

$$R_h = \frac{\sin \theta - \left[ (\epsilon - \cos^2 \theta) - j \frac{18\,000 \cdot \sigma}{f \text{ MHz}} \right]^{1/2}}{\sin \theta + \left[ (\epsilon - \cos^2 \theta) - j \frac{18\,000 \cdot \sigma}{f \text{ MHz}} \right]^{1/2}}$$

and

$\theta$  : grazing angle

$\epsilon$  : relative permittivity (or dielectric constant) of the Earth;

$\sigma$  : conductivity of the Earth (S/m);

$f_{\text{MHz}}$ : operating frequency (MHz).

(b) *Vertical polarization*

$$E_h' = E_i(r_1) - R_v E_i(r_2)$$

$$E_v = E_i(r_1) - R_v E_i(r_2)$$

where:

$E_h'$ : total horizontal component;

$E_v$ : total vertical component;

$R_v$ : complex reflection coefficient for vertically polarized waves defined as

$$R_v = \frac{\left[ \epsilon - j \frac{18\,000 \cdot \sigma}{f_{\text{MHz}}} \right] \sin \theta - \left[ (\epsilon - \cos^2 \theta) - j \frac{18\,000 \cdot \sigma}{f_{\text{MHz}}} \right]^{1/2}}{\left[ \epsilon - j \frac{18\,000 \cdot \sigma}{f_{\text{MHz}}} \right] \sin \theta + \left[ (\epsilon - \cos^2 \theta) - j \frac{18\,000 \cdot \sigma}{f_{\text{MHz}}} \right]^{1/2}}$$

## 4. Arrays of horizontal dipoles

### 4.1 *General considerations*

The half wavelength dipole is one of the radiating elements most commonly used at HF.

Although a horizontal dipole is often used on its own, arrays of dipoles are often used to obtain:

- increased gain;
- improved directional and slewable patterns.

When more complex arrays are used, an important aspect is the capability to operate within specific performance limits over a certain frequency range above and below the design frequency. This wide-band operating capability depends on various factors, such as the feeding arrangements, the dipole structure, etc.

Higher gains are achieved by arranging the dipole elements collinearly and/or stacking parallel dipoles in order to reduce the beamwidth of the main lobe and hence increase the directivity of the antenna.

The main beam of certain horizontal dipole arrays which have more than one feed point may be electrically slewed by feeding each stack or row of dipoles with equal currents having different phases.

Unidirectional patterns are generally obtained by the use of a reflector. This reflector can be comprised of either:

- an identical array of dipoles tuned to provide an optimum front-to-back ratio over a limited range of operating frequencies. In practice antennas of this form have a maximum operating frequency range which covers two adjacent broadcasting bands, giving a frequency range from the lowest to the highest frequency of approximately 1.25:1. It should be noted that this type of reflector is generally tuned to provide the optimum front-to-back ratio for a single frequency within the required frequency band and the front-to-back ratio can be expected to decrease if the antenna is operated at any other frequency. This type of reflector is known as either a "tuned dipole" or "parasitic" reflector. It can also be driven to obtain an improved performance. However this technique is not generally used; or
- a screen consisting of horizontal wires which act as an untuned reflector. In practice a number of antennas of this form can be operated over a maximum of five consecutive broadcasting bands giving an operating frequency range of up to 2:1. This range is limited by the performance of the radiating elements. This type of reflector is known as an "aperiodic reflector" or "screen reflector".

The front-to-back ratio of an aperiodic reflector depends on such factors as: number of wires per wavelength, wire gauge, distance between radiating elements and reflector, and size of reflector. To achieve a front-to-back ratio, which approaches the gain figure of the antenna would require a screen density of about 40 to 50 wires per wavelength for the highest operating band of the antenna.

## 4.2 Designation of arrays of horizontal dipoles

### 4.2.1 Arrays of horizontal dipoles arranged vertically (curtain antennas)

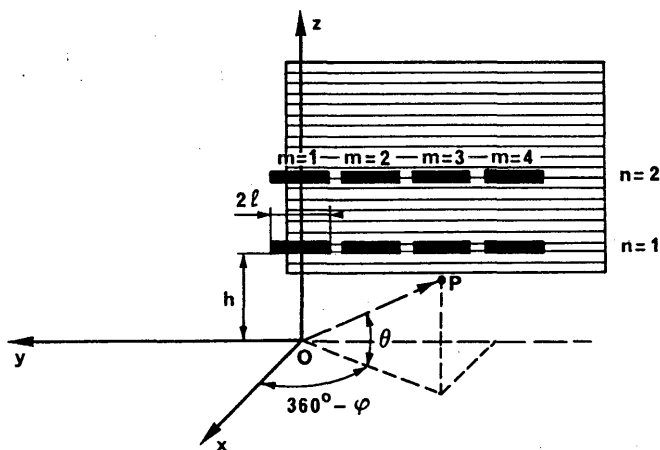
Type designation: H(R)(S)  $m/n/h$

where:

- H : array of horizontal dipoles arranged vertically;
- R : if specified, indicates the presence of a reflector;
- S : if specified, indicates that a phase shift in the current fed to adjacent collinear elements has been introduced to produce a slew of the azimuth of the main beam;
- $m$  : number of collinear elements in each row;
- $n$  : number of parallel elements normally spaced half a wavelength apart one above the other;
- $h$  : height of the lowest row of dipoles above the ground (wavelengths).

For example from Fig. 5 it can be seen that HR 4/2/1.0 indicates an array of horizontal dipoles arranged vertically with a reflector. In this case there are two horizontal rows of four half-wave elements of length  $2l$  at the design frequency, and the height ( $h$ ) of the lowest row is one wavelength above the ground.

FIGURE 5  
Curtain antenna



4.2.2 Arrays of horizontal dipoles arranged horizontally (tropical antennas)

Type designation: T(S)  $m/n/h$

where:

- T : array of horizontal dipoles arranged horizontally (tropical antenna);
- S : if specified, indicates that a phase shift in the current fed to adjacent collinear elements has been introduced to produce a slew of the elevation angle of the main beam from the vertical;
- $m$  : number of collinear elements in each row;
- $n$  : number of parallel rows spaced half a wavelength apart;
- $h$  : height of the dipoles above the ground (wavelengths).

For example from Fig. 6 it can be seen that a T 4/2/0.2 indicates an unslewed horizontal array of four horizontal collinear dipoles of length  $2l$  at the design frequency with two parallel rows, and where the height,  $h$ , is 0.2 wavelengths above the ground.

4.2.3 Omnidirectional arrays of horizontal dipoles

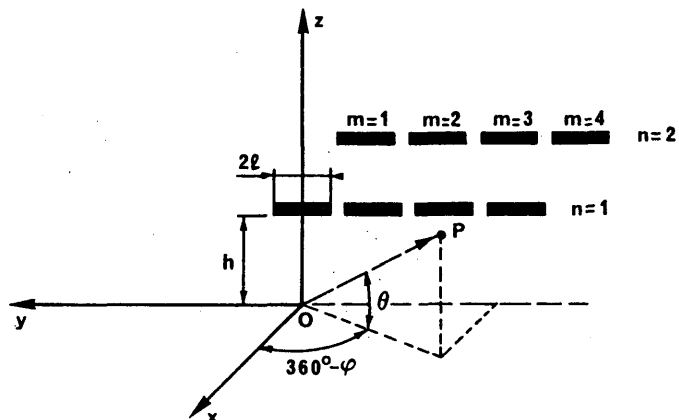
4.2.3.1 Quadrant antennas

Type designation: HQ  $n/h$

where:

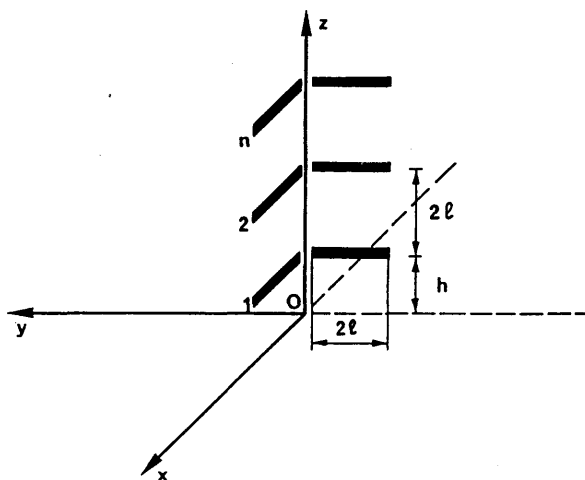
- HQ : quadrant antenna;
- $n$  : number of elements stacked one above the other;
- $h$  : height of the lowest row of dipoles above the ground (wavelengths).

FIGURE 6  
Tropical antenna



For example from Fig. 7 it can be seen that HQ 3/0.2 indicates a quadrant antenna of 3 sets of horizontal dipoles of length  $2l$  at the design frequency stacked vertically where the height,  $h$ , of the lowest dipoles is 0.2 wavelength above the ground.

FIGURE 7  
Quadrant antenna



#### 4.2.3.2 Crossed dipole antennas

Type designation: HX  $h$

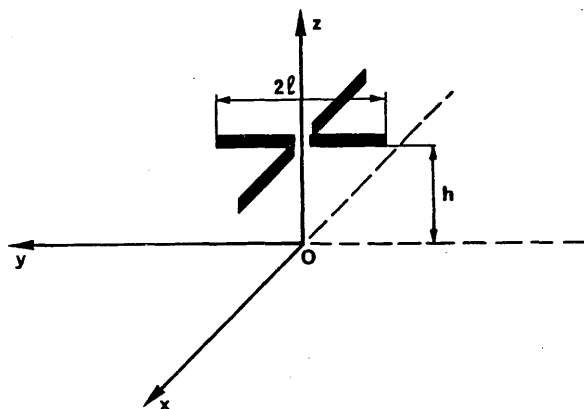
where:

HX : crossed dipole antenna;

$h$  : height of the dipoles above the ground (wavelengths).

For example from Fig. 8 it can be seen that HX 0.3 indicates a crossed dipole antenna of 2 horizontal dipoles of length  $2\ell$  crossing at right angles at their mid-points where the height,  $h$ , is 0.3 wavelengths above the ground.

FIGURE 8  
Crossed dipole antenna



#### 4.3 Slewing

The main beam of certain horizontal dipole arrays which have more than one feed point may be electrically slewed by feeding each stack or row of dipoles with currents having different phases.

Slewing is usually implemented in the azimuthal plane for arrays of horizontal dipoles arranged vertically. However vertical plane slewing is also possible and finds particular application in the case of tropical antennas.

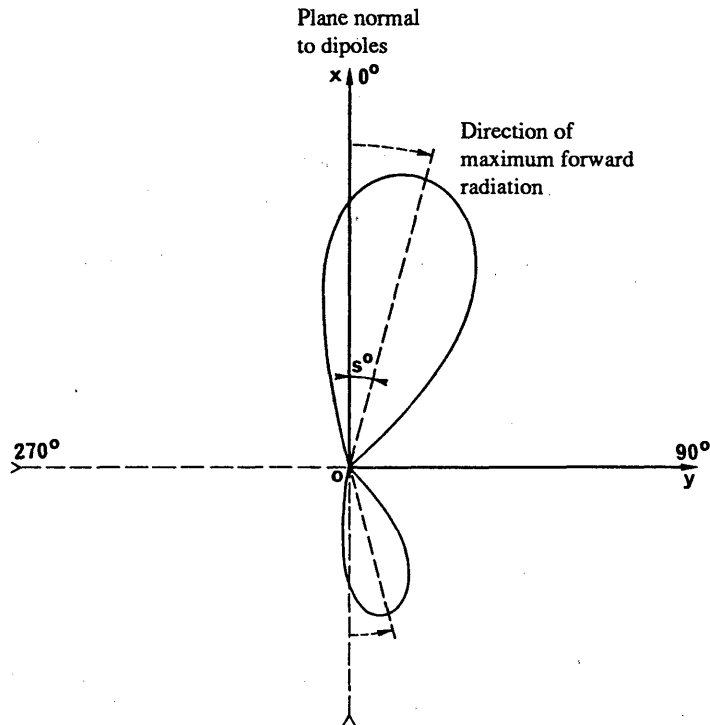
The main features of a horizontally slewed antenna are:

- the main beam is no longer in the direction normal to the plane of the dipoles,
- the forward horizontal radiation pattern is no longer symmetrical with respect to the direction normal to the plane of the dipoles,
- the backward radiation pattern is no longer symmetrical with respect to the direction normal to the plane of the dipoles, nor is it on the axis of the direction of the slewed maximum in the forward pattern. Slewing the forward radiation of an antenna in one direction (e.g. clockwise) will cause the back radiation to slew in the opposite direction (i.e. anticlockwise). Figure 9 shows the effect of slewing the forward radiation in a clockwise direction.

According to conventional methods of calculation, the slew angle  $s$  of the maximum radiation for horizontally slewed antennas is always less than the nominal slew angle introduced in the calculation. This nominal slew angle is sometimes quoted by the designer and is not therefore necessarily the value achieved in practice. Typically a slew  $s = 25.5^\circ$  will be achieved if a conventional calculation has been made with a nominal slew angle of  $30^\circ$  for a HRS  $4/n/h$  array.

It should also be noted that the slew angle  $s$ , does not always precisely define the centre of the horizontal pattern given by the mean of the angles at which maximum gain in the forward radiation pattern is reduced by 6 dB. This mean value called "effective slew",  $s_{eff}$ , provides a more accurate indication of the change in the coverage given by the main beam.

FIGURE 9  
Azimuthal pattern of a horizontally slewed antenna



The slew angle achieved in practice will depend on the ratio  $F_R$  of the operating to the design frequency, e.g. the value of the slewed angle, in comparison to the value achieved at  $F_R = 1.0$  is smaller for  $F_R < 1.0$  and larger for  $F_R > 1.0$ .

For a specified antenna, the maximum gain will decrease for increasing values of the slew angle. It is also to be noted that the elevation angle at which maximum radiation occurs will be affected by the value of  $F_R$ , but not by the slew angle  $s$ . In addition the main lobe to side lobe ratio of the antenna is decreased with increased slew.

#### 4.4 Arrays of horizontal dipoles arranged vertically

Arrays of horizontal dipoles arranged vertically (curtain antennas) are realized by aligning and/or stacking half wavelength dipoles in a vertical plane.

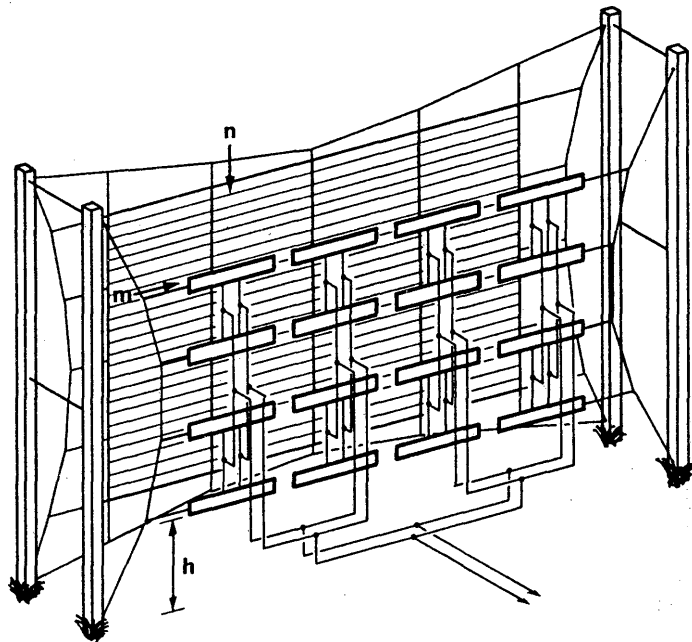
Two different basic feeding arrangements are used.

- centre-fed dipoles;
- end-fed dipoles.

In the centre-fed array, each dipole element has its own feeding point as shown in Fig. 10. Antennas with a number of pairs of half-wavelength dipoles in a row ( $m$ ) greater or equal to two, can be slewed.

FIGURE 10

Centre-fed dipole array with aperiodic reflector



In the end-fed array, two adjacent dipoles offer a common feeding point connected to a single transmission line as shown in Fig. 11 for the case of an aperiodic reflector. Figure 12 illustrates the case of an end-fed dipole array with tuned reflector. Slewing capability is provided only for cases when the number of the pairs of half-wavelength dipoles in a row ( $m$ ) is even.

FIGURE 11

End-fed dipole array with aperiodic reflector

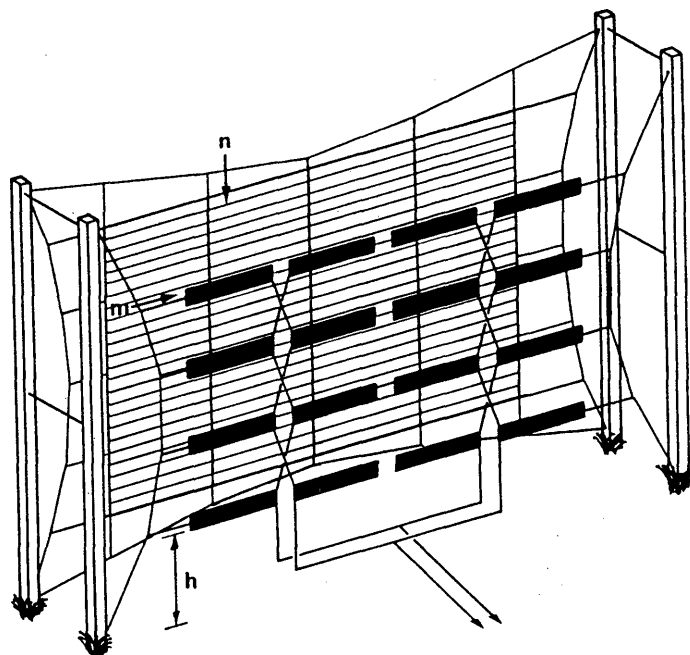
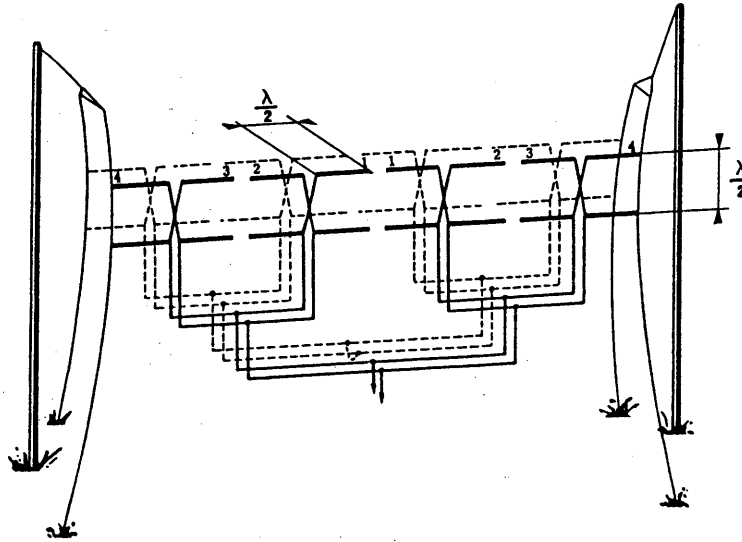


FIGURE 12  
End-fed dipole array with tuned reflector



Curtain antennas using centre-fed elements are of more modern design and, at the cost of a more complex feeding arrangement, offer greater slewing capabilities when compared to the corresponding end-fed type.

For example, an HRS  $4/n/h$  centre-fed dipole array with four feed points, can be slewed up to  $\pm 30^\circ$  and still maintain acceptable side-lobe levels.

A corresponding HRS  $4/n/h$  end-fed dipole array provides only two feed points spaced at about one wavelength. This spacing and the related feeding system which sets up a phase difference between the two halves of the array, result in a practical slewing capability of about  $\pm 15^\circ$  in the azimuthal plane. Greater slewing results in an undesirably large-amplitude sidelobe having a maximum gain value within 6 dB of that of the main beam.

The performance of arrays of horizontal dipoles arranged vertically is also a function of their multi-band operation capabilities.

Early types of curtain antennas were designed to operate on frequencies very close to the optimum design frequency so that they were called "single-band" antennas. This type of antenna, still in operation, is normally equipped with a tuned dipole reflector.

More modern tuned dipole reflector curtain antennas are designed to operate over two adjacent bands, that is for frequency ratios ranging from 0.9 to 1.1.

Wider operating frequency ranges (typically for frequency ratios up to 2:1) can presently be achieved by careful design of the radiating elements (normally centre-fed half-wavelength dipoles). Multiband antennas of modern design are usually equipped with a wire mesh aperiodic reflector placed at a suitable distance (in the order of 0.25 wavelength at the design frequency) from the driven elements.

A screen reflector may typically consist of a grid of horizontal wires with the diameter varying from 2.7 to 4.7 mm and with a spacing varying from 25 wires per wavelength to more than 100 wires per wavelength at the design frequency. A screen of at least 40 wires per wavelength is recommended for acceptable performance.

#### 4.5 *Arrays of horizontal dipoles arranged horizontally (tropical antennas)*

Radiation mainly concentrated at high elevation angles (up to 90°) and in most cases associated with a nearly circular azimuthal radiation pattern is achieved by using arrays of horizontal dipoles in a horizontal plane at a given height above the ground.

These antennas, also called tropical antennas, are often used for short-range broadcasting in tropical zones and consist of one or more rows of half-wave horizontal dipoles at a height above ground usually not exceeding 0.5 wavelength.

Slewing of the main beam in the z-y plane can be achieved by varying the phases of the feed current in the elements of the same row (along the y-axis).

The resulting pattern then shows a more or less pronounced main beam tilt in the z-y plane thus providing a directional effect useful for specific coverage situations.

#### 4.6 *Omnidirectional arrays of horizontal dipoles*

##### 4.6.1 *General considerations*

Non-directional short-range coverage in HF broadcasting generally requires the use of omnidirectional or near-omnidirectional antennas.

The vertical monopole (see § 7) provides an omnidirectional pattern but has some inherent limitations. A near-omnidirectional azimuthal pattern and better flexibility can be achieved with quadrant and crossed-dipole antennas. They consist of simple arrangements of horizontal dipoles whose height above ground determines the elevation angle at which maximum radiation occurs.

Antennas of this type are normally used in the lower part of the HF spectrum where short range broadcasting generally takes place. With careful design of the radiating elements, it is possible to realize antennas that can be operated over two (or even three) adjacent frequency bands. However, the resulting pattern shape shows a marked dependence on the frequency ratio.

##### 4.6.2 *Quadrant antennas*

The simplest form of quadrant antenna is represented by an arrangement of two end-fed half-wave dipoles placed at a right angle, as shown in Fig. 13. Another form of quadrant antenna sometimes encountered in practice, is shown schematically in Fig. 14. It consists of four elements placed in the form of a square and fed at opposite corners.

Quadrant antennas may also be stacked to achieve a more directive vertical radiation pattern and a higher directivity gain.

For simplicity, when calculating the pattern (see § 4.7.5.1) of a quadrant antenna, only the case of the simple antenna shown in Fig. 13, is considered.

FIGURE 13  
2-leg quadrant antenna

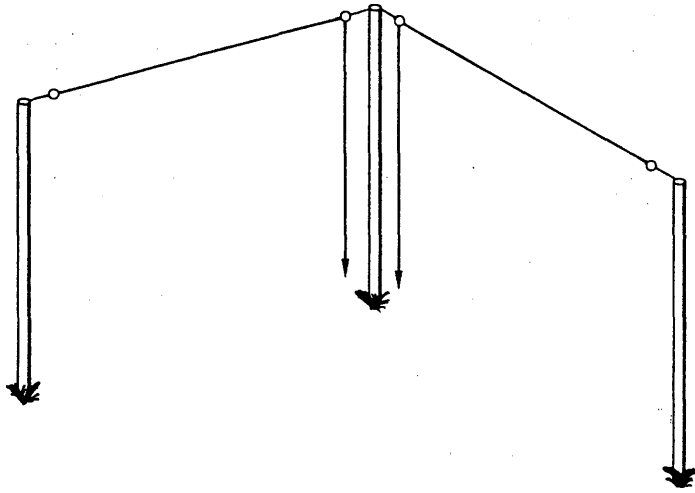
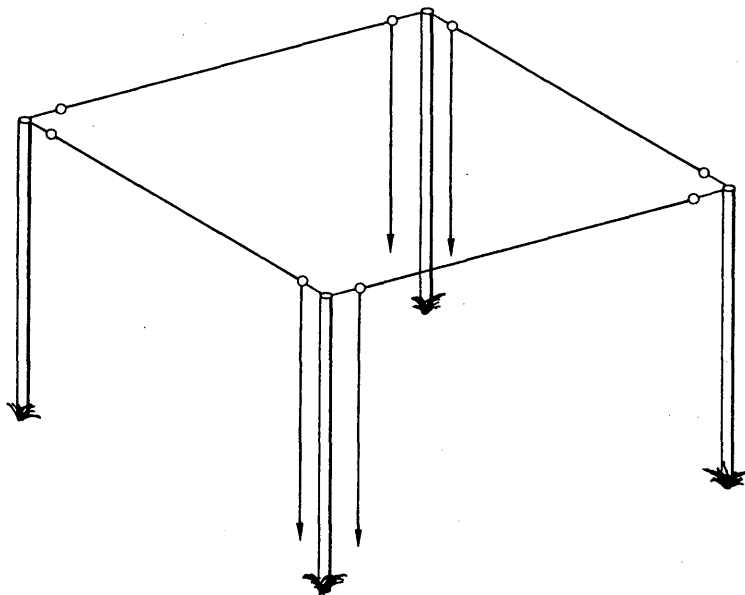


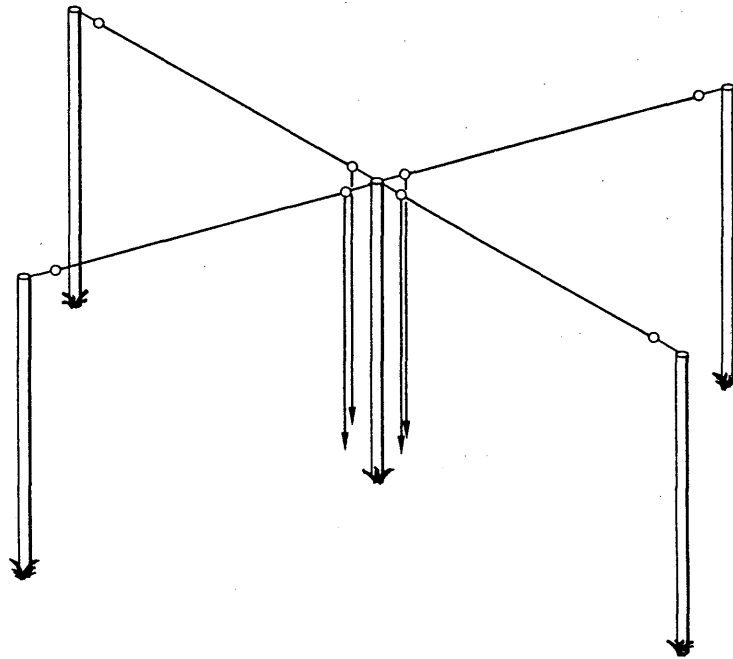
FIGURE 14  
4-leg quadrant antenna



#### 4.6.3 *Crossed-dipole antennas*

A crossed-dipole antenna consists of two centre-fed half-wave dipoles placed at a right angle to form a cross. The intersection point coincides with the radiating element feed point, as shown in Fig. 15.

FIGURE 15  
Crossed-dipole antenna



#### 4.7 *Calculation of the patterns of horizontal dipole arrays*

##### 4.7.1 *General considerations*

In the following section the calculation procedure used to derive the related radiation pattern for various horizontal dipole arrays and which has been implemented in the computer programs, is described.

The HF dipole array will be considered in the coordinate system of Fig. 1, for the following cases:

- aperiodic screen, centre-fed, half-wave dipole curtain arrays (Fig. 16);
- tuned reflector, centre-fed, half-wave dipole curtain arrays (Fig. 17);
- tuned reflector, end-fed, half-wave dipole curtain arrays (Fig. 18);
- centre-fed, half-wave dipole arrays for tropical broadcasting (Fig. 19).

FIGURE 16  
Centre-fed HR 4/4/ dipole array with aperiodic screen reflector

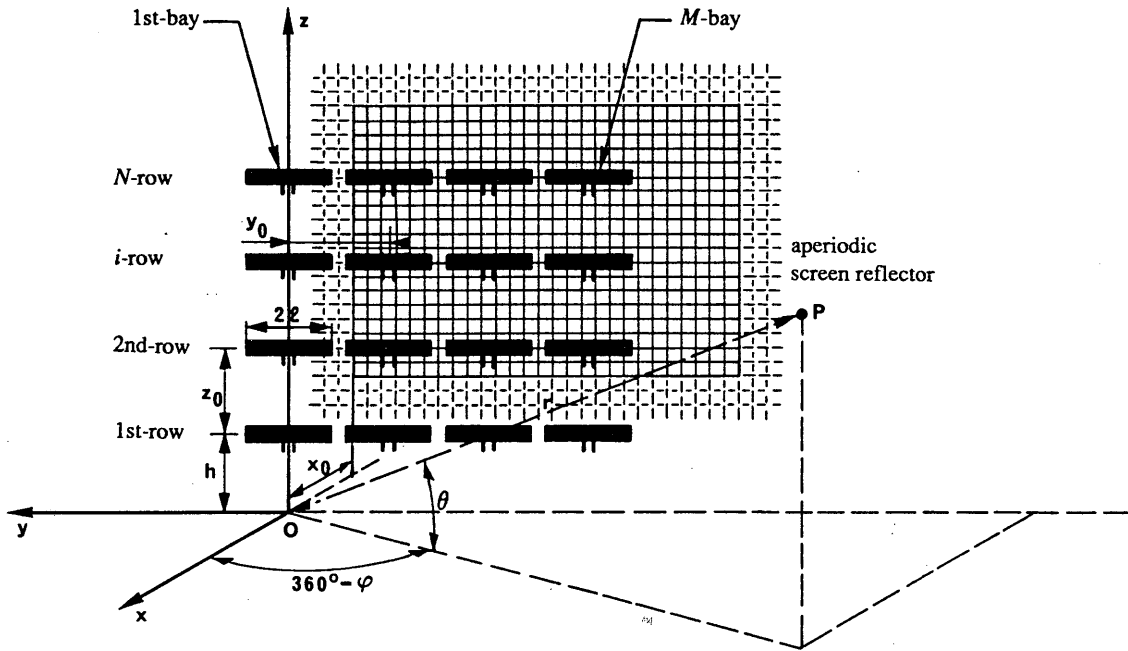


FIGURE 17  
Centre-fed HR 4/4/ dipole array with tuned dipole reflector

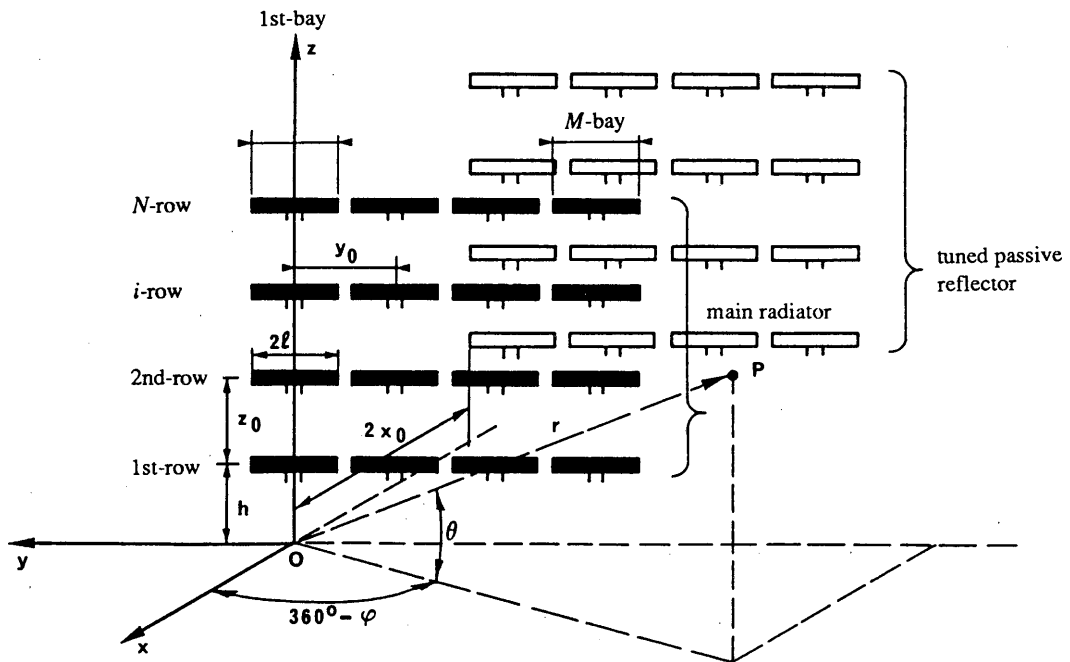


FIGURE 18  
End-fed HR 4/4/ dipole array with tuned reflector

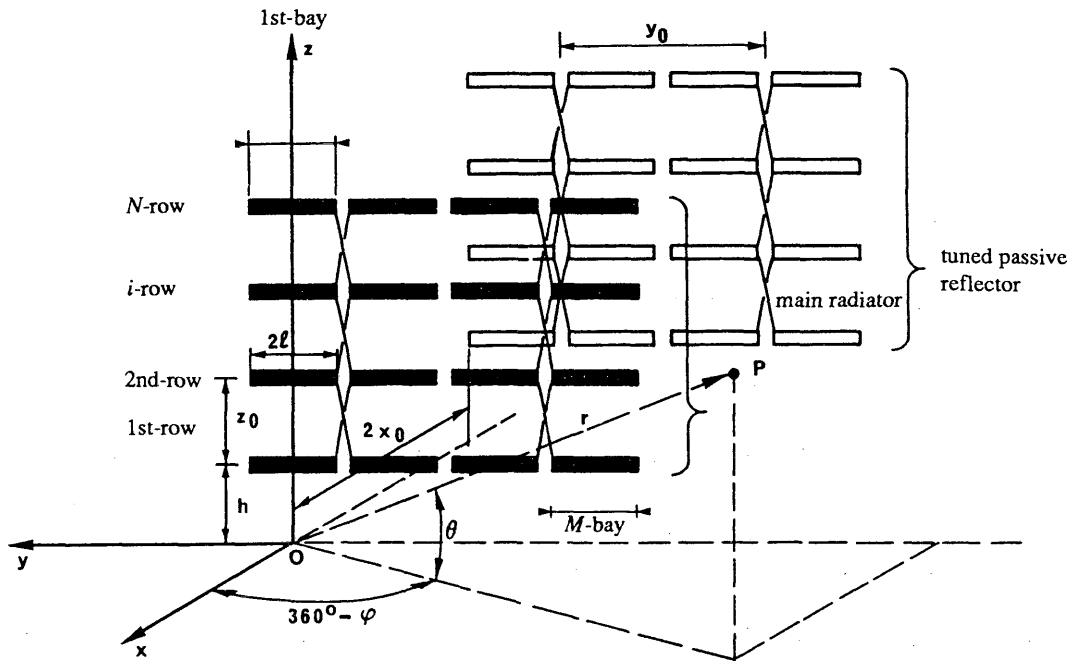
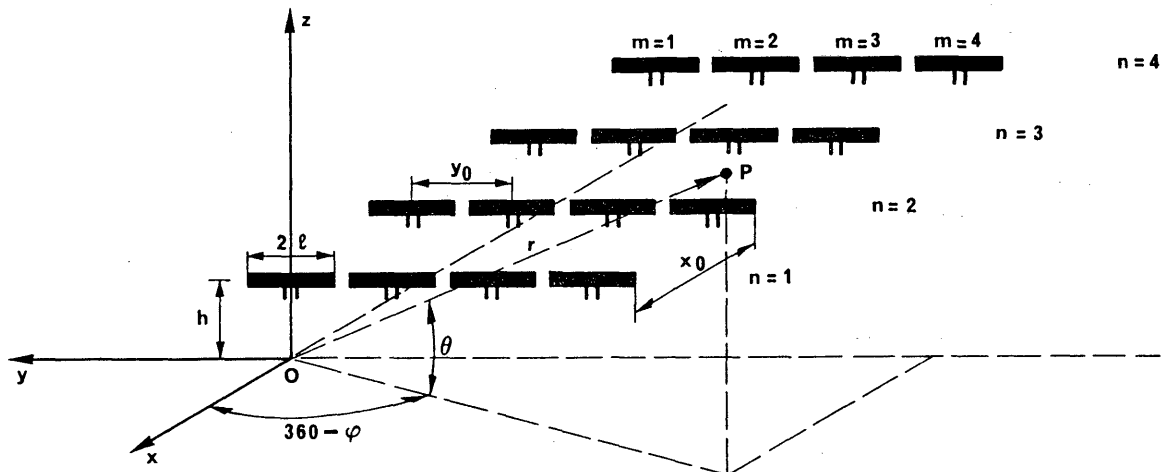


FIGURE 19  
Centre-fed T 4/4/ dipole array for tropical broadcasting



The array is considered to have a design frequency  $f_d$  (or wavelength  $\lambda_d$ ) and an operating frequency  $f$  (or wavelength  $\lambda$ ). The frequency ratio  $F_R$ , is given by:

$$F_R = f/f_d = \lambda_d/\lambda$$

The radiation pattern of a dipole array over flat, homogeneous and imperfect ground can be expressed by the following normalized radiation pattern function (see also [CCIR, 1978]):

$$F(\theta, \varphi) = K \cdot f(\theta, \varphi) \cdot S_x \cdot S_y \cdot S_z$$

where:

$K$ : normalizing factor to set  $|F(\theta, \varphi)|_{max} = 1$ , i.e. 0 dB;

$f(\theta, \varphi)$ : horizontal element pattern function;

$S_x$ : array factor for the x-direction, taking into account the presence of other elements or of a reflector;

$S_y$ : array factor for the y-direction, taking into account the presence of other elements along the y-axis;

$S_z$ : array factor for the z-direction, taking into account the presence of image elements due to an imperfect ground and of other elements along the z-axis.

The radiation pattern function,  $F(\theta, \varphi)$  is also expressed as the resultant of two electrical field components  $E_\theta$  and  $E_\varphi$  at a distant point P in the coordinate system of Fig. 1, i.e.:

$$F(\theta, \varphi) = K \cdot |E(\theta, \varphi)| = K \cdot \left[ |E_\theta(\theta, \varphi)|^2 + |E_\varphi(\theta, \varphi)|^2 \right]^{1/2}$$

with:

$$E_\theta(\theta, \varphi) = E_{\theta 1}(\theta, \varphi) \cdot S_x \cdot S_y \cdot S_\theta$$

$$E_\varphi(\theta, \varphi) = E_{\varphi 1}(\theta, \varphi) \cdot S_x \cdot S_y \cdot S_\varphi$$

where  $E_{\theta 1}(\theta, \varphi)$  and  $E_{\varphi 1}(\theta, \varphi)$  are the components of the horizontal element pattern function  $f(\theta, \varphi)$  and  $S_\theta$  and  $S_\varphi$  are the related components of the array factor  $S_z$ .

For a horizontal dipole having length  $2l$  at the design frequency, the electrical far field components have the following expression [Ma, 1974]:

$$E_{\theta 1}(\theta, \varphi) = -j 60 I \frac{e^{-jk r}}{r} \sin \varphi \sin \theta C_d$$

$$E_{\varphi 1}(\theta, \varphi) = -j 60 I \frac{e^{-jk r}}{r} \cos \varphi C_d$$

where:

- $I$ : amplitude of the current in the dipole,  
 $r$ : distance between the origin and the observation point and  
 $C_d$ : current distribution function of the radiating element.

Assuming a *sinusoidal* current distribution function:

$$C_d = \frac{\cos(kl \sin \varphi \cos \theta) - \cos kl}{1 - \sin^2 \varphi \cos^2 \theta}$$

where  $k = 2\pi/\lambda$  (phase constant).

Expressions for the current distribution function and the respective definitions of  $kl$  are given for the different types of arrays in the following sections.

#### 4.7.1.1 Centre-fed half-wave dipole arrays

Centre-fed half-wave dipole arrays include:

- aperiodic screen, centre-fed, half-wave dipole arrays;
- tuned reflector, centre-fed, half-wave dipole arrays;
- centre-fed, half-wave dipole arrays for tropical broadcasting.

For these cases  $2l = \lambda_d / 2$

and

$$kl = 2\pi / \lambda \cdot \lambda_d / 4 = F_R \cdot \pi/2$$

$$C_d = \frac{\cos(F_R \cdot \pi/2 \cdot \sin \varphi \cos \theta) - \cos(F_R \cdot \pi/2)}{1 - \sin^2 \varphi \cos^2 \theta}$$

#### 4.7.1.2 End-fed half-wave dipole arrays

For end-fed half-wave dipole arrays  $2l = \lambda_d$

and

$$kl = F_R \cdot \pi$$

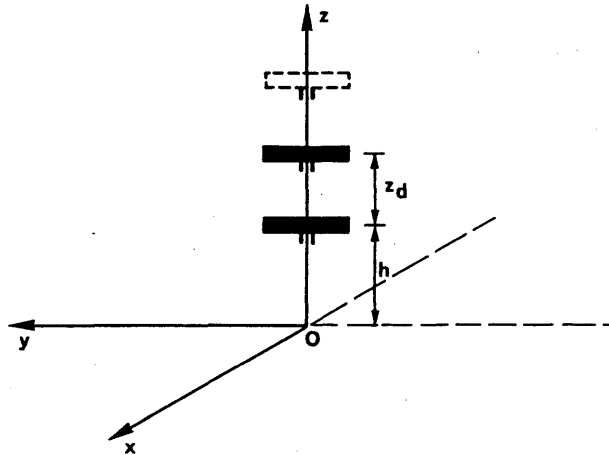
$$C_d = \frac{\cos(F_R \cdot \pi \cdot \sin \varphi \cos \theta) - \cos(F_R \cdot \pi)}{1 - \sin^2 \varphi \cos^2 \theta}$$

#### 4.7.2 Calculation of the array factor $S_z$

The array factor  $S_z$  takes into account the effect of stacking  $n$  elements along the vertical  $z$ -axis including their ground reflected components.

FIGURE 20

Stacking elements along z-axis



The array factor  $S_z$  has two components  $S_\theta$  and  $S_\phi$  corresponding to the respective electrical field components:

$$S_\theta = \sum_{i=0}^{n-1} e^{j(kh + ikz_d) \sin \theta} \left[ 1 - R_v e^{-2j(kh + ikz_d) \sin \theta} \right]$$

$$S_\phi = \sum_{i=0}^{n-1} e^{j(kh + ikz_d) \sin \theta} \left[ 1 + R_h e^{-2j(kh + ikz_d) \sin \theta} \right]$$

where:

- $z_d$ : vertical element spacing;
- $h$ : height of the lowest element above ground;
- $R_v$ : vertical reflection coefficient;
- $R_h$ : horizontal reflection coefficient.

Expressions for the respective array factor components are given for the different type of arrays in the following sections.

#### 4.7.2.1 Half-wave dipole arrays arranged vertically

Half-wave dipole arrays arranged vertically include:

- aperiodic screen, centre-fed, half-wave dipole arrays;
- tuned reflector, centre-fed, half-wave dipole arrays;
- tuned reflector, end-fed, half-wave dipole arrays;

For these cases  $z_d = \lambda_d / 2$  and  $kh + ikz_d = 2\pi h / \lambda + i\pi F_R$ .

Expressing  $h$  in wavelengths at  $f_d$  (i.e. as  $h / \lambda_d$ ), then:

$$kh + ikz_d = 2\pi F_R h / \lambda_d + i\pi F_R$$

and the components  $S_\theta$  and  $S_\phi$  are:

$$S_\theta = \sum_{i=0}^{n-1} e^{j\pi F_R(2h/\lambda_d + i)\sin\theta} \left[ 1 - R_v e^{-2j\pi F_R(2h/\lambda_d + i)\sin\theta} \right]$$

$$S_\phi = \sum_{i=0}^{n-1} e^{j\pi F_R(2h/\lambda_d + i)\sin\theta} \left[ 1 - R_h e^{-2j\pi F_R(2h/\lambda_d + i)\sin\theta} \right]$$

**4.7.2.2 Half-wave dipole arrays for tropical broadcasting**

For half-wave dipole arrays for tropical broadcasting  $n = 1$  and the formulae simplify as follows:

$$S_\theta = e^{j\pi F_R \cdot 2h/\lambda_d \cdot \sin\theta} \left[ 1 - R_v e^{-j4\pi F_R \cdot h/\lambda_d \cdot \sin\theta} \right]$$

$$S_\phi = e^{j\pi F_R \cdot 2h/\lambda_d \cdot \sin\theta} \left[ 1 - R_h e^{-j4\pi F_R \cdot h/\lambda_d \cdot \sin\theta} \right]$$

**4.7.3 Calculation of the array factor  $S_y$**

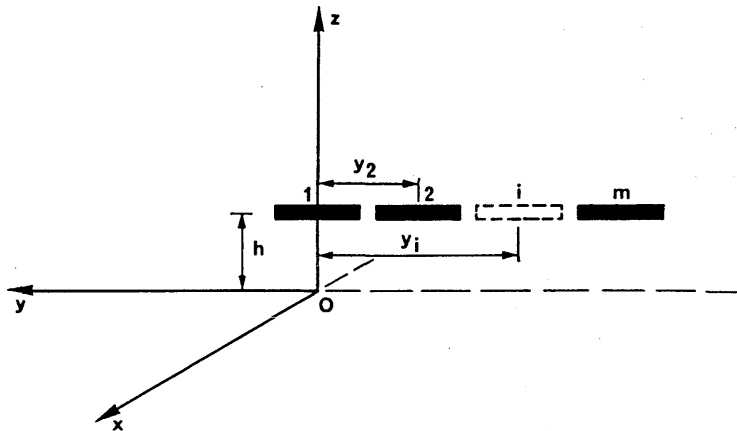
The array factor  $S_y$  takes into account the effect of  $m$ -elements along the  $y$ -axis (see Fig. 21) and it can be expressed [Ma, 1974] as:

$$S_y = \sum_{i=1}^m e^{jk y_i \cos\theta (\sin\phi - \sin s)}$$

where:

- $s$ : slew angle,
- $y_i$ : distance between the centre of the  $i$ -th element and the  $z$ -axis.

**FIGURE 21**  
**Elements aligned along y-axis**



The expressions for the array factor  $S_y$  are given for different types of arrays in the following sections.

4.7.3.1 Centre-fed, half-wave dipole arrays

For centre-fed, half-wave dipole arrays:

$$k y_i = i 2\pi / \lambda \cdot \lambda_d / 2 = i \pi F_R$$

and  $S_y$  can be expressed as:

$$S_y = \sum_{i=1}^m e^{j i \pi F_R \cos \theta (\sin \phi - \sin \alpha)}$$

4.7.3.2 End-fed, half-wave dipole arrays

For end-fed, half-wave dipole arrays:

$$k y_i = i 2\pi / \lambda \cdot \lambda_d = i 2\pi F_R$$

and  $S_y$  can be expressed as:

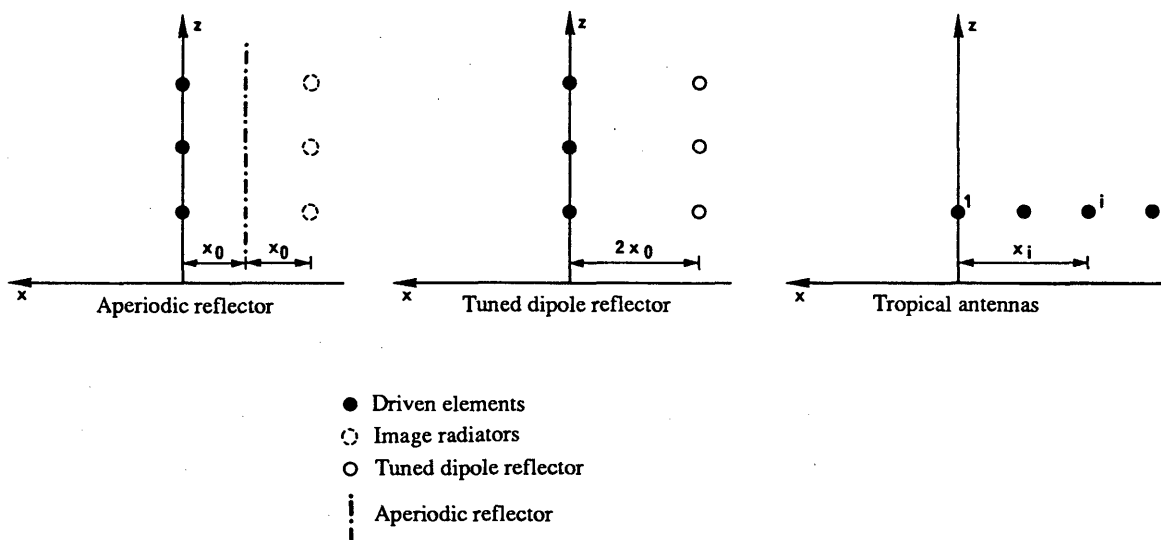
$$S_y = \sum_{i=1}^m e^{j i 2\pi F_R \cos \theta (\sin \phi - \sin \alpha)}$$

4.7.4 Calculation of the array factor  $S_x$

The array factor  $S_x$  takes into account the effect of placing  $n$ -elements along the  $x$ -axis in the case of arrays for tropical broadcasting and the presence of a reflector (tuned dipoles or aperiodic screen) in the remaining cases.

FIGURE 22

Elements or image elements aligned along  $x$ -axis



The expressions for the array factor  $S_x$  are given for different type of arrays in the following sections.

4.7.4.1 Aperiodic screen reflector antennas

The performance of aperiodic screen reflectors can be calculated from a mathematical model using the concept of an "image radiator" behind an infinite screen. This, however, only gives the forward pattern with sufficient accuracy. The magnitude of the back radiation to the rear of the screen is a function of the effectiveness of the screen and the distance of the dipole from the reflecting screen. For a screen of practical dimensions some energy will also be diffracted around the edge of the screen. The method used below for calculating the back radiation retains a directivity function shape generally similar to that calculated for the forward pattern.

Screen reflection factor

A reflecting screen composed of closely-spaced straight conductors parallel to the dipoles will reflect most of the energy incident upon it, while the remaining energy will pass through the screen.

The screen reflection factor  $q_r$  is defined as the ratio of reflected to incident energy, as follows:

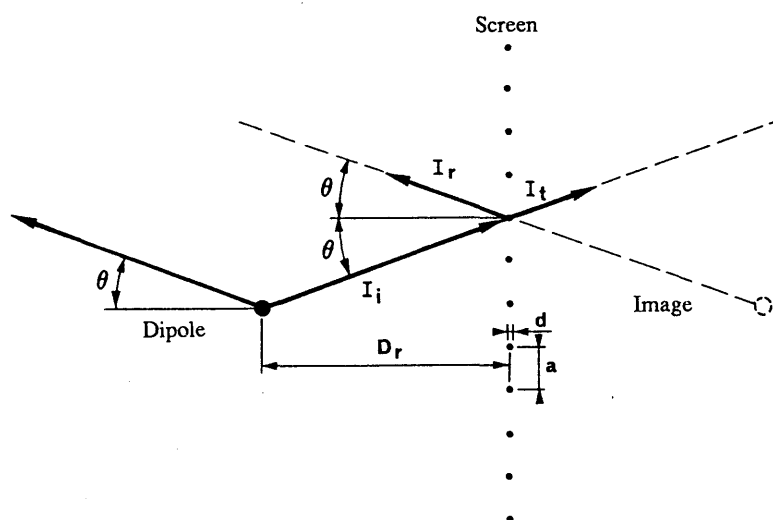
$$q_r = \frac{I_r}{I_i} = 1 - \frac{I_t}{I_i} = 1 - \frac{1}{\left[ 1 + \frac{1}{\left[ \log_e \left( \frac{a}{\pi \cdot d} \right) \cdot \frac{2a}{\lambda} \cos \theta \right]^2} \right]^{1/2}}$$

where:

- $d$ : diameter of the wire (mm)
- $a$ : wire spacing (m)
- $D_r$ : distance of dipoles from reflecting screen (m)
- $I_i$ : intensity of incident wave
- $I_r$ : intensity of reflected wave
- $I_t$ : intensity of transmitted wave
- $\theta$ : angle of incidence (or elevation).

FIGURE 23

Aperiodic reflecting screen and dipole (end view)



The radiation pattern can be expressed as:

$$F(\theta, \varphi) = F_D \cdot S_x$$

where:

$F_D$ : partial directivity function of the antenna, and

$S_x$ : array factor along the x-axis.

The array factor in front of the screen can be expressed as:

$$S_x = \left[ 1 + q_r^2 - 2q_r \cos(2 \cdot k \cdot D_r \cdot \cos \varphi \cos \theta) \right]^{1/2}$$

and the array factor behind the screen as :

$$S_x = (1 - q_r)$$

The front-to-back ratio (FTBR) can then be expressed as\* :

$$FTBR = 20 \log_{10} \cdot \frac{\left[ F_D \left[ 1 + q_r^2 - 2q_r \cos(2k D_r \cos \varphi \cos \theta) \right]_{max}^{1/2} \right]}{[F_D(1 - q_r)]_{max}}$$

In the particular case where :

$$F_R = 1, D_r = \lambda/4, \varphi = 0^\circ \text{ and } \theta = 0^\circ \text{ (or } 0^\circ \leq \theta \leq 20^\circ \text{ with small error)}$$

the radiation pattern in front of the screen becomes:

$$F(\theta, \varphi) = F_D \left[ 1 + q_r^2 - 2q_r \cos \pi \right]^{1/2} = F_D(1 + q_r)$$

and the radiation pattern behind the screen :

$$F(\theta, \varphi) = F_D(1 - q_r)$$

The front-to-back ratio will have the following expression:

$$FTBR = 20 \log_{10} \frac{F_D(1 + q_r)}{F_D(1 - q_r)} = 20 \log_{10} \frac{1 + q_r}{1 - q_r} \quad (1)$$

### Diffraction

The use of aperiodic reflecting screens of finite dimensions will result in diffraction around the edges of the screen. This in most cases can be expected to reduce the front-to-back ratio. The effect appears to be related to the proximity of the radiating elements to the edge of the screen.

At present, the effect of diffraction is not included in the mathematical model employed. Further studies are necessary before conclusions can be drawn.

### Reference screen

If the physical parameters of the aperiodic screen such as wire diameter and spacing and distance of the dipole from reflecting screen are not known, for planning purposes calculations may be performed using the following reference values (see § 4.4):

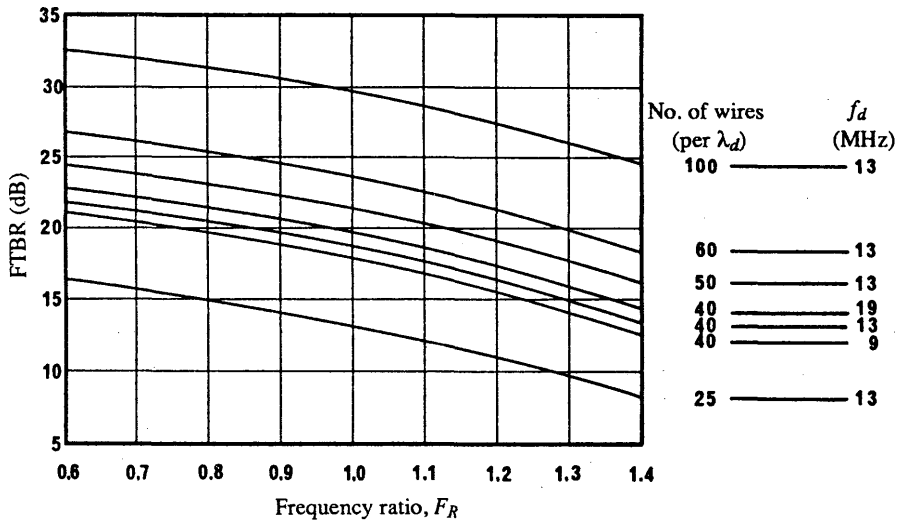
- wire diameter  $d = 3 \text{ mm}$ ;
- wire spacing  $\lambda/40$  (at design frequency);
- distance of dipole from reflecting screen,  $D_r = 0.25\lambda$  (at design frequency).

\* The front-to-back ratio (FTBR) is defined as the ratio of the maximum field strength in the forward radiation pattern to the maximum field strength in the backward radiation pattern.

Variation of front-to-back ratio with the parameters of aperiodic screen and the frequency ratio

Figure 24 shows for selected values of wire spacing (at the design frequency), the variation of FTBR with the frequency ratio  $F_R$  and the design frequency  $f_d$ , calculated according to (1).

FIGURE 24  
 Front-to-back ratio, FTBR, as a function of  
 the number of wires per wavelength at design frequency  $f_d$ ,  
 and frequency ratio  $F_R$



4.7.4.2 Tuned reflector antennas

Tuned reflector antennas include:

- centre-fed dipole arrays;
- end-fed dipole arrays.

For these cases the expression of the array factor  $S_x$  along the x-axis [Jasik, 1950; Aizenberg, 1948] is:

$$S_x = [1 + q^2 + 2q \cos(A - 2x_0 k \cos \varphi \cos \theta)]^{1/2}$$

where:

- $q$ : ratio between the current in the reflector and in the driven element
- $A$ : relative phase angle of the current in the reflector referred to the current in the driven element
- $2x_0$ : spacing between driven element and reflector.

The values  $q = 0.7$ ,  $A = \pi/2$  and  $2x_0 k = \pi/2$  are generally used for these antennas.

4.7.4.3 Centre-fed dipole arrays for tropical broadcasting

For centre-fed dipole arrays for tropical broadcasting the array factor can be expressed by:

$$S_x = \sum_{i=0}^{n-1} e^{-jkx_i \cos \varphi \cos \theta}$$

where:

$x_i$ : distance between the centre of the  $i$ -th element and the  $z$ -axis.

This distance is given by the expression:

$$x_i = i \lambda_d / 2$$

so that:

$$k x_i = i 2\pi / \lambda \cdot \lambda_d / 2 = i \pi F_R$$

and therefore:

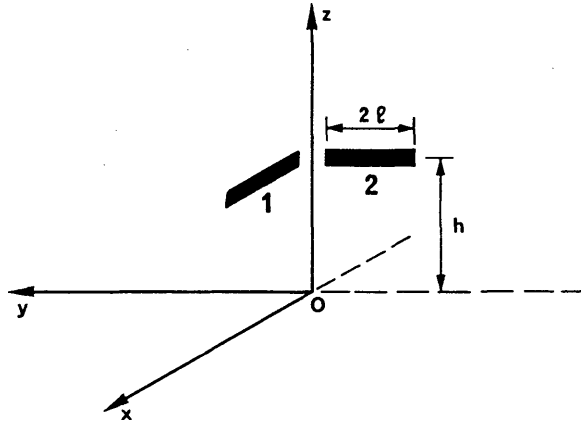
$$S_x = \sum_{i=0}^{n-1} e^{-j i \pi F_R \cos \varphi \cos \theta}$$

#### 4.7.5 Calculation of the patterns for omnidirectional arrays of horizontal dipoles

##### 4.7.5.1 Quadrant antennas

The quadrant antenna is schematically shown in Fig. 25, in the coordinate system of Fig. 1. The total field radiated by the array is the resultant of the field radiated by each dipole of length  $2l = \lambda_d / 2$  at the design frequency.

FIGURE 25  
Quadrant antenna



Considering dipole No. 1 aligned along the  $x$ -axis at height  $h$ , the electrical field components have the following expression:

$$E_{1\theta}(\theta, \varphi) = -j 60 I \frac{e^{-jk r}}{r} \cos \varphi \sin \theta C_d e^{j \Delta x} S_\theta$$

$$E_{1\varphi}(\theta, \varphi) = -j 60 I \frac{e^{-jk r}}{r} \sin \varphi C_d e^{j \Delta x} S_\varphi$$

where  $C_d$  is the current distribution function of the radiating element. Assuming a *sinusoidal* current distribution:

$$C_d = \frac{\cos(F_R \cdot \pi/2 \cdot \cos \varphi \cos \theta) - \cos(F_R \cdot \pi/2)}{1 - \cos^2 \varphi \cos^2 \theta}$$

The term  $e^{j\Delta x}$  takes into account the phase shift corresponding to the horizontal distance from origin of the centre of the dipole. It is expressed as:

$$e^{j\Delta x} = e^{-jk\ell \cos \theta \cos \varphi}$$

The array factors will have the following expressions:

$$S_\theta = e^{j\pi F_R \cdot 2h/\lambda_d \cdot \sin \theta} \cdot \left[ 1 - R_v e^{-j4\pi F_R \cdot h/\lambda_d \cdot \sin \theta} \right]$$

$$S_\varphi = e^{j\pi F_R \cdot 2h/\lambda_d \cdot \sin \theta} \cdot \left[ 1 + R_h e^{-j4\pi F_R \cdot h/\lambda_d \cdot \sin \theta} \right]$$

Considering dipole No. 2 aligned along the y-axis at height  $h$ , the electrical field components will have the following expressions:

$$E_{2\theta}(\theta, \varphi) = -j60 I \frac{e^{-jkr}}{r} \sin \varphi \sin \theta C_d e^{j\Delta y} S_\theta$$

$$E_{2\varphi}(\theta, \varphi) = -j60 I \frac{e^{-jkr}}{r} \cos \varphi C_d e^{j\Delta y} S_\varphi$$

and the current distribution function will have the following expression:

$$C_d = \frac{\cos(F_R \cdot \pi/2 \cdot \sin \varphi \cos \theta) - \cos(F_R \cdot \pi/2)}{1 - \sin^2 \varphi \cos^2 \theta}$$

The term  $e^{j\Delta y}$  takes into account the phase shift corresponding to the horizontal distance from origin of the centre of the dipole. It is expressed as:

$$e^{j\Delta y} = e^{-jk\ell \cos \theta \sin \varphi}$$

The array factors will have the same expression as for dipole No. 1.

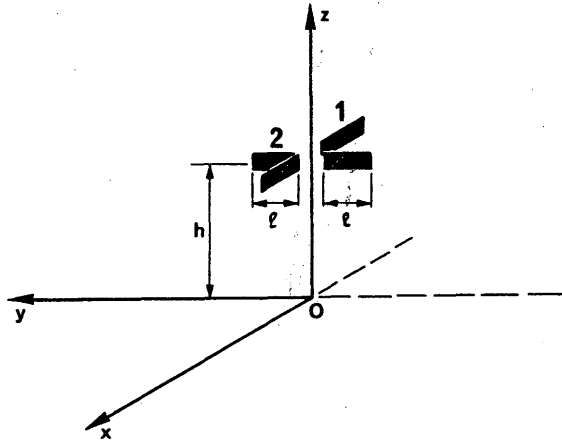
The total field radiated by the array is therefore:

$$|E(\theta, \varphi)| = \left[ |E_{1\theta}(\theta, \varphi) + E_{2\theta}(\theta, \varphi)|^2 + |E_{1\varphi}(\theta, \varphi) + E_{2\varphi}(\theta, \varphi)|^2 \right]^{1/2}$$

#### 4.7.5.2 Crossed-dipole antennas

The crossed-dipole antenna is schematically shown in Fig. 26, in the coordinate system of Fig. 1. The total field radiated by the array is the resultant of the field radiated by each dipole of length  $2\ell = \lambda_d / 2$  at the design frequency.

FIGURE 26  
Crossed-dipole antenna



Considering dipole No. 1 aligned along the x-axis at height  $h$ , the electrical field components have the following expression:

$$E_{1\theta}(\theta, \varphi) = -j 60 I \frac{e^{-jkr}}{r} \cos \varphi \sin \theta C_d S_\theta$$

$$E_{1\varphi}(\theta, \varphi) = j 60 I \frac{e^{-jkr}}{r} \sin \varphi C_d S_\varphi$$

where  $C_d$  is the current distribution function of the radiating element. Assuming a *sinusoidal* current distribution function:

$$C_d = \frac{\cos(F_R \cdot \pi/2 \cdot \cos \varphi \cos \theta) - \cos(F_R \cdot \pi/2)}{1 - \cos^2 \varphi \cos^2 \theta}$$

The array factors will have the following expressions:

$$S_\theta = e^{j\pi F_R \cdot 2h/\lambda_d \cdot \sin \theta} \cdot \left[ 1 - R_v e^{-j4\pi F_R \cdot h/\lambda_d \cdot \sin \theta} \right]$$

$$S_\varphi = e^{j\pi F_R \cdot 2h/\lambda_d \cdot \sin \theta} \cdot \left[ 1 + R_h e^{-j4\pi F_R \cdot h/\lambda_d \cdot \sin \theta} \right]$$

Considering dipole No. 2 aligned along the y-axis at height  $h$ , the electrical field components will have the following expressions:

$$E_{2\theta}(\theta, \varphi) = -j 60 I \frac{e^{-jkr}}{r} \sin \varphi \sin \theta C_d S_\theta$$

$$E_{2\varphi}(\theta, \varphi) = -j 60 I \frac{e^{-jkr}}{r} \cos \varphi C_d S_\varphi$$

and the current distribution function will have the following expression:

$$C_d = \frac{\cos(F_R \cdot \pi/2 \cdot \sin \varphi \cos \theta) - \cos(F_R \cdot \pi/2)}{1 - \sin^2 \varphi \cos^2 \theta}$$

The array factors have the same expression as for dipole No.1.

The total field radiated by the array is therefore :

$$|E(\theta, \varphi)| = \left[ |E_{1\theta}(\theta, \varphi) + E_{2\theta}(\theta, \varphi)|^2 + |E_{1\varphi}(\theta, \varphi) + E_{2\varphi}(\theta, \varphi)|^2 \right]^{1/2}$$

5. Log-periodic antennas

5.1 General considerations

Log-periodic dipole arrays are tapered linear arrays of dipole elements of varying length which operate over a wide frequency range. Wide band operation is achieved by assuming that different groups of elements radiate at different frequencies. The spacing between the elements is proportional to their length and the system is fed using a transmission line. As the frequency ratio varies, the elements which are at or near resonance, couple energy from the transmission line. The resulting radiation pattern is directional and has a broadly constant radiation characteristic over the full operating frequency range.

5.2 Designation of log-periodic antennas

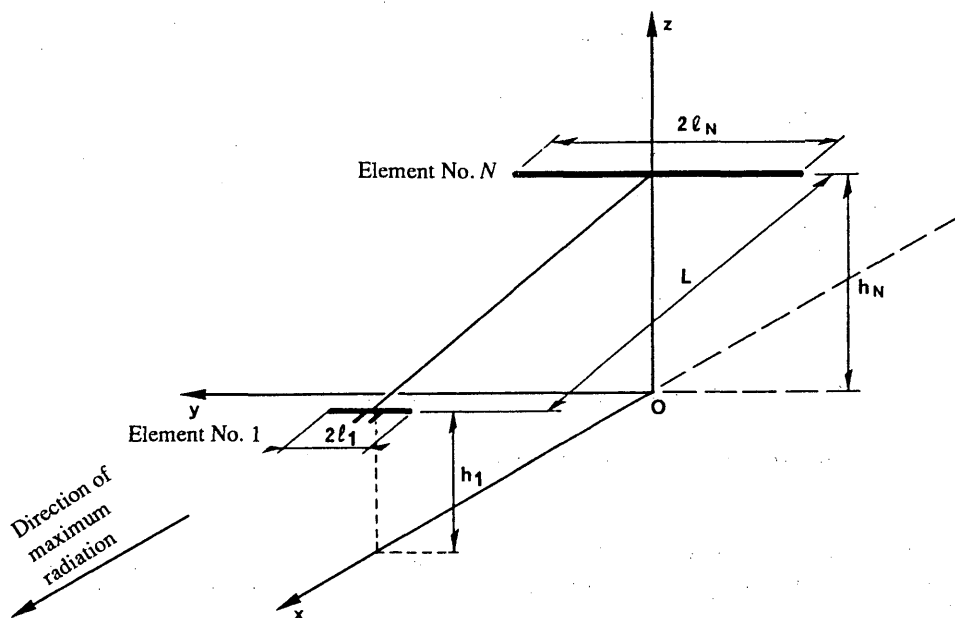
5.2.1 Horizontal log-periodic antennas

Type designation: LPH  $N / L / h_1 / h_N / l_1 / l_N / Z$

where:

- LPH : horizontal log-periodic antenna;
- $N$  : number of elements;
- $L$  : distance between the centres of the shortest and the longest element (m);
- $h_1$  : height of the shortest element (m);
- $h_N$  : height of the longest element (m);
- $l_1$  : half-length of the shortest element (m);
- $l_N$  : half-length of the longest element (m);
- $Z$  : impedance of the antenna internal feeder line ( $\Omega$ ).

FIGURE 27  
Designation of horizontal log-periodic array



### 5.2.2 Vertical log-periodic antennas

Type designation: LPV  $N / L / h_1 / h_N / l_1 / l_N / Z$

where:

LPV : vertical log-periodic antenna;

$N$  : number of elements;

$L$  : distance between the centres of the shortest and the longest element (m);

$h_1$  : height of the shortest element (m);

$h_N$  : height of the longest element (m);

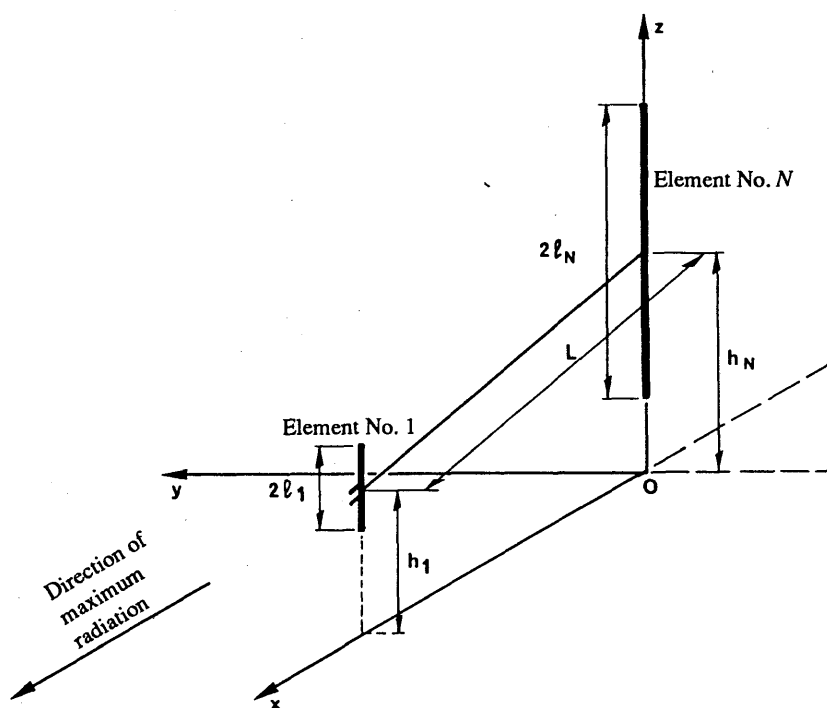
$l_1$  : half-length of the shortest element (m);

$l_N$  : half-length of the longest element (m);

$Z$  : impedance of the antenna internal feeder line ( $\Omega$ ).

FIGURE 28

Designation of vertical log-periodic array



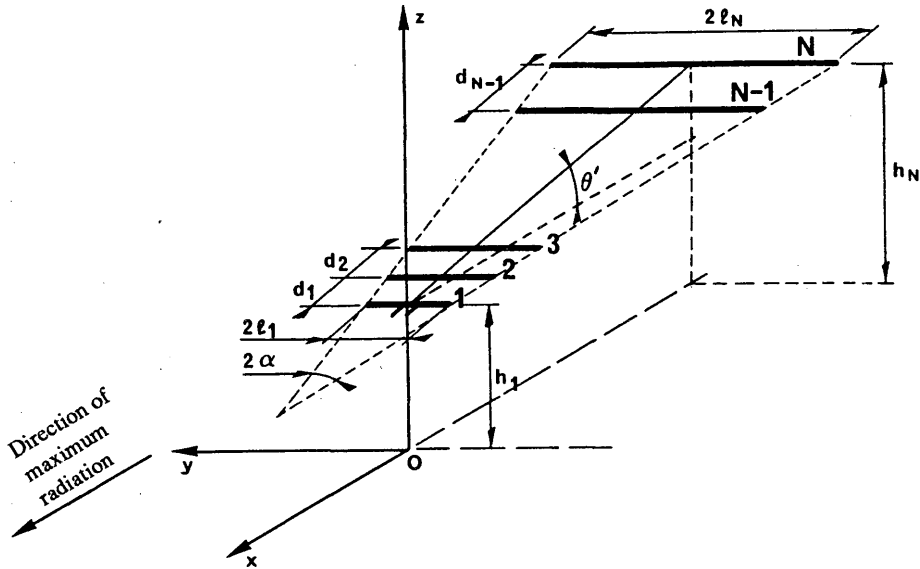
### 5.3 Calculation of the patterns for horizontal log-periodic antennas

Figure 29 shows an array made up of horizontal dipole elements whose length  $l$  and spacing  $d$  are related to the design ratio  $\tau$ .

Each of the geometrical parameters of a log-periodic array is shown in Fig. 29. The elements are spaced within a triangle according to the design ratio  $\tau$  which is given by the ratio of lengths of the elements:

$$\tau = l_i / l_{i+1} \quad (2)$$

FIGURE 29  
Horizontal log-periodic array



Theoretically this should also be the ratio of dipole radii, although this is not usually found in practice. The spacing factor is:

$$\sigma = d_i / 4 l_{i+1} = 0.25 (l - \tau) / \tan \alpha \quad (3)$$

where:

- $d_i$ : distance from the apex of the  $i$ -element, and
- $\alpha$ : half-apex angle.

The number of elements is determined mainly by the design ratio  $\tau$ . As  $\tau$  increases, the number of elements also increases. Antenna size is determined primarily by the spacing factor  $\sigma$ . As the boom length becomes greater  $\sigma$  increases.

The array is fed with alternate polarity, i.e. adjacent dipoles are connected in a "phase reversal" arrangement through a transmission line of impedance  $Z_0$ . The height of the first (lowest and shortest) dipole is  $h_1$ . The height  $h_i$  of the  $i$ -th dipole is:

$$h_i = h_1 + x_i \tan \theta' \quad (4)$$

where  $\theta'$  is the angle of elevation of the array axis (coinciding with its boom).

The angle  $\psi$  between the antenna dipoles and the direction of the observation point  $P(r, \theta, \phi)$  is given by:

$$\cos \psi = \cos \theta \cos \phi \quad (5)$$

The angle  $\psi_a$  between the antenna axis and the direction of the observation point is:

$$\cos \psi_a = - \cos \theta \cos \theta' \cos \phi + \sin \theta \sin \theta' \quad (6)$$

The distance from the centre of the  $i$ -th dipole to the observation point in far field conditions is given by:

$$r_i = r_1 + \cos \psi_a / \cos \theta' \quad (7)$$

The above relations are used in the calculation of the pattern.

5.3.1 Basic theory

In a log-periodic array of horizontal or vertical dipoles, the RF energy at a given frequency travels along the feeder until it reaches a region (active region) where the electrical lengths and phase relations are such as to produce radiation towards the short end through elements which are shorter than  $\lambda/2$ . Due to the cross-fed connection, fields produced ahead of this region (those in the transmission region) will cancel. The remaining region at the long end (the reflection region) has little effect since very little power travels beyond the active region.

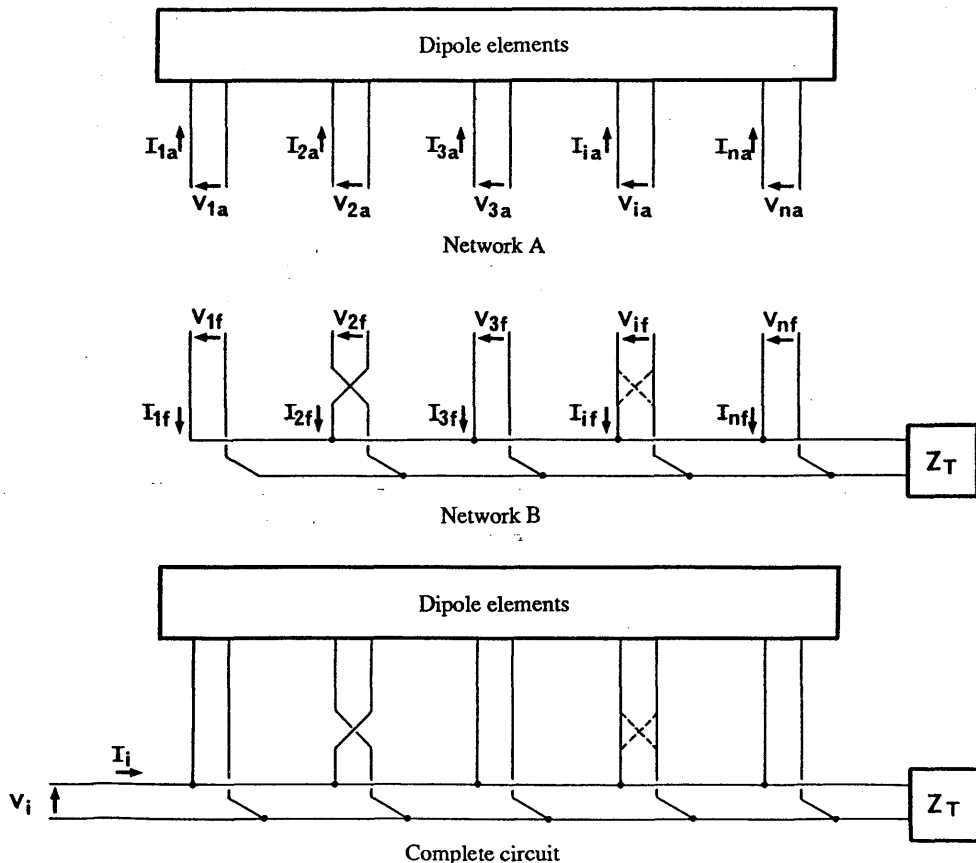
Assuming a lossless structure, the behaviour of the three regions can be described in terms of transmission line theory. The transmission region (short end) behaves like a feeder transmission line loaded by a capacitive reactance, the active region like a capacitance in parallel with a resistance and the reflection region like a shunt inductance. The overall effect is that of a filter network.

When the antenna is placed above a ground plane, the array axis is sloped so that the dipoles are at a constant electrical height above the ground. In the azimuthal plane the main beam pattern within the frequency range of the antenna, is similar to that of a  $\lambda/2$  dipole at a  $\lambda/4$  height above the ground. The analysis of the log-periodic antenna structure is usually carried out by separating the problem in two parts:

- the interior (circuit) problem which deals with the interaction of currents, voltages, etc., within the antenna system itself; and
- the exterior (radiation) problem which deals with the interaction of the antenna with the propagation medium.

The interior problem can be expressed as a matrix problem. The basis of the method of calculation has been described by [Carrel, 1961], where the array is represented by networks A and B as shown in Fig. 30.

FIGURE 30  
Schematic of the array network



Network A consists of the parallel radiating elements whose feed voltages and currents can be expressed in terms of self and mutual impedances so that:

$$[V_a] = [Z_a] \cdot [I_a] \quad \text{or} \quad [I_a] = [Z_a]^{-1} \cdot [V_a] \quad (8)$$

where:

- $I_a$ : 1 by  $N$  matrix of the feed base currents;
- $V_a$ : 1 by  $N$  matrix of the respective base voltages;
- $N_a$ : number of dipoles; and
- $Z_a$ :  $N$  by  $N$  open-circuit matrix of impedances.

The matrix elements on the main diagonal of  $[Z_a]$  represent the self-impedance of the dipoles and the off-diagonal elements represent the mutual impedances between dipoles indicated by the indices.

In a similar way the current-voltage relations for the feeder circuit shown in Fig. 30, can be expressed by:

$$[I_f] = [Y_f] \cdot [V_f] = [Y_f] \cdot [V_a] \quad (9)$$

where  $I_f$  and  $V_f$  are, respectively, the 1 by  $N$  matrix of the feed currents and of response voltages for each section of the transmission line constituting a complete feeder circuit, and  $[Y_f]$  is the associated  $N$  by  $N$  short-circuit admittance of the feeder. The elements of  $[Y_f]$  depend on the lengths of the transmission line in each section and the characteristic admittance  $Y_0$ , whose value is known once a choice or a design of the transmission line is made.

The analytical solution of the problem is obtained by calculating first the total input current matrix  $[I]$  by adding (8) and (9):

$$\begin{aligned} [I] &= [I_a] + [I_f] = [I_a] + [Y_f] \cdot [V_a] \\ &= [I_a] + [Y_f] \cdot [Z_a] \cdot [I_a] \\ &= ([U] + [Y_f] \cdot [Z_a]) \cdot [I_a] \end{aligned} \quad (10)$$

where  $[U]$  is the  $N$  by  $N$  unity matrix.

The elements of  $[I]$  represent the input currents at each node point (dipole bases) where the antenna and feeder circuits are combined. In practical cases all the matrix elements in  $[I]$  are zero except  $I_1$ , which is the only current source (at the base of the shortest dipole) for the entire array. Without loss of generality it can be assumed  $I_1=1$ , so that the dipole base currents  $[I_a]$  can be determined from (10) by matrix inversion:

$$[I_a] = ([U] + [Y_f] \cdot [Z_a])^{-1} \cdot [I] = ([U] + [Y_f] \cdot [Z_a])^{-1} \cdot [1 \ 0 \ \dots \ 0]^t \quad (11)$$

Referring to Fig. 30, the (sinusoidal) current distribution on the generic dipole can be expressed by [Ma, 1974]:

$$\begin{aligned} I_i(x) &= I_{mi} [\sin k(l_i - |x|)] \quad \text{for } k l_i < \pi/2 \\ I_i(x) &= I_{mi} [\sin k(|x|) - 1] \quad \text{for } k l_i = \pi/2 \end{aligned} \quad (12)$$

where it should be noted that  $I_i(0) = I_{ai}$ , with  $I_{ai}$  as calculated by (11).

The radiation pattern of the horizontal log-periodic array on a flat homogeneous and imperfect ground, can be expressed by the following normalized radiation pattern function:

$$F(\theta, \varphi) = K \cdot f(\theta, \varphi) \cdot S_\theta \cdot S_\varphi$$

where:

$K$ : normalizing factor to set  $|F(\theta, \varphi)|_{\max} = 1$ , i.e. 0 dB;

$f(\theta, \varphi)$ : horizontal element pattern function;

$S_\theta$ : array factor for the  $\theta$  direction; and

$S_\varphi$ : array factor for the  $\varphi$  direction.

The radiation pattern function is also expressed as (see § 4.7.1):

$$F(\theta, \varphi) = K \cdot |E(\theta, \varphi)| = K \cdot \left[ |E_\theta(\theta, \varphi)|^2 + |E_\varphi(\theta, \varphi)|^2 \right]^{1/2}$$

with

$$E_\theta(\theta, \varphi) = j 60 \frac{e^{-jk r}}{r} \sin \theta \sin \varphi S_\theta$$

and

$$E_\varphi(\theta, \varphi) = -j 60 \frac{e^{-jk r}}{r} \cos \varphi S_\varphi$$

or, neglecting the distance dependent term (not required for the determination of the radiation pattern):

$$E_\theta(\theta, \varphi) = |S_\theta| \sin \theta \sin \varphi$$

$$E_\varphi(\theta, \varphi) = -|S_\varphi| \cos \varphi$$

taking into account (4), (5), (6) and (7) the array factors can be written as:

$$\begin{aligned} S_\theta &= \sum_{i=1}^{Na} I_{mi} e^{jk x_i \cos \psi_a / \cos \theta} \cdot \left( 1 - R_v e^{-2jk h_i \sin \theta} \right) \cdot F_i \\ S_\varphi &= \sum_{i=1}^{Na} I_{mi} e^{jk x_i \cos \psi_a / \cos \theta} \cdot \left( 1 + R_h e^{-2jk h_i \sin \theta} \right) \cdot F_i \end{aligned} \quad (13)$$

where  $F_i$  is the  $i$ -th dipole radiation function expressed as:

$$F_i = \frac{\cos(k l_i \cos \theta \cos \theta') - \cos(k l_i)}{1 - \cos^2 \theta \cos^2 \theta'}$$

### 5.3.2 Calculation procedure

The calculation of radiation pattern according to the above formulae is more complicated than in the case of an array of horizontal dipoles. Actually the input current to each dipole is not a fixed value and should be determined frequency by frequency through a matrix inversion. This complication may lead to a rather cumbersome computer program coding and hence to some difficulties in integrating the real-time calculation routines in a more general planning system.

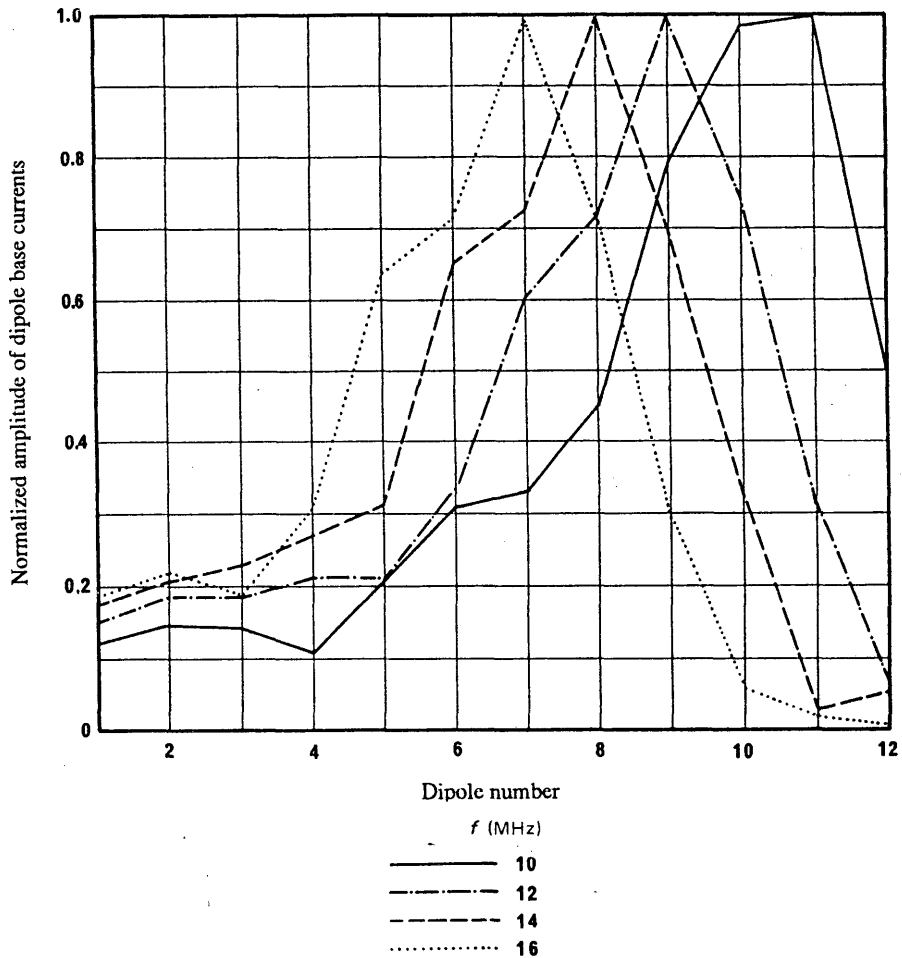
Furthermore it should be noted that even in the case of an exact calculation based on the above algorithms, some deviations of the resulting pattern from reality are unavoidable. These deviations may be more important than in the horizontal dipole case since the ratio of lengths  $\tau$  (see (2)) is theoretically also the ratio of dipole radii, so that the transversal dimension of the radiating element is also playing a role in the overall performance.

Since a more or less pronounced deviation is to be accepted, and also considering the planning context where the results are to be applied, an approximate but simpler and faster solution of the interior problem, as suggested by [Lloyd, 1983], will be described in the following section.

5.3.2.1 *Approximate solution of the interior problem*

The distribution of the amplitude and phase of the dipole base currents of a typical well-designed log-periodic array has been both measured and calculated. Examples of distributions of amplitude and phase calculated by [Ma, 1974] as a function of the dipole position for a particular antenna are shown in Figs. 31 and 32.

FIGURE 31  
 Normalized amplitude of dipole base currents of the  
 log-periodic dipole array in free space vs. dipole position and frequency

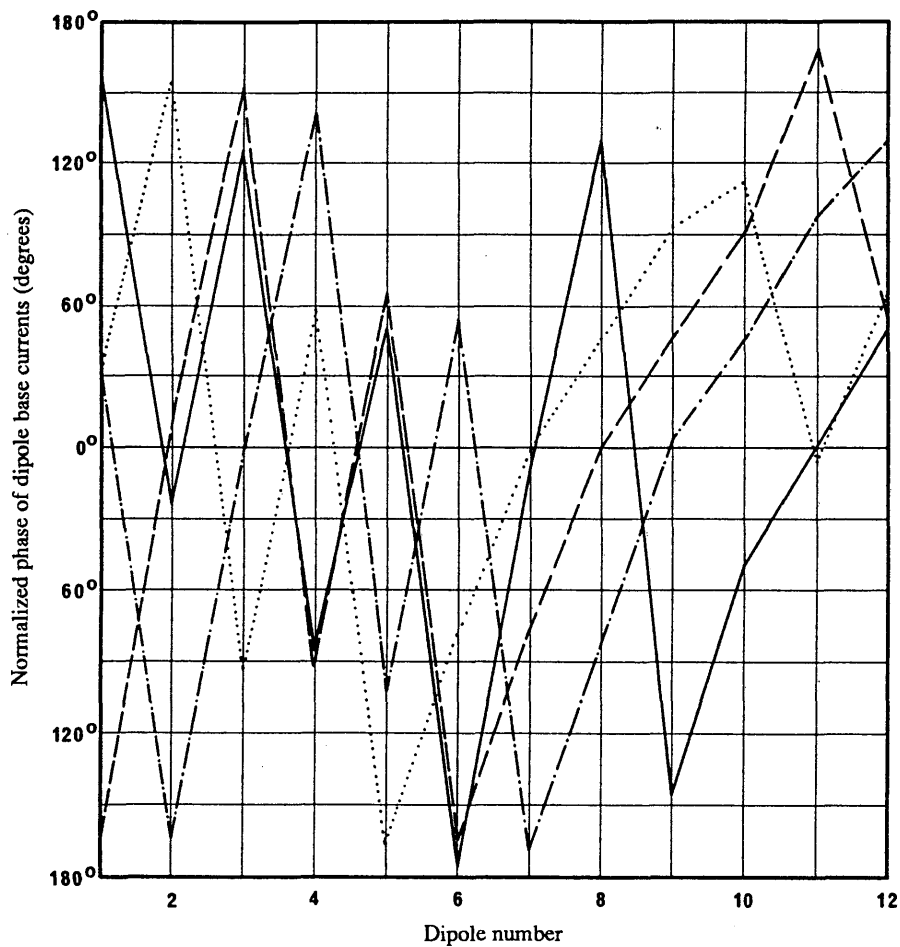


Figures 33 and 34 show the same distributions as a function of the element half-length at the various operating frequencies for the same case at frequency ranges of 10-32 MHz.

Although these curves have been calculated in free-space conditions, it is possible to derive a general current distribution curve that applies to any well-designed log-periodic array as shown in Fig. 35. This can be obtained by fitting suitable curves to Figs. 33 and 34.

FIGURE 32

Normalized phase of the dipole base currents of the same  
log-periodic dipole array in free space vs. dipole position and frequency



The phase has been normalized with that of the element having the largest current amplitude

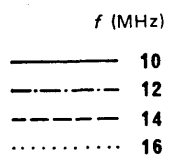
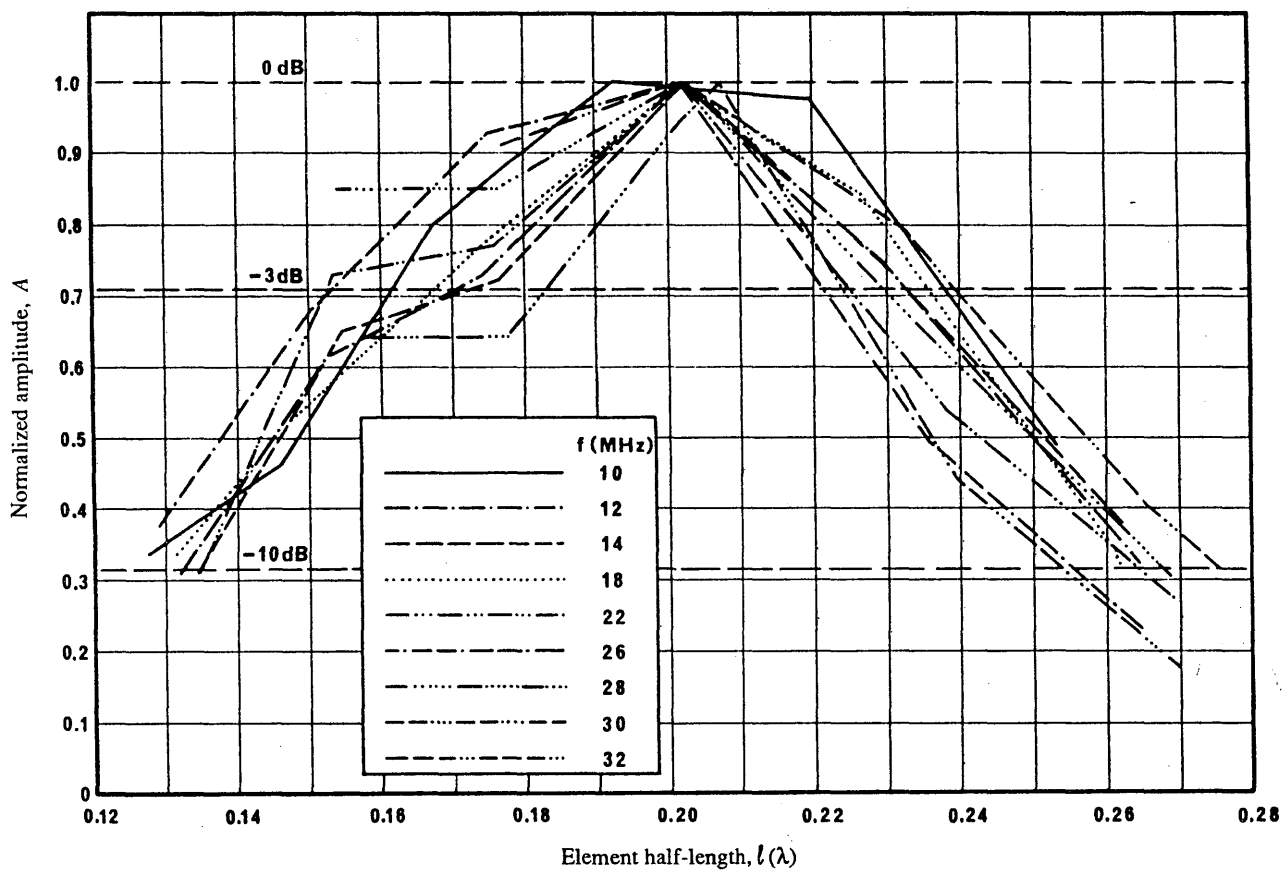


FIGURE 33  
 Normalized amplitude of dipole base currents  
 of the log-periodic dipole array in free space as a function  
 of the element half-length and frequency



The amplitude has been normalized with that of the element having the largest current amplitude.

FIGURE 34  
Normalized phase of dipole base currents  
of the log-periodic dipole array as a function of the element  
half-length and frequency

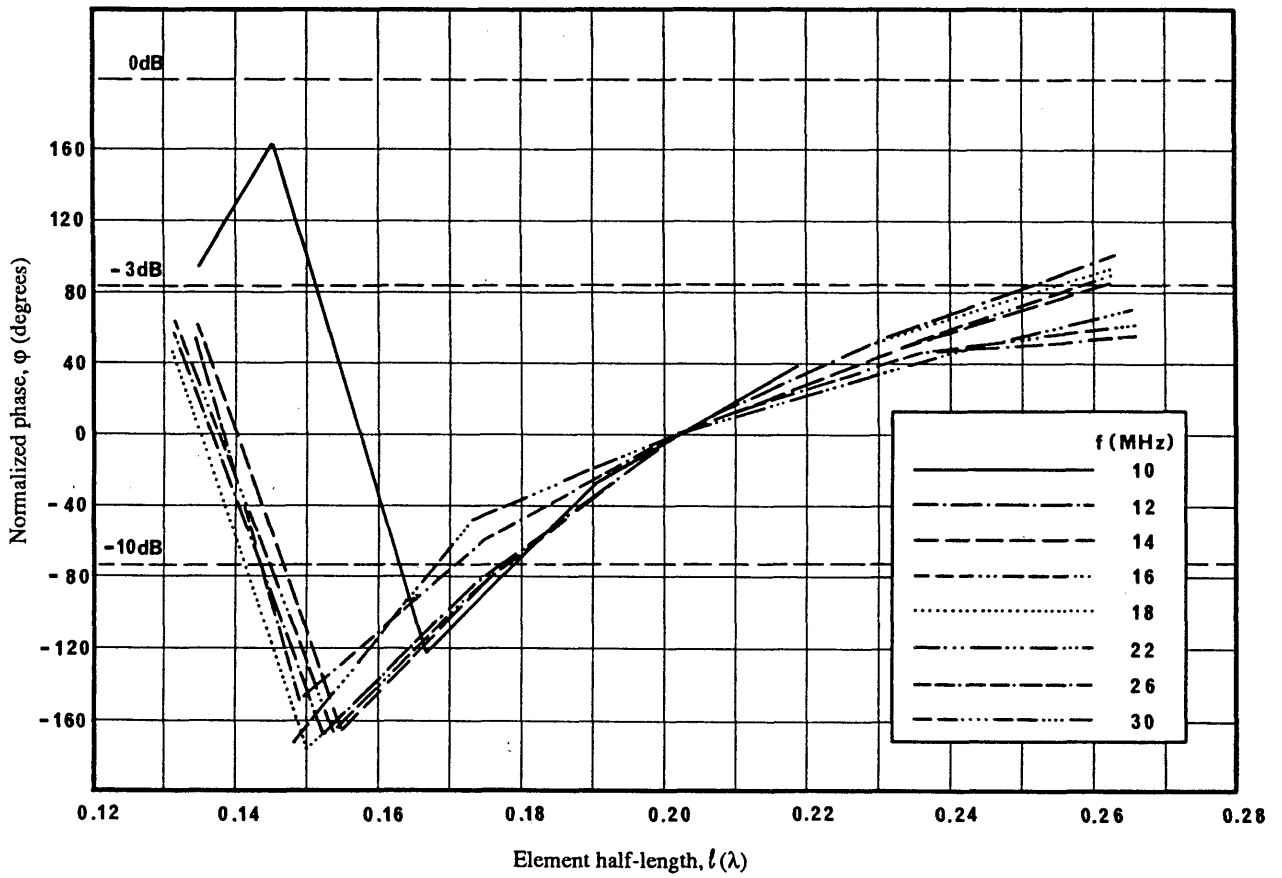
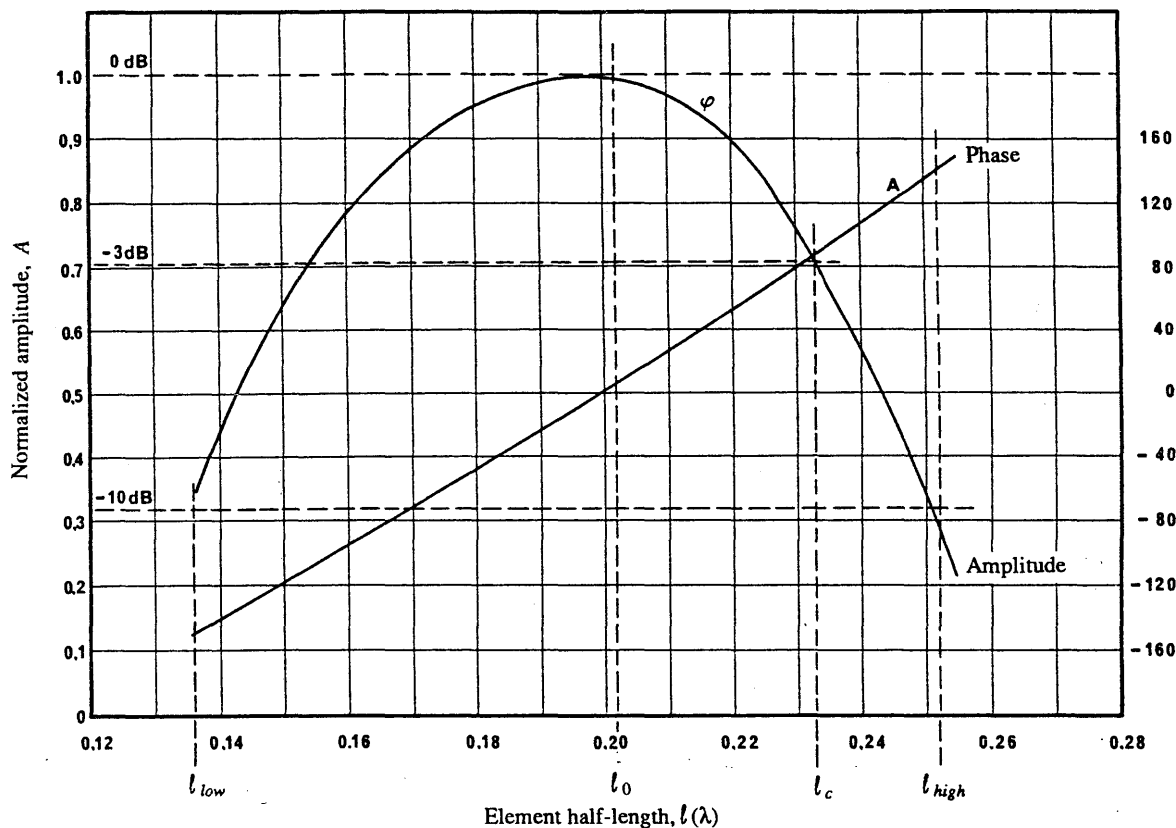


FIGURE 35  
 Extrapolated general curve of normalized  
 amplitude and phase of base currents as a function of element length



The usable bandwidth  $B_{ar}$  of the antenna depends on the relative bandwidth the antenna can cover before unacceptable effects are caused by the smallest or largest element. The high frequency limit is reached when the current of the smallest element is 10 dB below the maximum. This happens at a dipole length  $l_{low}$  (lengths are used here since the distance from apex varies with apex angle  $\alpha$ ). The low frequency limit is reached when the current in the longest element is 3 dB less than the maximum. This length is  $l_c$ . The maximum occurs at a length  $l_0$  and the upper 10 dB at a length  $l_{high}$ . The following empirical equations are used:

$$l_c = 0.5 S_h (Z_0, l/a)$$

where  $Z_0$  is the transmission line impedance,  $l/a$  is the element length to diameter ratio and  $S_h$  is a shortening factor [Carrel, 1961]. Figure 36 shows  $S_h$  as a function of  $Z_0$  for various values of  $l/a$  measured and calculated [Ma, 1974].

$$l_{low} = l_c / B_{ar}$$

$$B_{ar} = 1.1 + 30.7 \sigma (1 - \tau) \tag{14}$$

$B_{ar}$  is the usable active region bandwidth of the antenna as empirically proposed by [Carrel, 1961]. Figure 37 shows the measured values of  $B_{ar}$  in comparison with those given by equation (14).

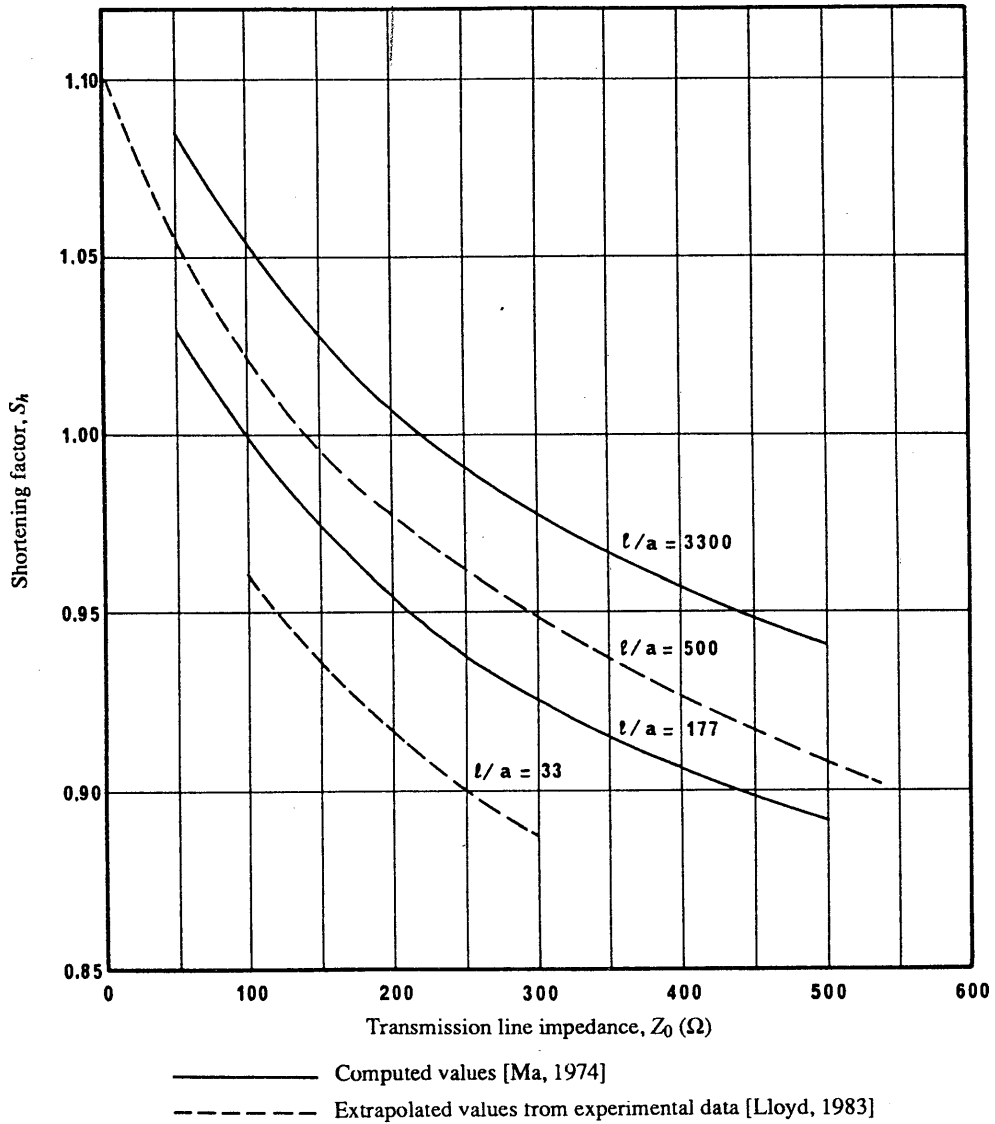
$$l_{high} = 1.1 l_c \tag{15}$$

and

$$l_0 = l_{low} + 0.7166 (l_c - l_{low}) \tag{16}$$

Equations (15) and (16) are designed to reproduce the curves of both [Carrel, 1961] and [Ma, 1974]. The coefficient 0.7166 is for  $l/a = 500$ . This value is used as the default value in calculations.

FIGURE 36  
Shortening factor  $S_h$  as a function of  $Z_0$  and  $l/a$



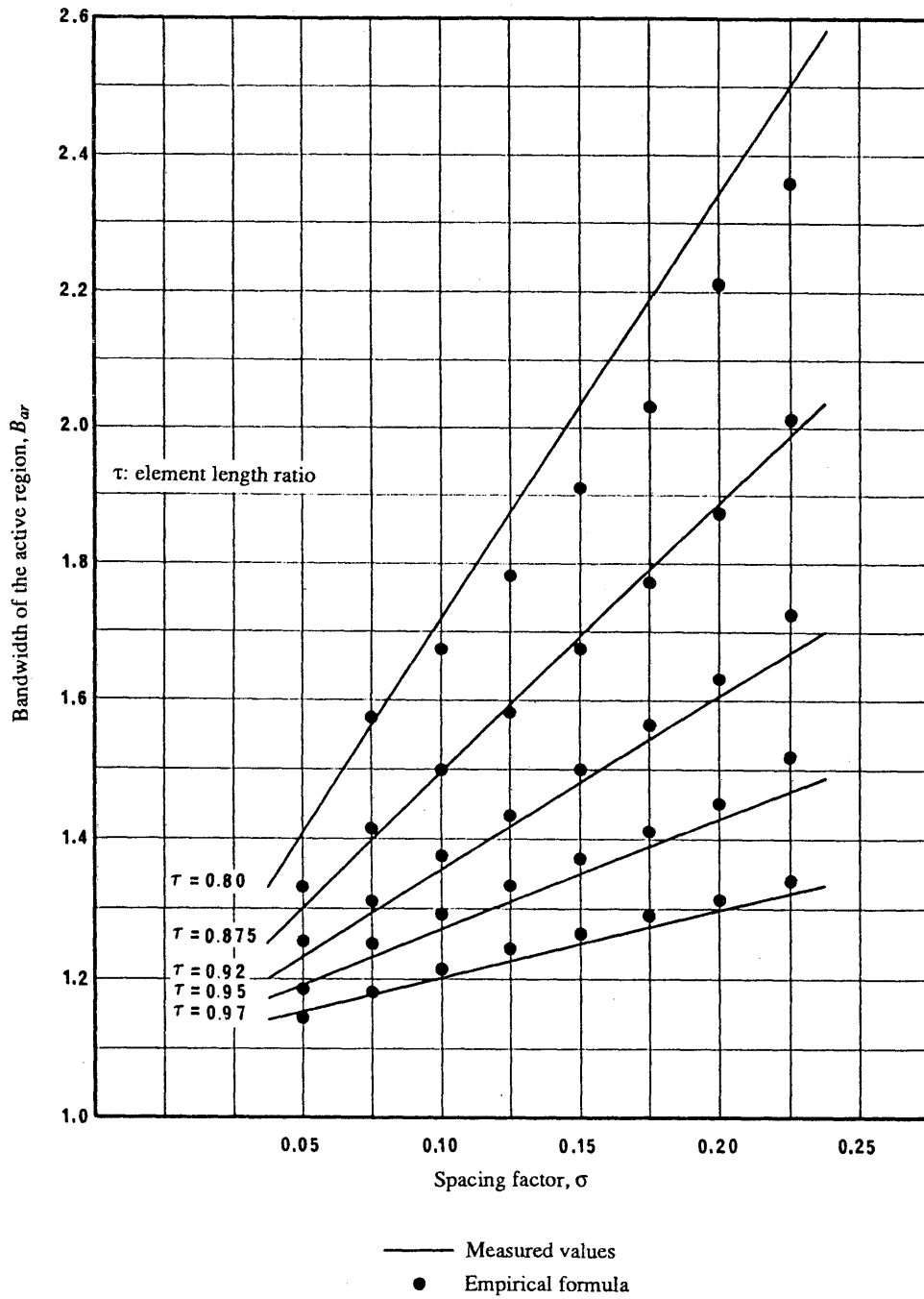
The procedure takes into consideration only those dipoles that fall in the active region between  $l_{low}$  and  $l_{high}$ . For each antenna case a curve similar to that of Fig. 35 is calculated and a current  $I_{bi}$  and phase evaluated for each dipole within the active region. All the dipole currents are then renormalized so that the maximum current is 1, since the dipole length will not usually correspond to  $l_0$ .

It should be recalled that the dipole currents of above represent the normalized base currents of the active dipoles. The currents  $I_{mi}$  appearing in the expression (13) of the array factors are the maximum (loop) currents in each dipole. Therefore it will be necessary to calculate them by applying (12) for  $x = 0$ , i.e.:

$$I_{mi} = I_{bi} / \sin(k l_i)$$

FIGURE 37

Bandwidth of the active region  $B_{ar}$  as a function of  $\sigma$  and  $\tau$



5.4 Calculation of the patterns for vertical log-periodic antennas

The vertical log-periodic array can be realized in two ways as indicated in Figs. 38 and 39. If constructed at a constant element centre height above the ground as in Fig. 38, the array will have broad-band characteristics, but the height factor resulting from ground reflection will be frequency dependent. In order to alleviate this problem, the array may be constructed with the element centres at variable height as shown in Fig. 39.

FIGURE 38

Vertical log-periodic antenna (element centres at fixed height)

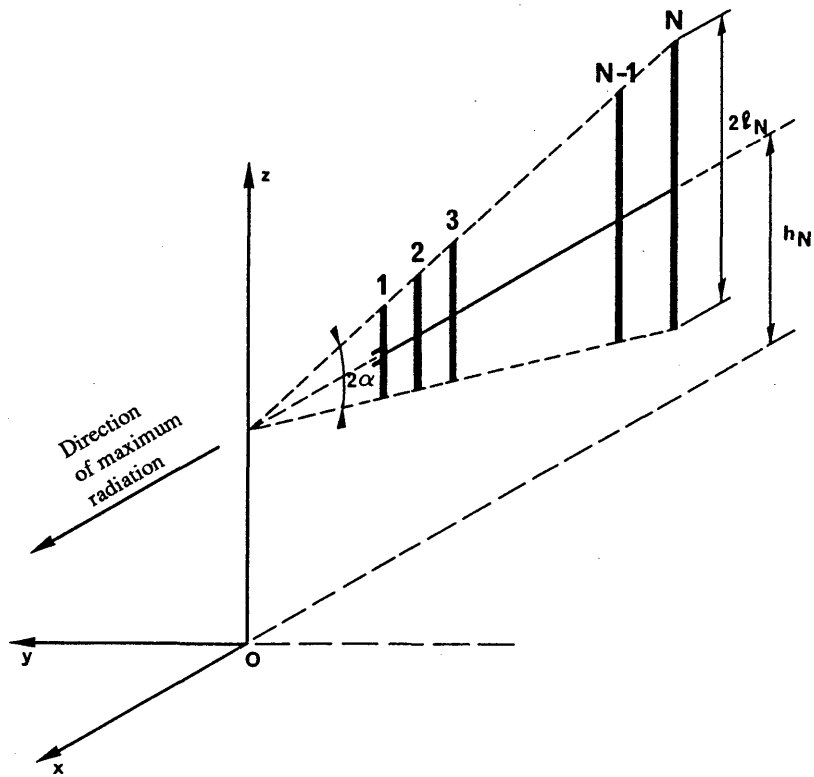
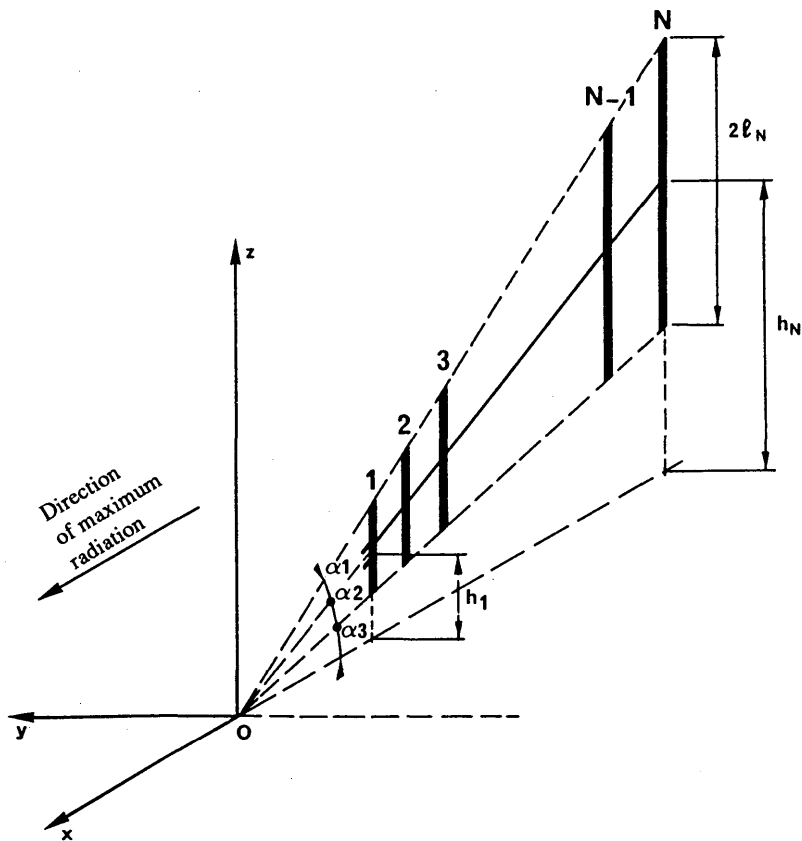


FIGURE 39

Vertical log-periodic antenna (element centres at variable height)



In the following section the case of a vertical log-periodic antenna with element centres at variable height will be considered as being the more general one.

Referring to Fig. 39 the array geometry is determined by the three angles  $\alpha_1, \alpha_2, \alpha_3$ . The spacing factor  $\sigma'$  (see (3)), may be written as:

$$\sigma' = d_i / 4 l_{i+1} = (1 - \tau) / 4 [\sin(\alpha_2 + \alpha_3) - \tan \alpha_3 \cos(\alpha_2 + \alpha_3)]$$

The height of each element is then expressed as:

$$h_i = l_i [1 + \sin \alpha_3 \cos(\alpha_2 + \alpha_3) / \sin \alpha_2]$$

The angle  $\psi_b$  between the antenna axis and the observation point is:

$$\cos \psi_b = \sin \theta \sin(\alpha_2 + \alpha_3) - \cos \theta \cos(\alpha_2 + \alpha_3) \cos \varphi$$

It is clear that when  $\alpha_1 = \alpha_2 = \alpha$  and  $\alpha_3 = -\alpha$  the case will be reduced to that of a vertical log-periodic array with the element centres at fixed height.

#### 5.4.1 Basic theory

The basic theory is essentially the same as described in § 5.3.1, with the following exceptions.

The electrical field components are expressed as:

$$E_\theta(\theta, \varphi) = 0$$

and

$$E_\varphi(\theta, \varphi) = j 60 \frac{e^{-jk r}}{r} S_v$$

or, neglecting the distance dependent term (not required for the determination of the radiation pattern):

$$E_\theta(\theta, \varphi) = 0$$

$$E_\varphi(\theta, \varphi) = S_v$$

the array factor  $S_v$  can be expressed by [Ma, 1974]:

$$S_v = \sum_{i=1}^N I_{mi} e^{jk x_i \cos \psi_b / \cos(\alpha_2 + \alpha_3)} \cdot e^{jk h_i \sin \theta} \cdot \left(1 + R_v e^{-2jk h_i \sin \theta}\right) \cdot F_i \quad (17)$$

where  $F_i$  is the  $i$ -th dipole radiation function:

$$F_i = \frac{\cos(k l_i \sin \theta) - \cos k l_i}{\cos \theta} \quad (18)$$

#### 5.4.2 Calculation procedure

The calculation procedure follows exactly as in the case of the horizontal log-periodic antenna described in § 5.3.2. The only difference is, of course, the different expressions for  $S_v$  and  $F_i$ , that need to be evaluated according to (17) and (18).

## 6. Rhombic antennas

### 6.1 General considerations

The rhombic antenna has been extensively used for HF communications. It continues to be used for fixed-services point-to-point links. It has also been used for HF broadcasting but is no longer recommended for this purpose (see Part 2, § 6.3). The antenna consists of four straight wires of the same length  $l$  arranged in the form of a rhombus (see Fig. 40).

A typical rhombic antenna design would use side lengths of several wavelengths and be at a height of between  $0.5-1.0 \lambda$  at the middle of the operating frequency range.

The rhombic antenna differs from the array of dipoles since it belongs to the travelling-wave antenna category, i.e. the currents in the conductors of the antenna are substantially travelling waves originated from the feeding point and propagating through the wires towards the terminating resistance.

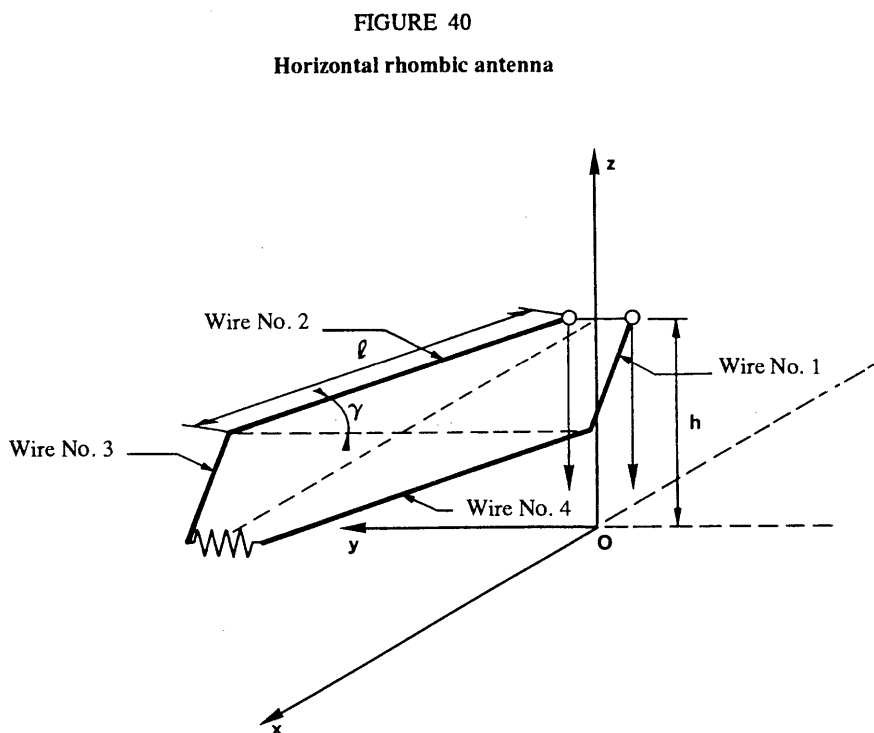
A considerable amount of power may be lost in the terminating resistance and represents the price that has to be paid for some desirable features such as simplicity of construction, relatively wide bandwidth of operation and high directivity gain.

### 6.2 Designation of rhombic antennas

Type designation: RH  $l / \gamma / h$

where (see Fig. 40):

- RH : horizontal rhombic antenna;
- $l$  : length of one side of the rhombus (m);
- $\gamma$  : one half of the interior obtuse angle of rhombus;
- $h$  : height of rhombus above ground (m).



6.3 Calculation of the patterns for rhombic antenna

Although the more general case is represented by a sloping rhombic antenna, this configuration is not frequently encountered and only the horizontal rhombic case will be considered.

The rhombic antenna radiation pattern will be calculated following the approach proposed by [Ma, 1974]. It consists of taking into account the contribution to the overall field produced by the individual conductors in the presence of an imperfect flat homogeneous ground.

With reference to Fig. 40, the four antenna conductors have been identified respectively by numbers 1 to 4.

Letting:

$$\cos \psi_1 = \cos \theta \sin (\varphi - \gamma)$$

$$\cos \psi_2 = \cos \theta \sin (\varphi + \gamma)$$

where  $\gamma$  is half of the obtuse angle of the rhombus, and letting also:

$$F_1 = \frac{1 - e^{-jkl(1 - \cos \psi_1)}}{1 - \cos \psi_1}$$

$$F_2 = \frac{1 - e^{-jkl(1 - \cos \psi_2)}}{1 - \cos \psi_2}$$

The field components resulting from the contribution of wire No. 1 and wire No. 2 are:

$$E'_\theta = E_{\theta 1} + E_{\theta 2} = 30 I_m \frac{e^{-jkr}}{r} F'_\theta$$

$$E'_\varphi = E_{\varphi 1} + E_{\varphi 2} = 30 I_m \frac{e^{-jkr}}{r} F'_\varphi$$

where:

$$F'_\theta = -\sin \theta \sin (\gamma + \varphi) \cdot F_1 \cdot (1 - R_v e^{-2jkh \sin \theta}) + \sin \theta \sin (\gamma - \varphi) \cdot F_2 \cdot (1 - R_v e^{-2jkh \sin \theta})$$

$$F'_\varphi = -\cos (\gamma + \varphi) \cdot F_1 \cdot (1 + R_h e^{-2jkh \sin \theta}) - \cos (\gamma - \varphi) \cdot F_2 \cdot (1 + R_h e^{-2jkh \sin \theta})$$

In the same way the field components resulting from the contribution of wire No. 3 and wire No. 4 are:

$$E''_\theta = E_{\theta 3} + E_{\theta 4} = 30 I_m \frac{e^{-jkr}}{r} F''_\theta$$

$$E''_\varphi = E_{\varphi 3} + E_{\varphi 4} = 30 I_m \frac{e^{-jkr}}{r} F''_\varphi$$

where:

$$F''_\theta = e^{-jkl(1 - \cos \psi_2)} \sin \theta \sin (\gamma + \varphi) \cdot F_1 \cdot (1 - R_v e^{-2jkh \sin \theta}) -$$

$$e^{-jkl(1 - \cos \psi_1)} \sin \theta \sin (\gamma - \varphi) \cdot F_2 \cdot (1 - R_v e^{-2jkh \sin \theta})$$

$$F''_\varphi = -e^{-jkl(1 - \cos \psi_2)} \cos (\gamma + \varphi) \cdot F_1 \cdot (1 + R_h e^{-2jkh \sin \theta}) -$$

$$e^{-jkl(1 - \cos \psi_1)} \cos (\gamma - \varphi) \cdot F_2 \cdot (1 + R_h e^{-2jkh \sin \theta})$$

The total field components can be expressed in the same way as:

$$E_{\theta} = E_{\theta 1} + E_{\theta 2} + E_{\theta 3} + E_{\theta 4} = 30 I \frac{e^{-jkr}}{r} (F'_{\theta} + F''_{\theta})$$

$$E_{\phi} = E_{\phi 1} + E_{\phi 2} + E_{\phi 3} + E_{\phi 4} = 30 I \frac{e^{-jkr}}{r} (F'_{\phi} + F''_{\phi})$$

The final expression of the total electrical field components is given by:

$$E_{\theta} = -240 j I \frac{e^{-jkr}}{r} e^{-jkl(1-\cos\psi_1)} e^{-jkl(1-\cos\psi_2)} \cdot (1 - R_v e^{-2jkh \sin\theta}) \cdot$$

$$\sin\theta \sin\varphi \sin\gamma \cdot \frac{\sin(kl(1-\cos\psi_1)/2)}{1-\cos\psi_1} \cdot \frac{\sin(kl(1-\cos\psi_2)/2)}{1-\cos\psi_2}$$

$$E_{\phi} = -240 j I \frac{e^{-jkr}}{r} e^{-jkl(1-\cos\psi_1)} e^{-jkl(1-\cos\psi_2)} \cdot (1 + R_h e^{-2jkh \sin\theta}) \cdot$$

$$\sin\gamma (\cos\varphi - \cos\gamma \cos\theta) \cdot \frac{\sin(kl(1-\cos\psi_1)/2)}{1-\cos\psi_1} \cdot \frac{\sin(kl(1-\cos\psi_2)/2)}{1-\cos\psi_2}$$

In the case of free-space radiation conditions ( $R_v = R_h = 0$ ), Table 1 gives values for the optimum interior angle vs.  $l/\lambda$ , as calculated by [Ma, 1974].

TABLE 1  
Optimum values for the half obtuse interior angle  $\gamma$  as a function  
of the rhombus leg length  $l/\lambda$  (wavelength)

$l/\lambda$	$\gamma_{opt}$ (degrees)
2	51.5
3	58.6
4	62.9
5	65.8
6	67.9
7	69.5

It is worth noting that the directivity gain by definition and as calculated, does not take into account the power dissipated in the terminating resistance.

Although the calculation procedure deals with the case of a single horizontal rhombic antenna, sometimes two rhombic antennas are stacked. In this case the overall gain is about 1 or 2 dB greater than a single rhombic; the azimuthal radiation pattern approximates that of a single rhombic and the vertical radiation pattern shows a slightly reduced beamwidth.

## 7. Vertical monopoles

Vertical monopoles are seldom used in HF broadcast transmission due to their low gain and non-directional properties. Their main application is confined to short-range omnidirectional broadcasting where economical and/or site constraints do not allow for the installation of radiating structures with better performance.

### 7.1 General considerations

A vertical monopole is considered to consist of an infinitely thin, electrically short (less than a half-wave) vertical radiating element erected on a reflecting plane.

To obtain efficient radiation from the antenna, if it is erected on poorly reflecting ground, an earth system normally consisting of a number of radial wires should be used. For the purposes of calculating radiation patterns, it is usually assumed that the input power is applied at the base of the antenna.

The vertical monopole provides an omnidirectional pattern on the azimuthal plane, however the associated vertical pattern is always significantly affected by the ground constants as well as by other physical parameters, e.g. the electrical antenna height, etc.

The presence of an earth system does not significantly affect the geometrical shape of the pattern, but it significantly affects the value of the absolute gain.

The vertical monopole will be considered in two basic conditions:

- above flat homogeneous imperfect ground, taking into account only ground reflection;
- above flat homogeneous imperfect ground with an earth system consisting of either a circular disk having infinite conductivity, or a number of radial wires of given length and diameter.

### 7.2 Designation of vertical monopoles

Type designation: VM  $h / a_s / N / d$

where (see Fig. 41):

VM : vertical monopole antenna;

$h$  : height of the monopole (m);

$a_s$  : earth system radius (m);

$N$  : number of radial wires in the earth system;

$d$  : diameter of the radial wires (mm).

### 7.3 Vertical monopole without an earth system

With reference to Fig. 42, a monopole with height  $h$  is considered on a flat homogeneous imperfect ground having conductivity  $\sigma$ , magnetic permeability  $\mu$ , and dielectric constant  $\epsilon$ .

FIGURE 41  
Designation of vertical monopoles

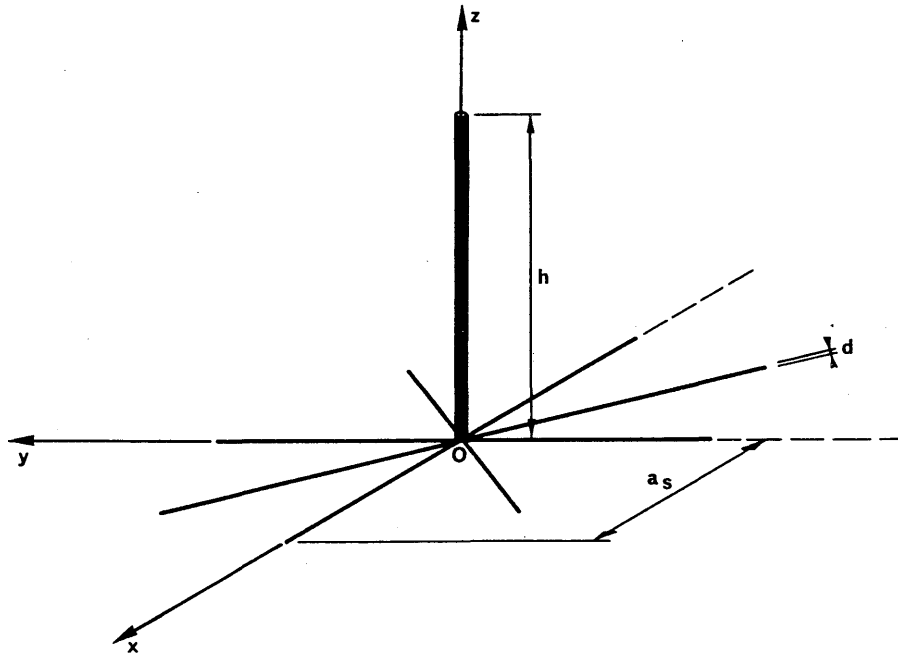
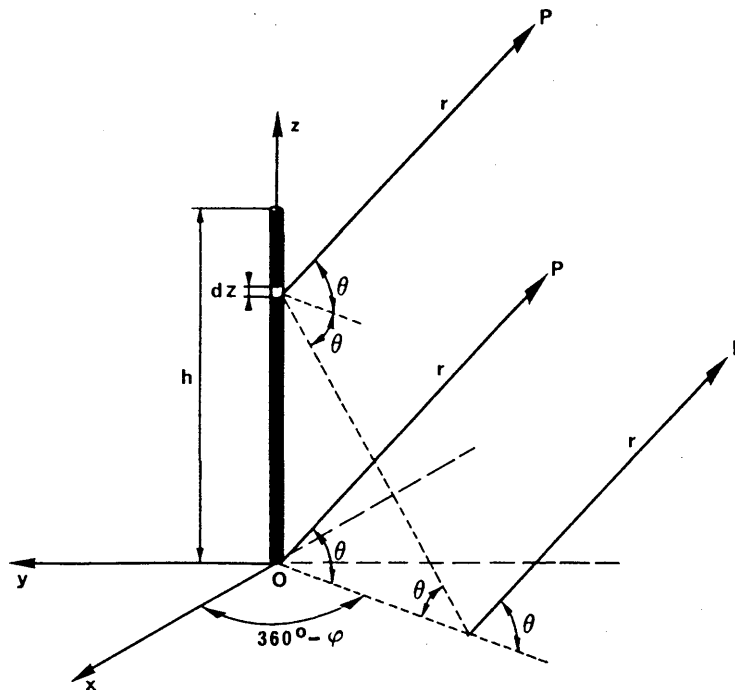


FIGURE 42  
Vertical monopole without earth system on imperfect ground



The general expression for the electrical field components [Ma, 1974] is:

$$E_{\theta}^0 = j \frac{30 k}{r} e^{-j k r} \cos \theta \int_0^h I(z) e^{j k z \sin \theta} \cdot [1 + R_v e^{-j k z \sin \theta}] dz$$

$$E_{\phi} = 0$$

where:

$E_{\theta}^0$ : the electrical field radiated without the earth system.

If the horizontal cross-section of the vertical monopole is very small compared to its height, the current distribution can be assumed as sinusoidal.

With this assumption the integral term in the previous equation can be easily calculated and the resulting equation re-written as:

$$E_{\theta}^0 = j 30 I \frac{e^{-j k r}}{r} \cdot \frac{A_2 + j B_2 + R_v (A_2 - j B_2)}{\cos \theta} = j 30 I \frac{e^{-j k r}}{r} \cdot f_{\theta}^0 \quad (19)$$

where:

$$A_2 = \cos(k h \sin \theta) - \cos k h$$

$$B_2 = \sin(k h \sin \theta) - \sin \theta \sin k h, \text{ and}$$

$R_v$ : reflection coefficient for vertically polarized waves.

The radiation pattern function in the vertical plane is expressed by the second term of the above equation. In the case of a perfectly conducting ground  $R_v = 1$  and the electrical field becomes:

$$E_{\theta}^{\infty} = j 60 I \frac{e^{-j k r}}{r} \cdot \frac{\cos(k h \sin \theta) - \cos k h}{\cos \theta} = j 60 I \frac{e^{-j k r}}{r} \cdot f_{\theta}^{\infty} \quad (20)$$

#### 7.4 Vertical monopole with an earth system

##### 7.4.1 Vertical monopole with an earth system consisting of a solid circular disk having infinite conductivity

The earth system considered in this section is schematically represented in Fig. 43.

The electrical field  $E_{\theta}$  under these circumstances can be expressed [Wait, 1956; Monteath, 1958] as follows:

$$E_{\theta} \simeq E_{\theta}^0 + \Delta E_{\theta} = E_{\theta}^0 \left[ 1 + \frac{\Delta E_{\theta}}{E_{\theta}^0} \right] \quad (21)$$

where:

$E_{\theta}^0$ : the electrical field radiated without the earth system as given by equation (19);

$\Delta E_{\theta}$ : electrical field variation due to the presence of the earth system.

According to the compensation theorem [Monteath, 1958], the electrical field can be written as:

$$E_{\theta} \simeq E_{\theta}^0 \cdot \left[ 1 - k \cdot \eta_g \cdot \frac{e^{-jk r}}{r} \cdot \frac{1}{E_{\theta}^{\infty}} \int_{\rho=0}^{a_s} H_{\phi}^{\infty}(\rho, 0) \cdot J_1(k \rho \cos \theta) \rho \cdot d\rho \right] \quad (22)$$

where:

$k$ :  $2\pi / \lambda$ , phase constant in free-space conditions;

$\lambda$ : wavelength in free-space conditions;

$a_s$ : earth system radius;

$\eta_g$ : ground surface impedance;

$E_{\theta}^{\infty}$ : electrical field radiated in the case of a perfectly conducting ground;

$H_{\phi}^{\infty}(\rho, 0)$ : magnetic field expressed in cylindrical coordinates  $(\rho, \phi, z)$ , radiated in the case of a perfectly conducting ground, invariable with  $\phi$ , and calculated at  $z = 0$ ;

$J_1$ : Bessel function of the first kind.

In the case of a sinusoidal current distribution, the magnetic field  $H_{\phi}^{\infty}(\rho, 0)$  can be expressed as:

$$H_{\phi}^{\infty}(\rho, 0) = \frac{jI}{2\pi\rho} \cdot \left[ e^{-jk[\rho^2+h^2]^{1/2}} - e^{-jk\rho} \cos kh \right] \quad (23)$$

where  $I$  represents the antenna loop current.

Substituting in (22), the previously determined expressions (19) and (20) for the electrical and magnetic fields, the following expression is obtained:

$$E_{\theta} \simeq j30I \frac{e^{-jk r}}{r} \cdot f_{\theta}^0 \left\{ 1 - \frac{\eta_g \cdot k}{\eta_0 \cdot f_{\theta}^{\infty}} \int_{\rho=0}^{a_s} \left[ e^{-jk[\rho^2+h^2]^{1/2}} - e^{-jk\rho} \cos kh \right] \cdot J_1(k\rho \cos \theta) d\rho \right\}$$

where the final expression for the vertical radiation pattern function is given by:

$$f_{\theta} = f_{\theta}^0 \left\{ 1 - \frac{k \cdot \eta_g}{\eta_0} \cdot \frac{1}{f_{\theta}^{\infty}} \int_{\rho=0}^{a_s} \left[ e^{-jk[\rho^2+h^2]^{1/2}} - e^{-jk\rho} \cos kh \right] \cdot J_1(k\rho \cos \theta) d\rho \right\}$$

where  $\eta_0 = 120 \pi$  ( $\Omega$ ), free space intrinsic impedance.

For the determination of the antenna pattern, only the modulus of the above expression needs to be calculated. It should be noted that the integral shown can only be calculated by numerical methods.

#### 7.4.2 Vertical monopole with an earth system consisting of a number of radial wires of given length and diameter

The earth system considered in this section is schematically represented in Fig. 44.

FIGURE 43

Vertical monopole with an earth system consisting of a circular disk with infinite conductivity

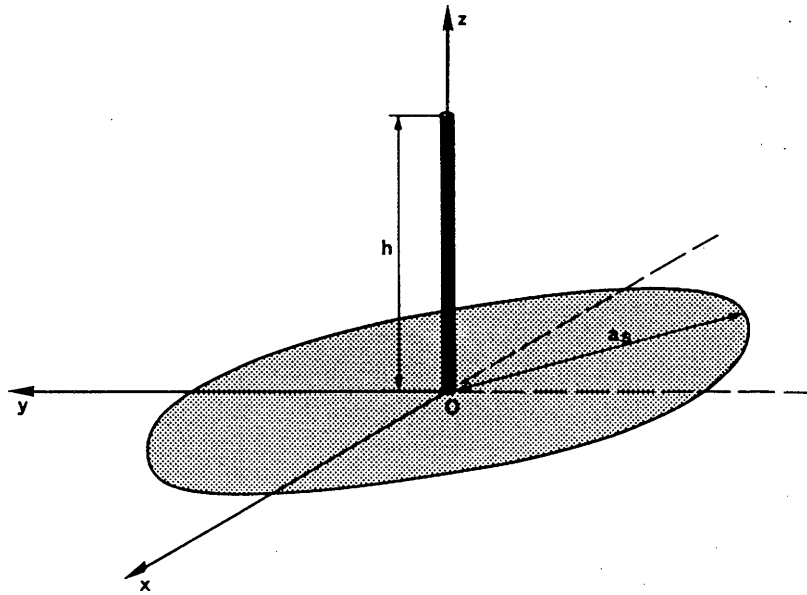
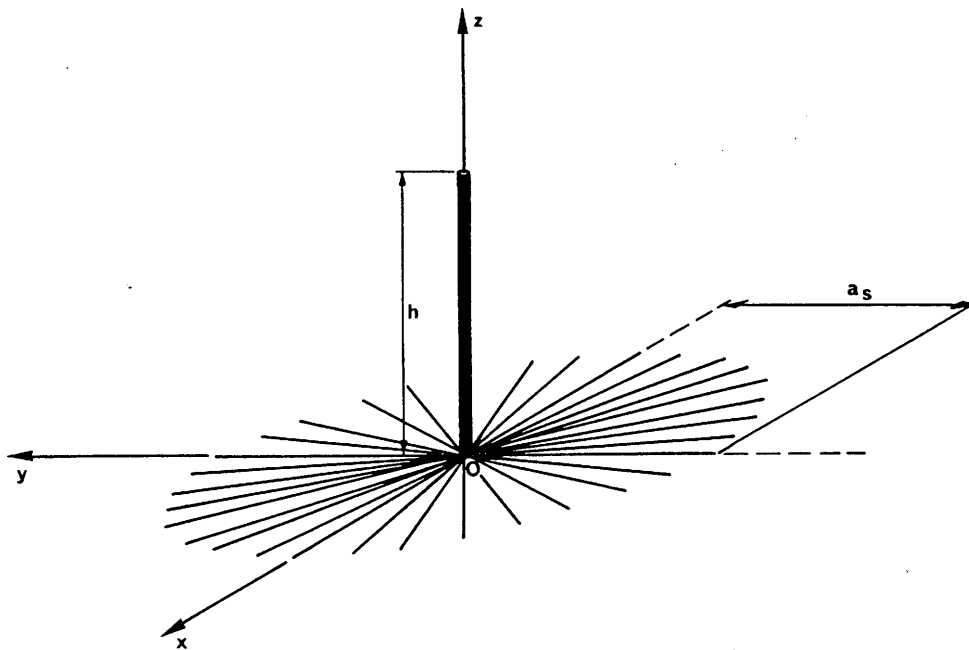


FIGURE 44

Vertical monopole with an earth system consisting of radial wires



The electrical field  $E_\theta$ , can again be expressed (see (21)), as:

$$E_\theta \simeq E_\theta^0 + \Delta E_\theta = E_\theta^0 \left[ 1 + \frac{\Delta E_\theta}{E_\theta^0} \right]$$

where:

$E_\theta^0$ : electrical field radiated without earth system,

$\Delta E_\theta$ : electrical field variation due to the presence of the earth system.

According to the compensation theorem, the above expression can be re-written as:

$$E_\theta = E_\theta^0 \cdot \left[ 1 - \frac{e^{-jk r}}{r} \cdot \frac{k}{E_\theta^\infty} \int_{\rho=0}^{a_s} W'(k, \rho) [\eta_g - \eta_\rho(\rho)] \cdot H_\phi^\infty(\rho, 0) \cdot J_1(k \rho \cos \theta) \rho \, d\rho \right] \quad (24)$$

where:

$W'(k, \rho)$ : attenuation function of the ground wave [Norton, 1941],

$k = 2\pi/\lambda$ : phase constant in free space propagation conditions,

$\lambda$ : wavelength in free space,

$a_s$ : earth system radius,

$\eta_g$ : ground surface impedance,

$\eta_\rho$ : resulting impedance from paralleling of  $\eta_g$  and  $\eta_w$ ,

$E_\theta^\infty$ : electrical field radiated in case of perfectly conducting ground,

$H_\rho^\infty(\rho, 0)$ : magnetic field (in cylindrical coordinates  $(\rho, \phi, z)$ , radiated in case of perfectly conducting ground, invariable with  $\phi$ , and calculated at  $z = 0$ ,

$J_1$ : Bessel function of the first kind.

Assuming a sinusoidal current distribution the expression of  $H_\phi^\infty(\rho, 0)$  is given by equation (23).

The exact evaluation of  $W'(k, \rho)$  is difficult, however at the distances of interest it approximates unit value and zero phase. This approximation is assumed in developing the expressions that follow.

The impedance  $\eta_\rho$  is obtained by paralleling of the earth system surface reactance  $\eta_w$  and the ground surface impedance  $\eta_g$ , whose expressions respectively are:

$$\eta_w = j \eta_0 \frac{2\pi \rho}{N \lambda} \log_e \left( \frac{2\rho}{Nd} \right)$$

where

$\rho$ : radial distance,

$N$ : number of the wires,

$d$ : diameter of wire,

and

$$\eta_g = \frac{\eta_0}{\epsilon_{rc}} (\epsilon_{rc} - 1)^{1/2}$$

where

$\epsilon_{rc}$ : relative complex ground dielectric constant.

Substituting expressions (19) and (20) in (24), the following expression is obtained:

$$E_\theta \simeq j 30 I \frac{e^{-jk r}}{r} \cdot f_\theta^0 \left\{ 1 - \frac{k}{f_\theta^\infty} \int_{\rho=0}^{a_s} \frac{\eta_g - \eta_\rho(\rho)}{\eta_0} \left[ e^{-jk[\rho^2+h^2]^{1/2}} - e^{-jk\rho \cos kh} \right] \cdot J_1(k\rho \cos \theta) d\rho \right\}$$

and the vertical radiation function has the following expression:

$$f_\theta = f_\theta^0 \left\{ 1 - \frac{k}{f_\theta^\infty} \int_{\rho=0}^{a_s} \frac{\eta_g - \eta_\rho(\rho)}{\eta_0} \cdot \left[ e^{-jk[\rho^2+h^2]^{1/2}} - e^{-jk\rho \cos kh} \right] \cdot J_1(k\rho \cos \theta) d\rho \right\}$$

For the determination of the antenna pattern only the modulus of the above function is to be calculated. It should be noted that the integral shown in the formula can only be calculated by numerical methods.

## 8. Pattern examples

Annex I includes a number of antenna types for which the following examples of patterns are given:

- the vertical pattern at maximum gain,
- the horizontal pattern at maximum gain and
- the Sanson-Flamsteed projection of the forward and backward radiation patterns.

Patterns for various cases of frequency ratio  $F_R$  and slew angle  $s$  are also included.

## REFERENCES

- AIZENBERG, G.Z. [1948] *Antenni dlia Magistralnoi Radiosviazi*. Sviazizdat.
- CARREL, R. [1961] The design of log-periodic antennas. IRE International Convention Record 1961, 6.
- CCIR [1978] *Antenna diagrams*.
- JASIK, J.J. [1950] *Antenna Engineering Handbook*. McGraw-Hill Book Co., Inc., New York, USA.
- LLOYD, J.L. [1983] Computation of thin linear antennas. NTIA Report 83-136, US Dept. of Commerce, Office of Telecommunications, Institute for Telecommunication Sciences, Boulder, CO 80303, USA.
- MA, M.T. [1974] *Theory and Application of Antenna Arrays*. J. Wiley & Sons, Inc., New York, USA.
- MONTEATH, G.D. [1958] The effect of the ground constant and of an earth system on the performance of a vertical medium-wave aerial. IEE Monograph No. 279 R.

- NORTON, K.A. [1941] The calculation of ground-wave field intensity over a finitely conducting spherical Earth. *Proc. IRE*, Vol. 29, 623.
- WAIT, J.R. [1956] Effect of the ground screen on the field radiated from a monopole. *IRE Trans. Ant. Prop.*, Vol. AP-4, 2, 179-181.

## BIBLIOGRAPHY

- CCIR [1953] Antenna diagrams.
- CCIR [1984] Antenna diagrams.
- CCIR [1990] Broadcasting service (sound). Volume X – Part I, XVIIth Plenary Assembly, Düsseldorf, Germany (Federal Republic of).
- EATON, J.L. and THODAY, R.D.C. [June, 1977] Computer-aided wideband antenna design in the broadcast Band II. *Proc. IEE*, Vol. 124, 6.
- HILL, D.A. and WAIT, J.R. [1973] Calculated pattern of a vertical antenna with a finite radial wire ground system. *Radio Sci.*, Vol. 8, 1, 81-86.
- JASIK, J.J. [1984] *Antenna Engineering Handbook*. McGraw-Hill Book Co., Inc. New York, USA.
- JORDAN, E.C. [1968] *Electromagnetic Waves and Radiating Systems*. Prentice-Hall, Inc., Englewood Cliffs, New Jersey, USA.
- KRAUS, J.D. [1950] *Antennas*. McGraw-Hill Book Co., Inc., New York, USA.
- MA, M.T. and WALTERS, L.C. [1969] Power gains for antennas over lossy plane ground. ESSA Tech. Rep. ERL 104-ITS 74, US Dept. of Commerce, Environmental Science Services Administration, Boulder CO 80303, USA.
- MANTON, R.G. [1977] The design of aperiodic reflecting screen for HF arrays. BBC Technical Note No. 48.
- MOULLIN, E.B. [1949] *Radio Aerials*. Oxford University Press, Amen House, London, UK.
- SCHELKUNOFF, S.A. [1951] *Electromagnetic Waves*. D. Van Nostrand Co., Inc., New York, USA.
- SCHELKUNOFF, S.A. and FRIIS, H.T. [1952] *Antennas: Theory and Practice*. J. Wiley & Sons, Inc., New York, USA.
- STRATTON, J.A. [1941] *Electromagnetic Theory*. McGraw-Hill Book Co., Inc., New York, USA.
- WILENSKY, R. [January, 1981] Wide Bandwidth Dipole Curtain Antennas: a Guide for Shortwave Broadcasters. *International Broadcast Engineer*.

*CCIR Documents*

- [1982-86]: 10/183 (Hungary (People's Republic of)).
- [1986-90]: 10/101 (CCIR Secretariat), IWP 10/1-7 (Italy), IWP 10/1-42 (CCIR Secretariat), IWP 10/1-46 Germany (Federal Republic of), IWP 10/1-60 (Rev.1) (CCIR Secretariat), IWP 10/1-65 (Italy), IWP 10/1-69 (CCIR Secretariat), IWP 10/1-79 (CCIR Secretariat), IWP 10/1-80 (Italy), IWP 10/1-102 (United Kingdom), IWP 10/1-107 (The Netherlands).

## PART 2

**Practical aspects of HF transmitting antennas****1. Introduction**

The high-frequency antenna radiation patterns illustrated in Part 1, § 8 are theoretical patterns derived from mathematical models. It should be noted that these patterns are for antennas over flat homogeneous ground of average conductivity as described in Part 1, § 3.

Antenna arrays and feeders are, however, very complex systems and the radiation may be influenced by a great number of parameters which cannot always be defined, e.g. construction deficiencies, the environment and the real reflection situation. These subjects are discussed further in the following chapters.

The actual radiation pattern of an antenna at a specific location can only be determined by measurement on site.

**2. Measurements of antenna radiation patterns****2.1 Method of measurement**

The method employed to determine the actual radiation pattern of an antenna is usually by airborne measuring equipment. The measuring receiver is mounted in a helicopter (the preferred type of aircraft for these measurements) and receives transmissions from the antenna under test. Reciprocity is of course valid. However it should be borne in mind that a rather high transmitter power may be required to ensure a sufficient signal to interference ratio particularly in pattern nulls.

It is obvious that an attempt to measure the radiation by using ground based measuring equipment will not give the real horizontal pattern at the take-off angle corresponding to maximum gain in the vertical pattern.

**2.2 Considerations when using a helicopter for the measurements**

When measuring the radiation patterns of HF antennas, reflections have to be considered as composing part of the radiated lobes. Thus the optimum measuring distance has to be a compromise between the necessary accuracy (far field condition) and flying time.

A generally used formula to calculate the minimum measuring distance with a sufficient tolerance to the far field condition is :

$$d = 2h^2 / \lambda$$

where:

$d$  : measuring distance (m);

$h$  : aperture (m) of the antenna including its image and parasitic radiators;

$\lambda$  : wavelength (m).

In practice a measuring distance of 2000 to 2500 m is often used. However careful consideration has to be taken of the surroundings. A greater distance may be needed if there are other high power transmitters operating at the site.

Normally a set of measured radiation patterns for an HF antenna consists of one horizontal radiation pattern (HRP) and one vertical radiation pattern (VRP) for each operating condition of the antenna. The HRP is measured at the elevation angle of the maximum radiation in the main lobe and the VRP is measured as a cross section through the main lobe at maximum radiation.

The accuracy of the results depends on the performance of the field strength and location measurement equipment in the helicopter. Therefore careful consideration has to be given to the following points:

- the receiving antenna characteristics and its mounting on the helicopter;
- the test receiver (field strength meter), including the cables;
- the position determining system for giving true three dimensional coordinates and guidance to the pilot.

To ensure reliability the HRP should, at least in the main lobe, be measured on two separate occasions.

### 2.3 *Measuring equipment*

A radiation pattern measuring system may include the following components:

- a test receiver with:
  - high dynamic range;
  - high electromagnetic compatibility (EMC);
  - high ruggedness and stability (vibrations in the helicopter and temperature variations);
- a receiving antenna mounted in such a manner that the influence of the helicopter on the field pattern of the antenna is reduced to a minimum. For example a magnetic antenna such as a loop or ferrite rod mounted at least 3 m below the helicopter is often used;
- position determining facilities in the helicopter and/or on the ground. Commonly used methods are either tracking or ranging using terrestrial or satellite based systems;
- control, data-logging and processing facilities linking the individual components through a data-bus.

A signal source having a stable and calibrated output power level. This source could be the normal transmitter.

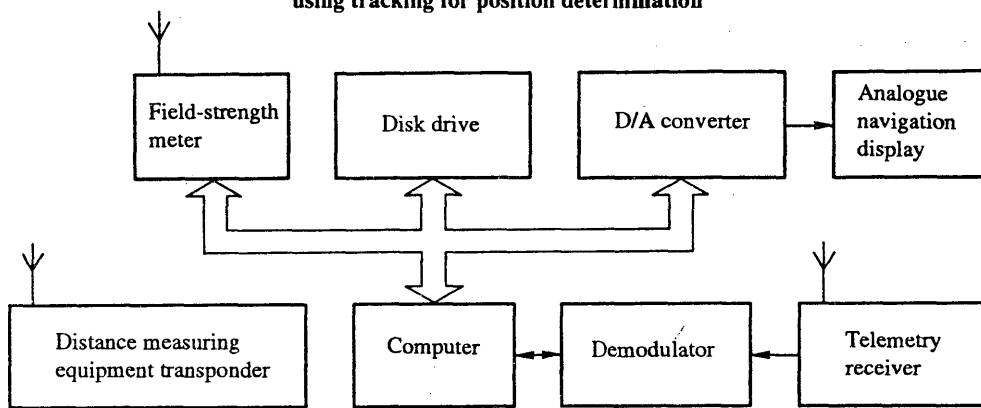
Figures 45 and 46 show simplified block diagrams of two measuring systems having different position determination equipment.

### 2.4 *Measurement procedures*

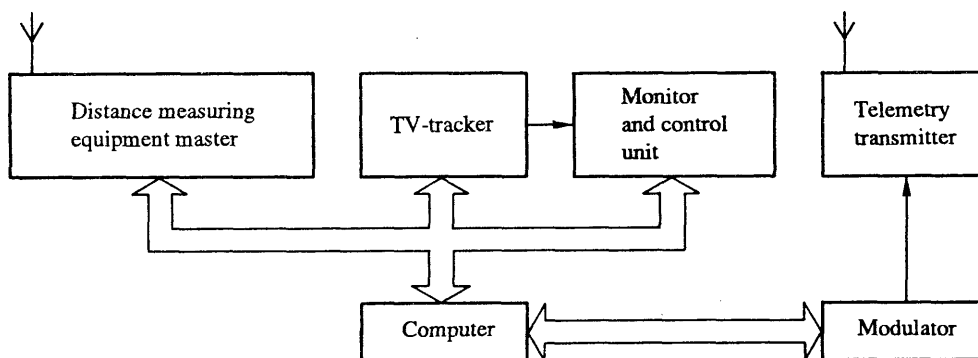
Before the actual measurement takes place, careful preparation is needed. The equipment on board the helicopter as well as that on the ground must be checked and proper operation must be verified. The signal generator or the normal transmitter, whichever is used to power the antenna under test has to be set and its power level calibrated. It may be helpful to have some modulation on the transmission to facilitate aural recognition while the measurements are being made.

FIGURE 45

Block diagram of measuring equipment using tracking for position determination



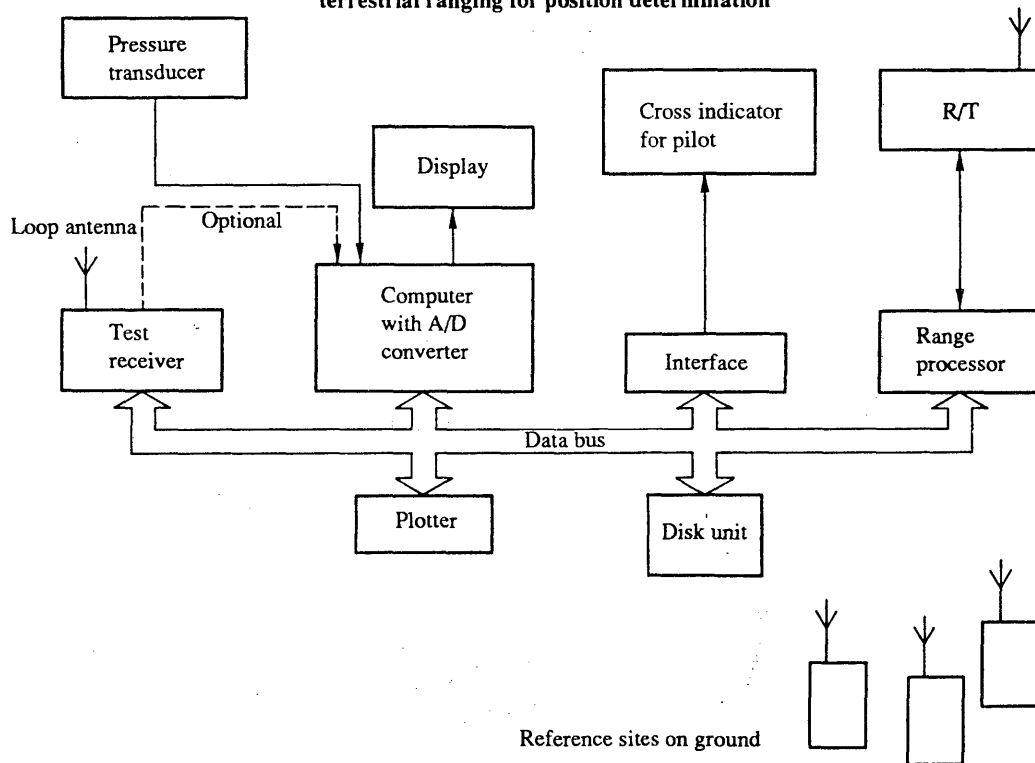
(a) Equipment in helicopter



(b) Ground-based equipment

FIGURE 46

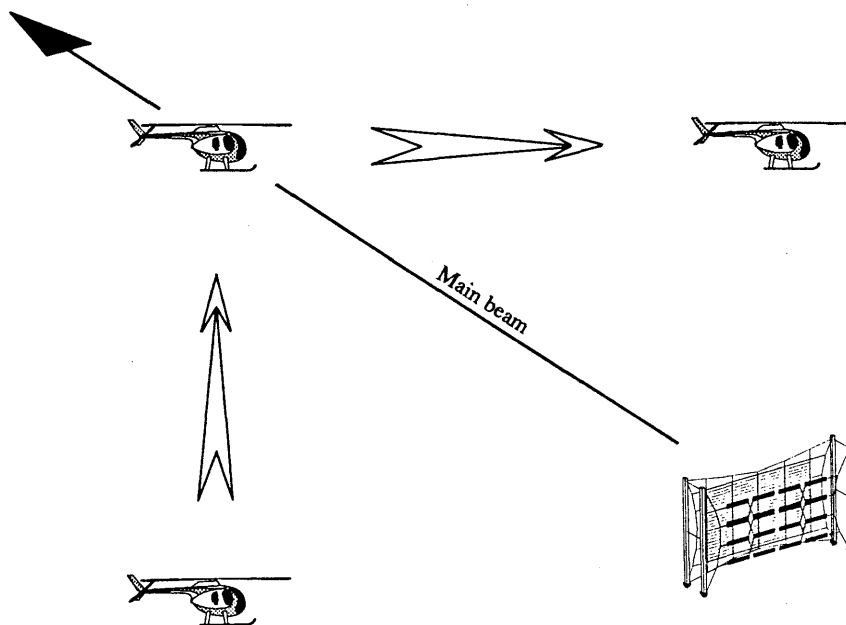
Block diagram of measuring equipment using terrestrial ranging for position determination



During the measurement flight the helicopter should follow predetermined routes, as described below. The actual flight paths are recorded using the output from the position determining equipment which gives the actual position of the helicopter in relation to the antenna under test. This helicopter position information, which is presented to the pilot in real-time, allows the correct flight path to be maintained in order to obtain the best accuracy.

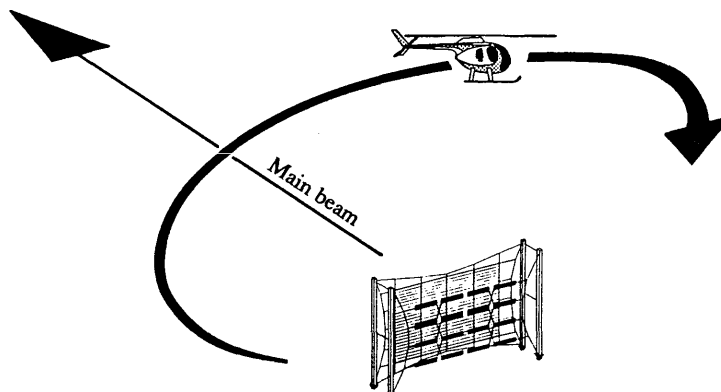
Ideally, a VRP is measured by flying a semicircle over the top of the antenna starting at the azimuthal angle of maximum radiation while simultaneously taking samples of the field strength. However, as it is difficult for the pilot to keep to such a precise flight path, a modified flight path may have to be used. Such a flight path can be a combination of a vertical climb at a known position and an approach flight at known altitude as shown in Fig. 47. In this type of flight path it is important to maintain the correct azimuthal position of the helicopter as deviation can spoil the measurement results.

FIGURE 47

**Flight path for the VRP measurement**

The results of the vertical measurement give the elevation angle for maximum radiation (the main lobe maximum) at which the HRP should be measured. The helicopter then flies in a circle around the antenna at a constant radius at an altitude corresponding to this elevation angle as shown in Fig. 48.

FIGURE 48

**Flight path for the HRP measurement**

For this flight path it is important that the correct elevation angle be exactly kept since compensation for any deviation is difficult.

If the measured values, in the form of an antenna pattern, are displayed to the operator in the helicopter, the proper operation of the measurement system can be verified while the flight is in progress.

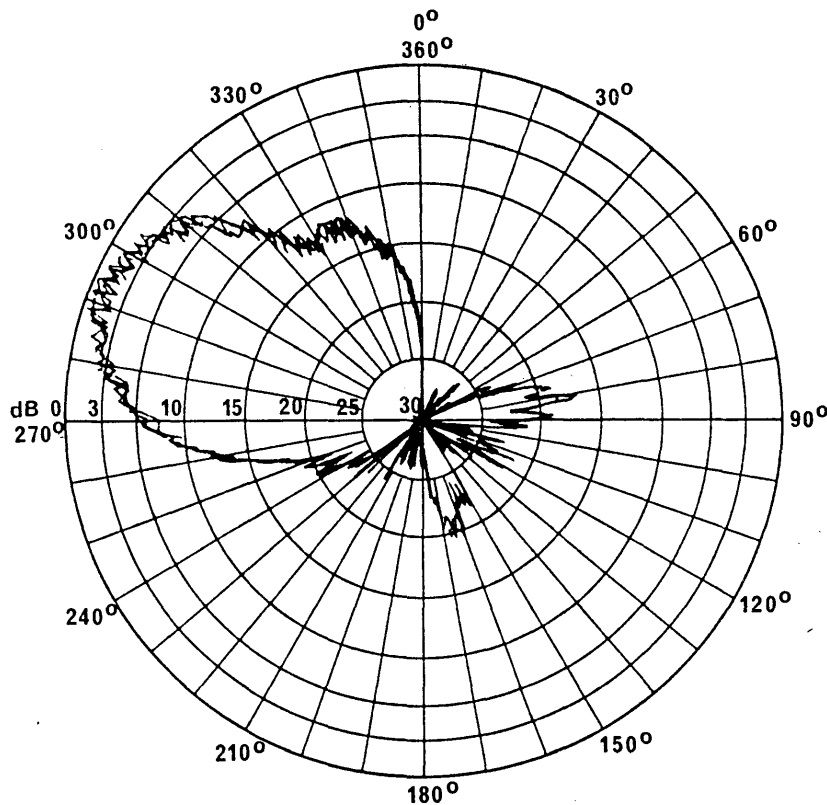
The test receiver should be able to measure in an averaging mode so that one single signal level sample consists of an average over a specific time (e.g. 100 ms) so as to eliminate the influence of modulation. The flight of the helicopter and the capability of the measurement system should be such that at least two samples per degree in the horizontal plane and at least five samples per vertical degree are stored by the system along with their correlated position data.

2.5 *Processing the measured data*

In a subsequent analysis the samples of signal level are converted into field strength values at a normalised distance taking into account the characteristics of the receiving antenna and the position information. At this stage any samples that are obviously erroneous should be discarded.

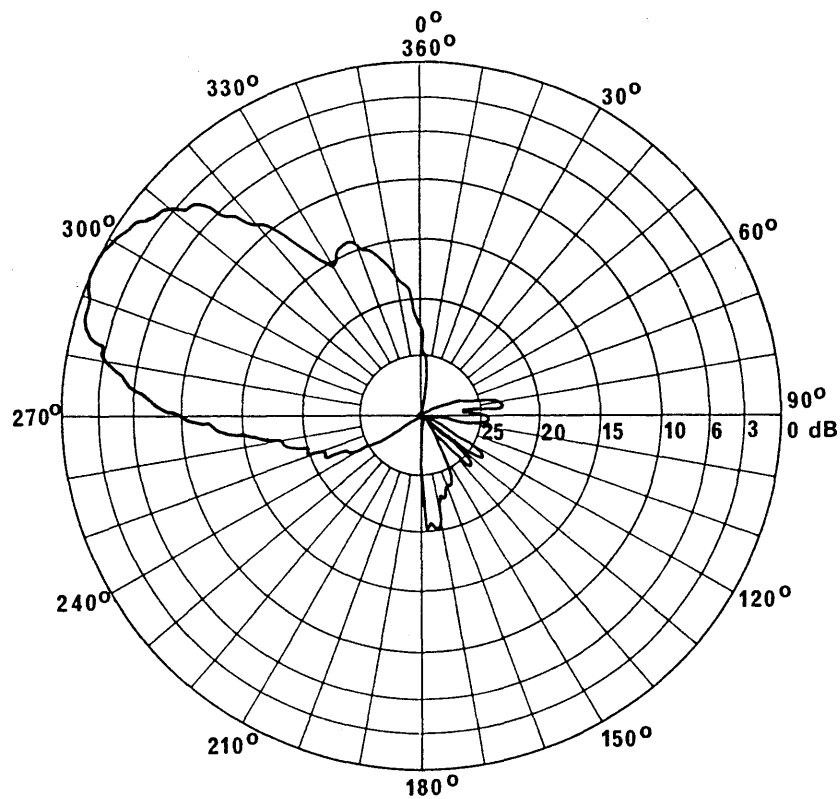
A direct plot of the remaining field strength samples will generally contain ripple as shown in Fig. 49.

FIGURE 49  
 HRP using validated field-strength samples collected  
 on three complete flights around the antenna



If a smoothed pattern is required the data are further processed using a filtering function. A final plot using these filtered values is shown in Fig. 50. This figure is plotted in a polar-logarithmic scale which allows examination of sidelobes and minima. Other formats and scales could be used.

FIGURE 50  
Final HRP after filtering and scaling of data



The gain of the antenna in the direction of maximum radiation can be derived as the ratio  $e.i.r.p./P_{in}$ , where  $P_{in}$  is the power fed to the antenna and e.i.r.p. is derived from the measured field strength and the corresponding distance.

The directivity gain of the antenna can be estimated from the shape of the measured horizontal and vertical radiation patterns assuming that the shape of the vertical radiation pattern is identical for all azimuth directions.

### 3. Comparison of theoretical and measured radiation patterns

Meaningful comparisons between theoretical and measured radiation patterns have proved to be very difficult to make.

Measurements on certain antennas have shown that variations in performance are the result of many factors which are not easily isolated.

This is illustrated in Figs. 51a and b, and 52a and b which give the measured and theoretical radiation patterns in both the horizontal and vertical planes of a HR 4/4/0.6 horizontal dipole antenna with an aperiodic screen reflector.

Although the main radiation lobe has approximately the same shape, there are differences in the number, size and position of the side lobes.

FIGURE 51a

Measured HRP of a multiband centre-fed HR 4/4/0.6 antenna with aperiodic screen reflector, at  $F_R = 1.0$

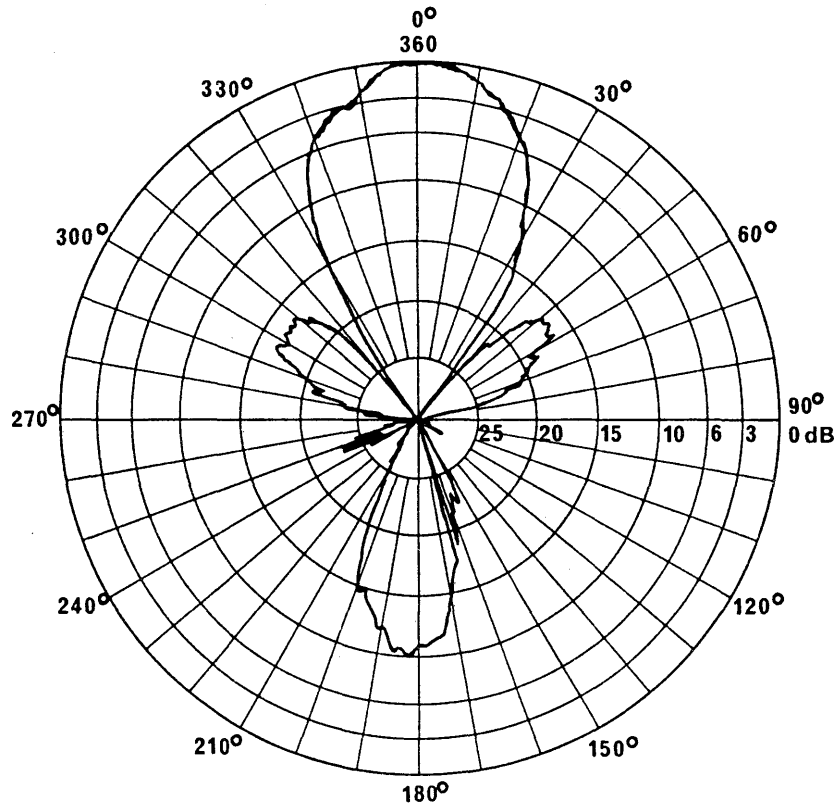


FIGURE 51b

Theoretical HRP of the antenna of Fig. 51

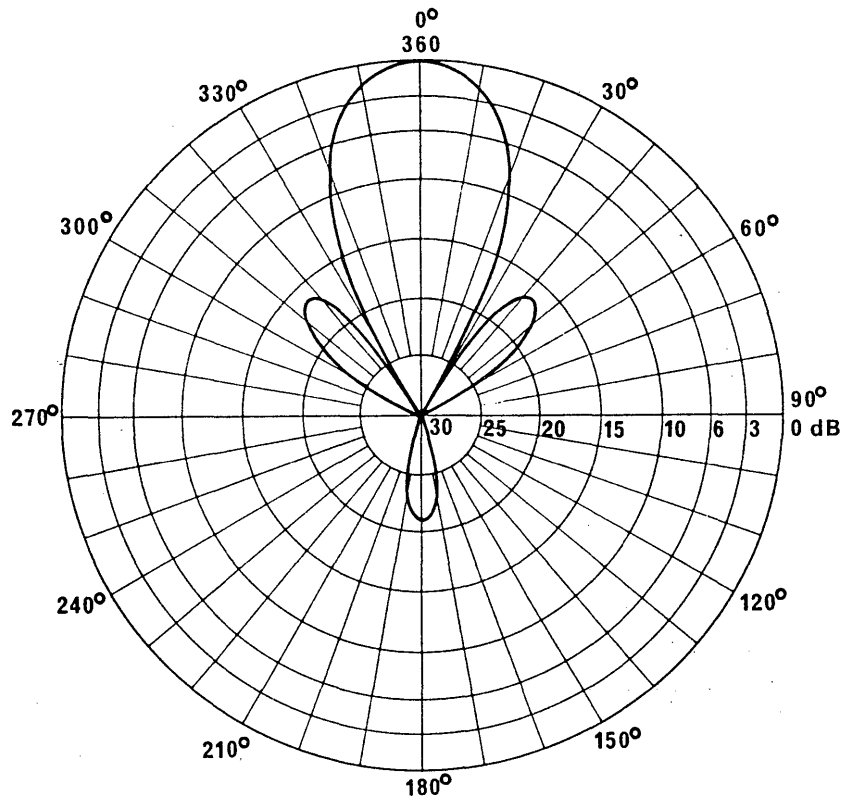


FIGURE 52a  
Measured VRP of the antenna of Fig. 51

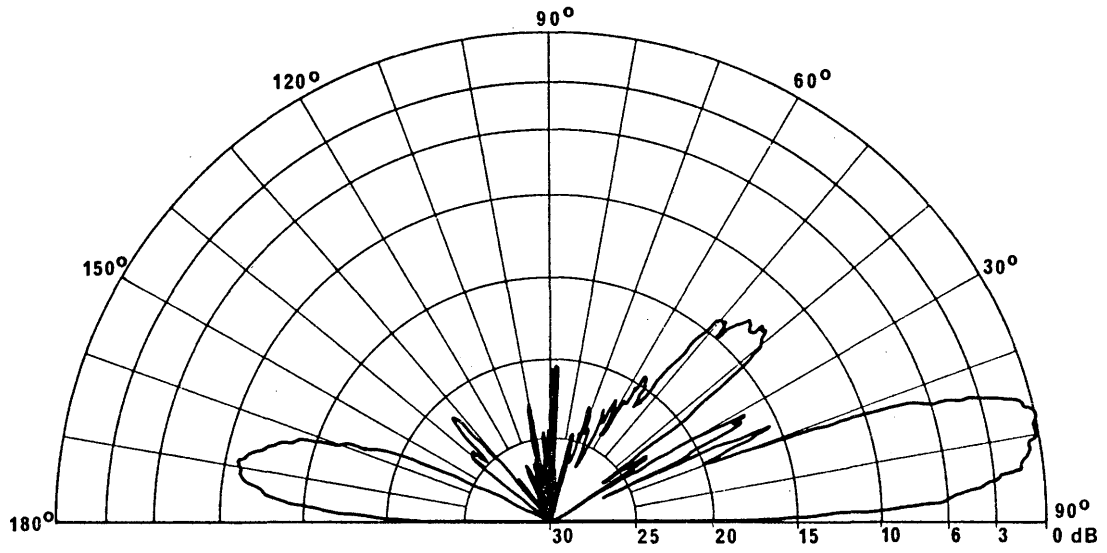
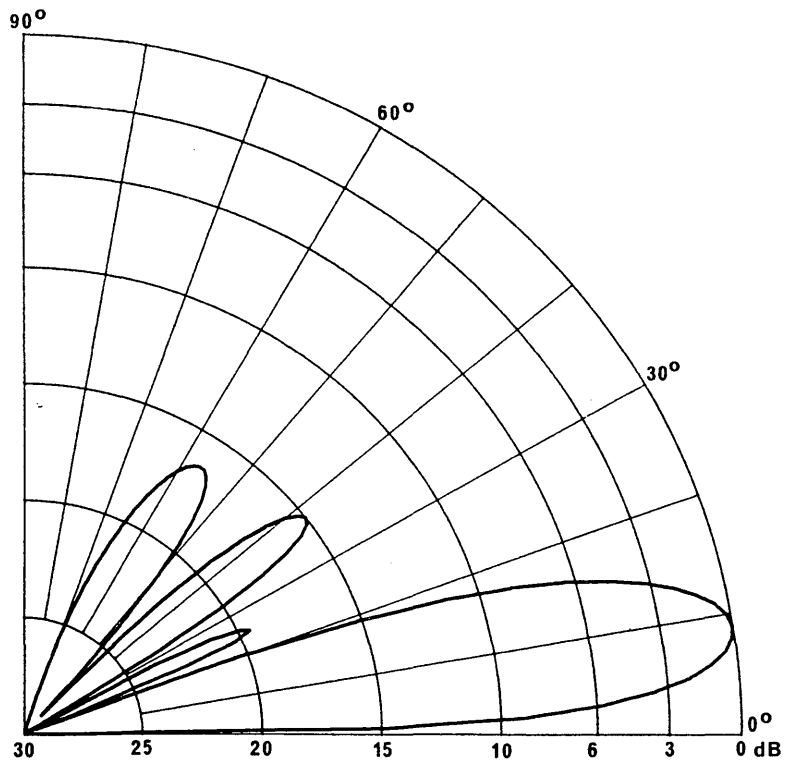


FIGURE 52b  
Theoretical VRP of the antenna of Fig. 51a



3.1 Comparison of theoretical and measured front-to-back ratios

Figure 53 shows a comparison of measured and calculated front-to-back ratio (FTBR) values for a HR 4/4/1.0 antenna. Figure 54 shows the comparison for other types of curtain antenna and different reflecting screen parameters. In both figures the calculated FTBR is for an aperiodic screen with 50 wires per wavelength as in § 4.7.4.1, Part 1, Fig. 23.

FIGURE 53  
Measured and calculated FTBR values for a HR 4/4/1.0 antenna

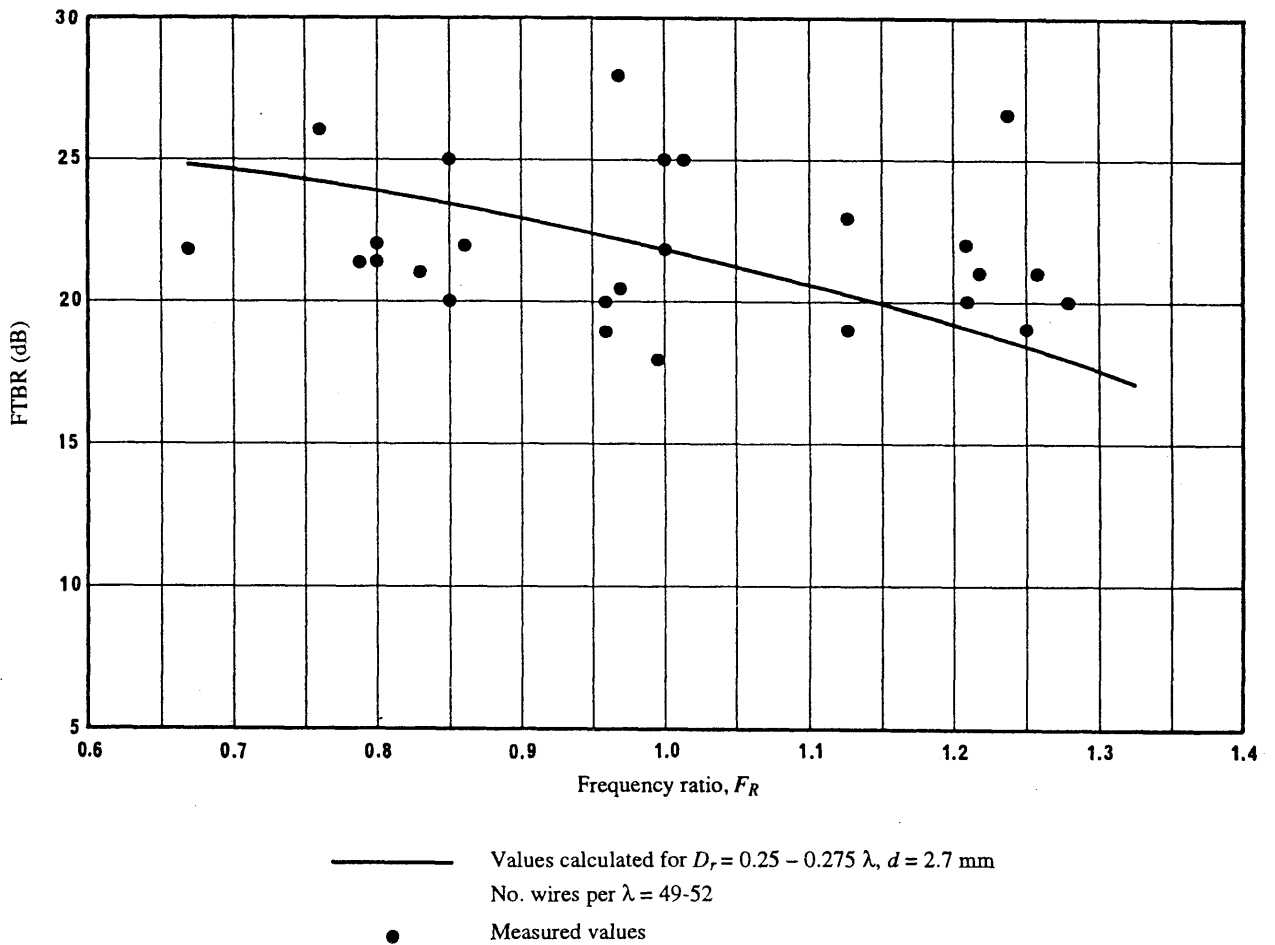
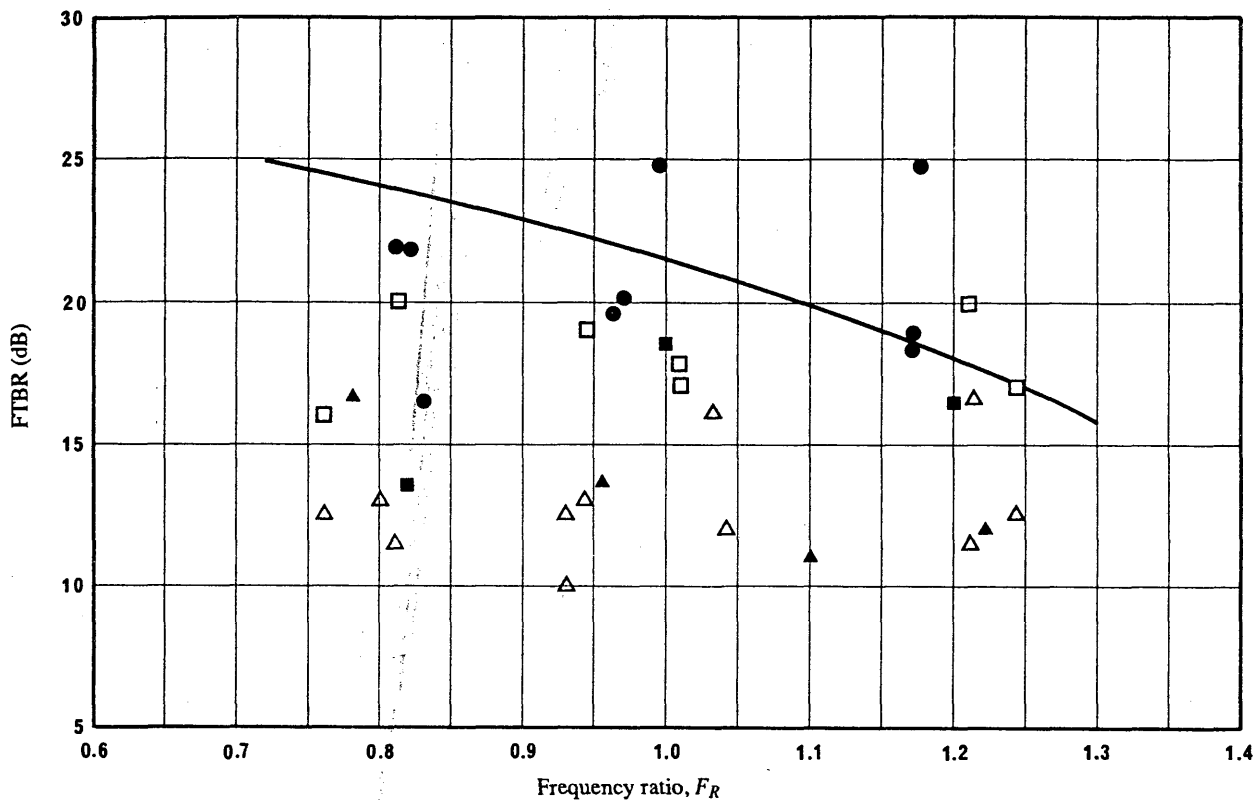


FIGURE 54

Measured and calculated FTBR values for various antenna types



— Values calculated for  $D_r = 0.3 \lambda$ ,  $d = 2.7$  mm  
No. wires per  $\lambda = 47 - 50$

Measured values:

● HR 4/4/1.0

□ HR 4/3/0.55

■ HR 2/4/1.0

△ HR 2/3/0.6

▲ HR 2/2/0.4

#### 4. Influence of surrounding environment on radiation patterns

The following factors are known to have an influence on HF antenna radiation patterns.

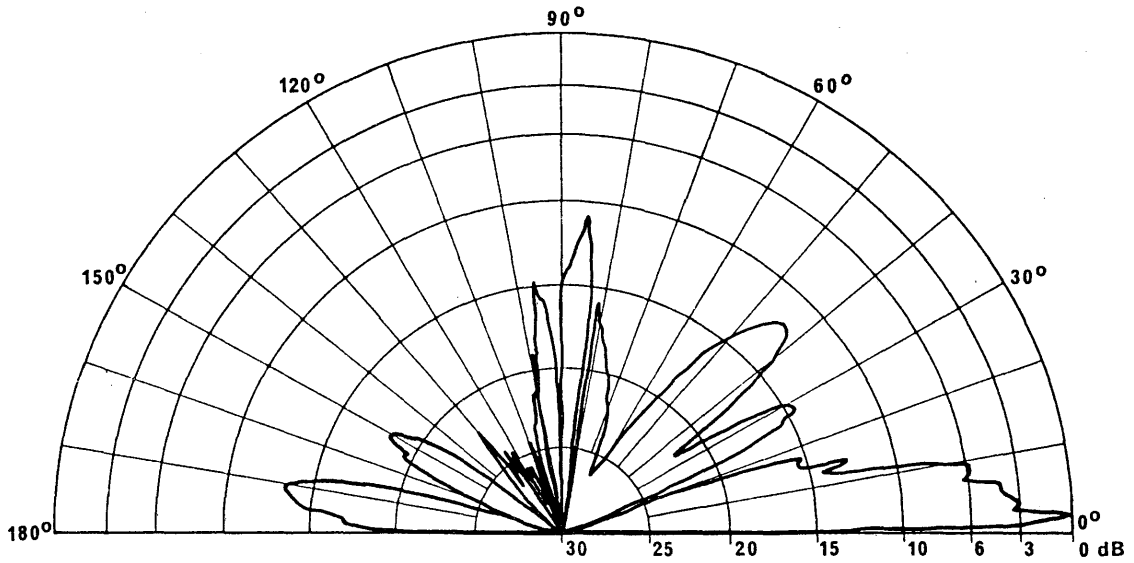
##### 4.1 Ground topography

The theoretical sample radiation patterns given in Part 1, § 8 assume the antenna is sited on flat homogeneous ground of average ground conductivity. Any perturbation of the ground (slopes, hills, valleys, etc.) will produce image currents that differ in position and value from those used in the calculations. This will lead to a modified radiation pattern. Depending on the type of antenna used, the radiation pattern can be significantly modified by ground perturbations extending up to several kilometres from the antenna.

Figure 55 illustrates the effect of irregular ground profile on the VRP of an HR 4/4/0.5 antenna.

FIGURE 55

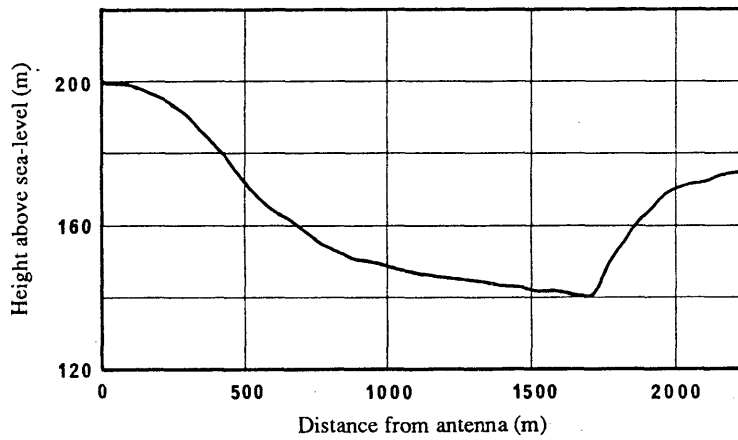
Vertical radiation pattern measured at 21.56 MHz of a HR 4/4/0.5 antenna  
(operating frequency range: 11-21 MHz), centre-fed, aperiodic screen, no slew



The ground to the front of the antenna slopes down to a valley before rising again as shown in Fig. 56.

FIGURE 56

Ground profile in front of HR 4/4/0.5 antenna



In this case the elevation angle at maximum gain is significantly less than the theoretical angle assuming flat ground in front of the antenna.

It should also be noted that the converse is true; if the ground in the front of the antenna rises with increasing distance from the antenna, the elevation angle will be greater than the theoretical elevation at maximum gain.

#### 4.2 *Ground conductivity*

The calculated radiation patterns are based on average ground conductivity. However, there are changes in the vertical pattern, particularly for vertically polarized antennas, if the actual ground conductivity is significantly different to the average values assumed.

#### 4.3 *Other site structures*

High gain HF antennas are physically large and need substantial supporting structures as well as large areas of land.

Many transmitting sites require a number of antennas to cope with the range of bands and azimuths required to cover a range of target areas throughout the day, seasons and sunspot cycle.

The following factors are known to adversely affect the radiation performance of antennas:

- coupling of energy to adjacent antennas;
- any obstruction in the foreground of the antenna e.g.:
  - transmitter buildings
  - high structures, e.g. church towers
  - high-tension towers
  - antenna guys
  - trees
  - feeder lines.

In particular cases, the forward radiation of one antenna can be modified by the presence of one or more other antennas.

Figure 57 illustrates the effect on the HRP of an HR 4/4/0.5 antenna obstructed by the screens of other antennas about 600 m away. The layout of the antennas is illustrated in Fig. 58. The horizontal radiation pattern (HRP) is distorted and there are significant differences in the size and location of the sidelobes compared to the theoretical HRP. The vertical radiation pattern (VRP) is also affected. Not only is the angle of elevation at maximum gain higher than expected, but also the VRP sidelobes are greater in amplitude.

FIGURE 57

HRP measured at 15.39 MHz of a HR 4/4/0.5 antenna (operating frequency range: 11-21 MHz),  
centre fed, aperiodic screen, slew angle:  $-20^\circ$

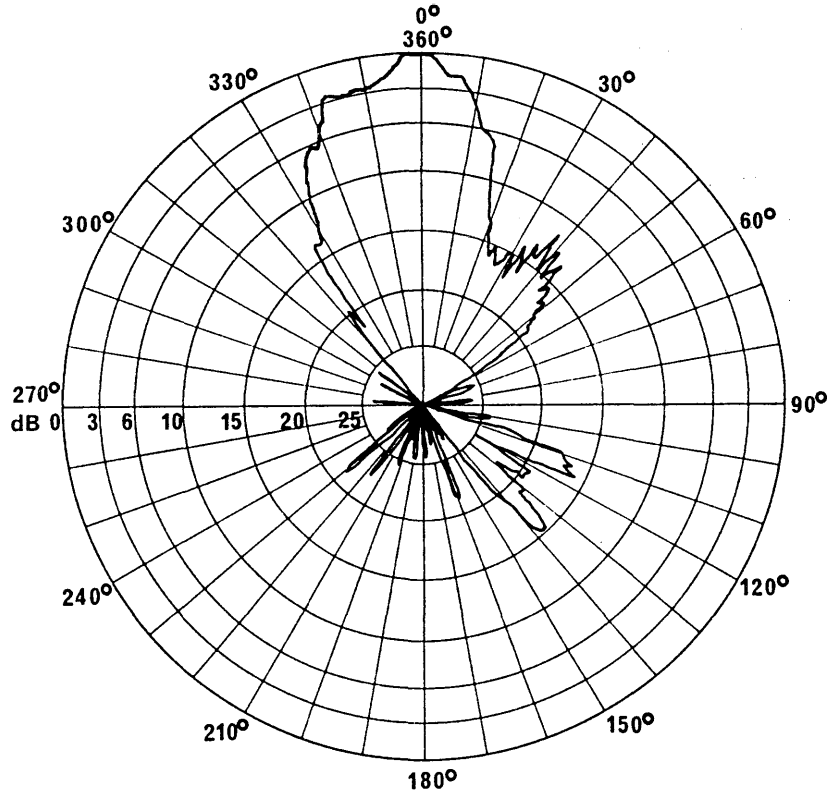
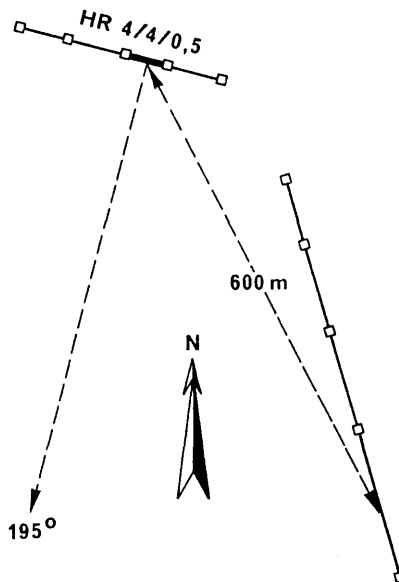


FIGURE 58

Layout of antennas



## 5. Variations in practical antenna performance

The example HF antenna radiation diagrams contained in Part 1, § 8 show the calculated performance for antennas having the design criteria specified in Part 1.

Variations in the performance of practical antennas from the ideal case, are due to the actual choices made by the manufacturer of the physical and electrical parameters required to achieve an economical design.

For example the main sources of variation in the performance of curtain antennas are:

- spacing of wires in reflecting screen;
- thickness of wires in reflecting screen;
- spacing of reflecting screen from dipoles;
- size of the reflecting screen in relation to the size of the array of dipoles;
- spacing between dipoles both horizontally and vertically;
- design frequency of antenna;
- effective thickness of dipoles;
- physical arrangement of the supporting structures (e.g., guys, catenaries).

### 5.1 Azimuthal pattern

Figures 59 and 60 illustrate the variation in performance in HRP that can be expected for nominal antennas HR 4/4/1.0 supplied by different antenna manufacturers and operated at different transmitting sites.

Figure 61 shows the theoretical horizontal radiation pattern of an HR 4/4/1.0 antenna using the default parameters.

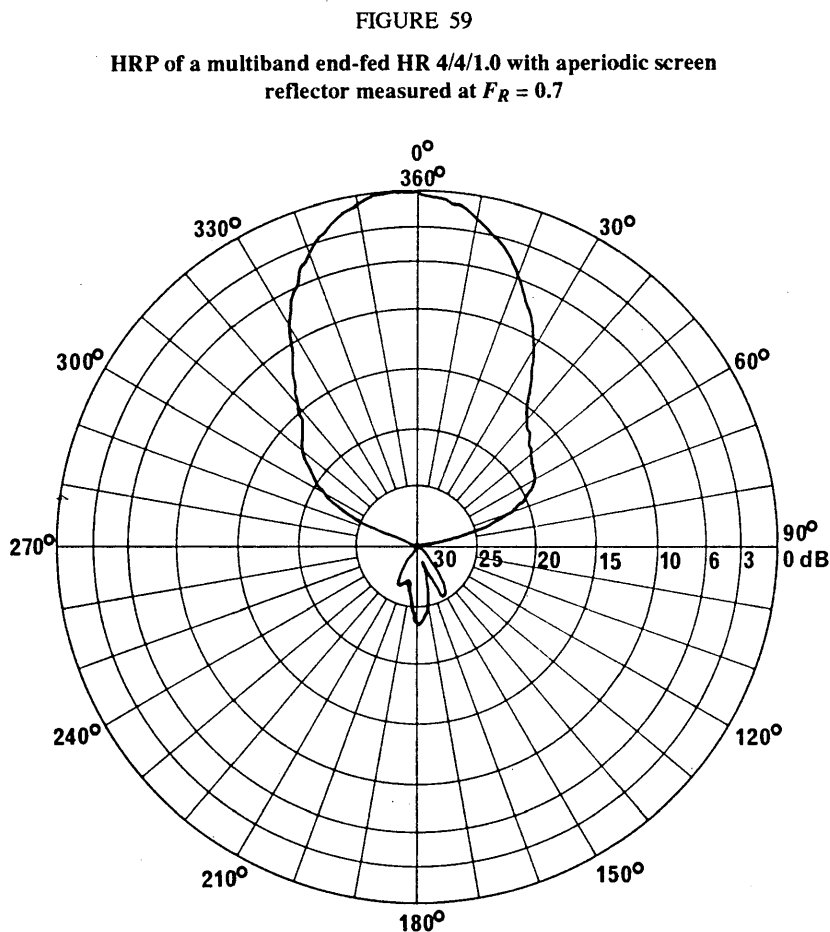


FIGURE 60

HRP of a different multiband end-fed HR 4/4/1.0 antenna with aperiodic screen reflector, measured at  $F_R = 0.7$

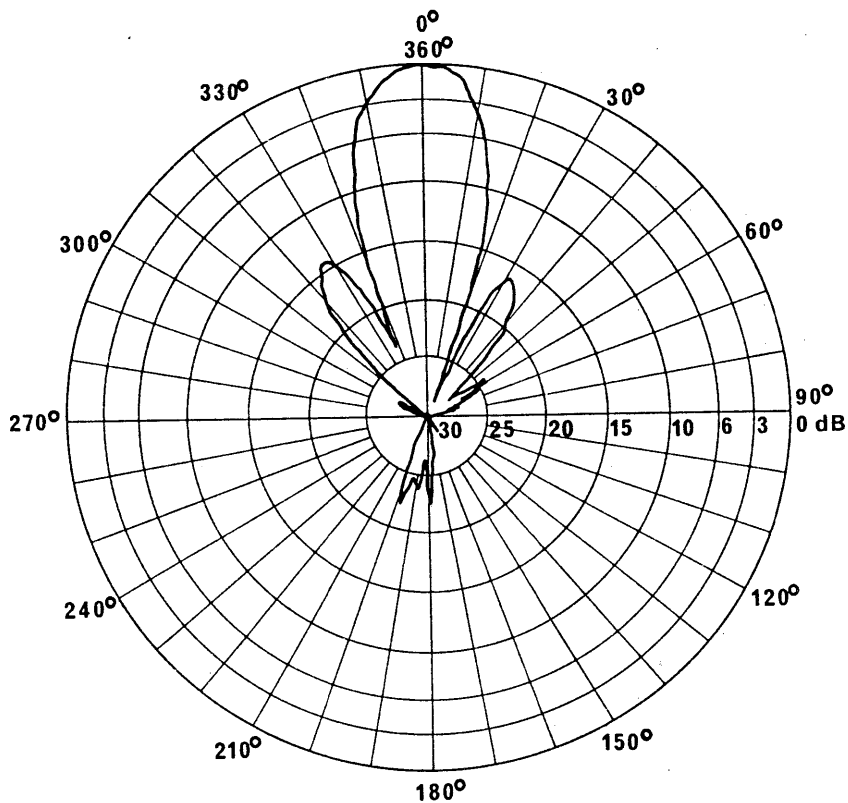
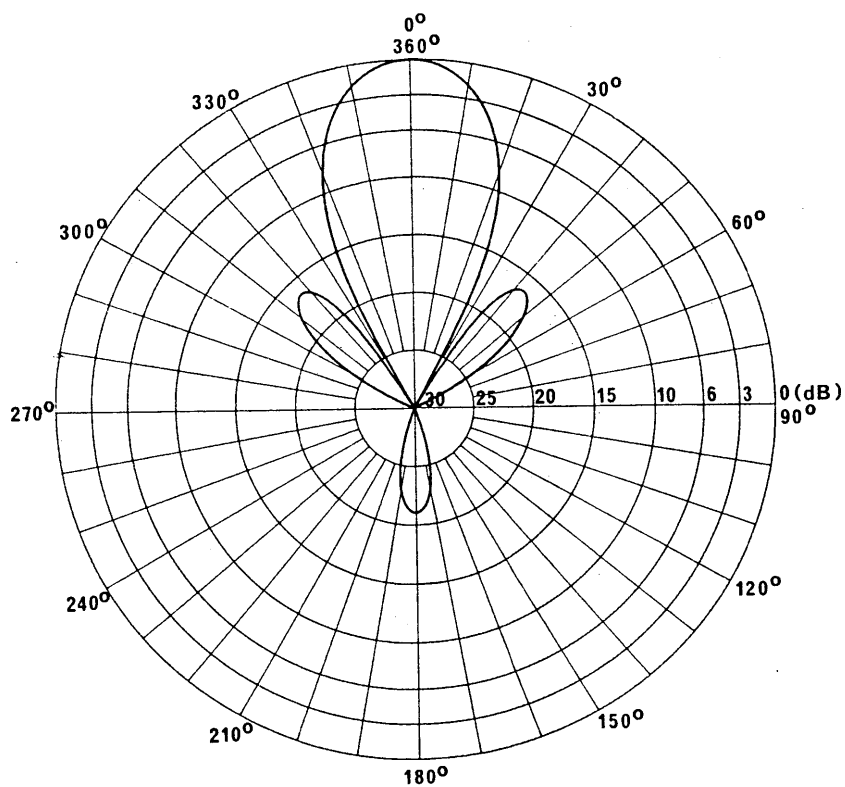


FIGURE 61

Theoretical HRP of an end-fed HR 4/4/1.0 antenna with aperiodic screen reflector calculated at  $F_R = 0.7$



## 5.2 Slewed pattern

It should also be noted that antenna designers implement the slewing of HF horizontal dipole antennas by various methods. Generally the method of slewing used, results in the actual slew angle being less than that specified. This is described in Part 1, § 4.3.

However, this reduction can be compensated for in some antenna designs so that in practice the specified slew angle is achieved over the full frequency range of the antenna.

This is illustrated in Figs. 62 and 63. Figure 62 is the measured HRP of a horizontally slewed HRS 4/4/0.5 antenna having a nominal slew angle of  $+25^\circ$ . The slew achieved in practice is approximately  $+25^\circ$  and is maintained over the full frequency range of the antenna.

Figure 63 is the measured HRP of a horizontally slewed HRS 4/4/1.0 antenna having a nominal slew angle of  $+30^\circ$ . The slew achieved in practice is approximately  $25^\circ$ .

FIGURE 62  
 HRP of a multiband centre-fed HRS 4/4/0.5 antenna  
 with aperiodic screen reflector slewed by  $+25^\circ$  from fundamental  
 azimuth of  $275^\circ$ , measured at  $F_R = 0.7$

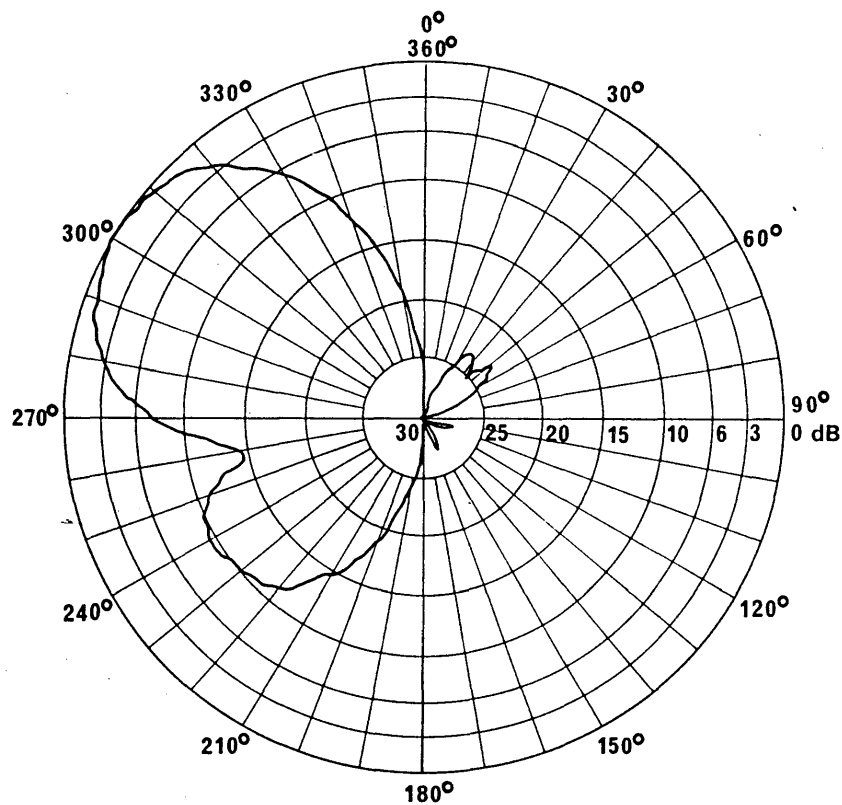
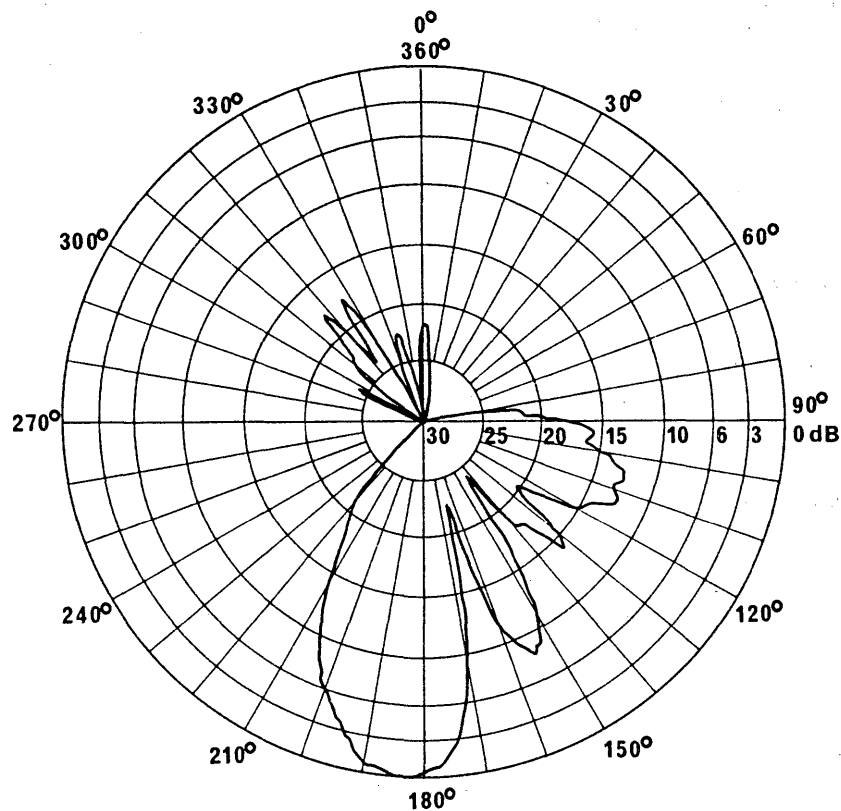


FIGURE 63

HRP of a multiband centre-fed HRS 4/4/1.0 antenna  
with aperiodic screen reflector slewed by  $+30^\circ$  from fundamental  
azimuth of  $160^\circ$ , measured at  $F_R = 1.3$



## 6. Suitability and application of antennas

### 6.1 Horizontal dipole antennas

Horizontal dipole antennas are the most common form of antenna used for HF broadcasting. They can be designed to realize closely any performance specification or pattern which is commonly required.

### 6.2 Rotatable curtain antennas

A rotatable curtain antenna usually consists of two arrays of dipole elements supported on either side of a common reflecting screen. If each of the curtain arrays has an operating frequency range of one octave, all shortwave bands between 6 and 26 MHz can be covered.

These antennas are mechanically rotated so that the main beam of radiation is at the desired azimuth. The time needed for this mechanical movement is typically less than 5 min for a full  $360^\circ$  rotation.

A rotatable curtain antenna is particularly suitable for physically small sites where there is requirement to transmit in a large number of azimuthal directions.

### 6.3 *Rhombic antennas*

Rhombic antennas are not recommended for HF broadcasting as:

- the main lobe is narrow in both horizontal and vertical planes which could result in the required service area not being reliably covered because of the variations in the ionosphere;
- there are a large number of sidelobes of a size sufficient to cause interference to other broadcasts;
- a significant proportion of the transmitter power is dissipated in the terminating impedance.

### 6.4 *Fixed azimuth log-periodic antennas*

Log-periodic antennas have the advantage of a wide frequency range. They are commonly used for short distance broadcasts as they have wide beamwidth and low gain.

### 6.5 *Rotatable log-periodic antennas*

Rotatable log-periodic antennas generally have horizontal radiating elements. In the case where they are mounted on a horizontal boom, the vertical radiation pattern will show an increased number of lobes with increasing operational frequency.

Although rotatable log-periodic antennas are used for both short, medium and long range broadcasting they are recommended for special purposes only e.g. for short distances at low and medium frequencies and for long distances at the highest frequency bands, where wide beamwidth is acceptable.

## BIBLIOGRAPHY

### *CCIR Documents*

[1986-90]: IWP 10/1-25 (Italy and Vatican City State), IWP 10/1-26 (France), IWP 10/1-31 (The Netherlands), IWP 10/1-34 (United Kingdom), IWP 10/1-35 (United Kingdom), IWP 10/1-36 (Deutsche Welle), IWP 10/1-57 (Norway), IWP 10/1-58 (United Kingdom), IWP 10/1-59 (United Kingdom), IWP 10/1-62 (Finland), IWP 10/1-73 (Norway), IWP 10/1-83 (Sweden), IWP 10/1-84 (Sweden), IWP 10/1-85 (United Kingdom), IWP 10/1-86 (Finland), IWP 10/1-87+Add.1 (The Netherlands), IWP 10/1-93 (United Kingdom), IWP 10/1-95 (United Kingdom).

## ANNEX I

## Pattern examples

Examples of patterns are given for the following antenna types and for the specified cases of frequency ratio  $F_R$  and slew angle  $s$ .

## 1. Curtain antennas

1.1 *Curtain antennas without reflector*

H	1/1/0.3	$F_R = 1$	(see Fig. 64)
---	---------	-----------	---------------

1.2 *Curtain antennas with tuned reflector*

HR	2/1/0.5	$F_R = 1$	$s = 0^\circ$	(see Fig. 65)
----	---------	-----------	---------------	---------------

HRS	2/2/0.5	$F_R = 1$	$s = 0^\circ, 15^\circ$	(see Figs. 66 and 67)
-----	---------	-----------	-------------------------	-----------------------

1.3 *Curtain antennas with aperiodic screen reflector*

HRS	2/2/0.5	$F_R = 1$	$s = 0^\circ, 15^\circ$	(see Figs. 68 and 69)
-----	---------	-----------	-------------------------	-----------------------

HRS	4/3/0.5	$F_R = 1$	$s = 0^\circ$	(see Fig. 70)
-----	---------	-----------	---------------	---------------

HRS	4/4/0.5	$F_R = 0.7, 1.0, 1.4$	$s = 0^\circ, 30^\circ$	(see Figs. 71 to 76)
-----	---------	-----------------------	-------------------------	----------------------

HRS	4/4/1.0	$F_R = 1$	$s = 0^\circ$	(see Fig. 77)
-----	---------	-----------	---------------	---------------

## 2. Tropical antennas

T	1/2/0.3	$F_R = 1$	$s = 0^\circ$	(see Fig. 78)
---	---------	-----------	---------------	---------------

T	2/2/0.5	$F_R = 1$	$s = 0^\circ, 15^\circ$	(see Figs. 79 and 80)
---	---------	-----------	-------------------------	-----------------------

## 3. Log-periodic antennas

LPH	18/35/30/30/3/26/89	(see Fig. 81)
-----	---------------------	---------------

LPV	18/45/3/17/6/34/220	(see Fig. 82)
-----	---------------------	---------------

## 4. Quadrant antennas

HQ	1/0.3	(see Fig. 83)
----	-------	---------------

## 5. Crossed dipole antennas

HX	0.3	(see Fig. 84)
----	-----	---------------

## 6. Rhombic antennas

RH	90/55/15	(see Fig. 85)
----	----------	---------------

## 7. Vertical monopoles

VM	12.5/12.5/120/3	(see Fig. 86)
----	-----------------	---------------

FIGURE 64a

Vertical pattern at 0° azimuth angle

Curtain antenna without reflector  
 H 1/1/0.3  
 $F_R = 1$   
 $\theta = 47^\circ$   
 $G_i = 5.9 \text{ dB}$

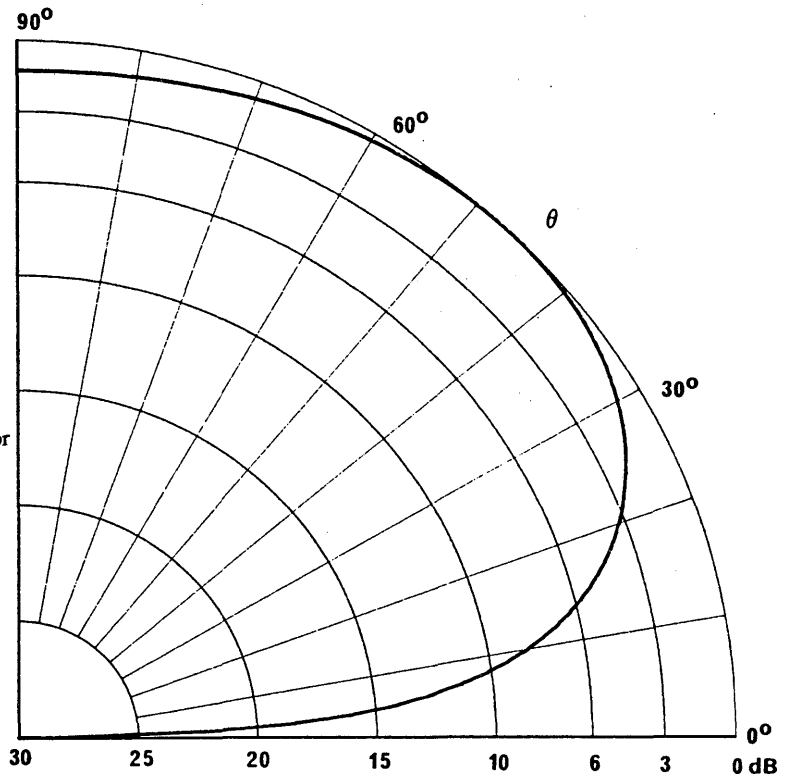


FIGURE 64b

Horizontal pattern at 47° elevation angle

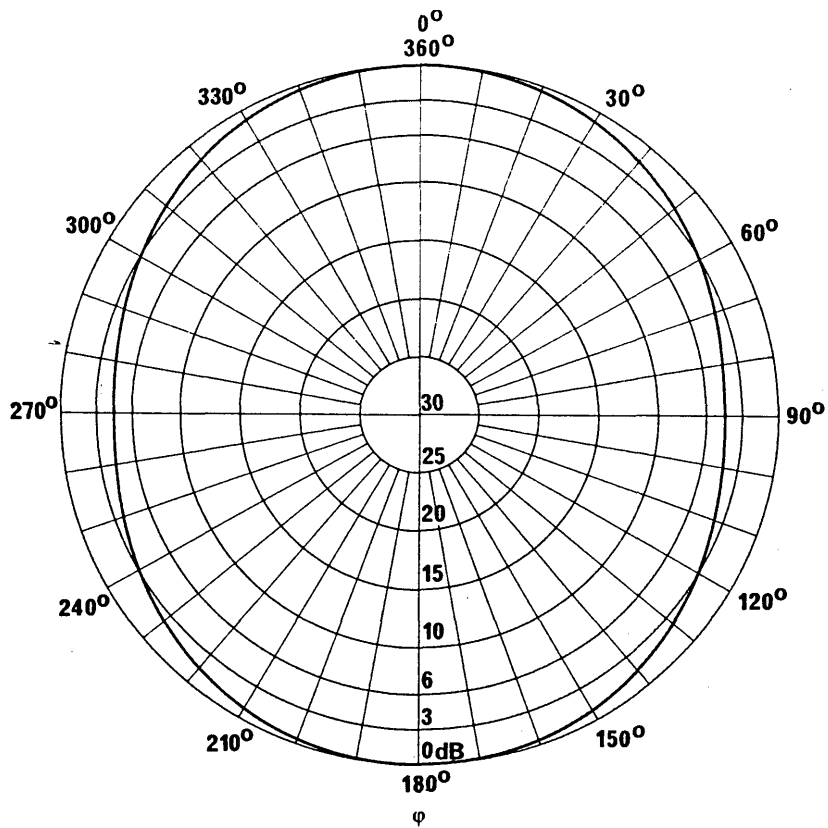


FIGURE 64c  
Forward radiation pattern

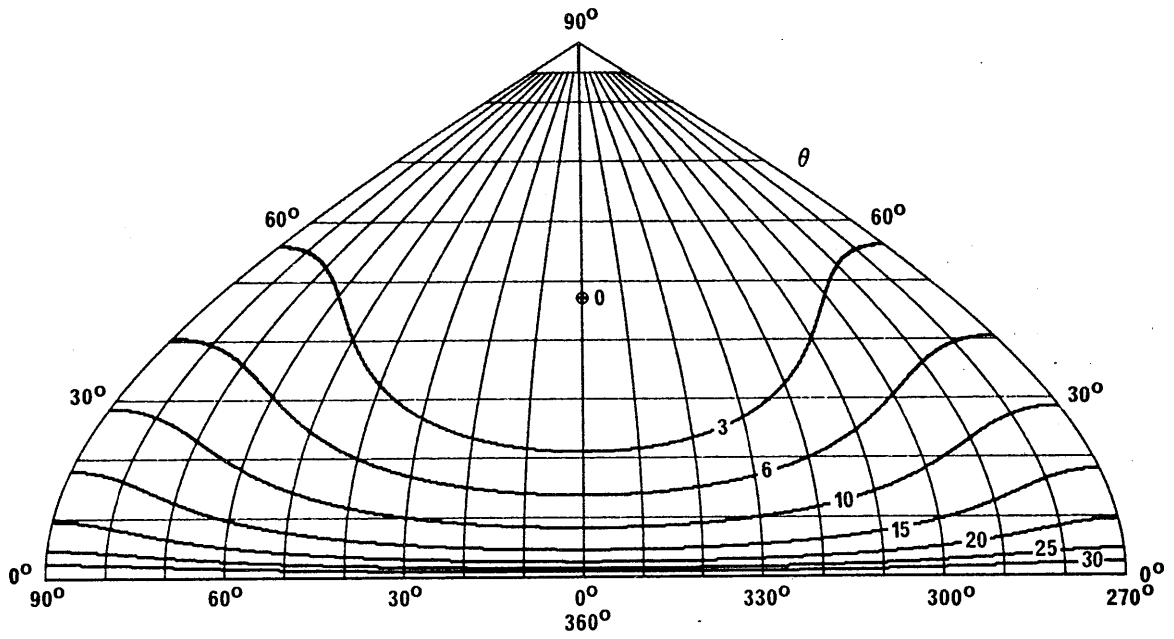


FIGURE 64d  
Backward radiation pattern

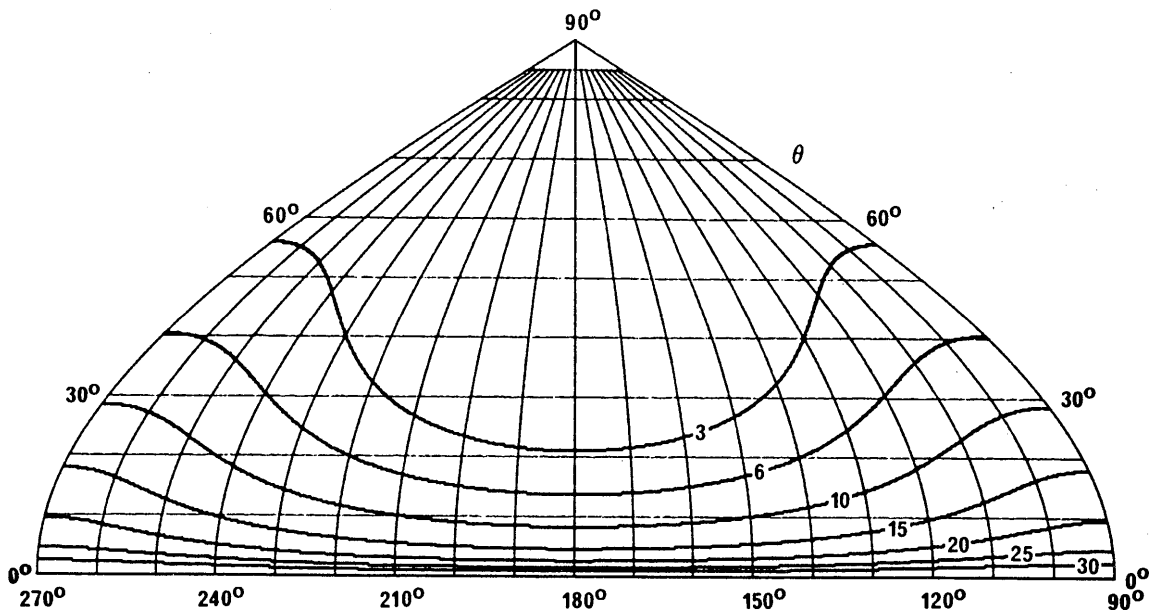


FIGURE 65a

Vertical pattern at 0° azimuth angle

Curtain antenna with tuned reflector  
 H R 2/1/0.5  
 $F_R = 1$   
 $\theta = 27^\circ$   
 $G_i = 12.6 \text{ dB}$

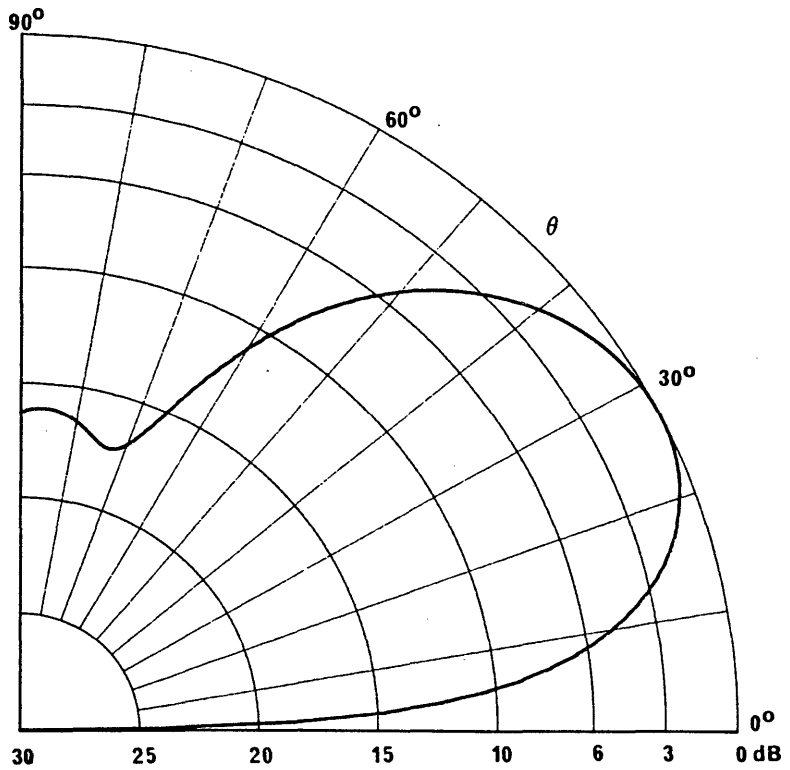


FIGURE 65b

Horizontal pattern at 27° elevation angle

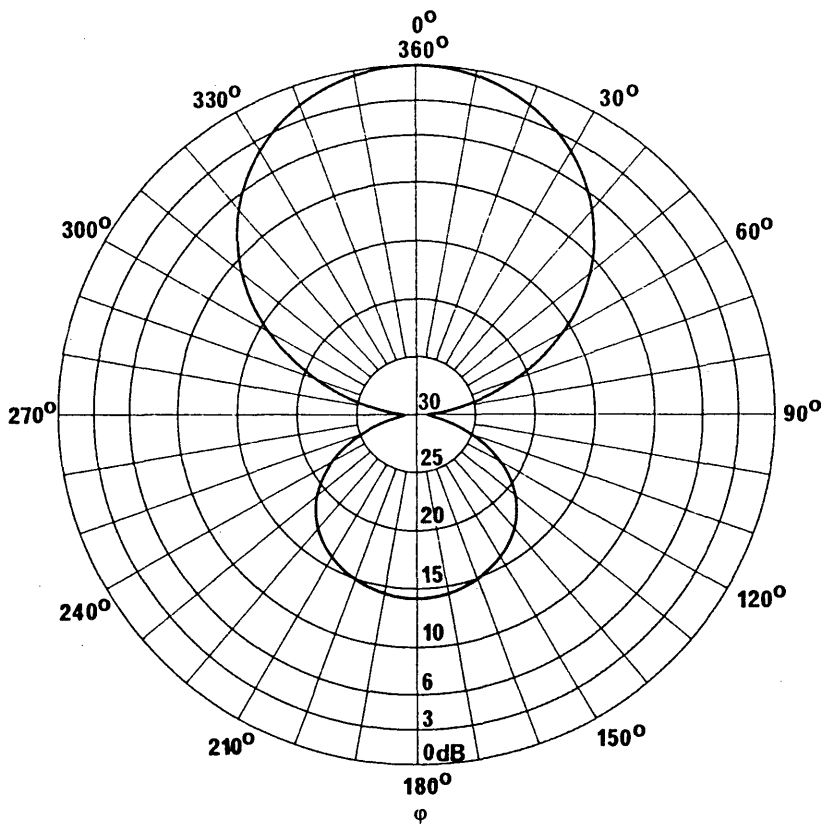


FIGURE 65c  
Forward radiation pattern

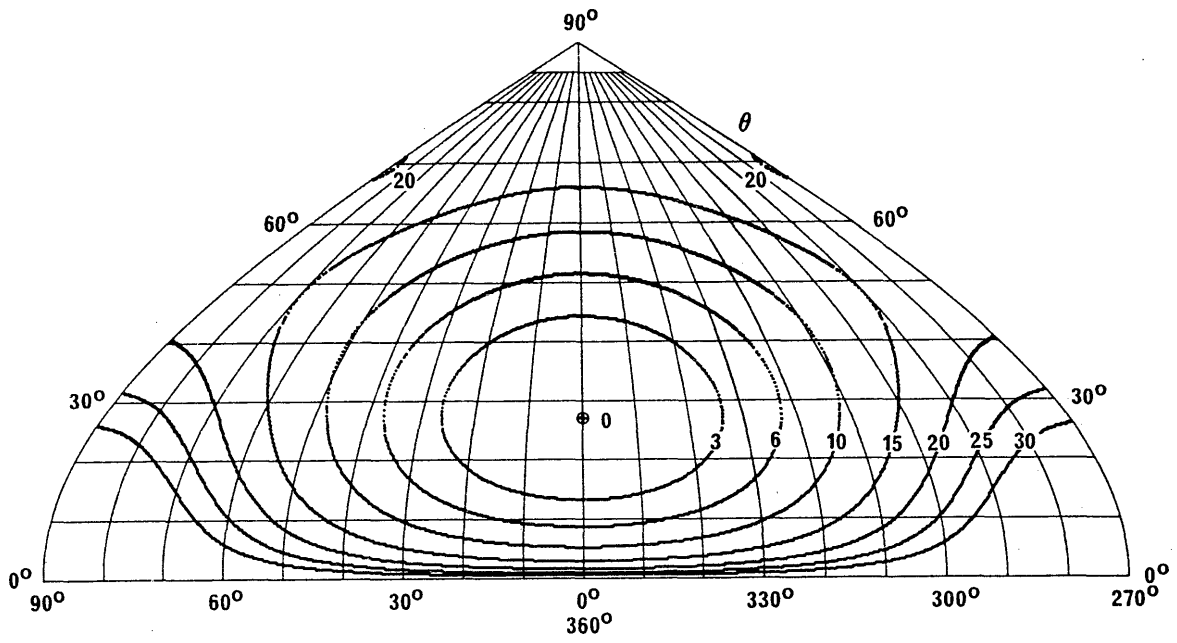


FIGURE 65d  
Backward radiation pattern

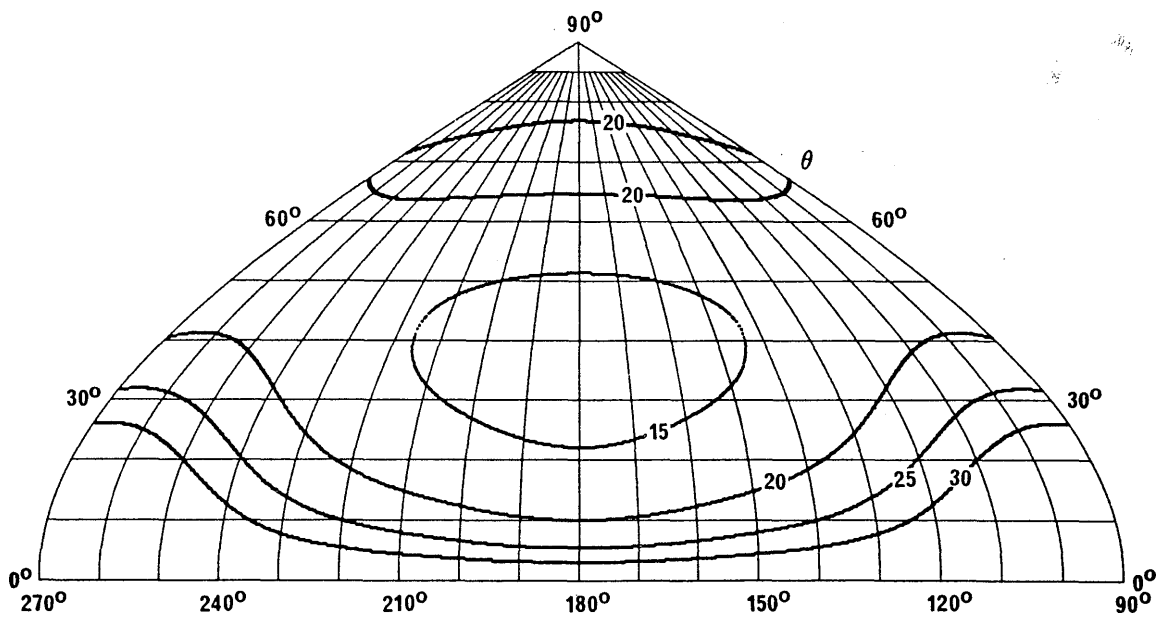


FIGURE 66a

Vertical pattern at 0° azimuth angle

Curtain antenna with  
tuned reflector  
HR 2/2/0.5  
 $F_R = 1$   
 $\theta = 17^\circ$   
 $G_i = 15.5$  dB

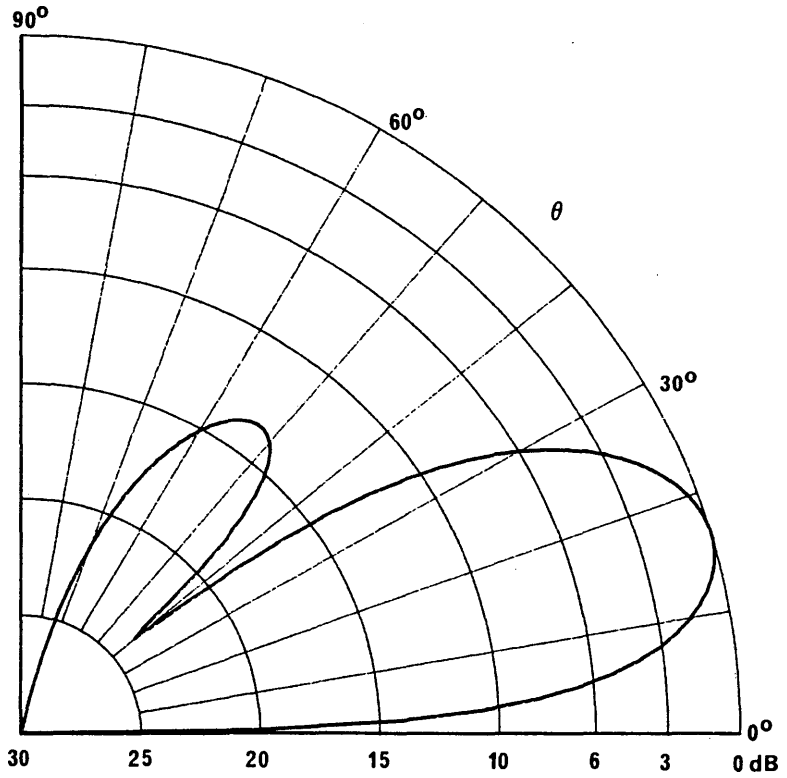


FIGURE 66b

Horizontal pattern at 17° elevation angle

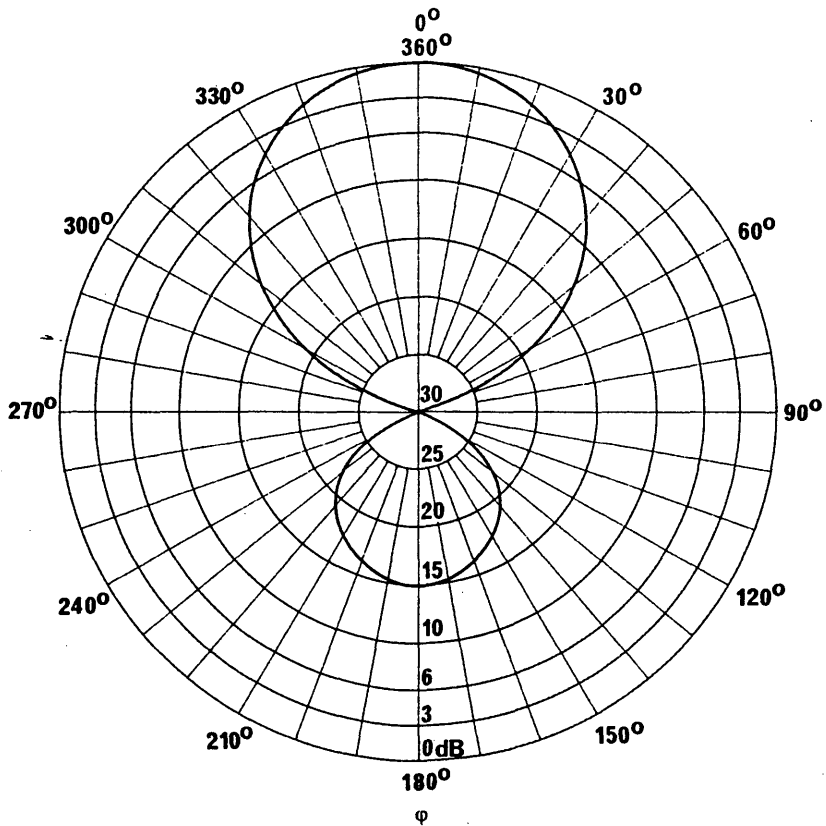


FIGURE 66c  
Forward radiation pattern

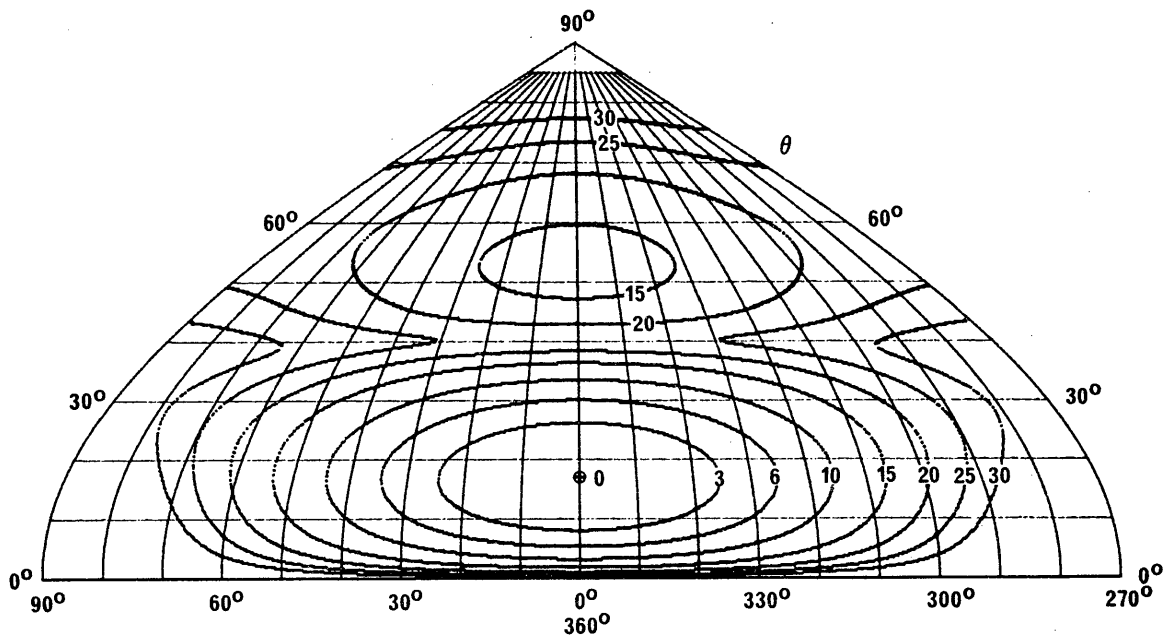


FIGURE 66d  
Backward radiation pattern

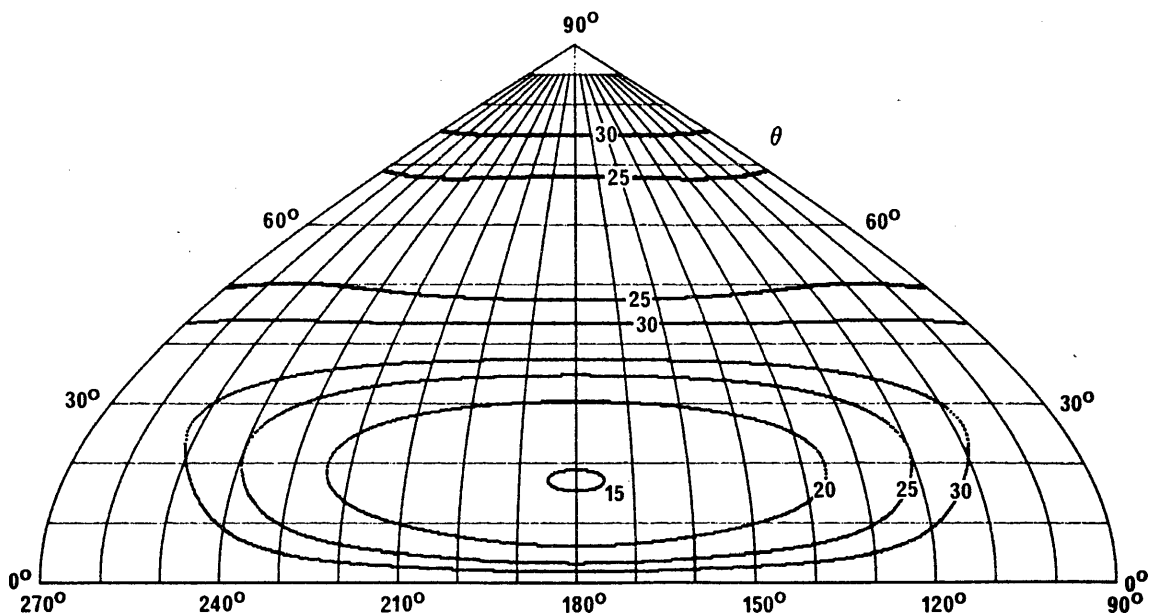


FIGURE 67a

Vertical pattern at 9° azimuth angle

Curtain antenna with  
tuned reflector  
HRS 2/2/0.5  
 $F_R = 1$   
 $s = 15^\circ$   
 $\theta = 17^\circ$   
 $\phi = 9^\circ$   
 $G_i = 15.5 \text{ dB}$

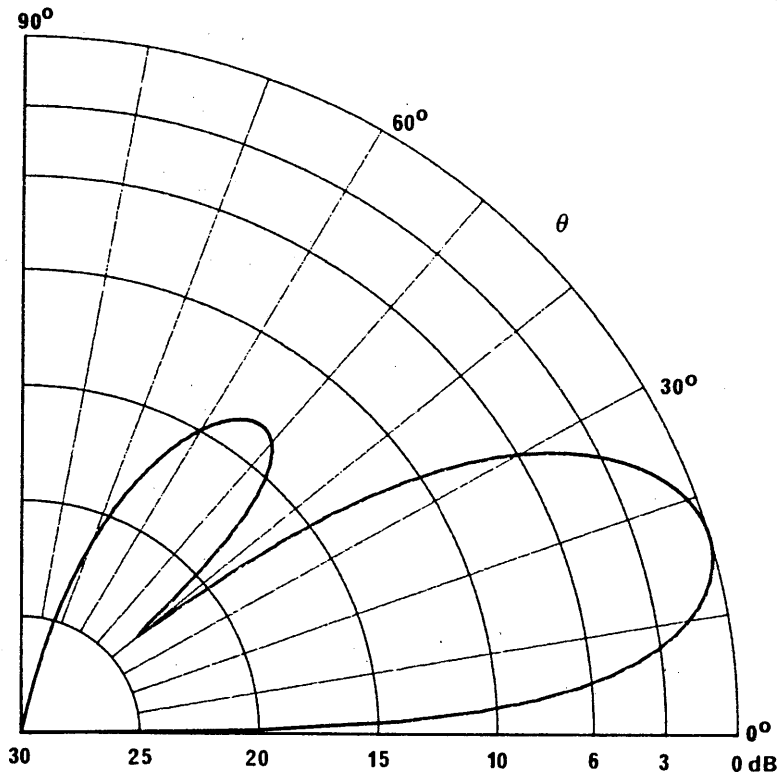


FIGURE 67b

Horizontal pattern at 17° elevation angle

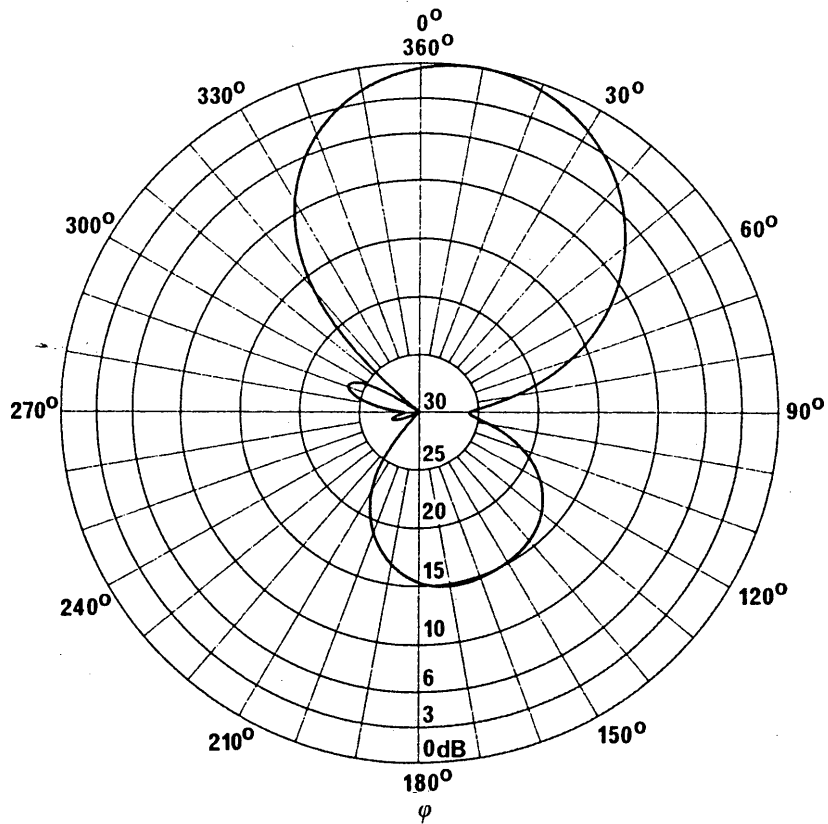


FIGURE 67c  
Forward radiation pattern

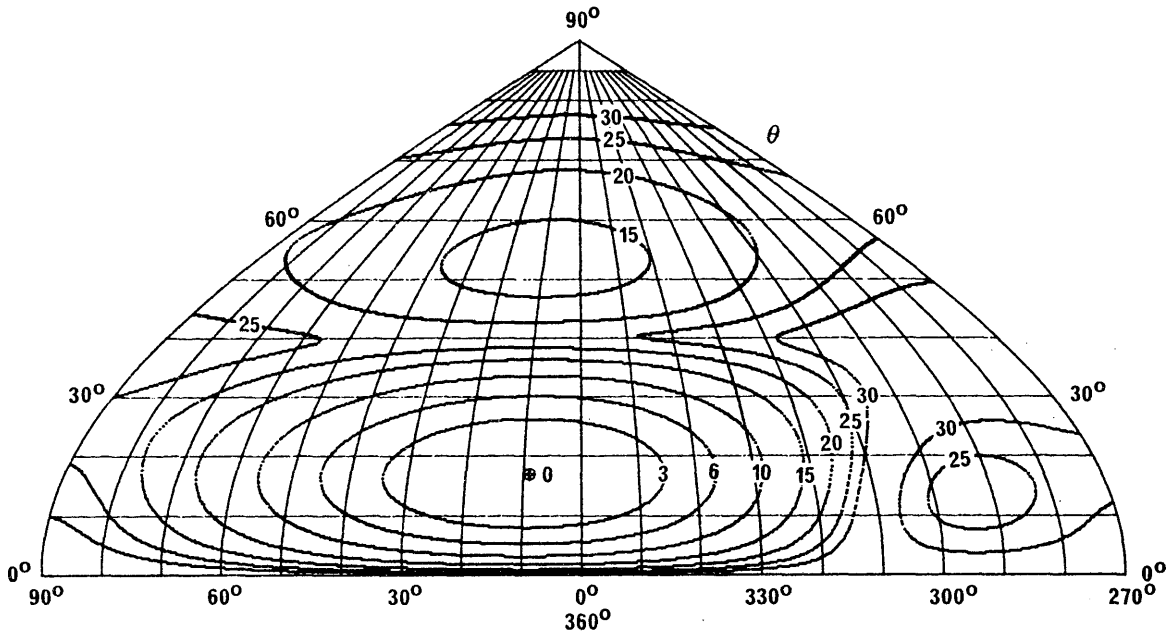


FIGURE 67d  
Backward radiation pattern

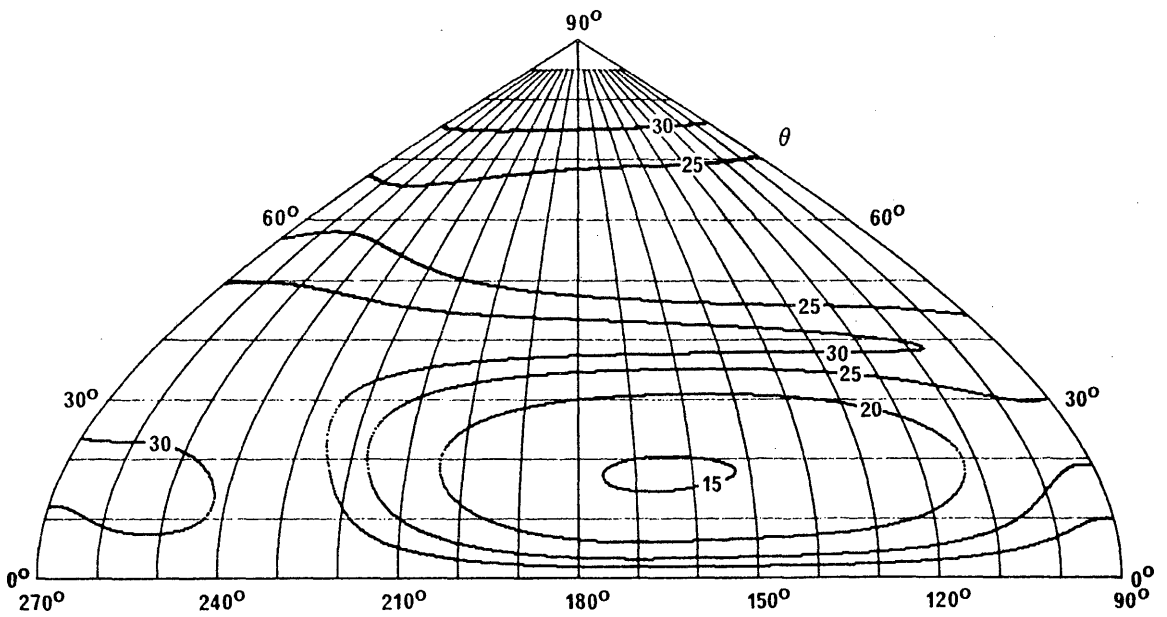


FIGURE 68a

Vertical pattern at 0° azimuth angle

Curtain antenna with aperiodic screen reflector  
 HR 2/2/0.5  
 $F_R = 1$   
 $\theta = 17^\circ$   
 $G_i = 16.0$  dB

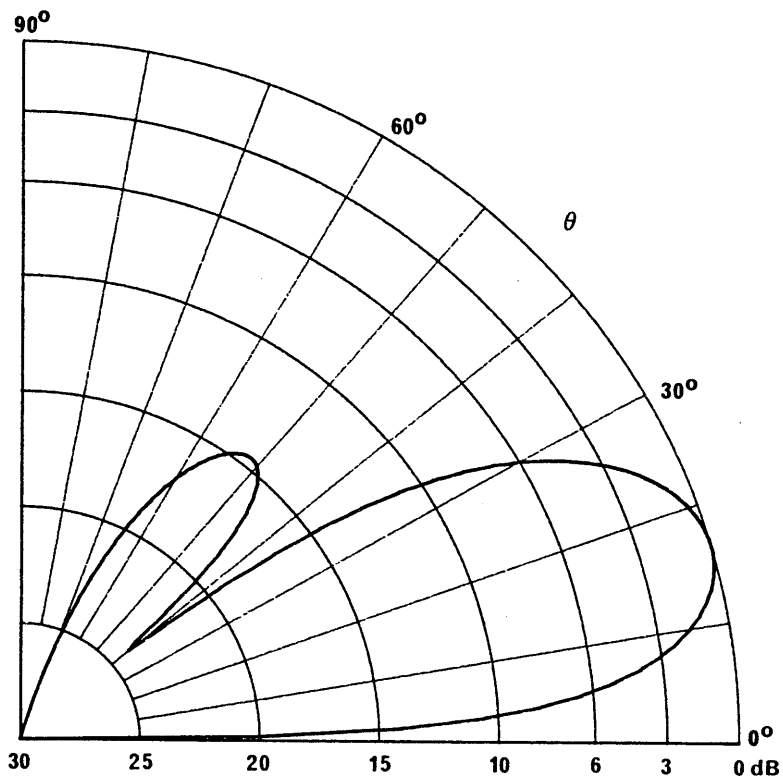


FIGURE 68b

Horizontal pattern at 17° elevation angle

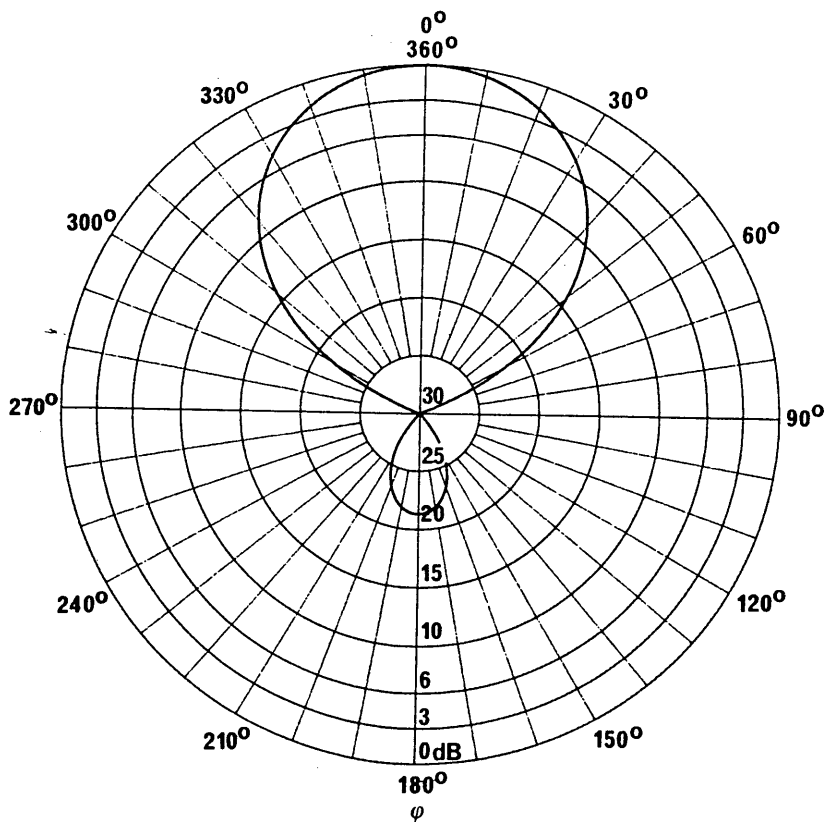


FIGURE 68c  
Forward radiation pattern

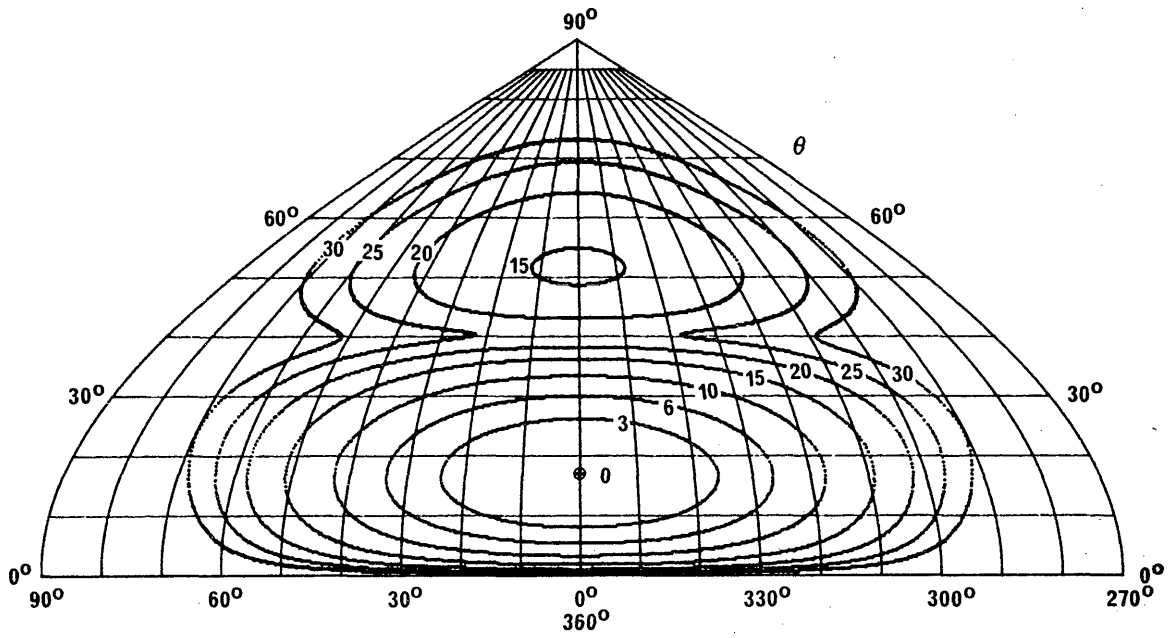


FIGURE 68d  
Backward radiation pattern

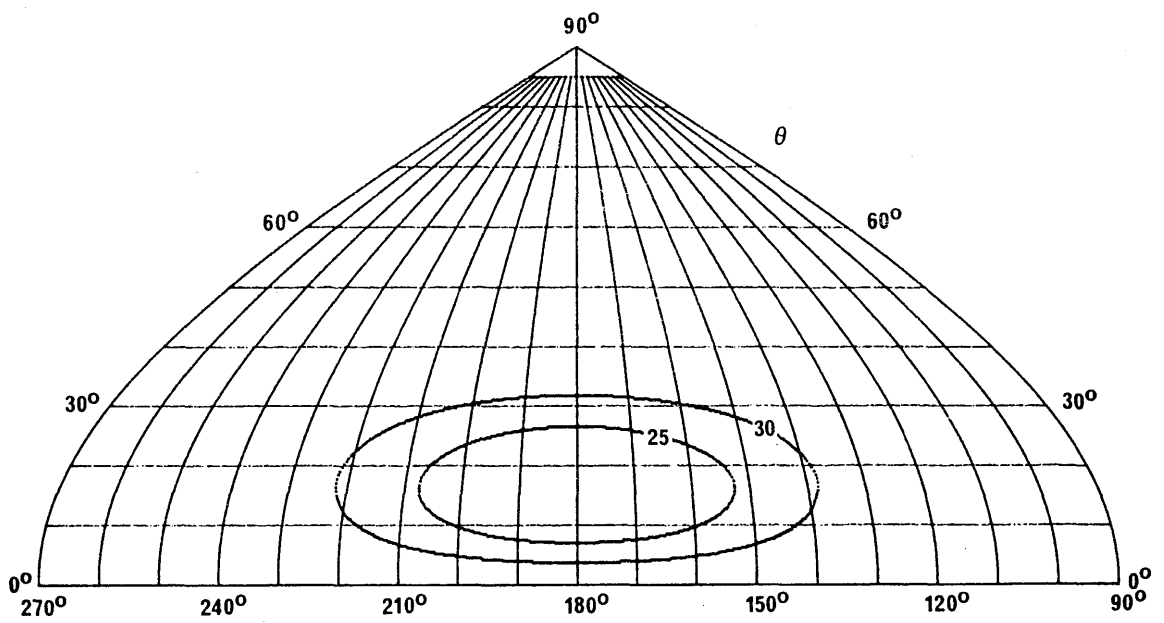


FIGURE 69a  
Vertical pattern at 9° azimuth angle

Curtain antenna with aperiodic  
screen reflector  
HRS 2/2/0.5  
 $F_R = 1$   
 $s = 15^\circ$   
 $\theta = 17^\circ$   
 $\phi = 9^\circ$   
 $G_i = 16.0 \text{ dB}$

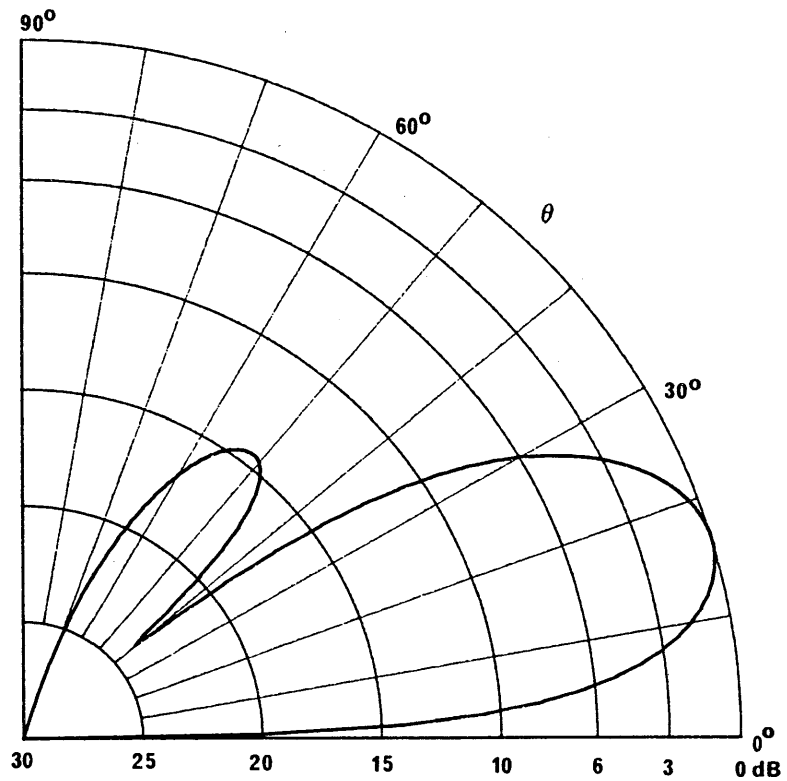


FIGURE 69b  
Horizontal pattern at 17° elevation angle

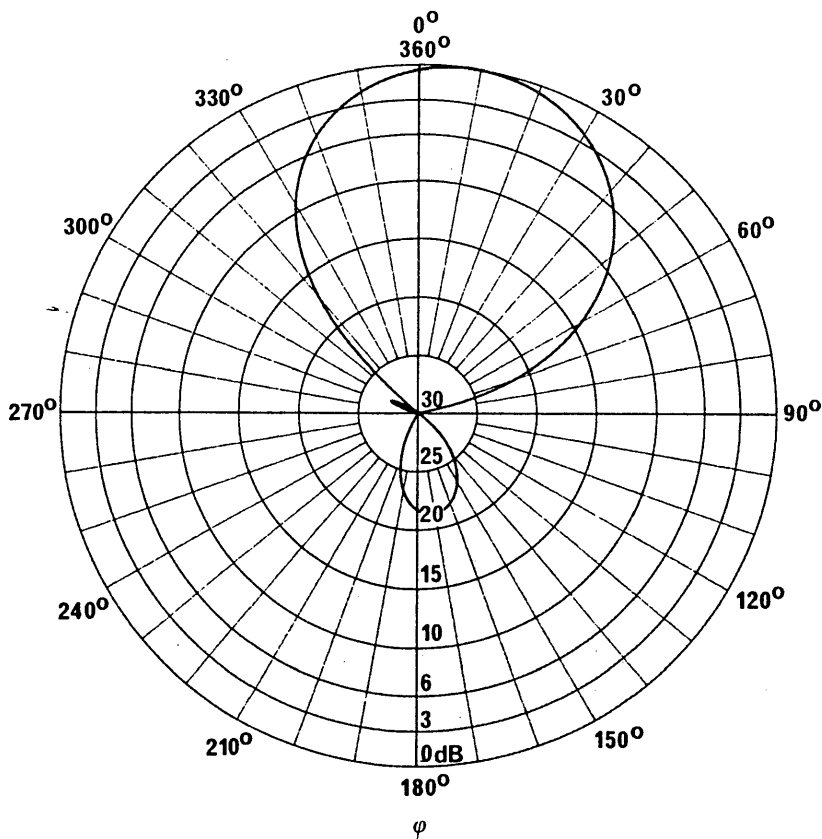


FIGURE 69c  
Forward radiation pattern

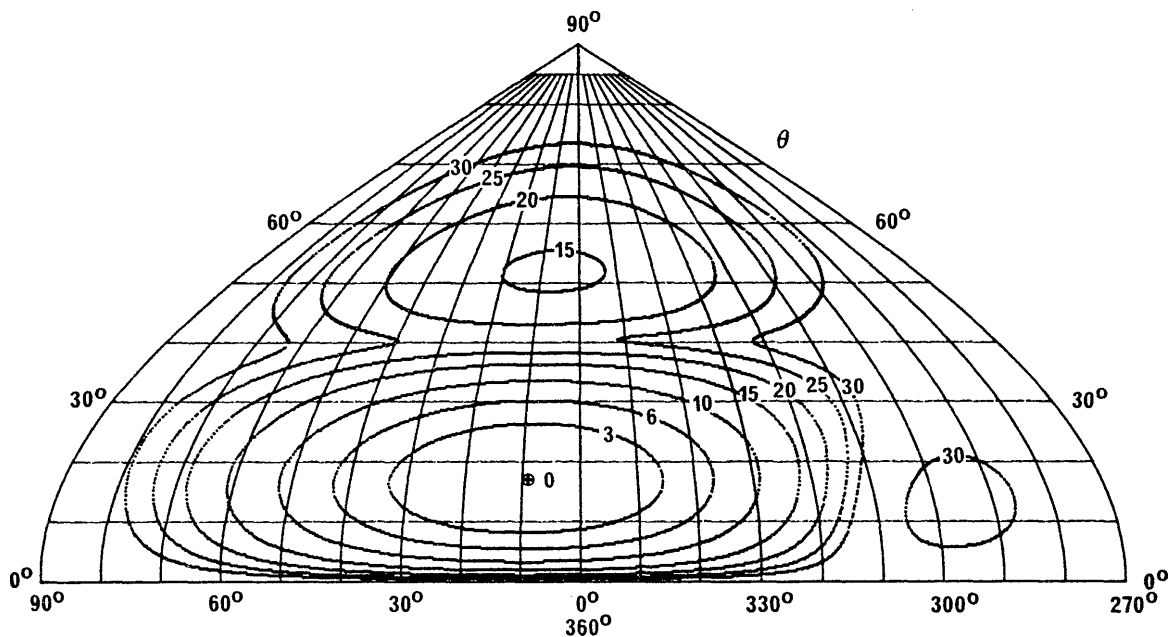


FIGURE 69d  
Backward radiation pattern

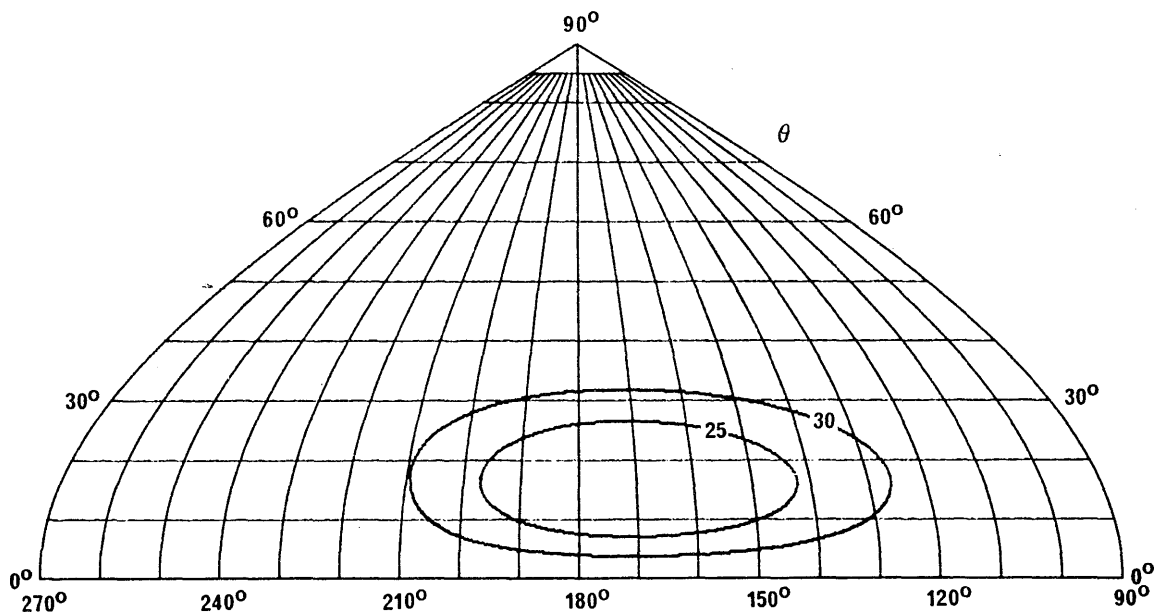


FIGURE 70a

Vertical pattern at 0° azimuth angle

Curtain antenna with aperiodic  
screen reflector  
HR 4/3/0.5  
 $F_R = 1$   
 $\theta = 12^\circ$   
 $G_i = 20.1$  dB

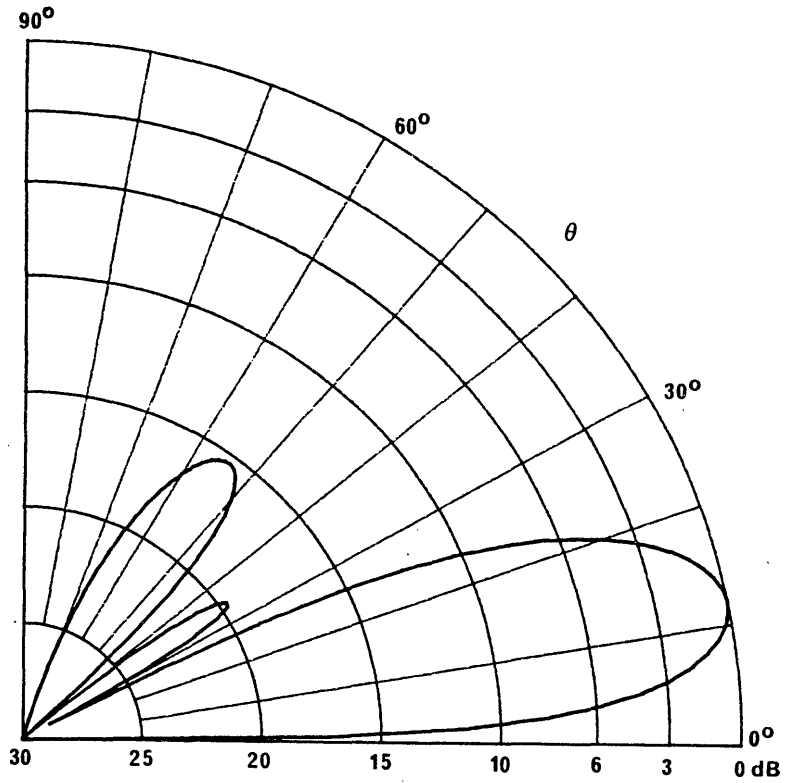


FIGURE 70b

Horizontal pattern at 12° elevation angle

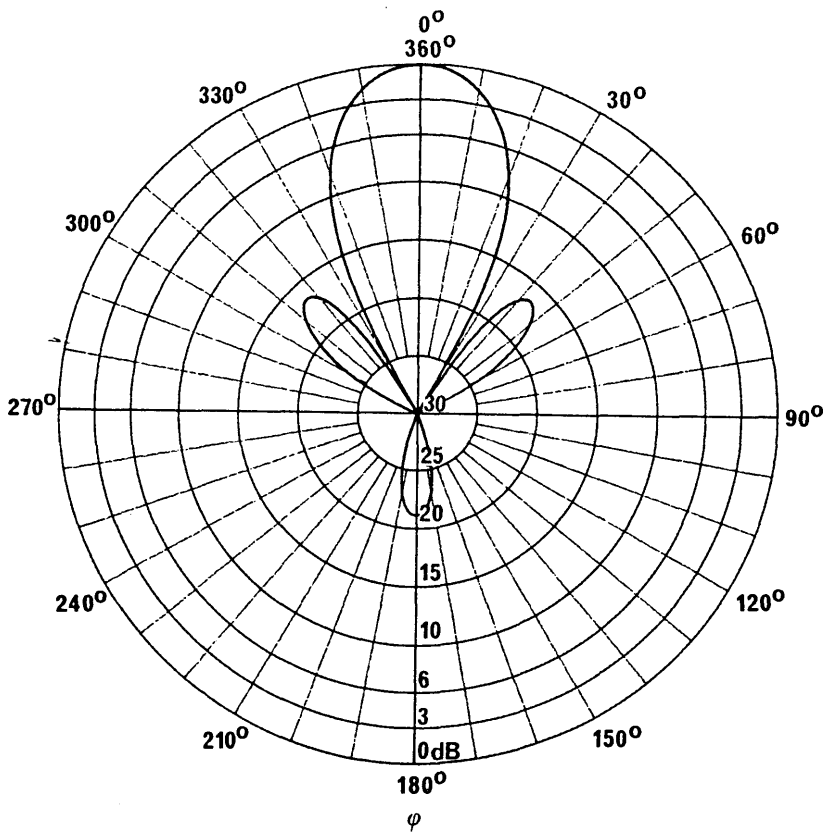


FIGURE 70c  
Forward radiation pattern

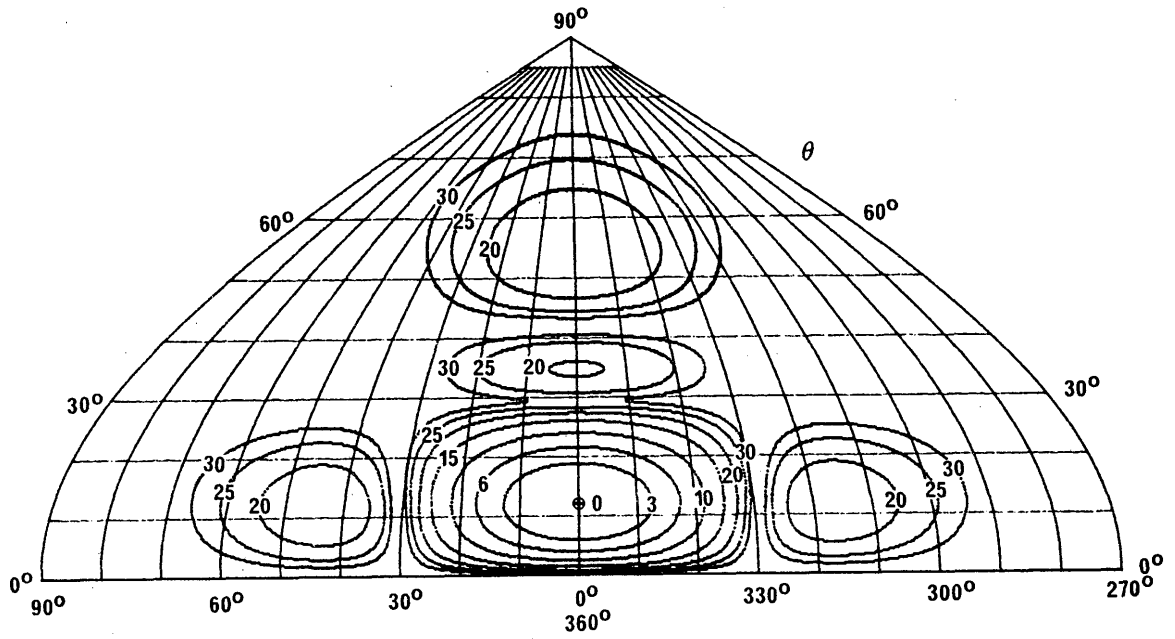


FIGURE 70d  
Backward radiation pattern

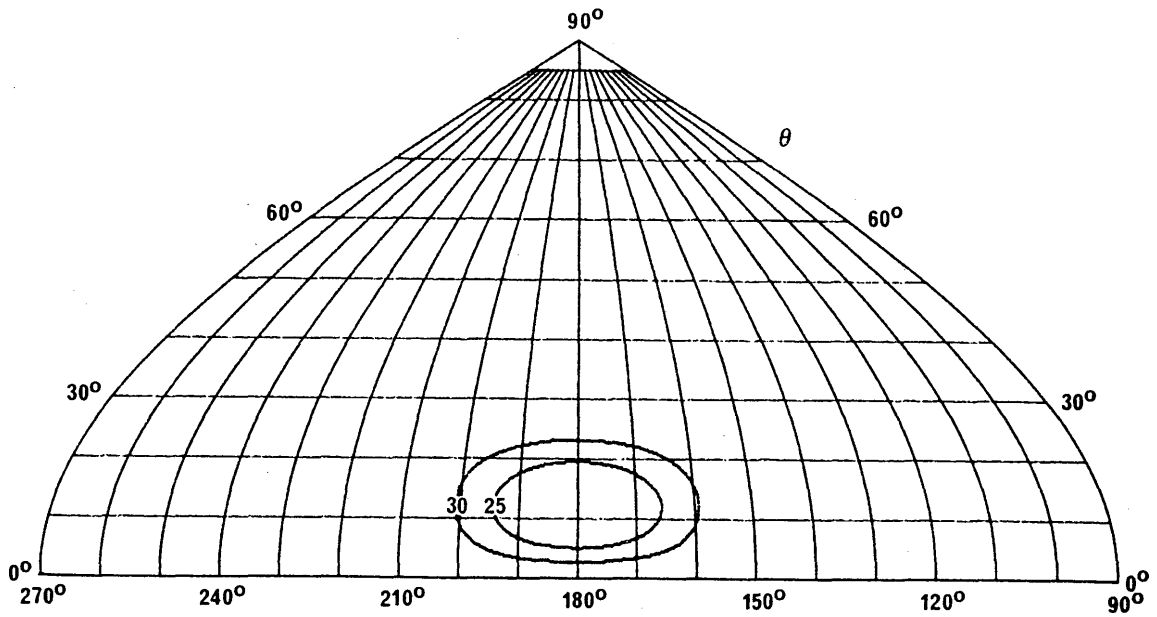


FIGURE 71a

Vertical pattern at 0° azimuth angle

Curtain antenna with aperiodic screen reflector

HR 4/4/0.5

$F_R = 0.7$

$\theta = 13^\circ$

$G_i = 18.6 \text{ dB}$

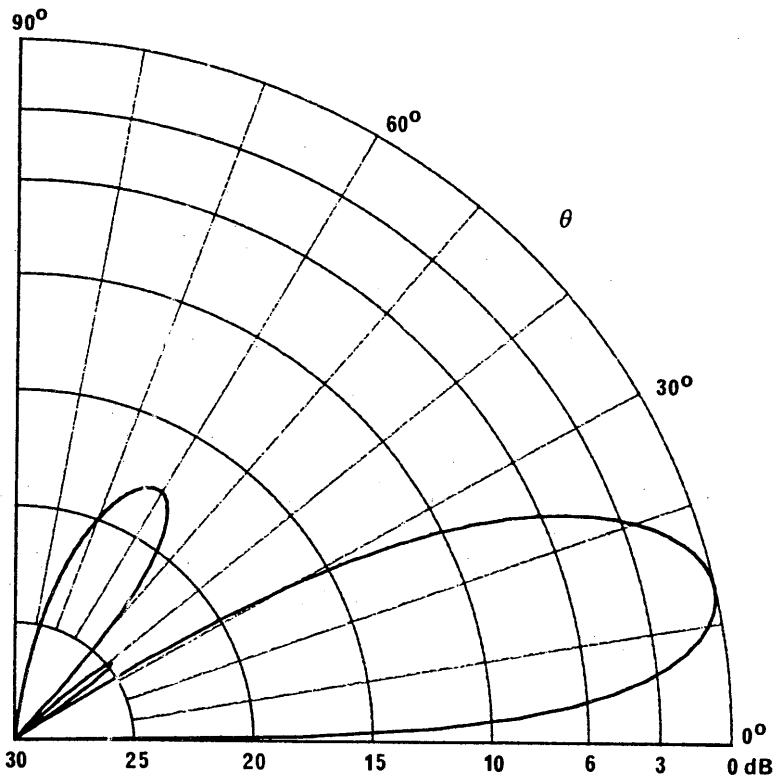


FIGURE 71b

Horizontal pattern at 13° elevation angle

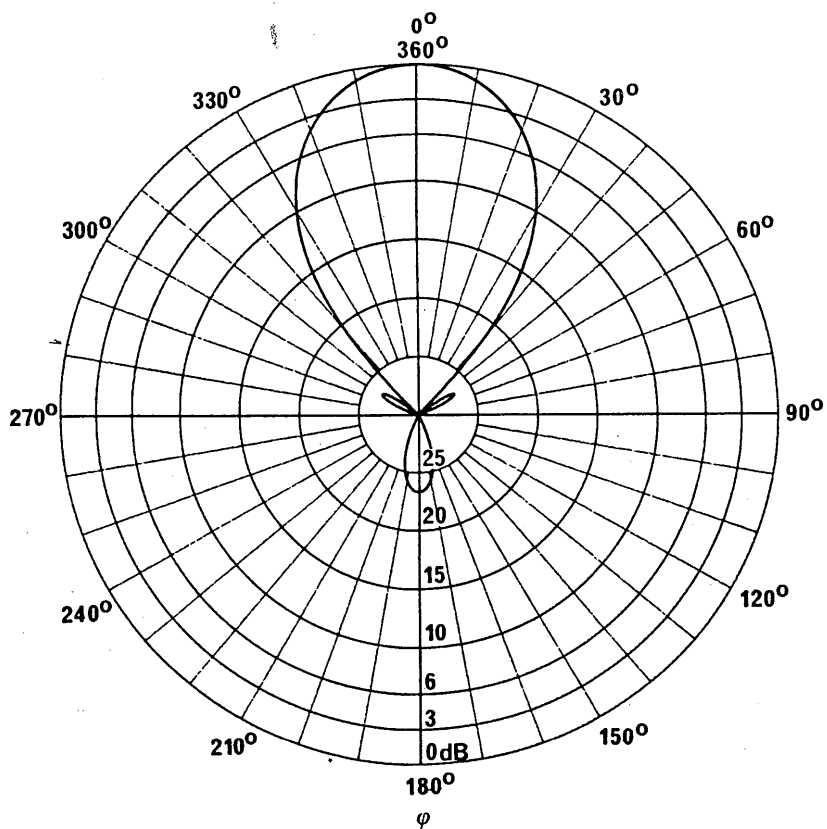


FIGURE 71c  
Forward radiation pattern

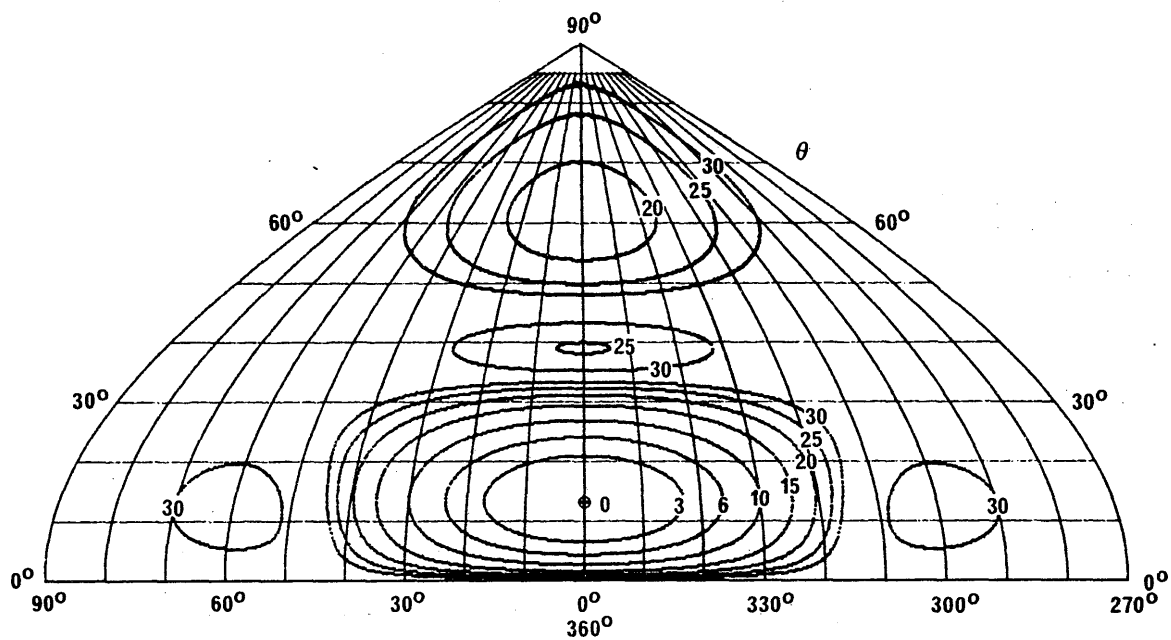


FIGURE 71d  
Backward radiation pattern

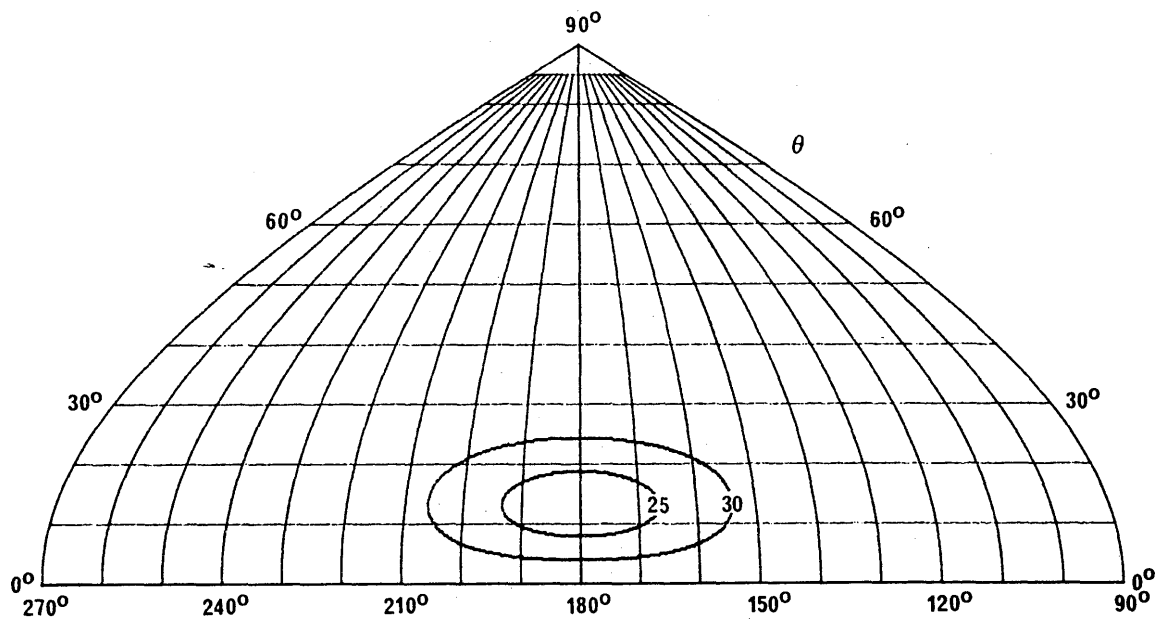


FIGURE 72a

Vertical pattern at 22° azimuth angle

Curtain antenna with aperiodic screen reflector

HRS 4/4/0.5

$F_R = 0.7$

$s = 30^\circ$

$\theta = 13^\circ$

$\phi = 22^\circ$

$G_i = 18.4 \text{ dB}$

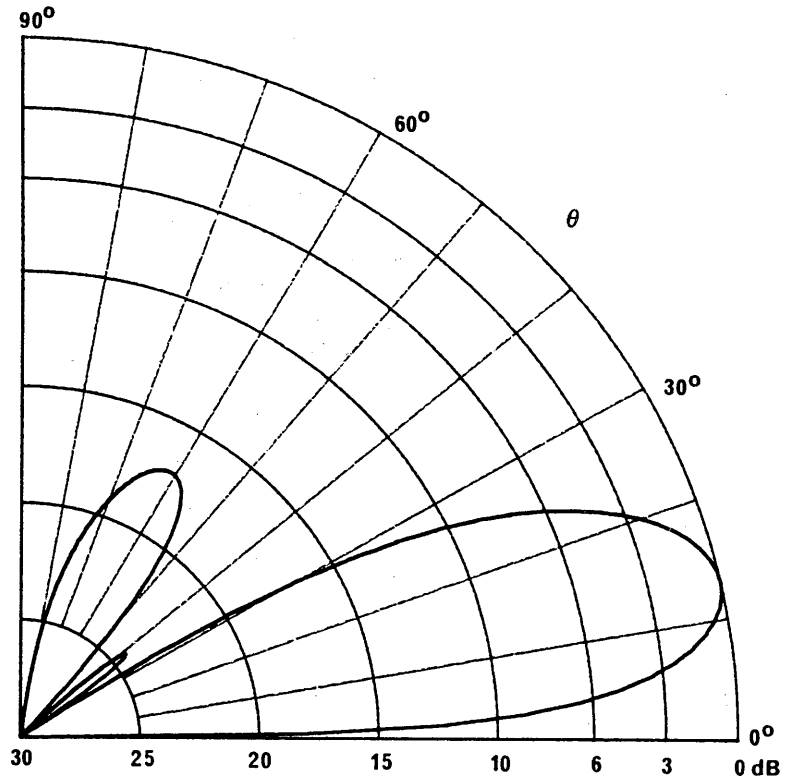


FIGURE 72b

Horizontal pattern at 13° elevation angle

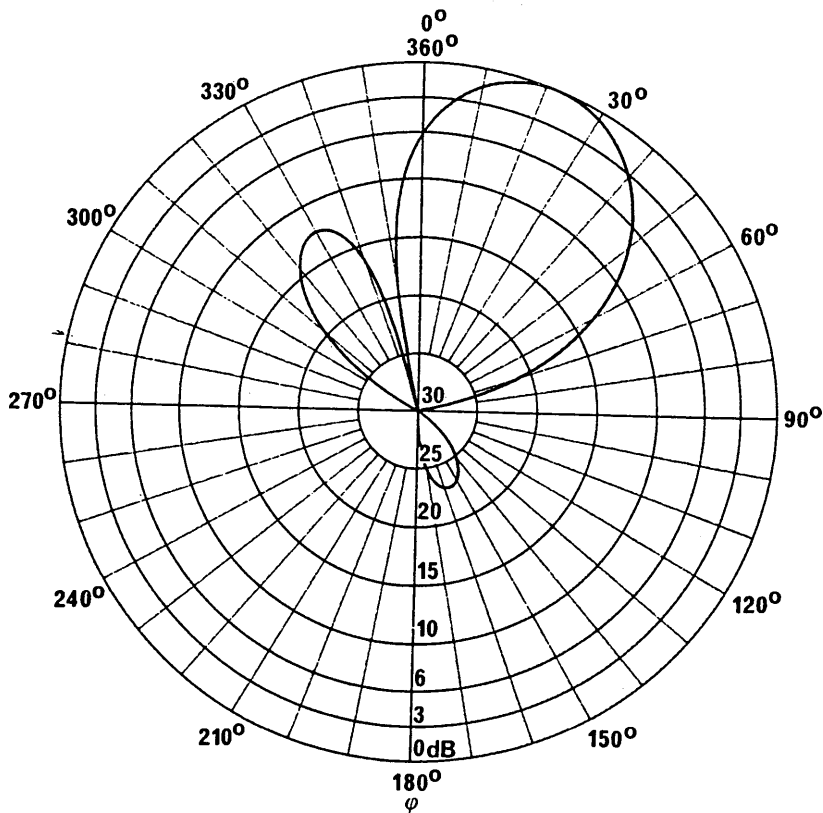


FIGURE 72c  
Forward radiation pattern

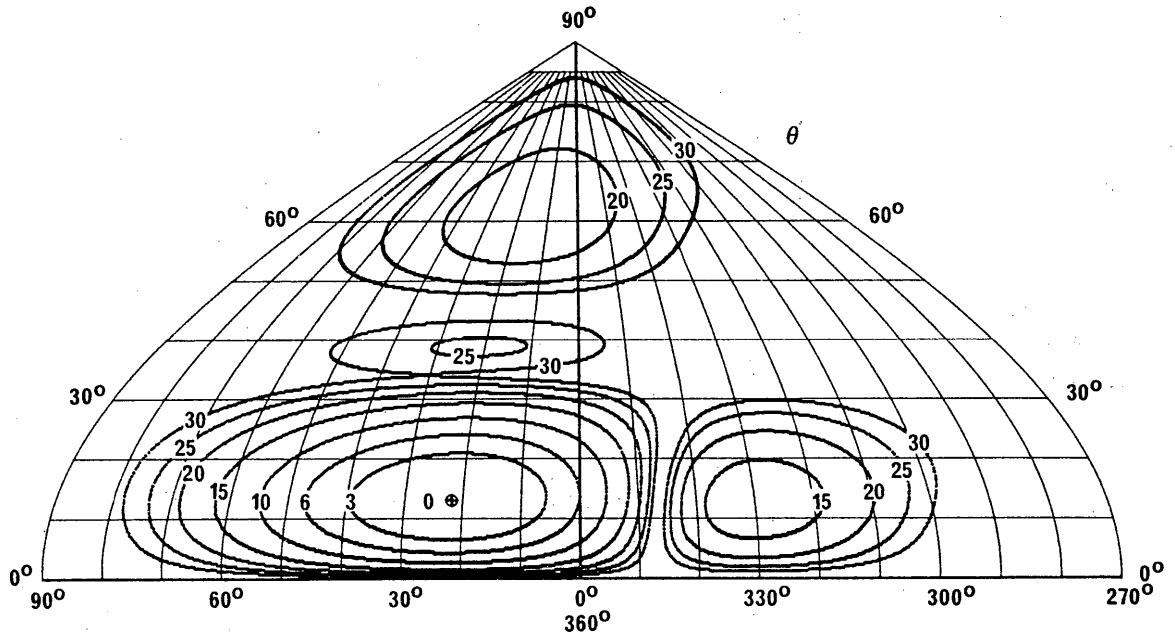


FIGURE 72d  
Backward radiation pattern

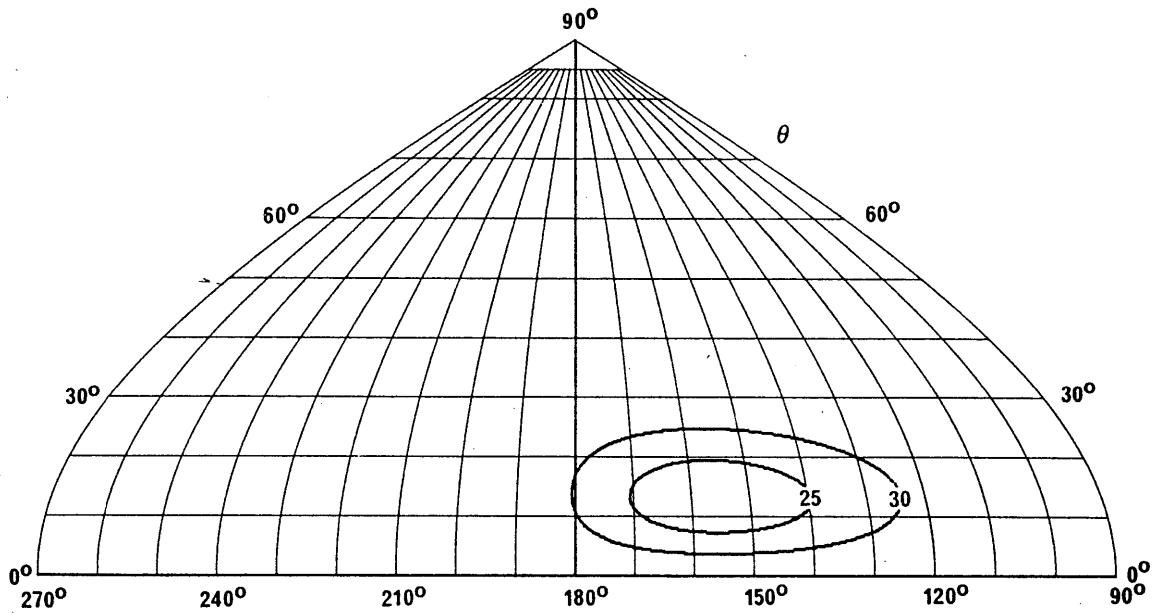


FIGURE 73a

Vertical pattern at 0° azimuth angle

Curtain antenna with aperiodic  
screen reflector  
HR 4/4/0.5  
 $F_R = 1.0$   
 $\theta = 9^\circ$   
 $G_i = 21.2$  dB

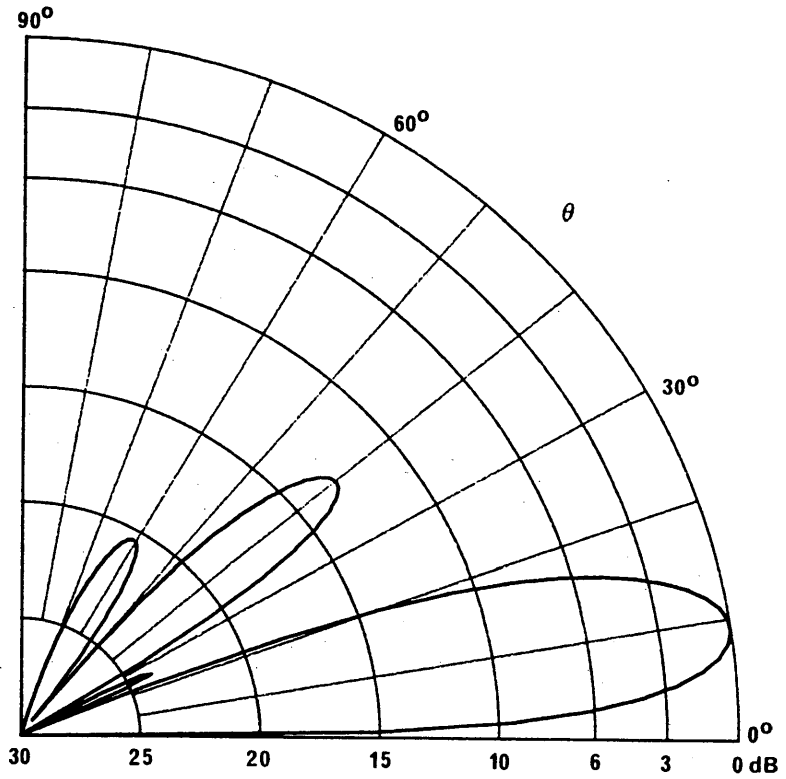


FIGURE 73b

Horizontal pattern at 9° elevation angle

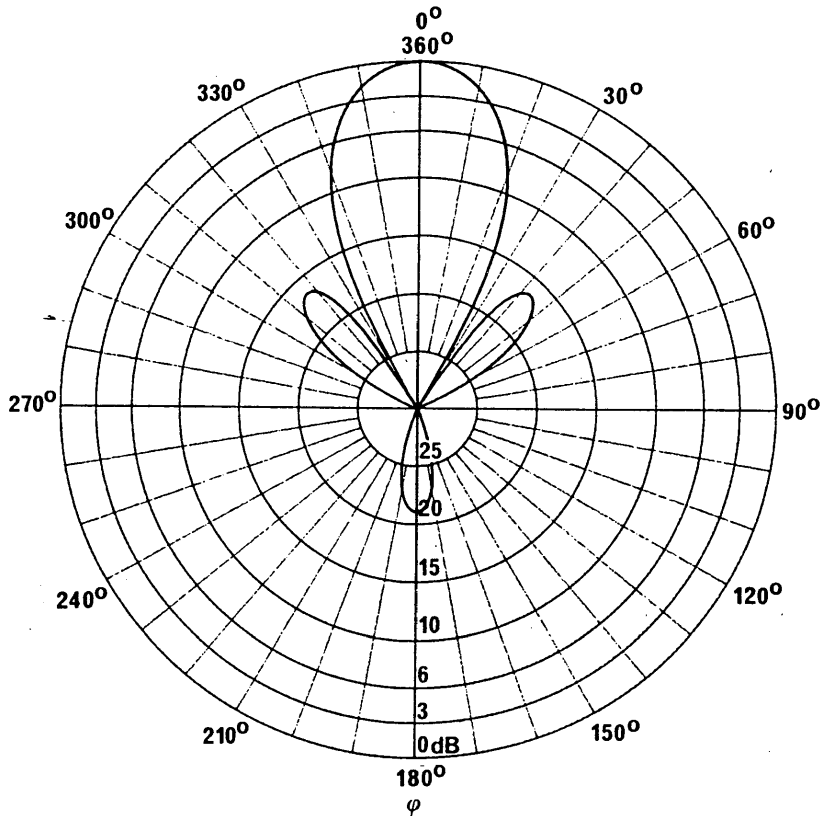


FIGURE 73c  
Forward radiation pattern

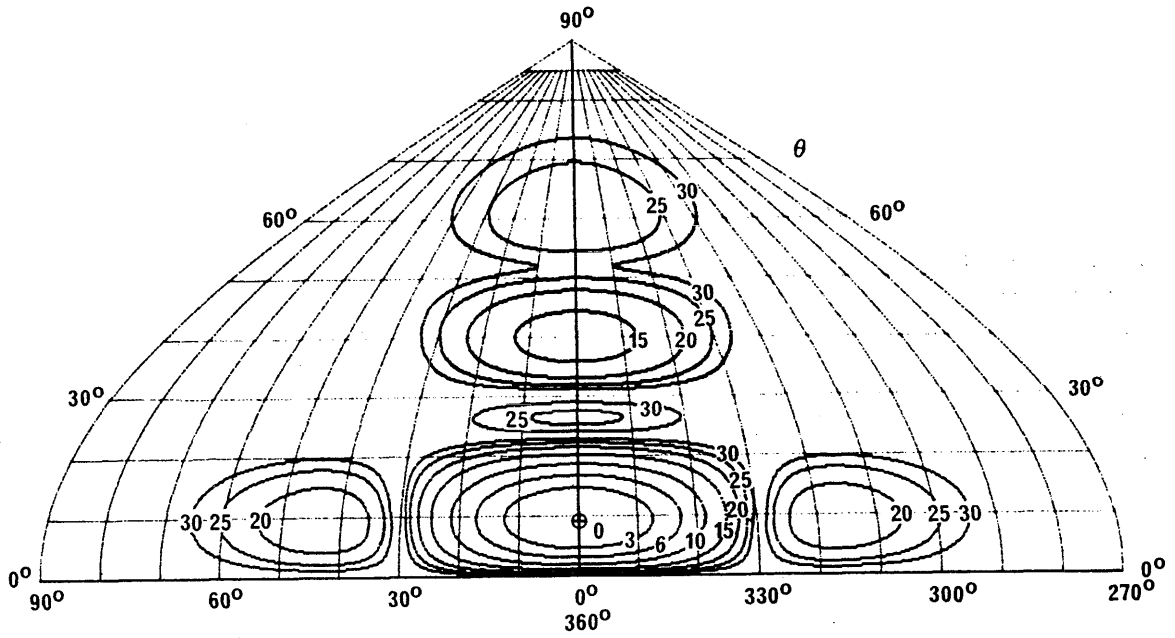


FIGURE 73d  
Backward radiation pattern

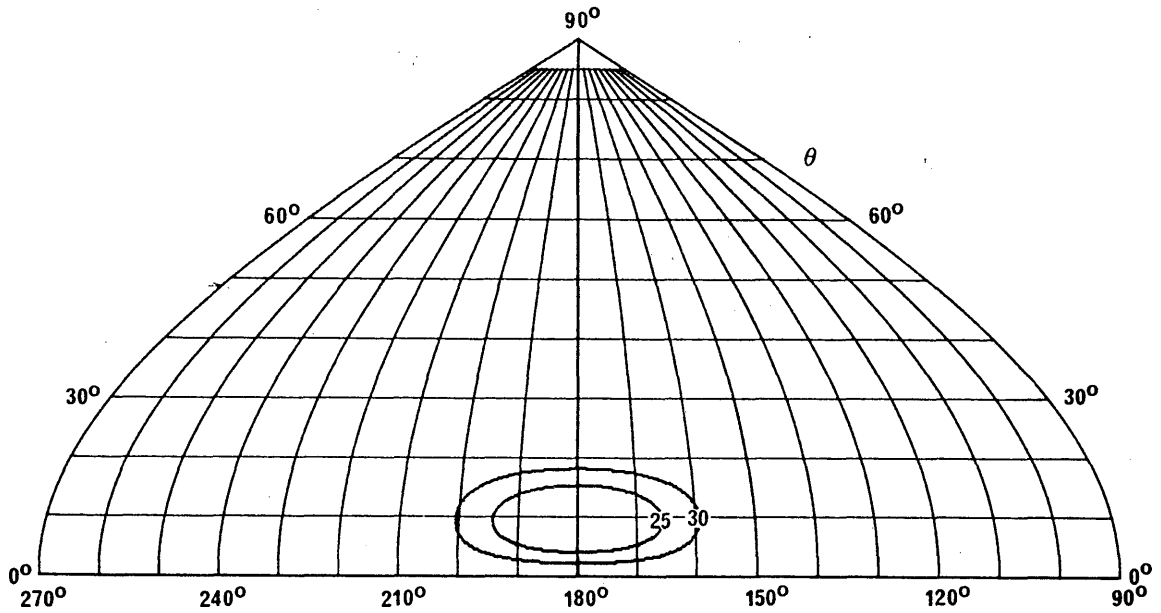


FIGURE 74a

Vertical pattern at 26° azimuth angle

Curtain antenna with  
aperiodic screen reflector

HRS 4/4/0.5

$F_R = 1.0$

$s = 30^\circ$

$\theta = 9^\circ$

$\phi = 26^\circ$

$G_i = 20.8 \text{ dB}$

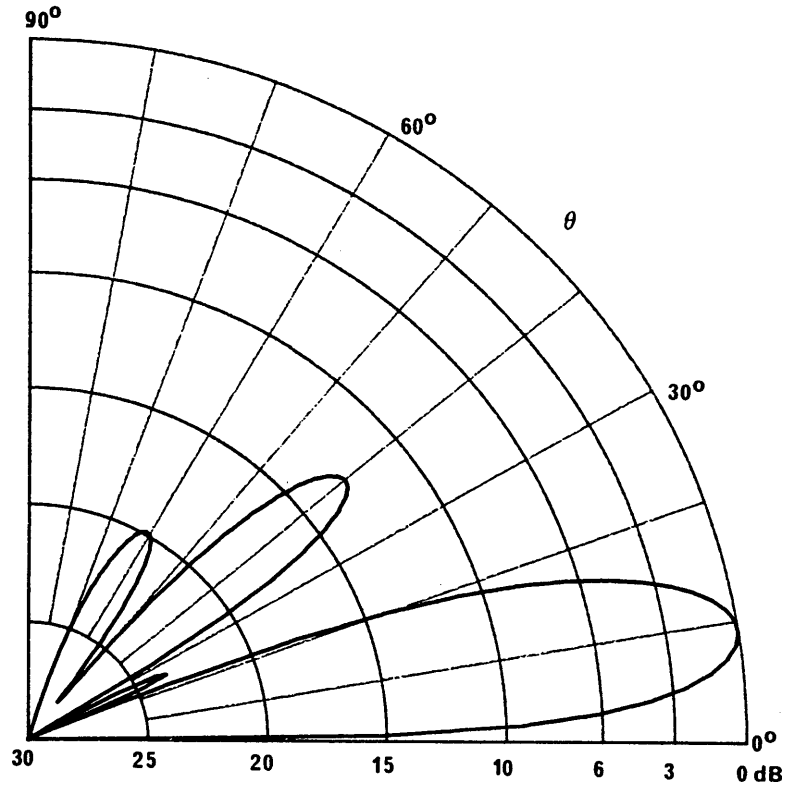


FIGURE 74b

Horizontal pattern at 9° elevation angle

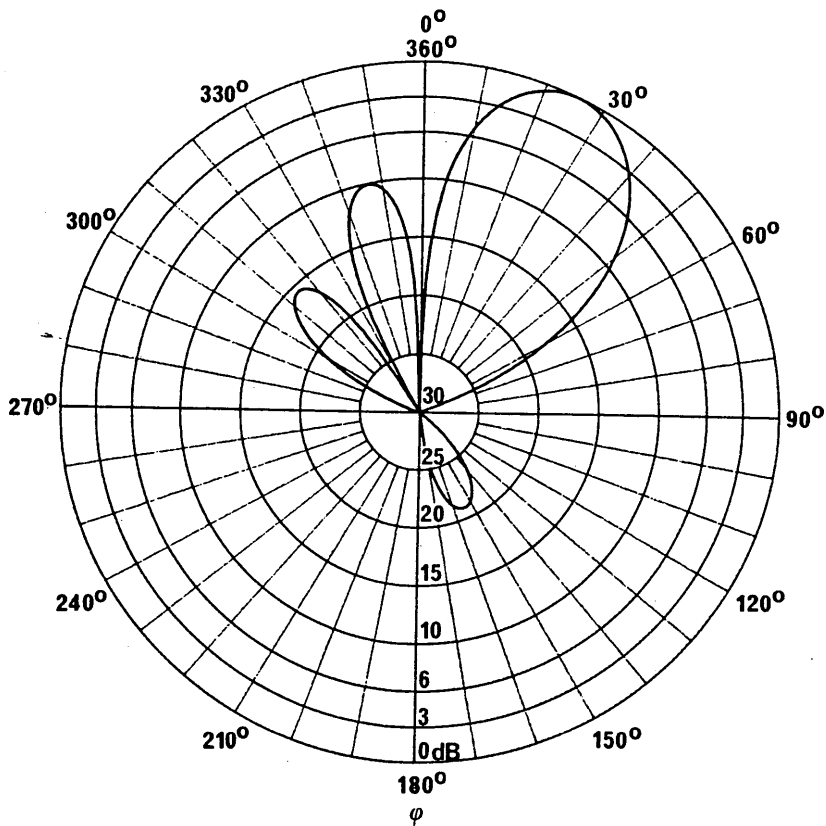


FIGURE 74c  
Forward radiation pattern

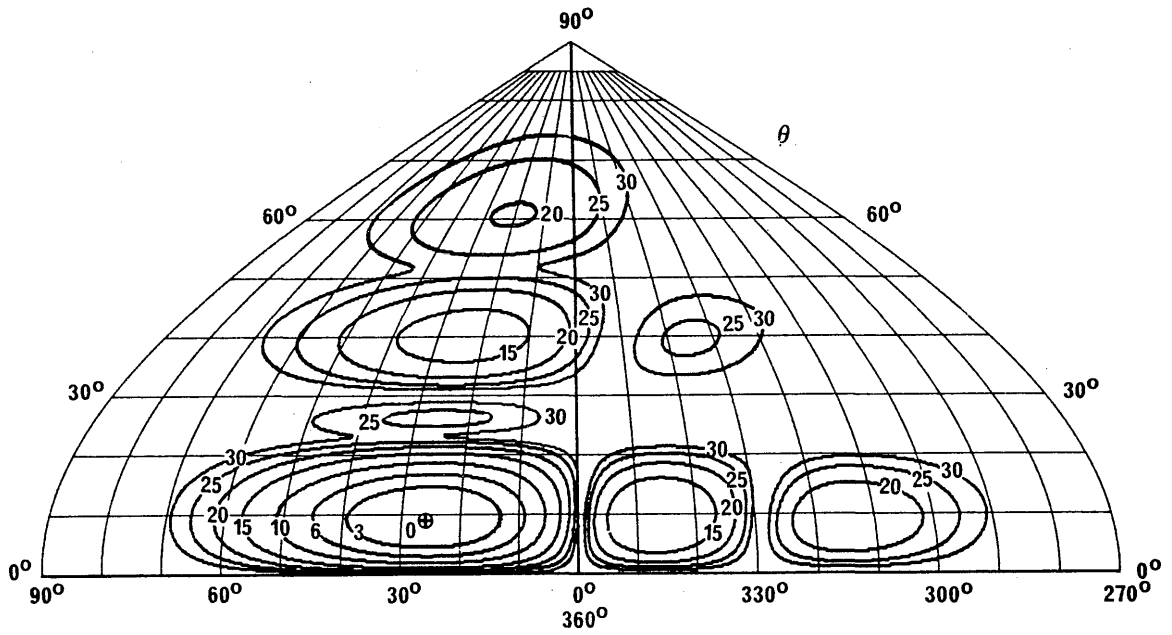


FIGURE 74d  
Backward radiation pattern

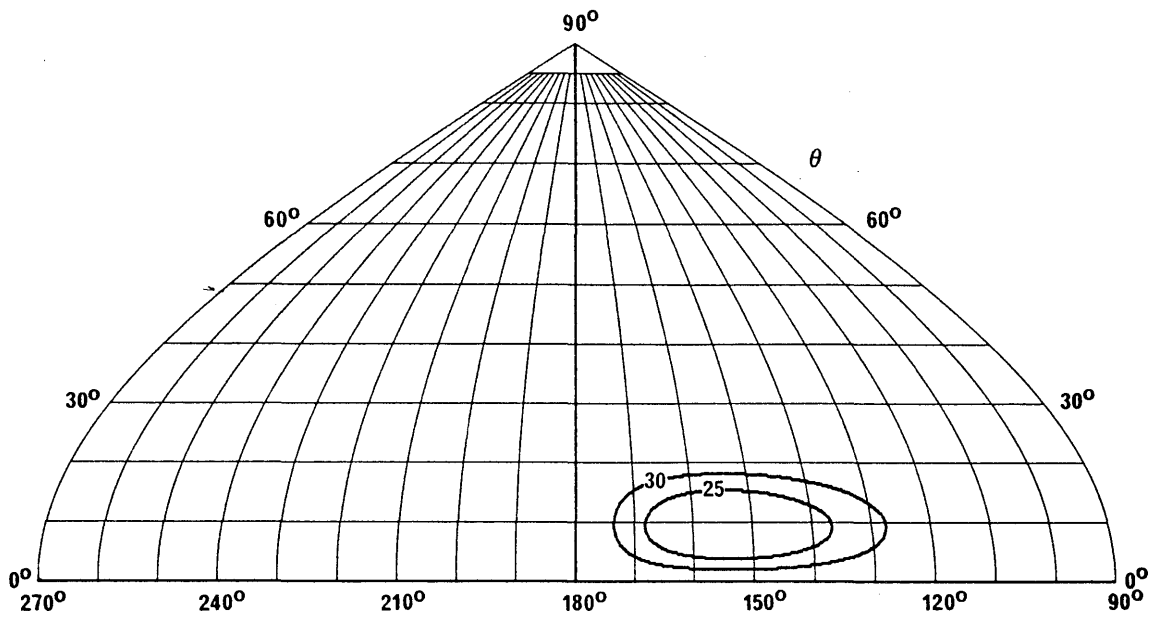


FIGURE 75a

Vertical pattern at 0° azimuth angle

Curtain antenna with aperiodic  
screen reflector  
HR 4/4/0.5  
 $F_R = 1.4$   
 $\theta = 7^\circ$   
 $G_i = 23.2$  dB

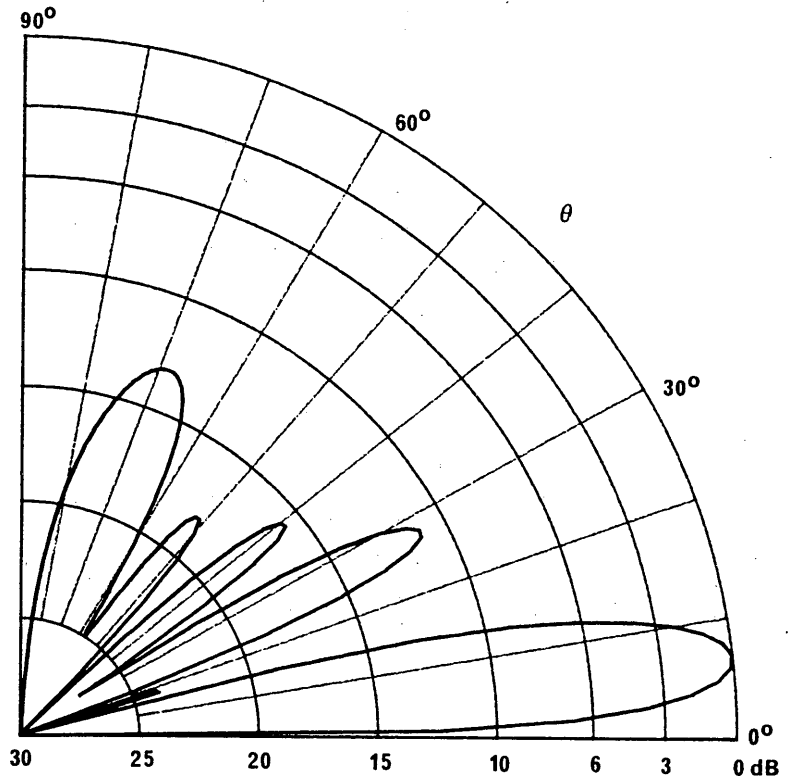


FIGURE 75b

Horizontal pattern at 7° elevation angle

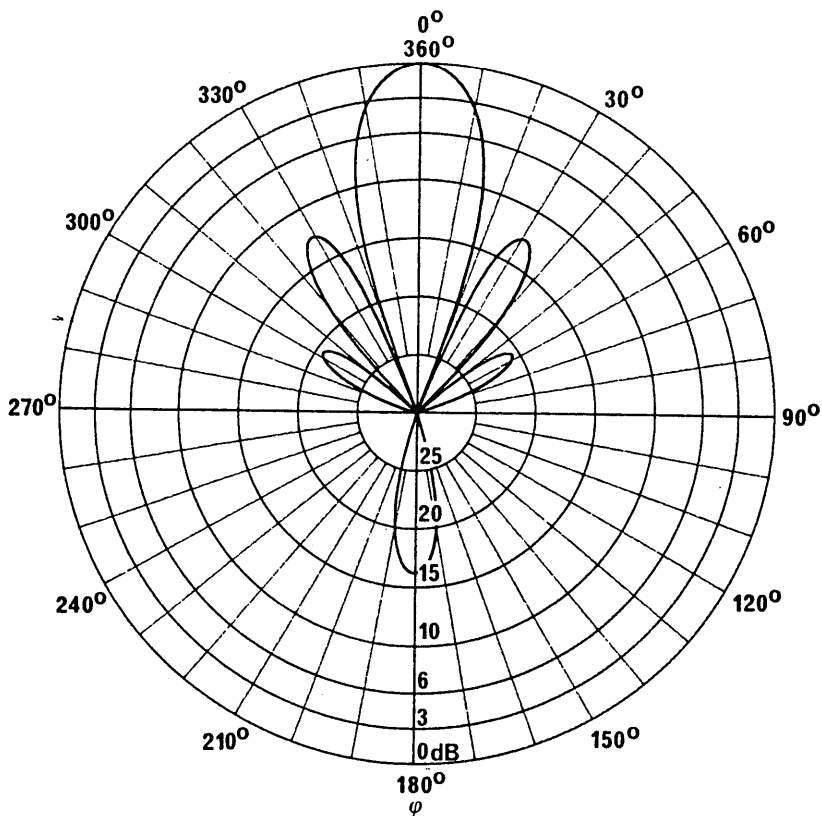


FIGURE 75c

Forward radiation pattern

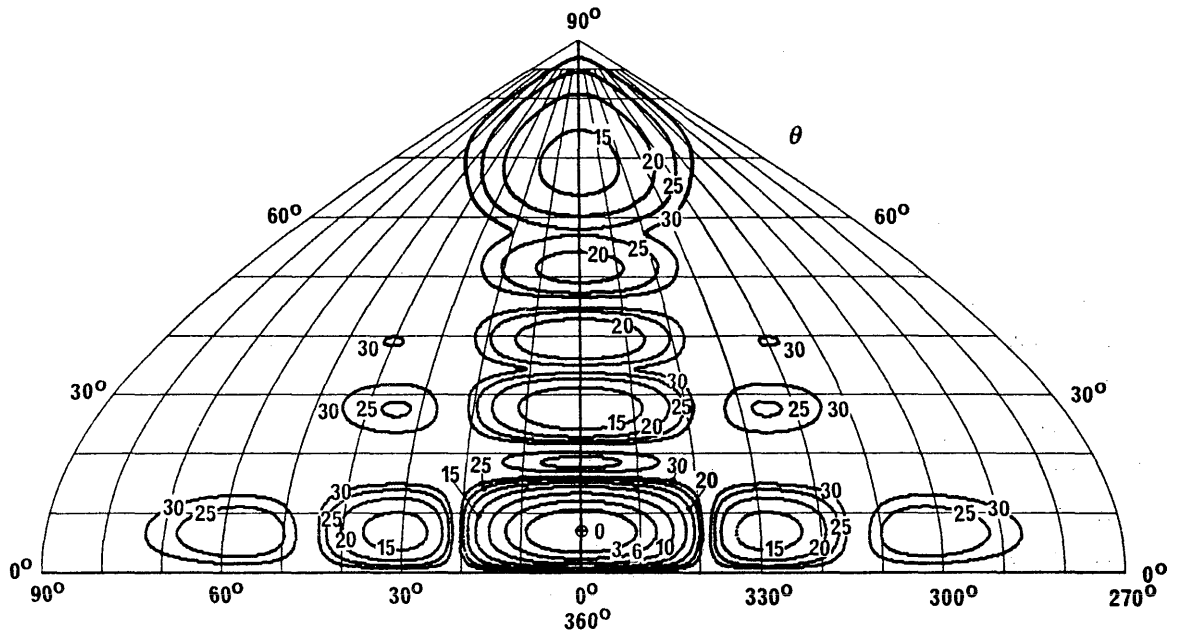


FIGURE 75d

Backward radiation pattern

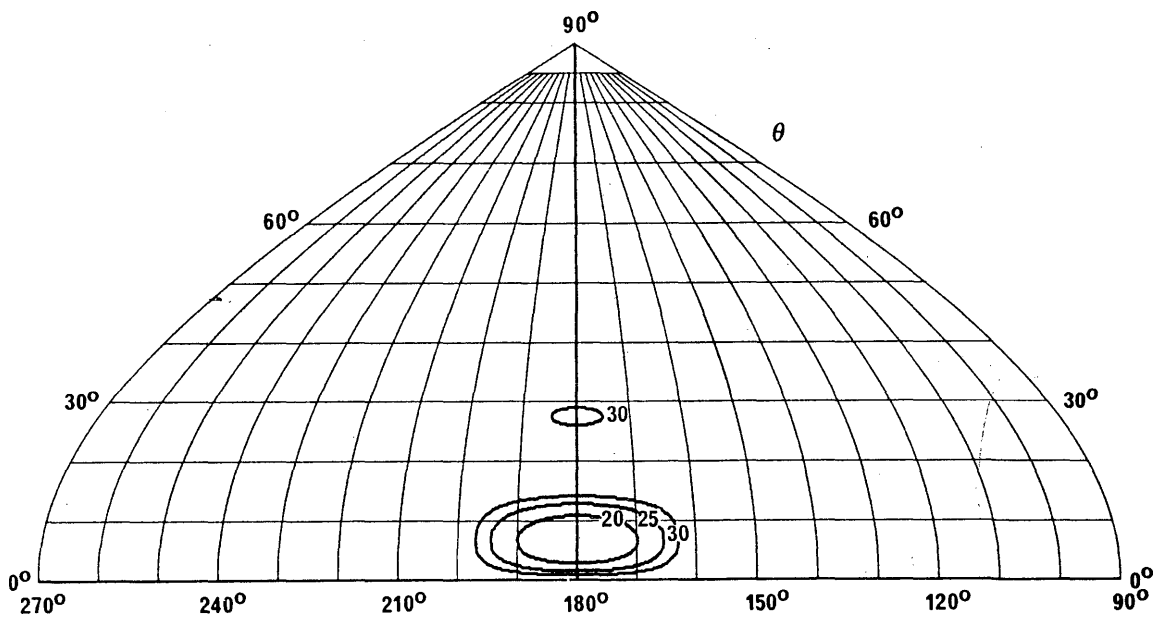


FIGURE 76a

Vertical pattern at 28° azimuth angle

Curtain antenna with aperiodic screen reflector  
 HRS 4/4/0.5  
 $F_R = 1.4$   
 $s = 30^\circ$   
 $\theta = 7^\circ$   
 $\phi = 28^\circ$   
 $G_i = 22.2$  dB

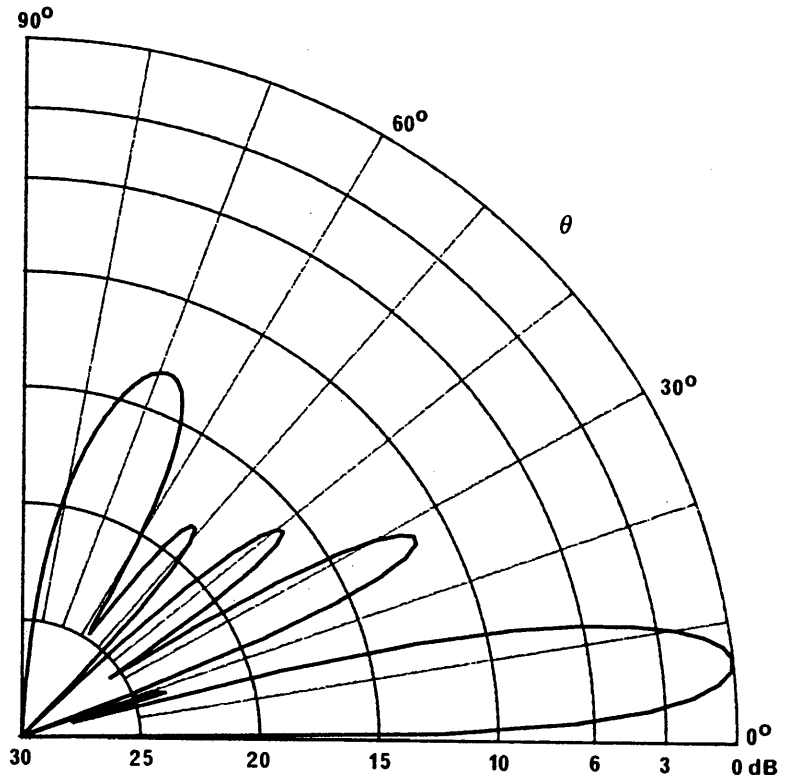


FIGURE 76b

Horizontal pattern at 7° elevation angle

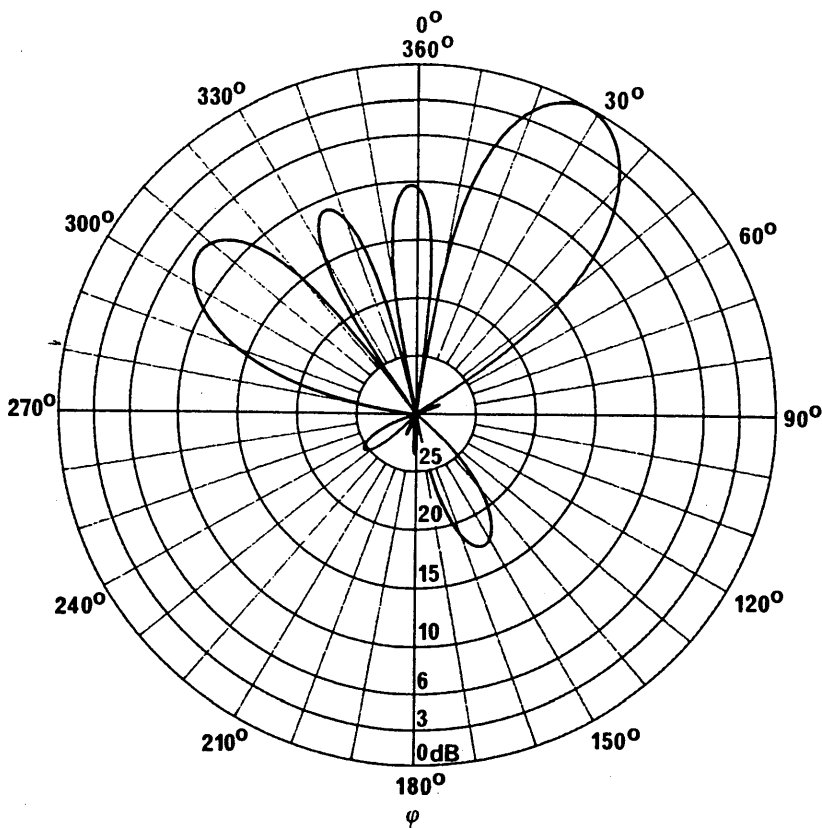


FIGURE 76c

Forward radiation pattern

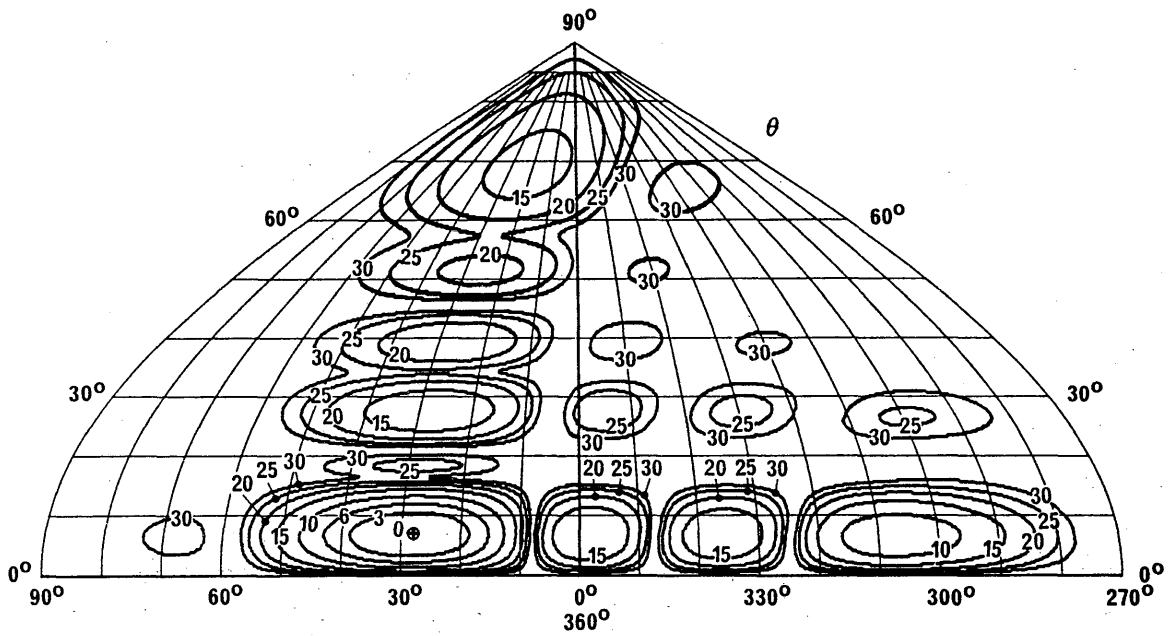


FIGURE 76d

Backward radiation pattern

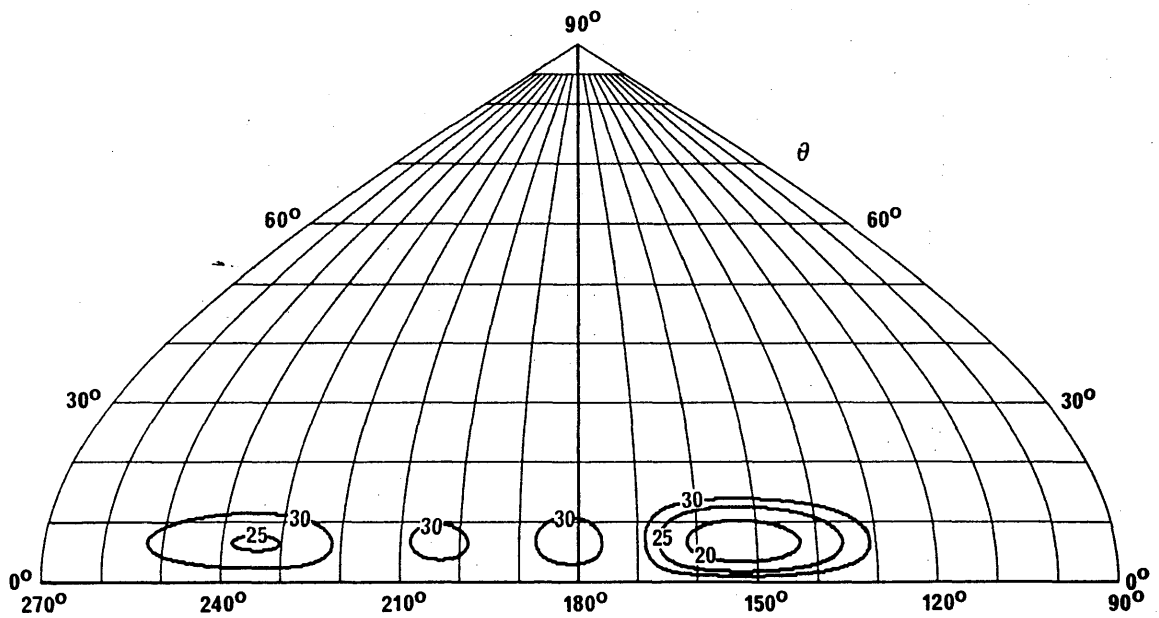


FIGURE 77a

Vertical pattern at 0° azimuth angle

Curtain antenna with aperiodic screen reflector

HR 4/4/1.0

$F_R = 1$

$\theta = 7^\circ$

$G_i = 22.0$  dB

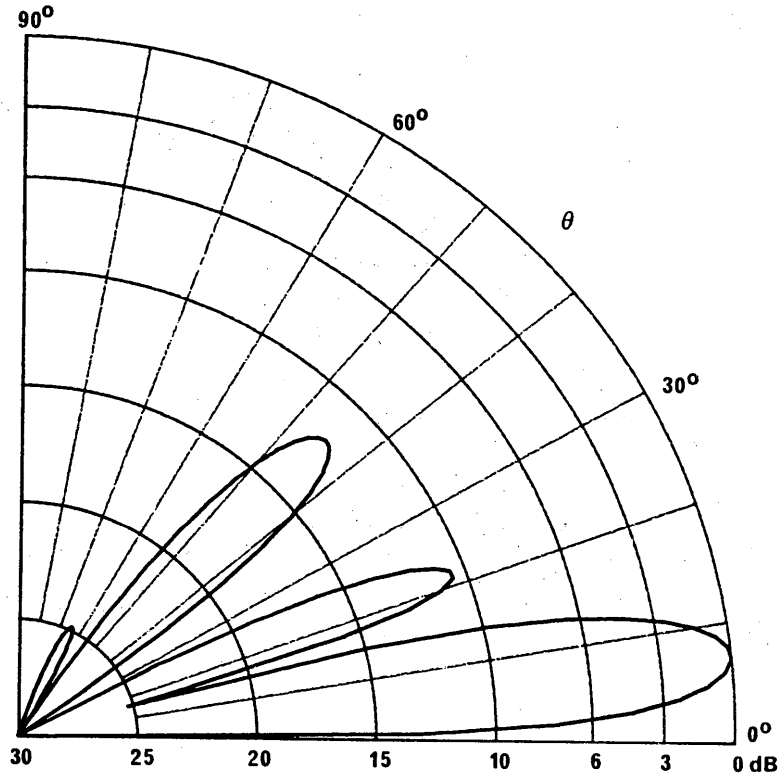


FIGURE 77b

Horizontal pattern at 7° elevation angle

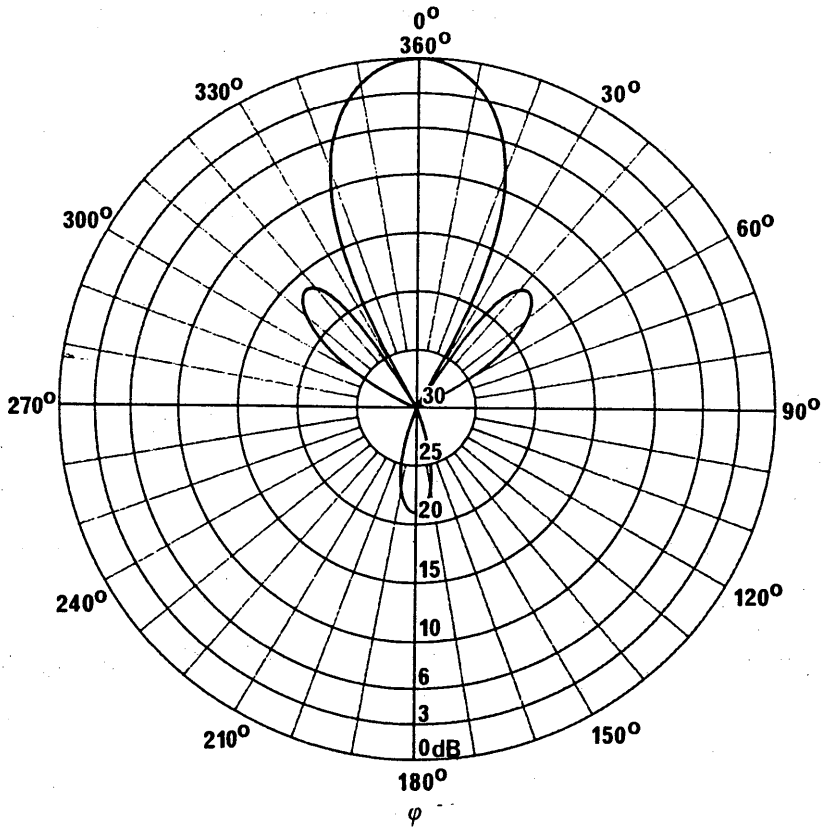


FIGURE 77c  
Forward radiation pattern

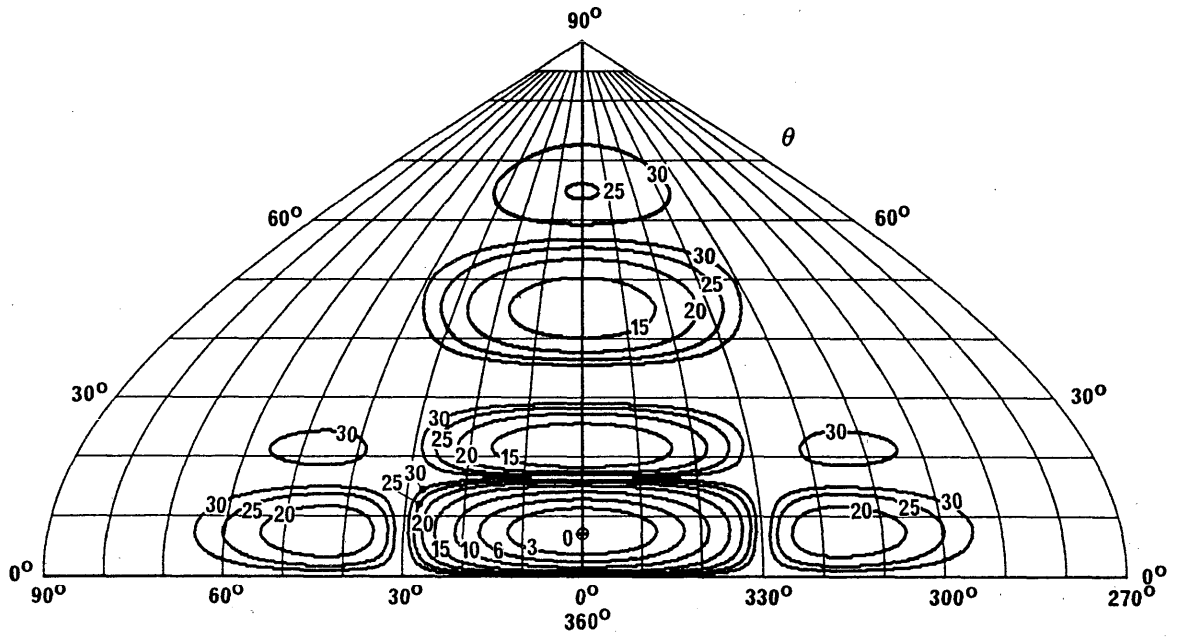


FIGURE 77d  
Backward radiation pattern

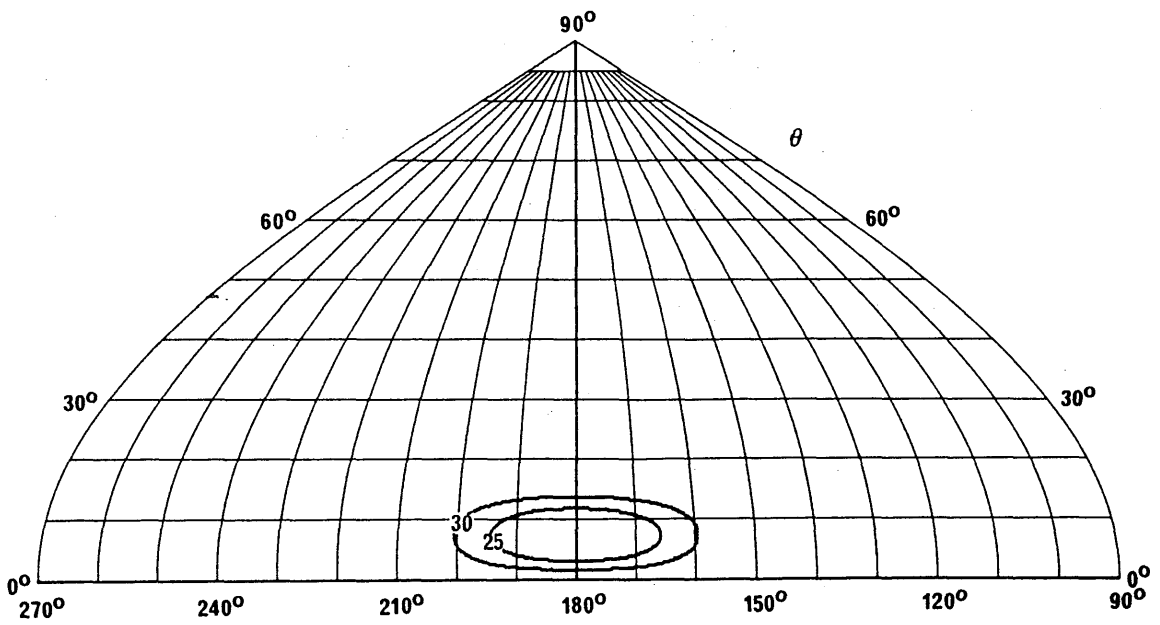


FIGURE 78a

Vertical pattern at 0° azimuth angle

Tropical antenna  
T 1/2/0.3  
 $F_R = 1$   
 $\theta = 90^\circ$   
 $G_i = 7.3 \text{ dB}$

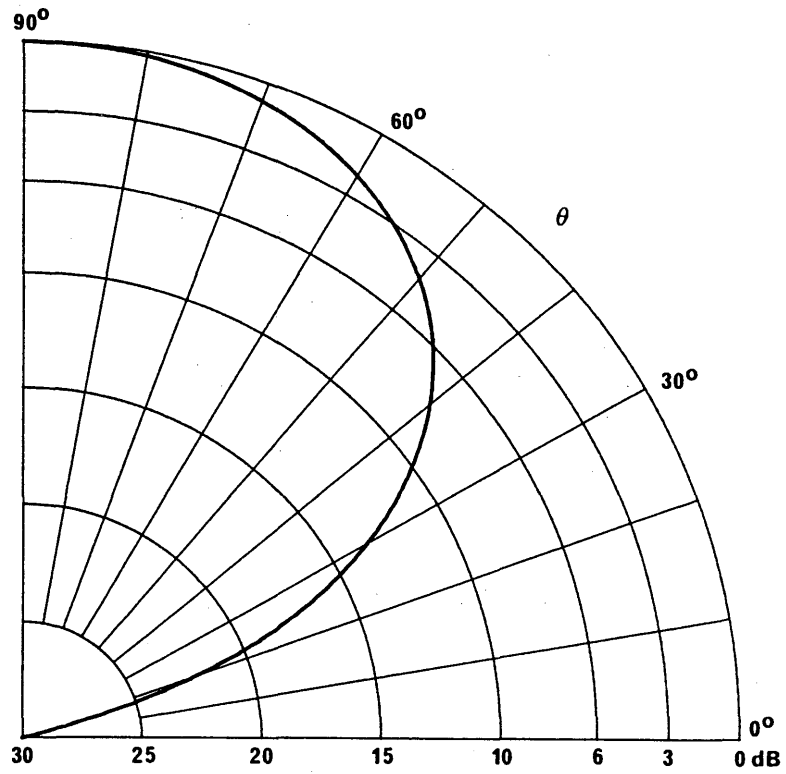


FIGURE 78b

Horizontal pattern at 45° elevation angle

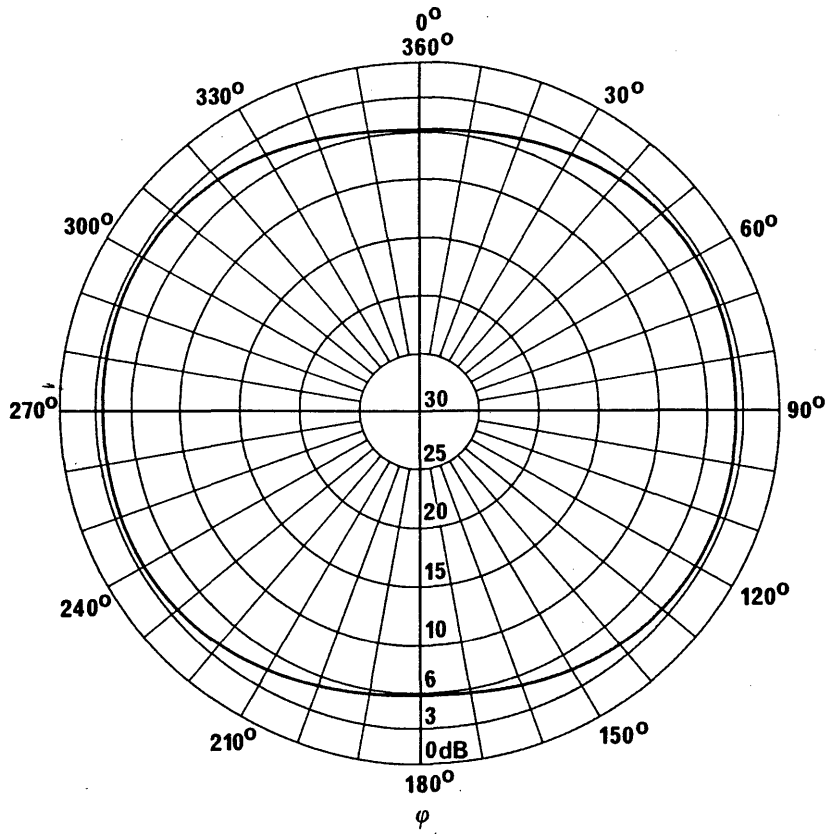


FIGURE 78c  
Forward radiation pattern

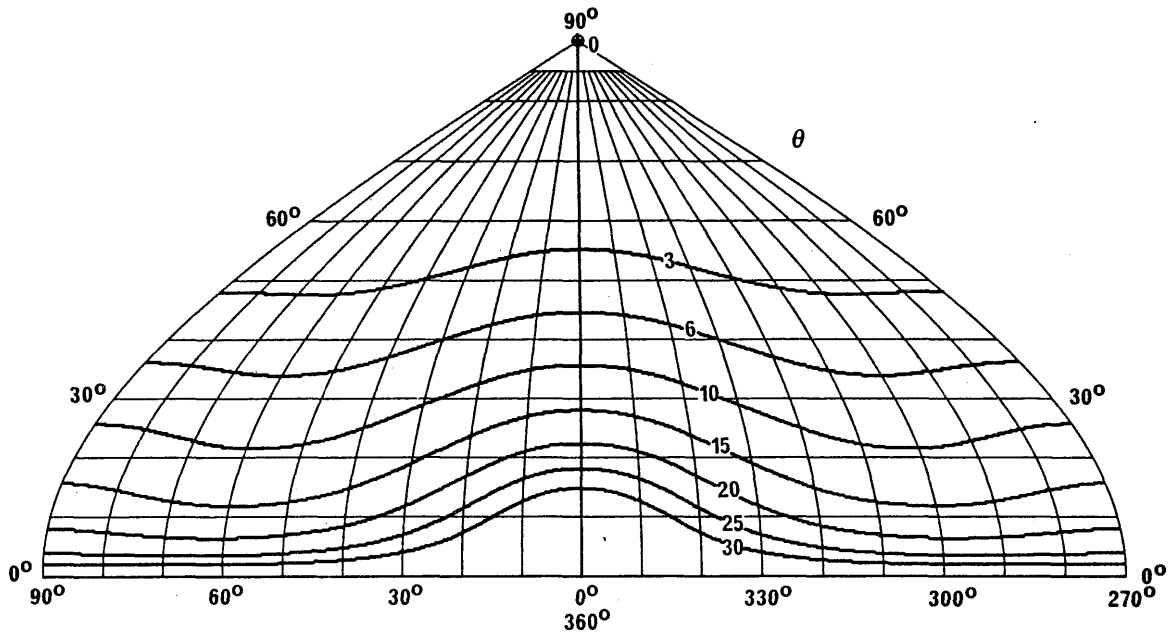


FIGURE 78d  
Backward radiation pattern

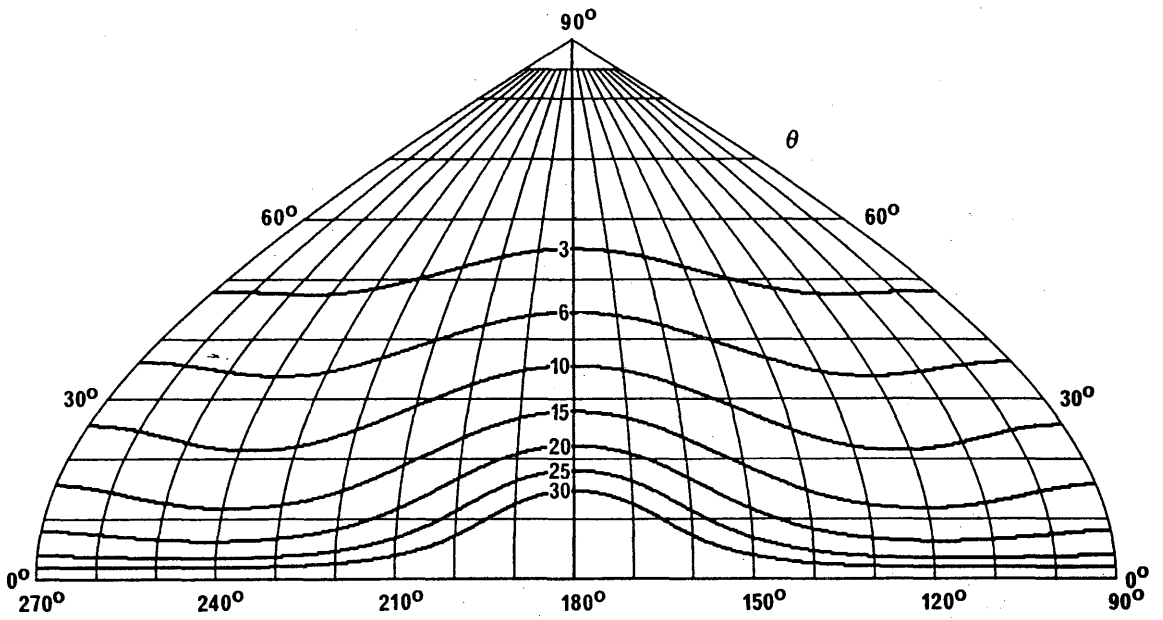


FIGURE 79a

Vertical pattern at 12° azimuth angle

Tropical antenna  
T 2/2/0.5  
 $F_R = 1$   
 $\theta = 45^\circ$   
 $\phi = 12^\circ$   
 $G_i = 6.4 \text{ dB}$

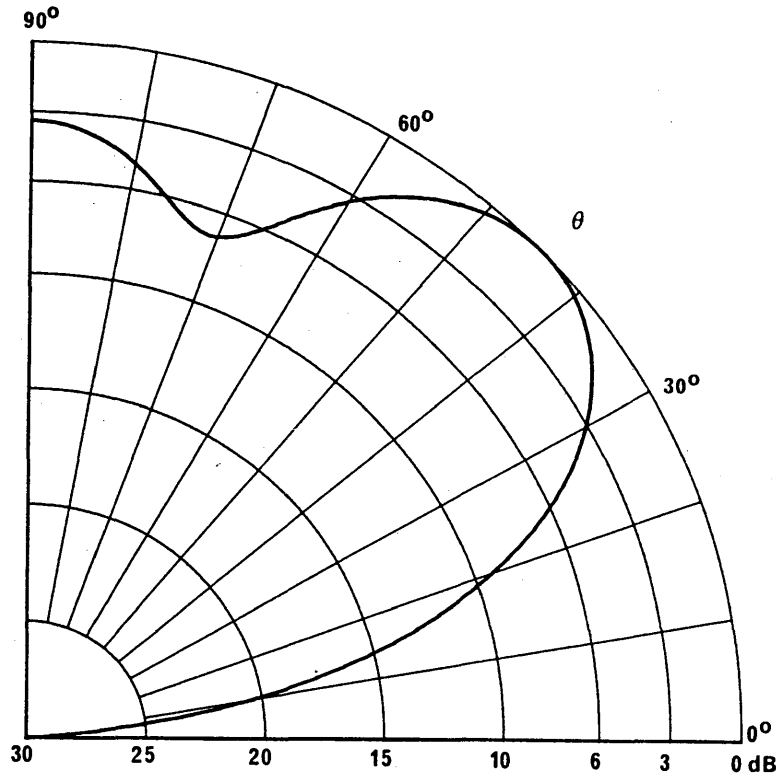


FIGURE 79b

Horizontal pattern at 45° elevation angle

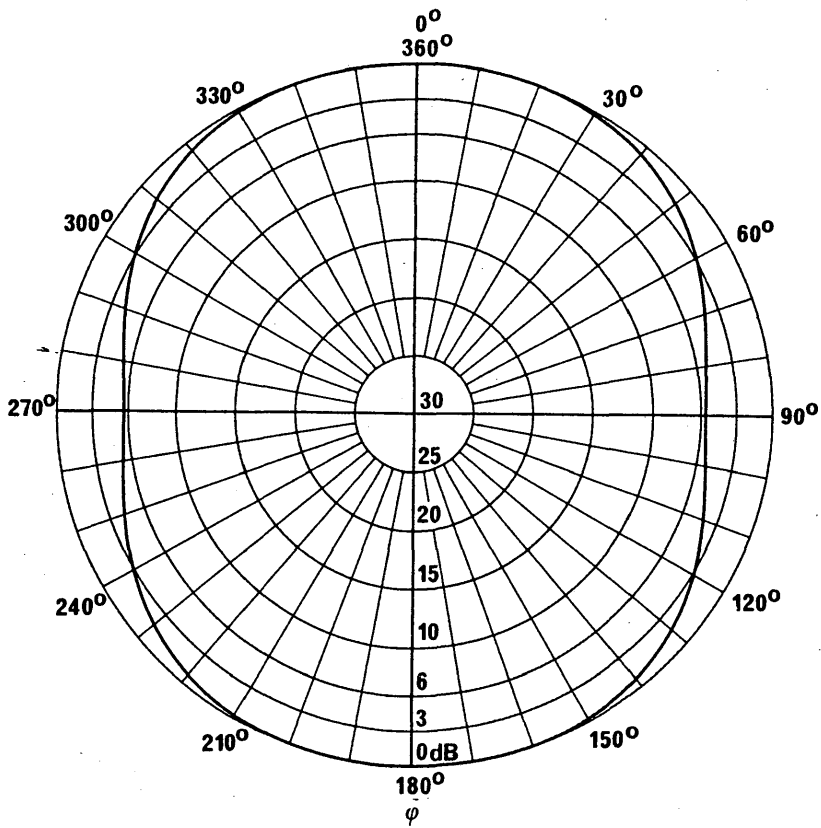


FIGURE 79c  
Forward radiation pattern

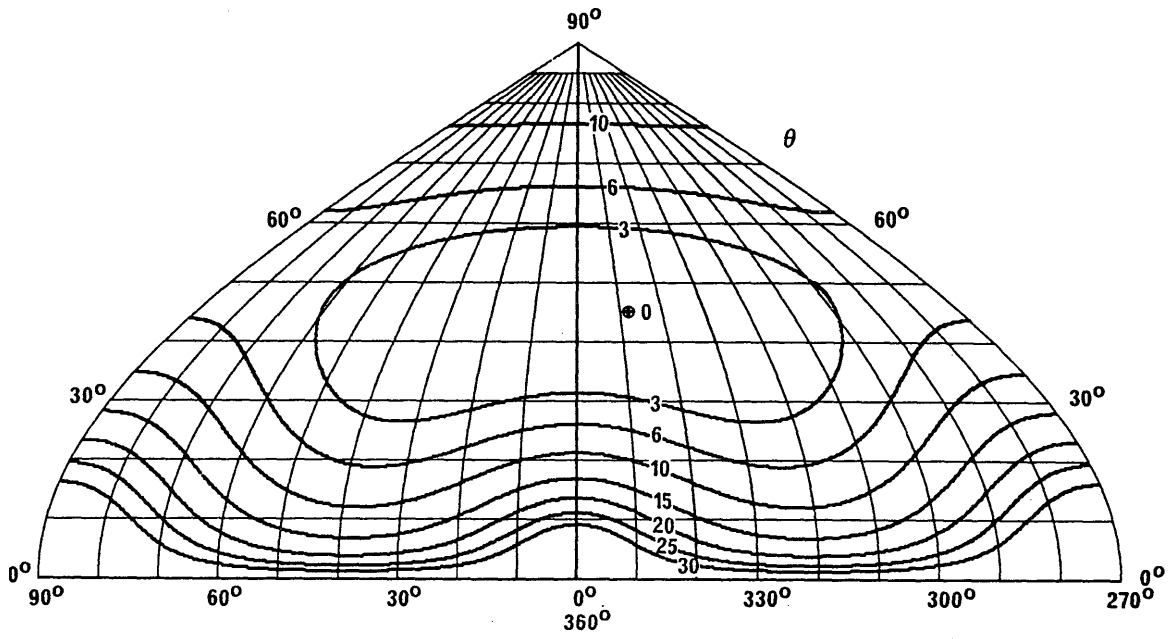


FIGURE 79d  
Backward radiation pattern

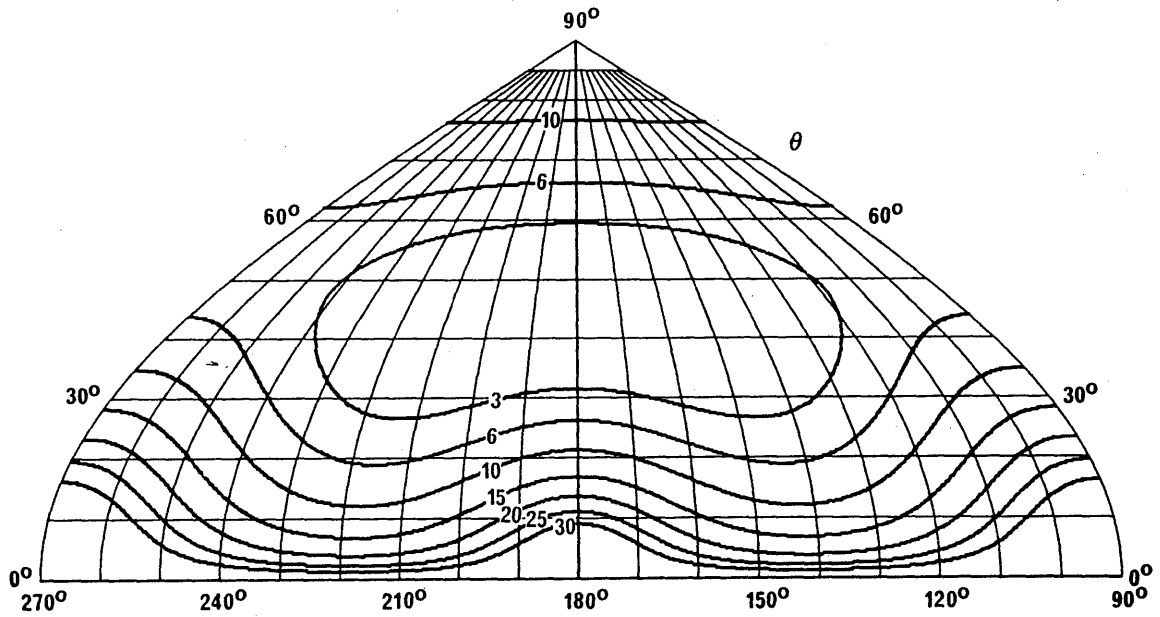
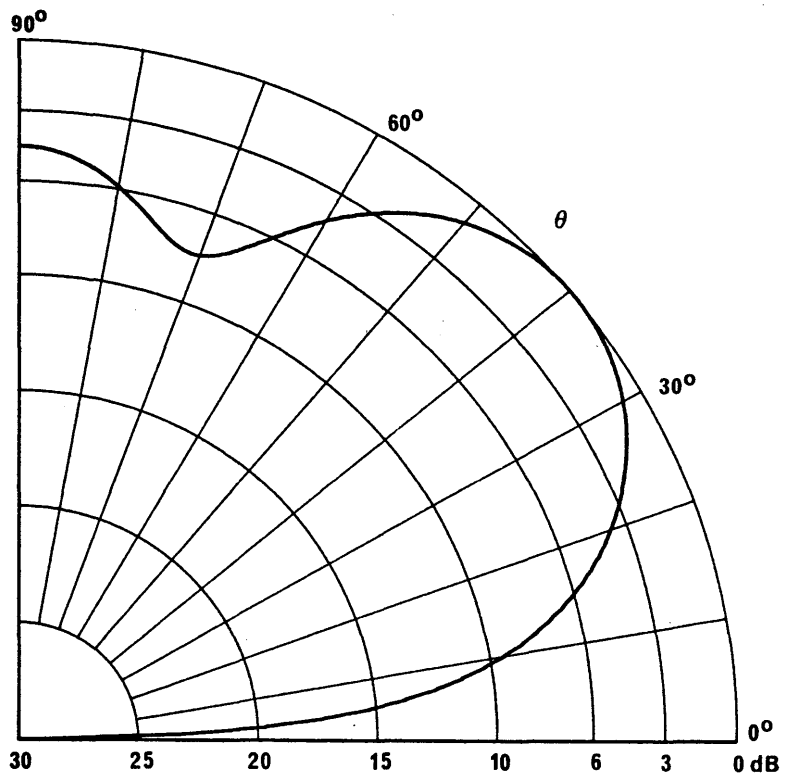


FIGURE 80a

Vertical pattern at 37° azimuth angle



Tropical antenna

T 2/2/0.5

$F_R = 1$

$s = 15^\circ$

$\theta = 40^\circ$

$\varphi = 37^\circ$

$G_i = 7.3 \text{ dB}$

FIGURE 80b

Horizontal pattern at 40° elevation angle

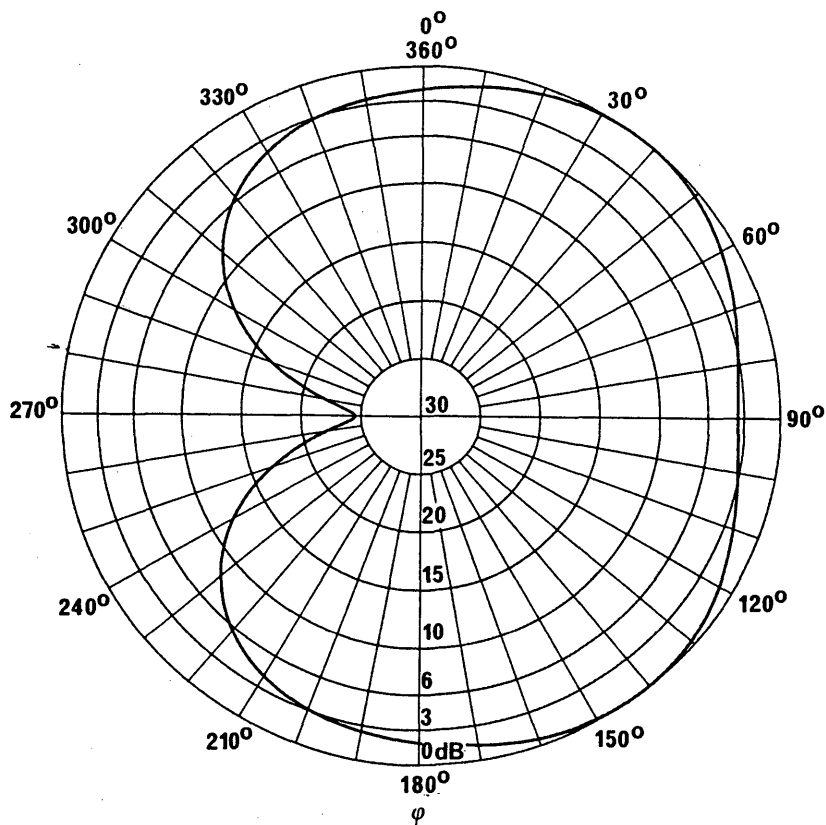


FIGURE 80c  
Forward radiation pattern

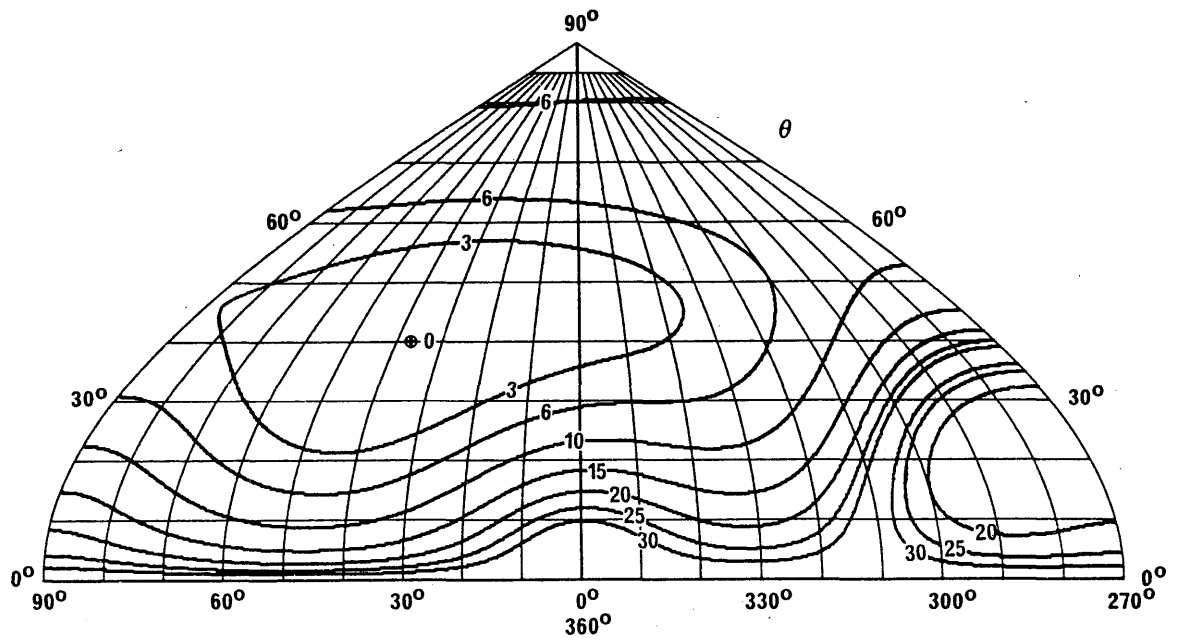


FIGURE 80d  
Backward radiation pattern

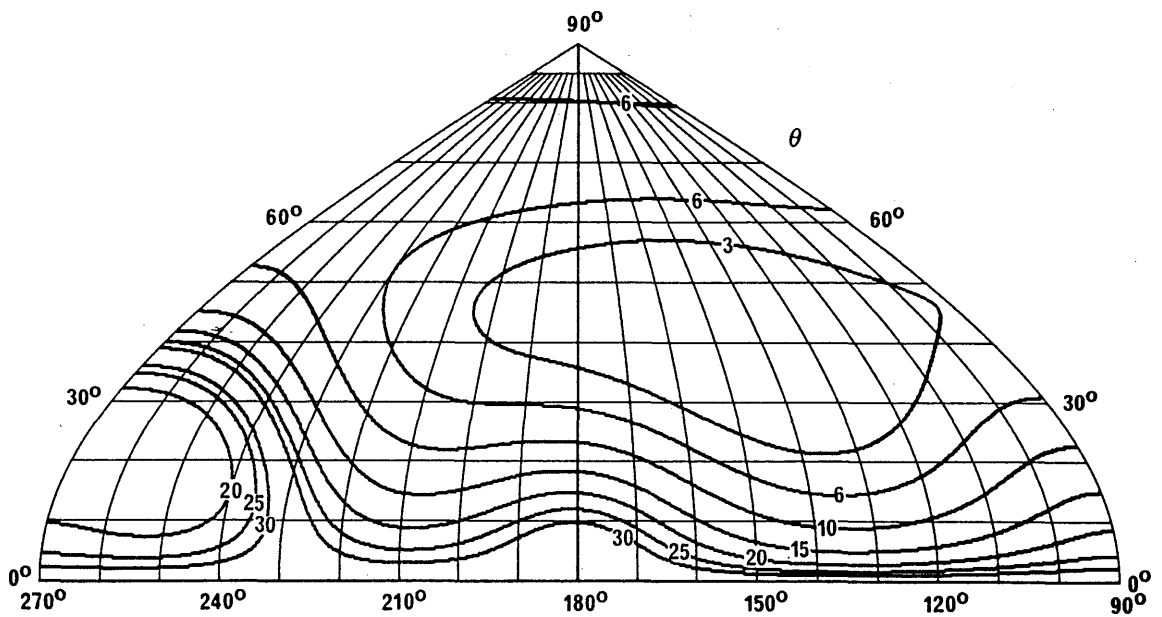


FIGURE 81a

Vertical pattern at 0° azimuth angle

Horizontal log-periodic antenna  
 LPH 18/35/30/3/26/89  
 $f = 10 \text{ MHz}$   
 $\theta = 14^\circ$   
 $G_i = 17.3 \text{ dB}$

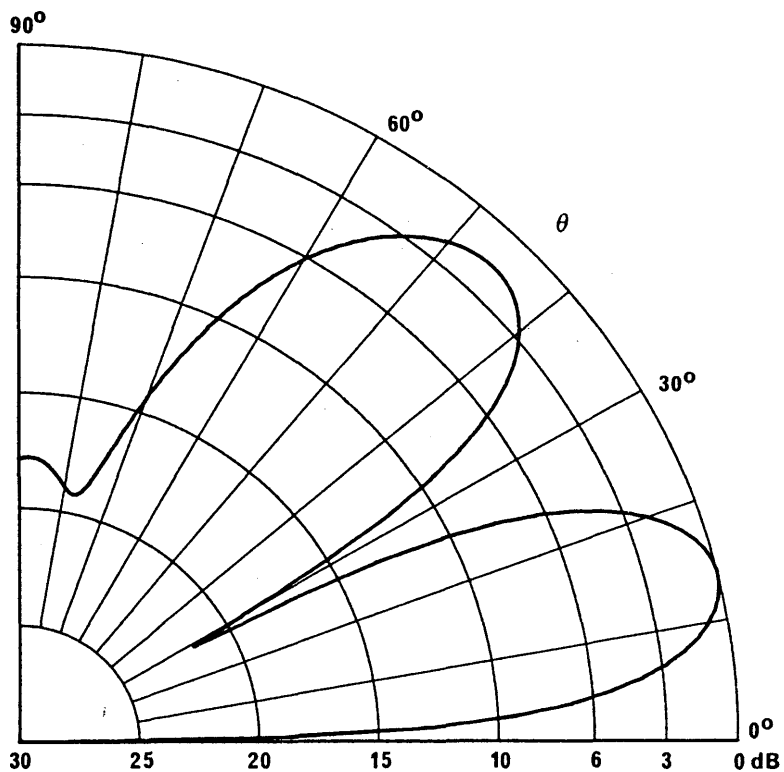


FIGURE 81b

Horizontal pattern at 14° elevation angle

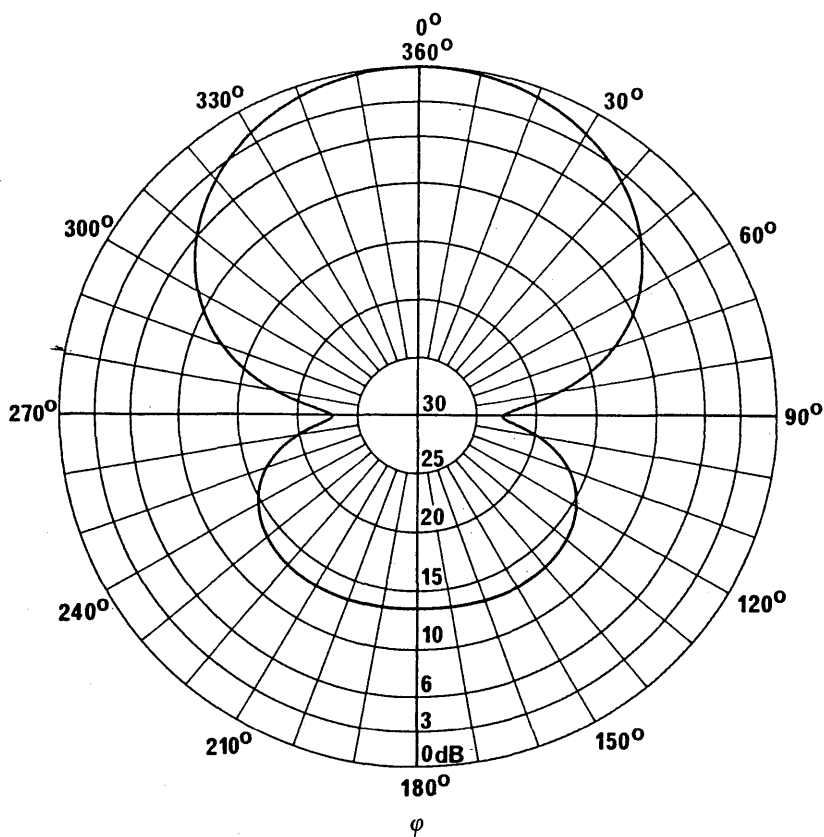


FIGURE 81c  
Forward radiation pattern

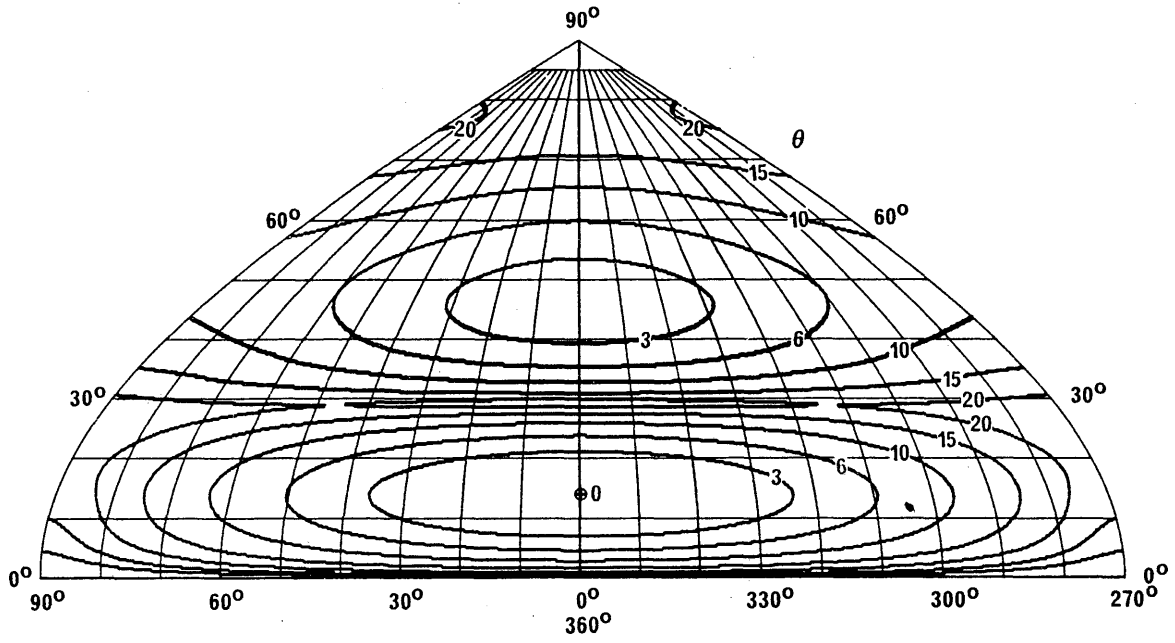


FIGURE 81d  
Backward radiation pattern

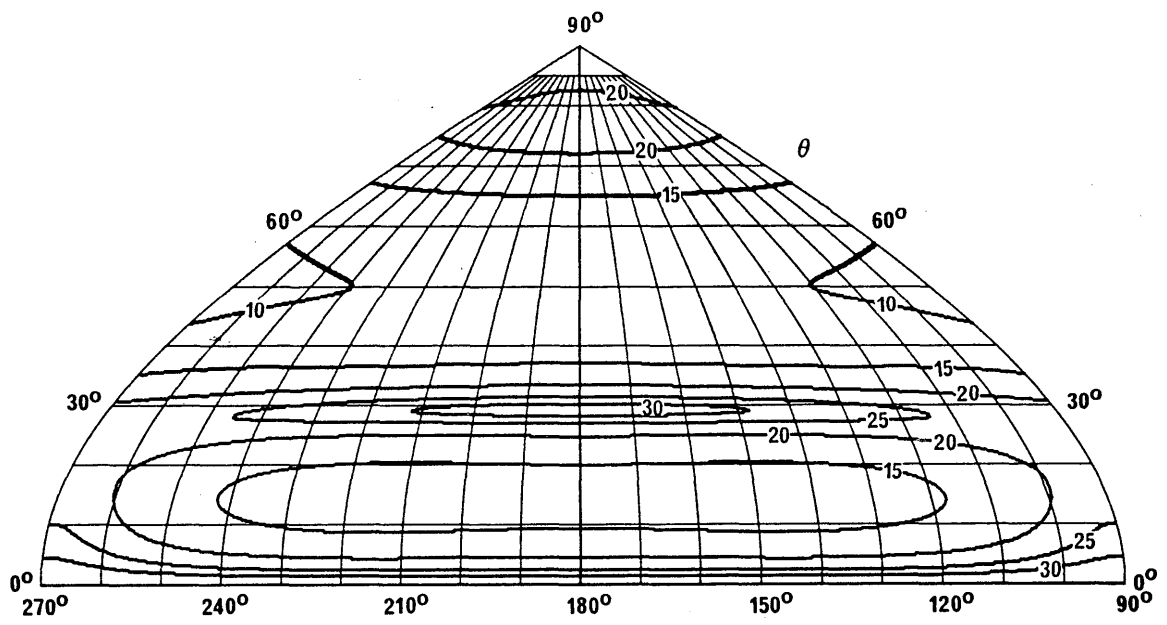


FIGURE 82a

Vertical pattern at 0° azimuth angle

Vertical log-periodic antenna  
 LPV 18/45/3/17/6/34/220  
 $f = 10 \text{ MHz}$   
 $\theta = 17^\circ$   
 $G_i = 2.4 \text{ dB}$

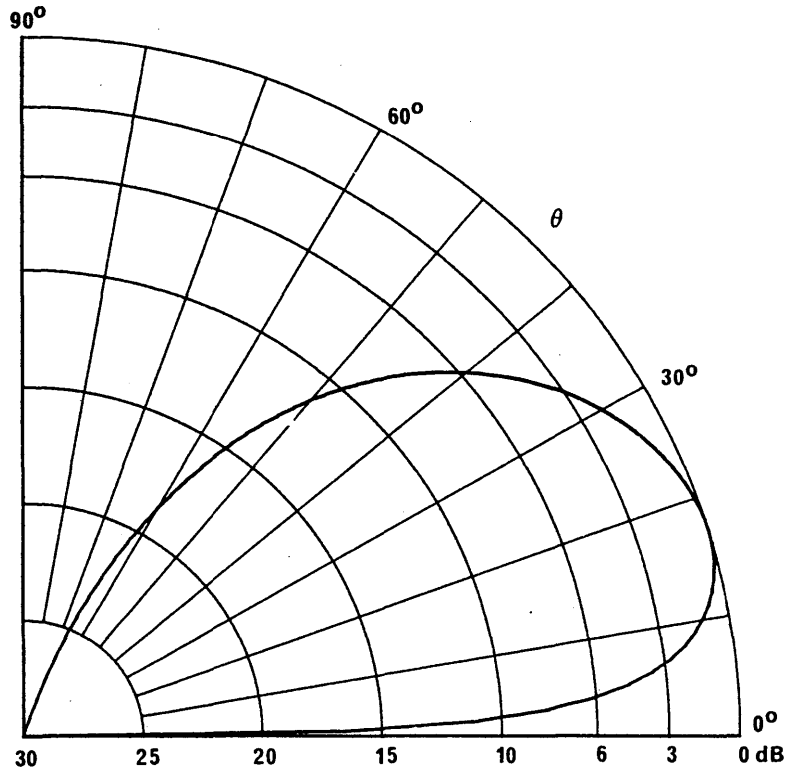


FIGURE 82b

Horizontal pattern at 17° elevation angle

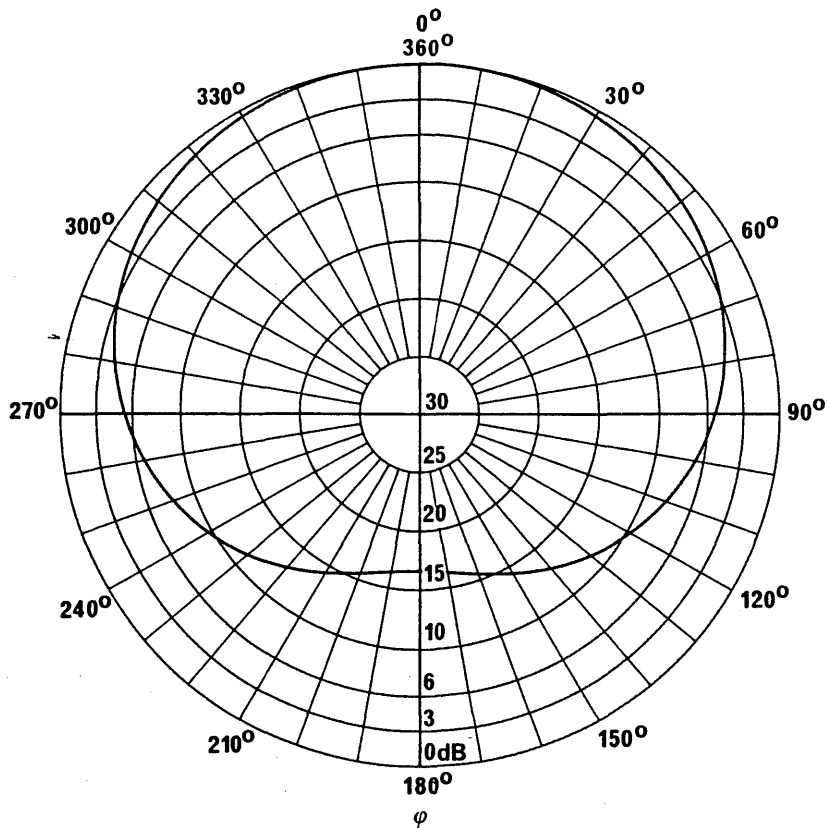


FIGURE 82c

Forward radiation pattern

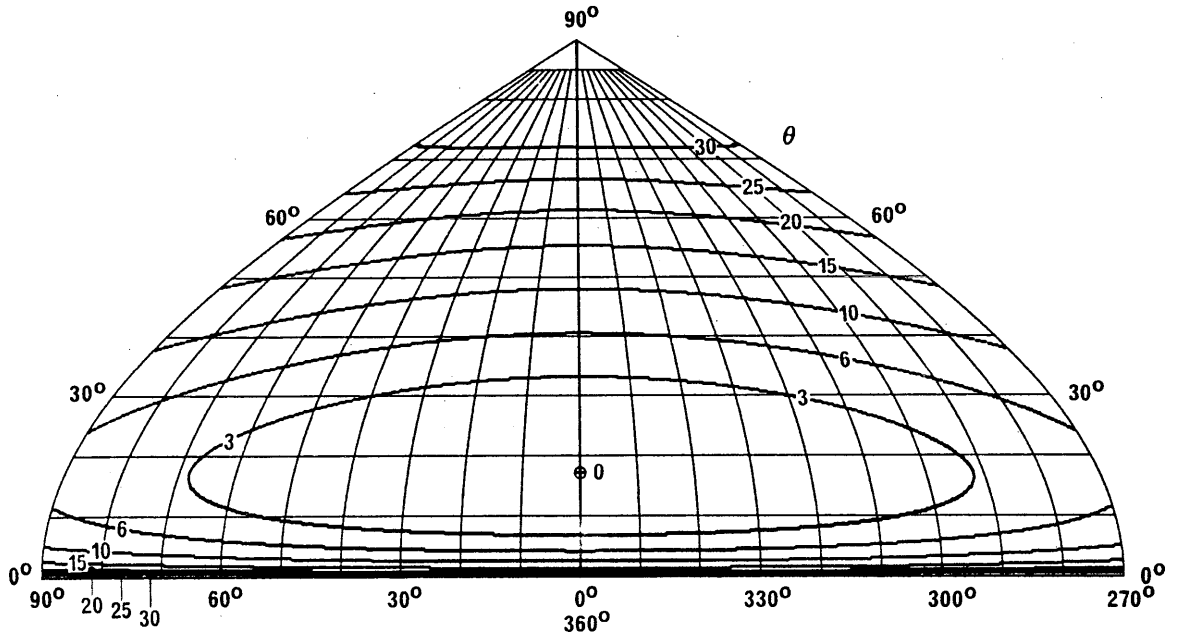


FIGURE 82d

Backward radiation pattern

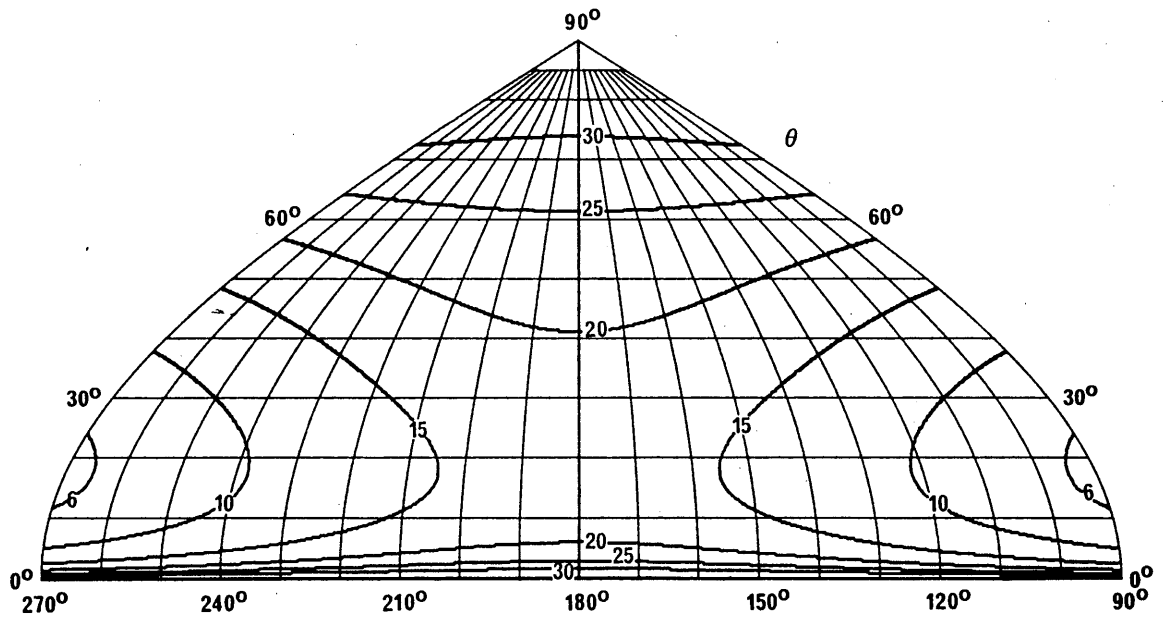


FIGURE 83a

Vertical pattern at 0° azimuth angle

Quadrant antenna  
 HQ 1/0.3  
 $\theta = 51^\circ$   
 $G_i = 5.3 \text{ dB}$

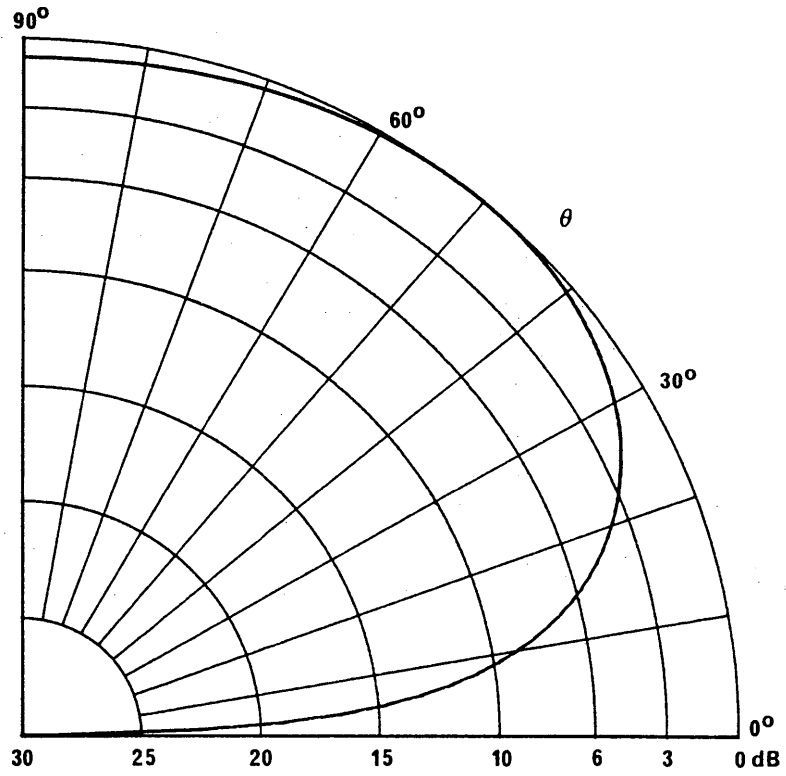


FIGURE 83b

Horizontal pattern at 51° elevation angle

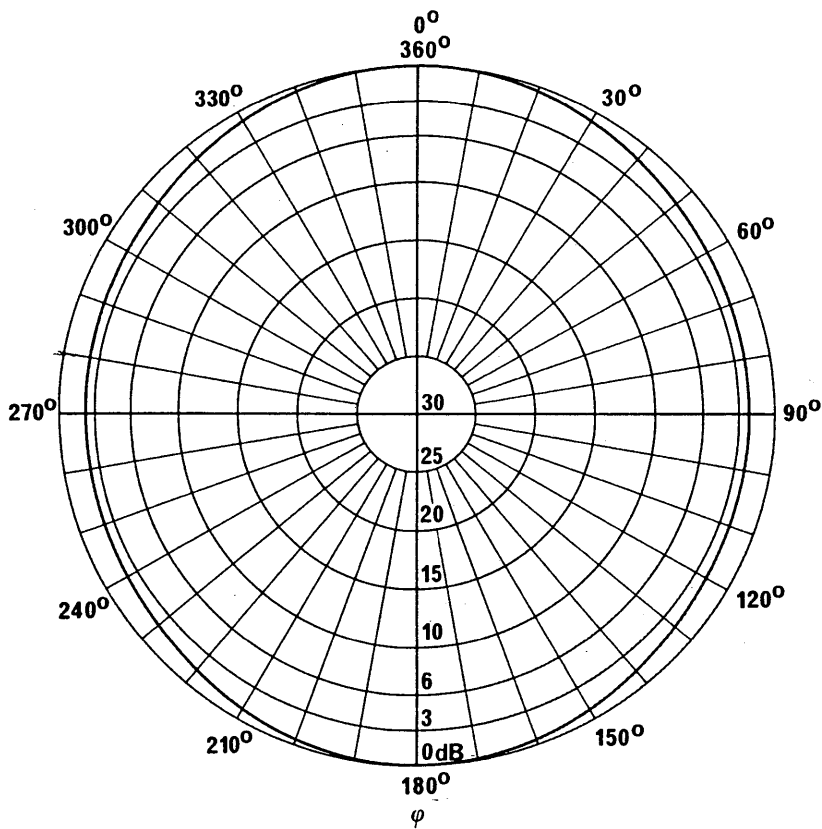


FIGURE 83c  
Forward radiation pattern

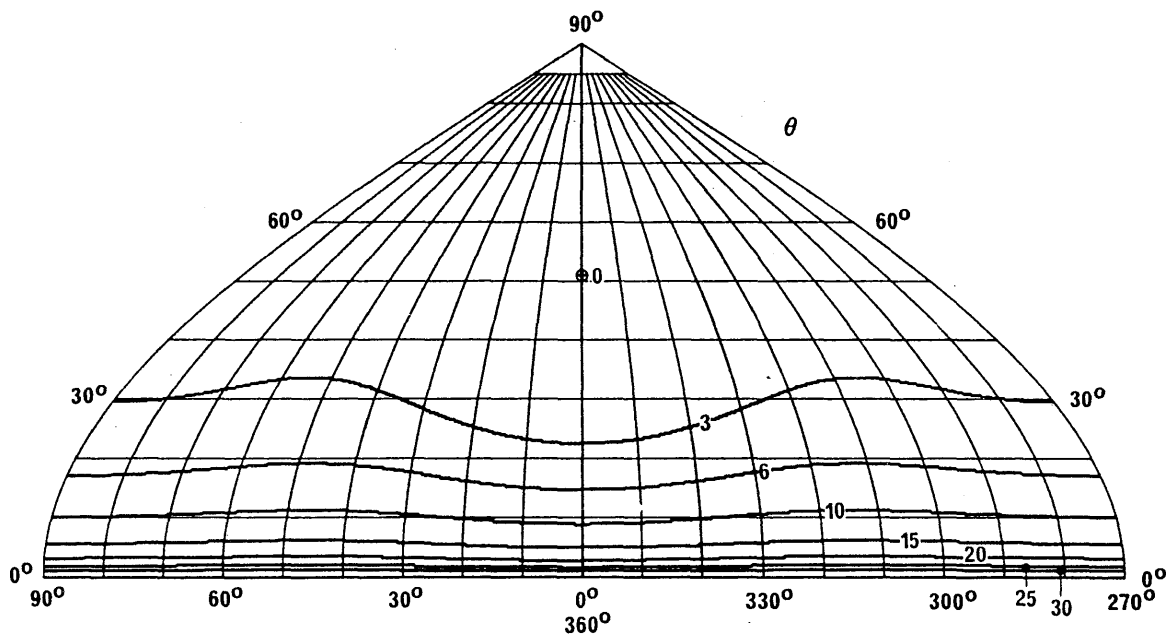


FIGURE 83d  
Backward radiation pattern

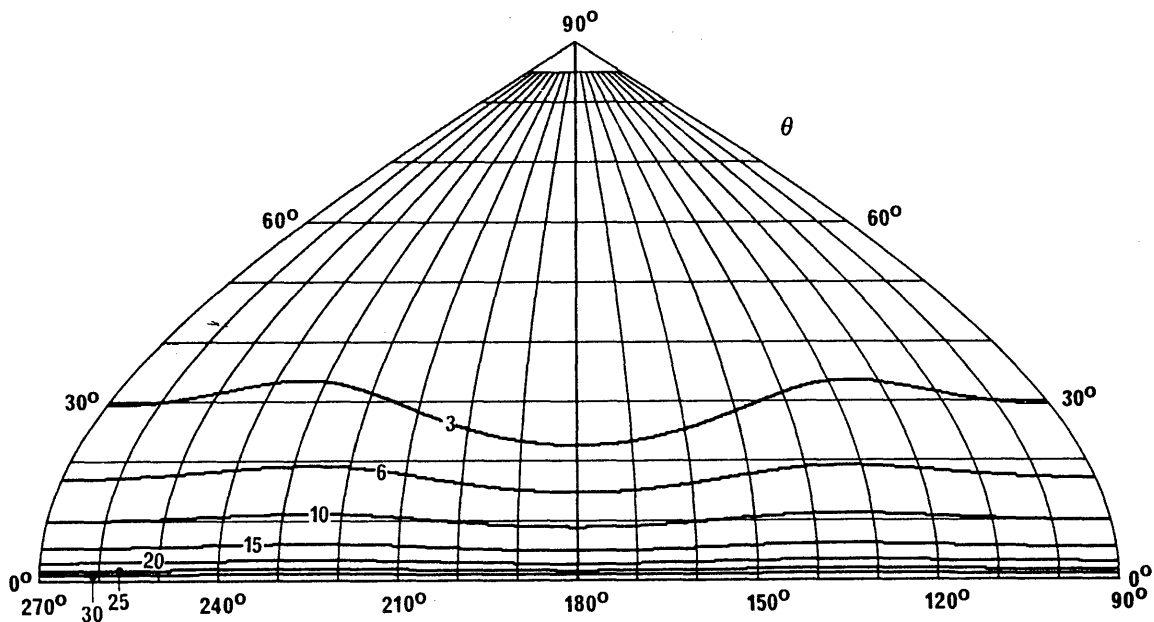


FIGURE 84a

Vertical pattern at 0° azimuth angle

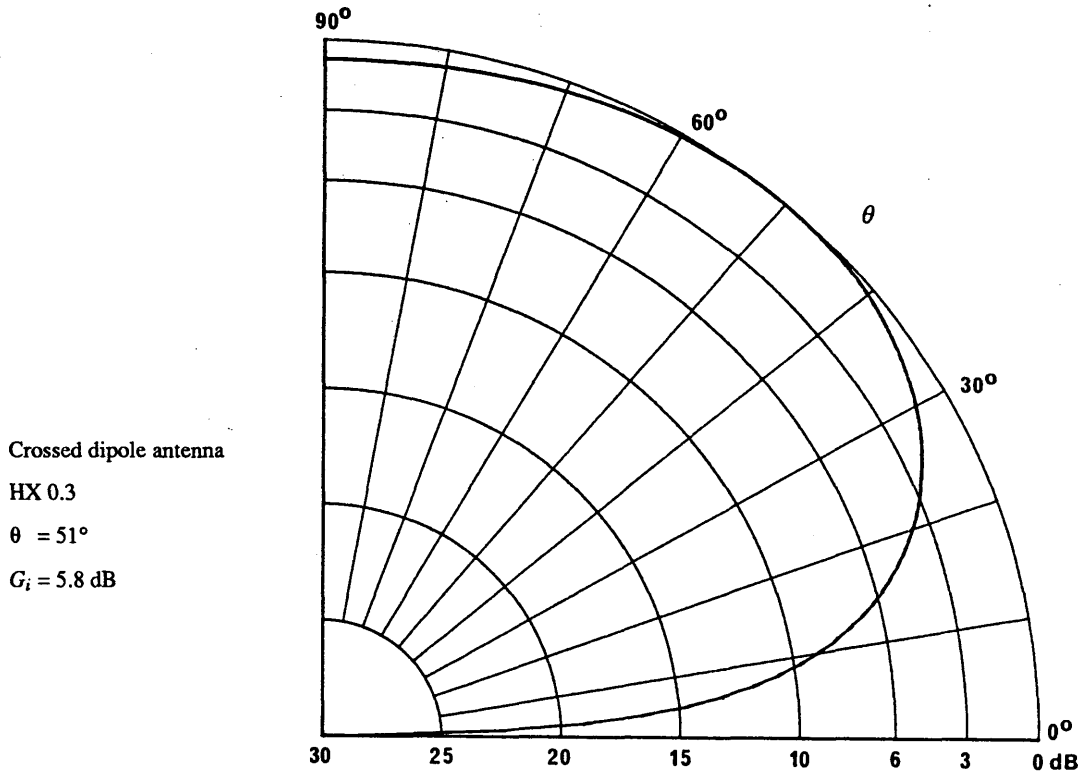


FIGURE 84b

Horizontal pattern at 51° elevation angle

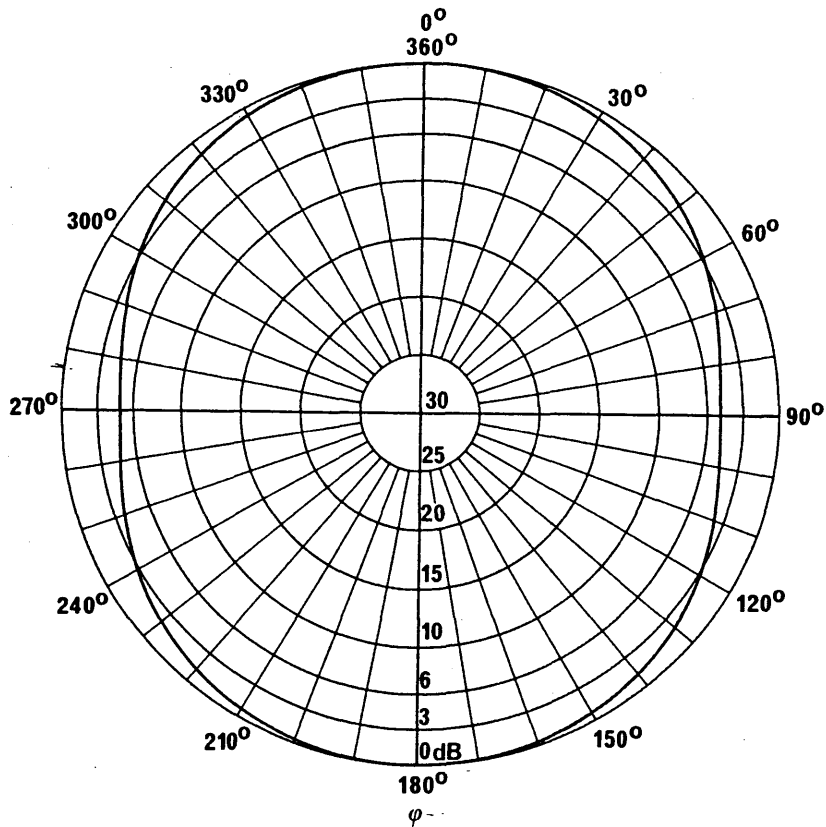


FIGURE 84c  
Forward radiation pattern

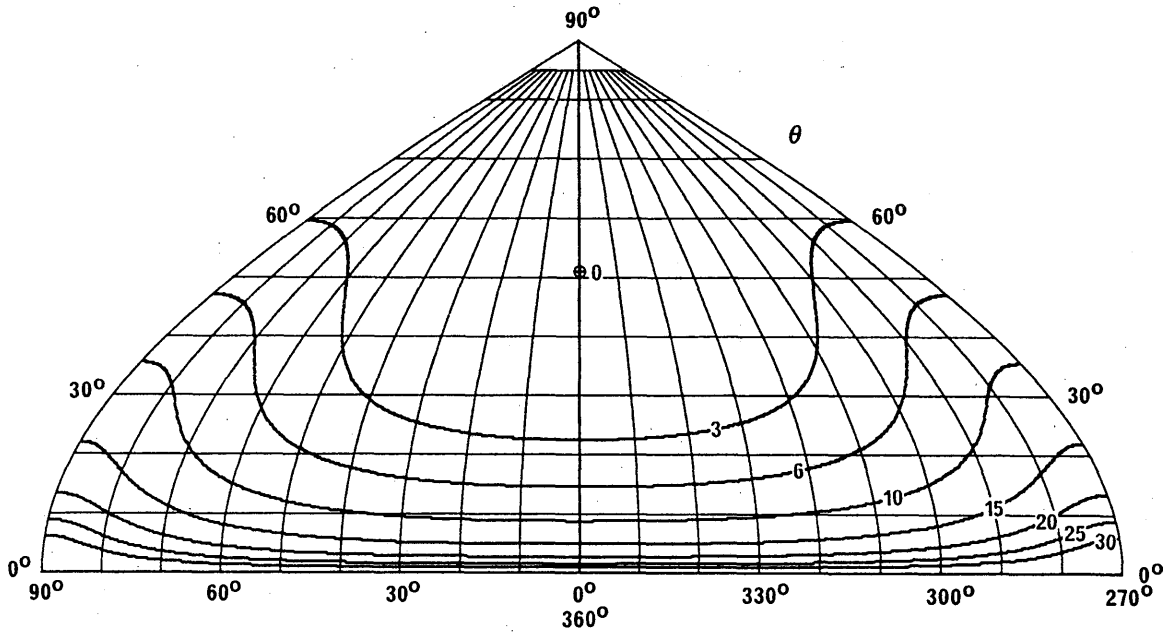


FIGURE 84d  
Backward radiation pattern

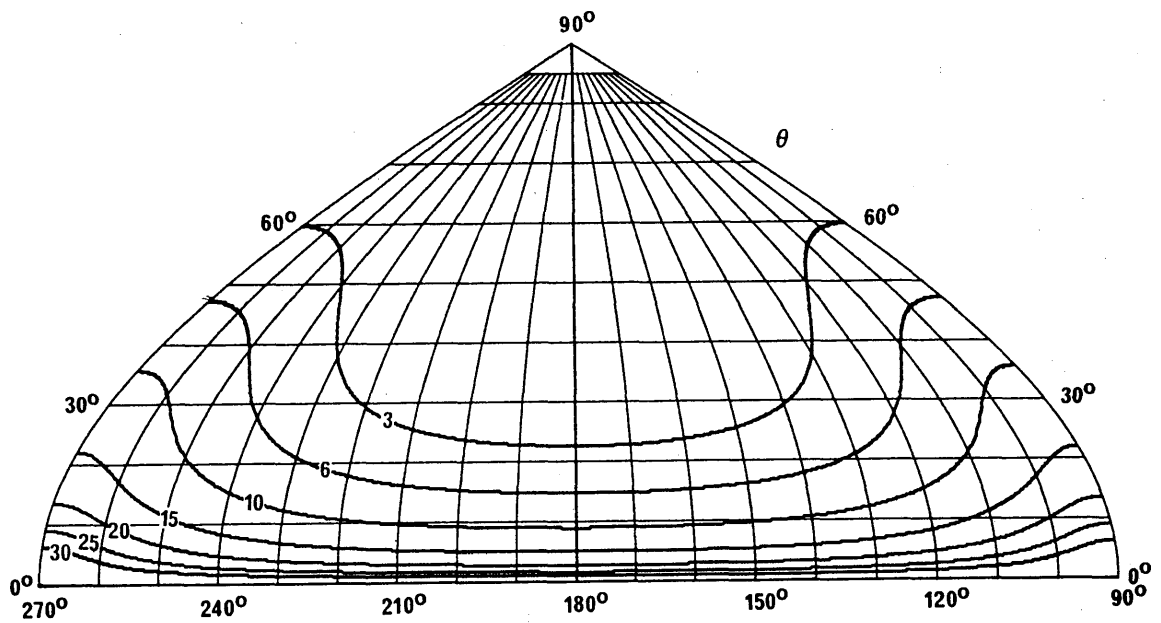


FIGURE 85a

Vertical pattern at 0° azimuth angle

Rhombic antenna  
 RH 90/55/15  
 $f = 10 \text{ MHz}$   
 $\theta = 15^\circ$   
 $G_i = 14.4 \text{ dB}$

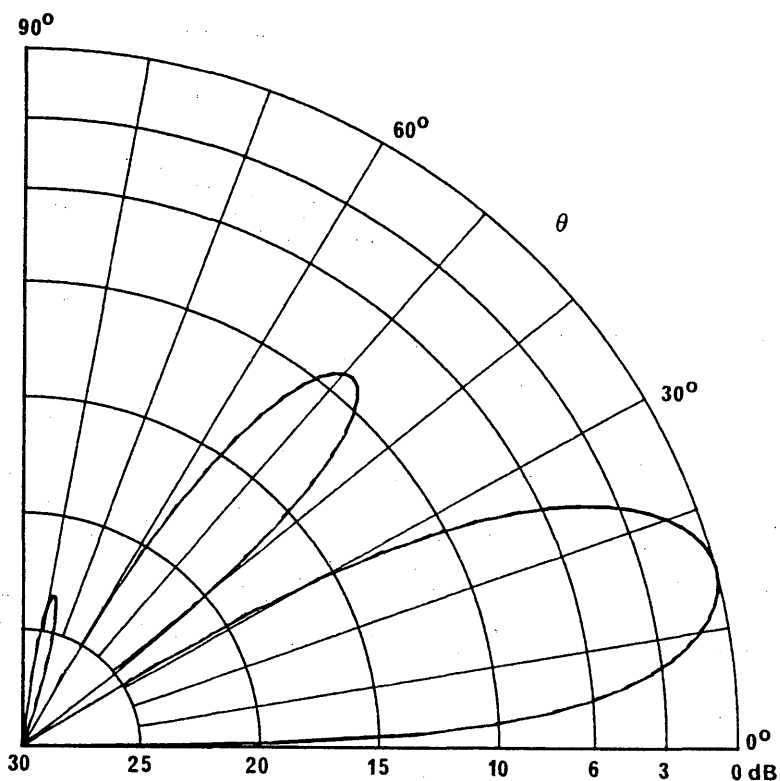


FIGURE 85b

Horizontal pattern at 15° elevation angle

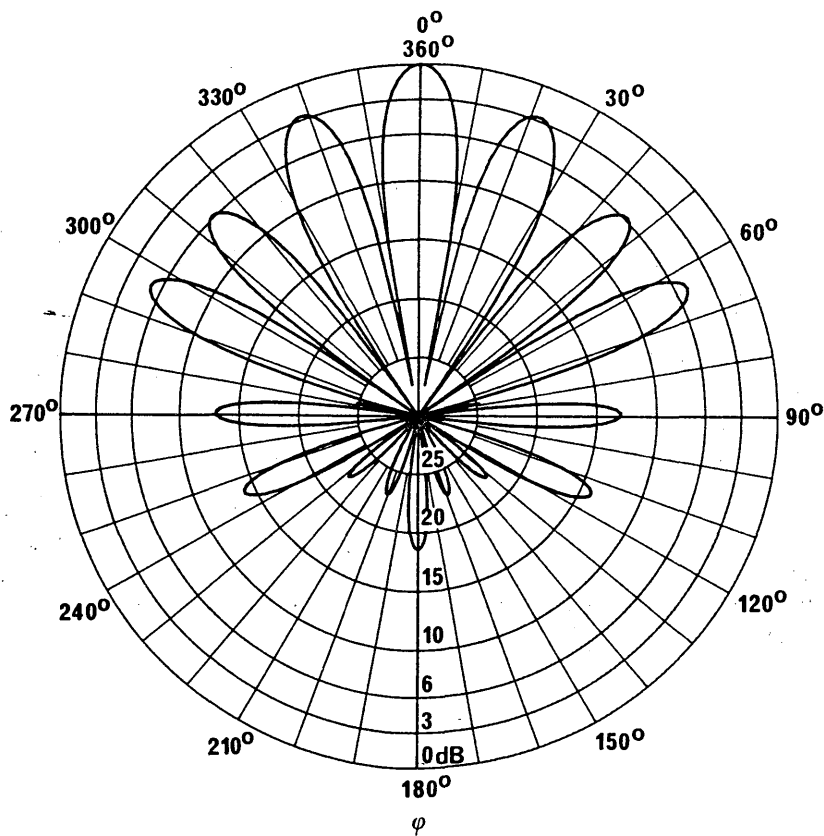


FIGURE 85c  
Forward radiation pattern

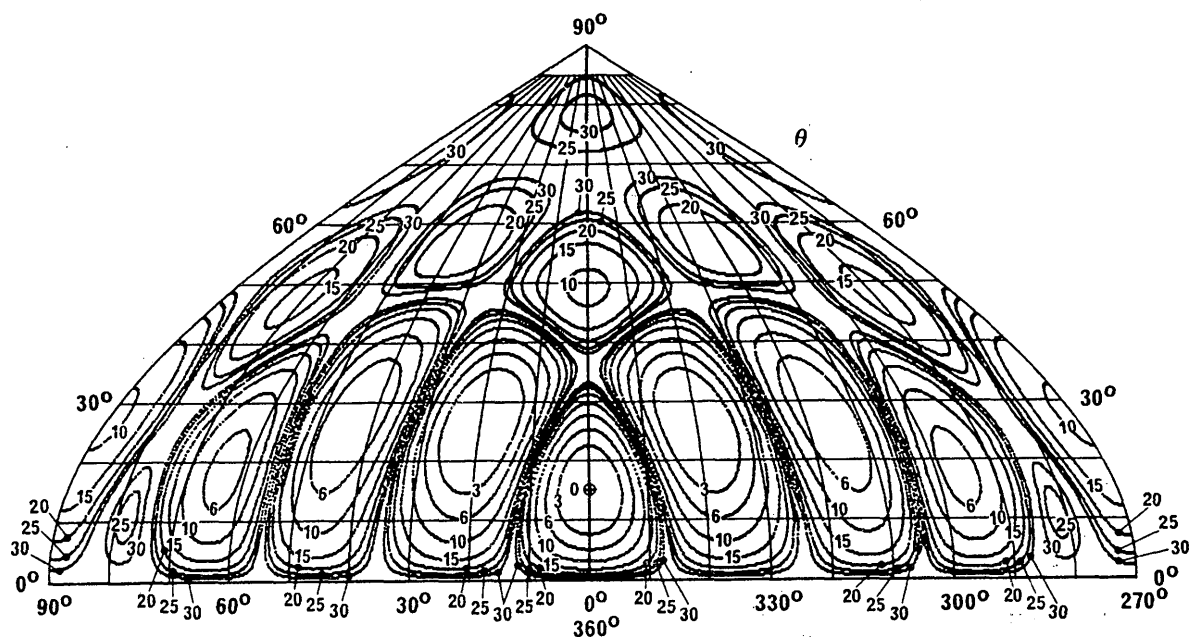


FIGURE 85d  
Backward radiation pattern

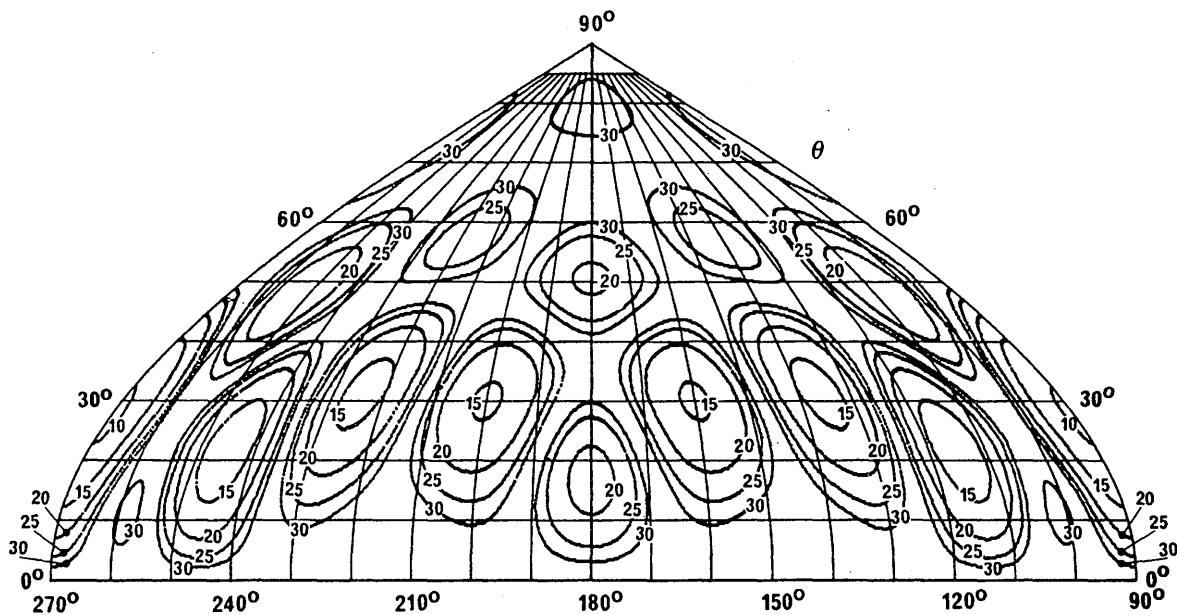


FIGURE 86a

Vertical pattern at 0° azimuth angle

Vertical monopole  
 VM 12.5/12.5/120/3  
 $\theta = 24^\circ$   
 $G_i = 0.6$  dB

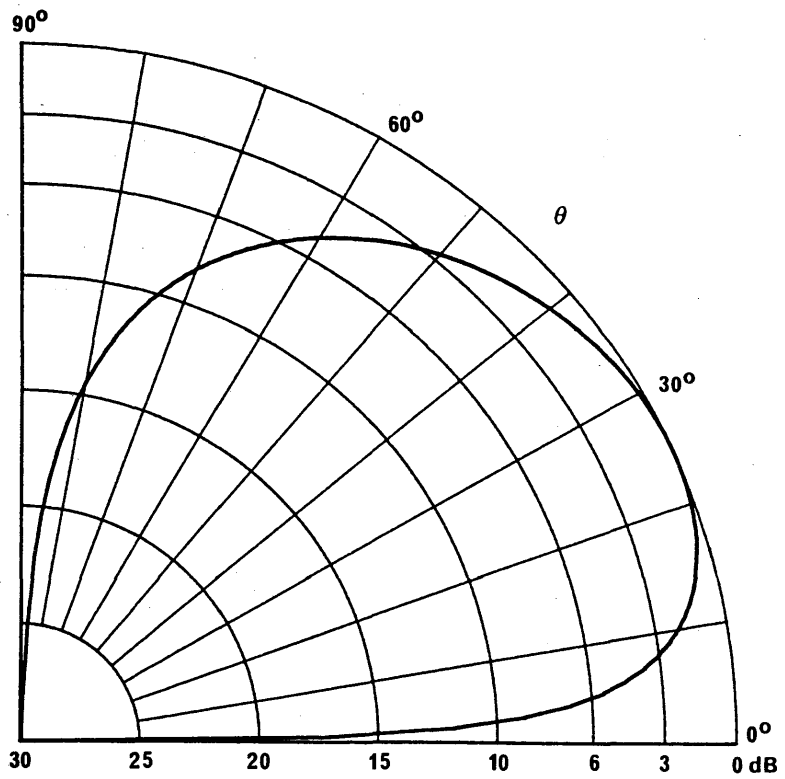


FIGURE 86b

Horizontal pattern at 24° elevation angle

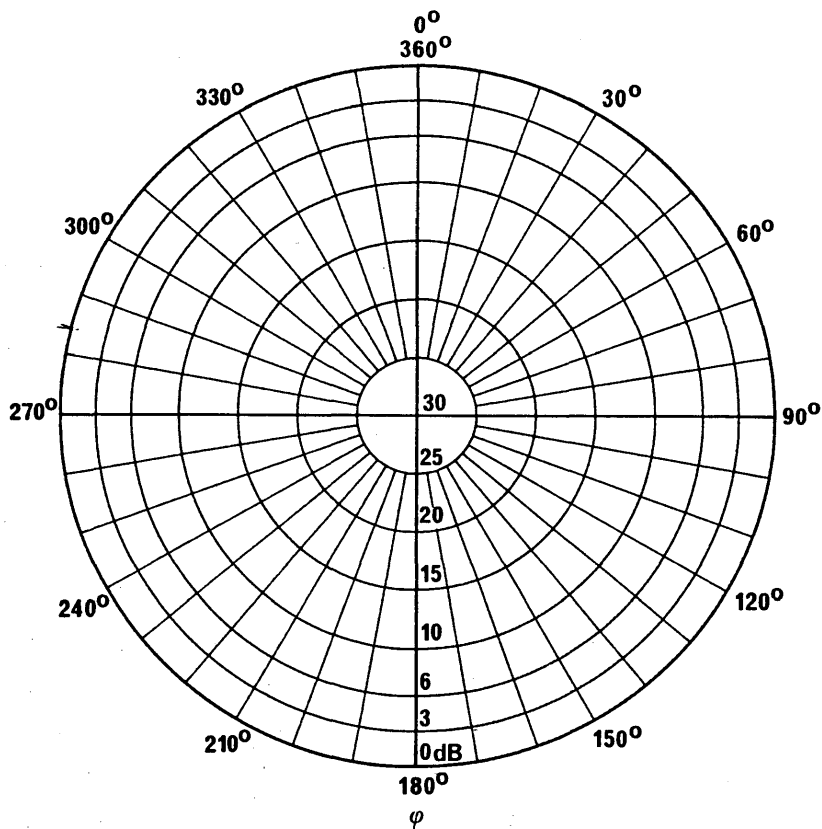


FIGURE 86c

Forward radiation pattern

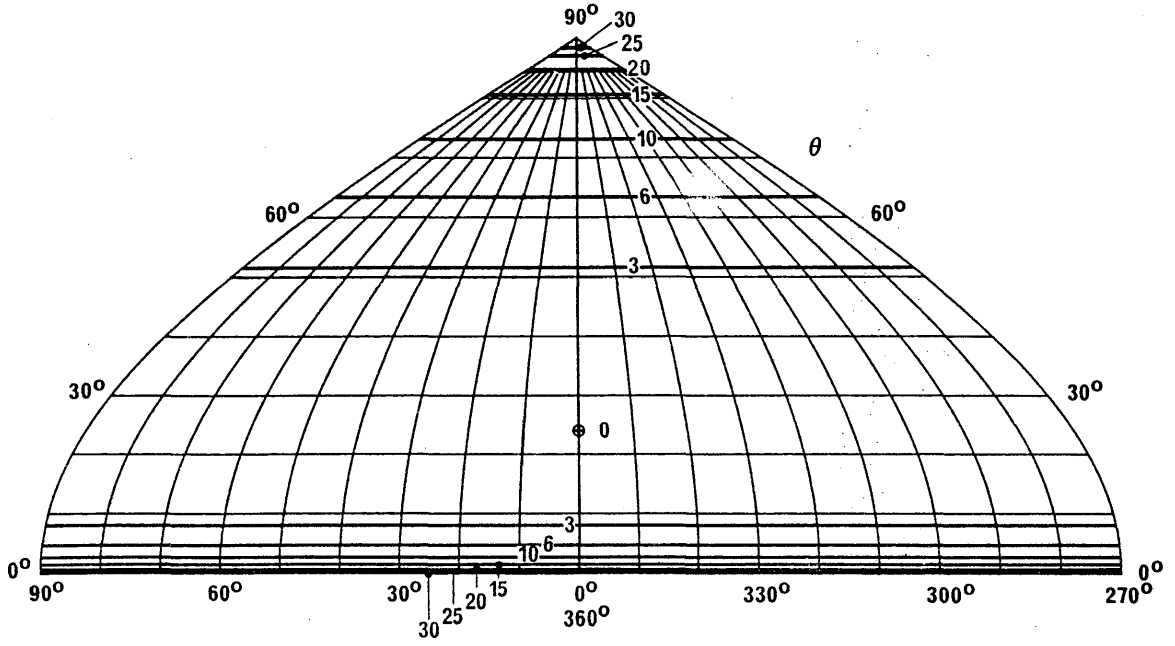
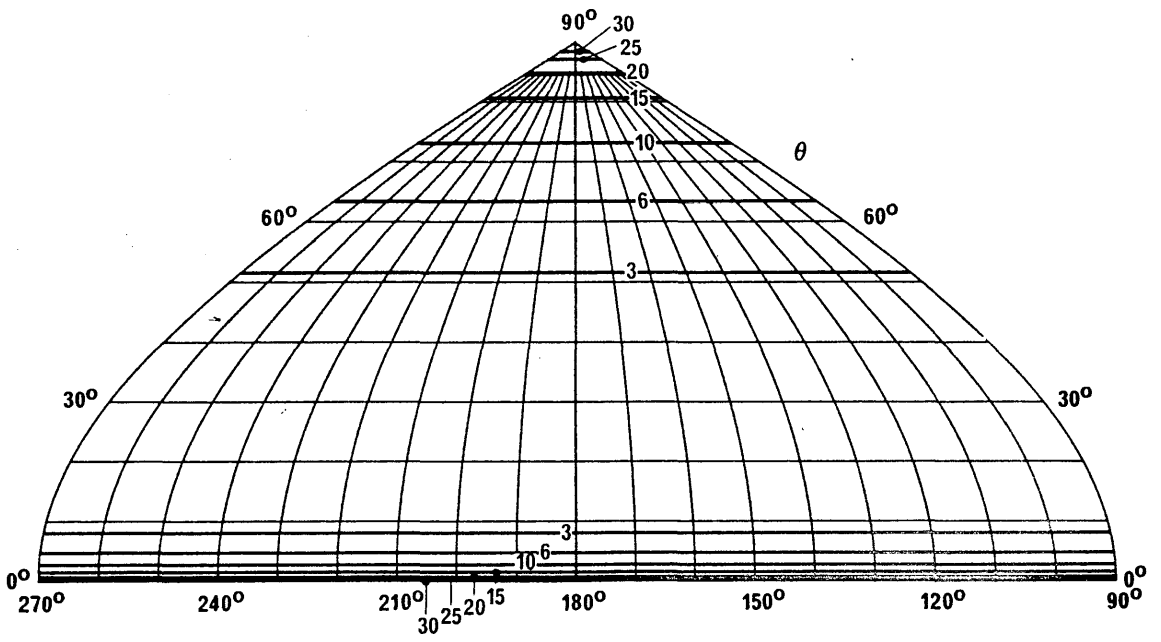


FIGURE 86d

Backward radiation pattern





Printed in Switzerland

ISBN 92-61-04431-X